Investigating the Associations Between *Plasmodium* Infections and Autoimmunity in sub-Saharan Africa

Rinter Karimi Kimathi

BSc, MSc

Submitted in fulfilment of the requirements for the Degree of Doctor of Philosophy

Institute of Infection, Immunity, and Inflammation

College of Medical, Veterinary & Life Sciences

University of Glasgow

October 2024

Abstract

Autoimmune diseases affect 5- 8% of the global population and are known to occur due to a misguided immune response towards the host, consequently affecting several organs. Importantly, infections are considered key environmental triggers of autoimmunity and contribute to the onset of autoimmune diseases, though this idea remains controversial. In this research, I focus on malaria, a disease caused by *Plasmodium species*, which has been linked to autoimmunity through the induction of anti-self-antibodies, with higher levels of autoantibodies associated with disease severity. By contrast, there is evidence suggesting that autoantibodies play a crucial role in anti-malarial protection, with increased autoantibodies shown to inhibit parasite growth. Thus, autoantibodies play a dual role in protection and pathology. However, this raises a crucial question on whether the induction of autoimmune antibodies during malaria increases predisposition to autoimmune disease later in life.

Herein, anti-citrullinated protein autoantibodies (ACPA) commonly associated with clinical diagnosis of rheumatoid arthritis and their corresponding native peptides were first screened using ELISA in mice infected with the model pathogen *Plasmodium chabaudi*. This approach was chosen to investigate whether *Plasmodium* triggers ACPA production, providing insights into the potential link between *Plasmodium* infections and autoimmunity. Subsequently, the impact of heightened antibody responses to both the native and citrullinated peptides on the development of a model of experimental arthritis in mice was assessed. Extending the findings to humans, serum samples obtained from individuals residing in areas with varying levels of malaria exposure were examined for the presence of autoimmune markers using ELISA and protein microarray assays. This was followed by assessing differential cellular immune phenotypes using flow cytometry.

Interestingly, increased levels of antibody responses to both the native and citrullinated peptides were observed in the *P. chabaudi*-infected mice with levels comparable to those observed in a chronic experimental arthritis model. However, despite the elevated autoantibodies, under the experimental conditions used in

our study, infection-induced autoantibodies did not appear to influence the outcome of either acute or chronic experimental arthritis in mice.

Furthermore, expanding our findings to adults and children residing in malaria-endemic areas, I observed that individuals living in high malaria transmission areas exhibited elevated antibody responses to both the native and citrullinated peptides compared to those in low transmission areas. Interestingly, a similar trend was observed in children, particularly children with uncomplicated and severe malaria who had increased levels of autoantibodies compared to healthy children. In addition, protein microarray data suggested that individuals from a high malaria transmission area had an overall increase in autoimmune reactivity. Notably, higher levels of antibodies against both the native and citrullinated peptides were also associated with increased frequency of atypical B cells ($CD27^{-}$ $CD21^{-}CD11c^{+}$T-bet^{+}) and a reduction in the levels of FOXP3 regulatory T cells.

My research indicates that *Plasmodium* infection leads to a broad spectrum of autoantibodies, including responses to both the native and citrullinated peptides as well as extracellular antigens, mirroring a profile of increased autoantibodies typically observed in autoimmune diseases. Moreover, in this study, I report the presence of elevated antibody responses to these peptides in both *Plasmodium* infected mice and humans residing in areas of high *Plasmodium falciparum* transmission. Notably, the pre-existing autoantibody response to these peptides from a single *Plasmodium* infection episode did not modulate susceptibility to experimental autoimmune arthritis. Thus, the effect and role of chronic exposures to *P. falciparum* infections on the risk of developing autoimmune diseases in people living in endemic areas cannot be ruled out and should be determined.

Table of Contents

Table of Contents

List of Tables

List of Figures

Dedication

This work is dedicated to the memory of my father, John Kimathi, whose love and sacrifices continue to inspire me.

To my husband, David, and my daughter, Naila, thank you for your unwavering support, sacrifices and believe in me. This achievement would not have been possible without your unwavering support.

Acknowledgement

First, I would like to thank the Almighty God for seeing me through the start and completion of this project, for the gift of a sound mind, good health, and provision that made this journey possible.

To my primary supervisor, Paul Garside, thank you for the opportunity to work on such an exciting research project. Your guidance, encouragement, and the freedom you granted me to explore with the project have shaped not only my work but also my confidence as a scientist. I'm grateful for the insightful suggestions with the project, and professional advice. It has been a pleasure to work with such a wonderful mentor and teacher.

To my secondary supervisor, Hannah Scales, thank you for your patience, especially at the start in guiding me through the lab work, animal studies, and flow cytometry. I remember starting with animal work and feeling less confident, but your support enabled me to overcome those challenges, I still never got bitten! Your attention to detail has been truly inspiring, showing me what it takes to be a brilliant scientist.

To my third supervisor, Francis, thank you for your guidance with the human samples and for facilitating such a valuable collaboration, providing me access to these samples was crucial to this work, and I am deeply appreciative of your support.

A special thanks to the lab team at KEMRI-Wellcome, Kilifi, Kenya, particularly Jennifer, and Jedidah, for your help with the human samples. To Ken Mwai, Jacqueline Waeni, and Joy Kabagenyi, I am incredibly grateful for your assistance with navigating the complexity of data analysis for the protein microarray. To John Cole, thank you for your patience and guidance as I worked through the protein array data.

To the entire LIVE lab team, thank you for creating such a collaborative and supportive environment. To my assessors, Jim and Carl, your feedback was

instrumental in shaping the direction of my project thank you for your insight and time.

I would also like to extend my gratitude to the CRF team and the flow cytometry team at KEMRI and Glasgow for their support throughout this journey. To the Wellcome Trust IIB management team, especially Jacqueline and Megan, thank you for making my time as a funded PhD student a smooth and rewarding experience. Your willingness to answer my questions and help with any issues made all the difference.

To my fellow PhD students, Zaydah, Martha, and Lizzie, my time in Glasgow has been so much richer because of you. From our random meetups for “coffee”/ lunch to babysitting my daughter so I could focus on lab work, without a worry I am eternally grateful. In you, I gained not only colleagues but lifelong friends who became my family. Thank you for being my sounding boards when things got tough. I also want to thank Diana, for always being a great sounding board and constantly nudging me to keep writing.

To my family, especially my late father, thank you for your love, support, and the sacrifices you made to facilitate my dreams. I am incredibly grateful that you saw the beginning of this journey, though you are no longer here, I know you would be proud of this milestone.

To my mother thank you for being my pillar of strength, especially during the early stages of my PhD. Your constant encouragement and love have meant more to me than words can express.

To my brothers, and my in-laws, your continued love and support have been deeply felt, and I am grateful to have you in my life.

To my husband, David there are no words to express how grateful I am. Thank you for every single sacrifice, for being my rock, and for holding everything together when I couldn’t. From moving countries with me to stepping up as the main parent for months while I focused on this, you’ve been my unwavering support. I am deeply grateful for standing by my side as I pursued my goals. Your constant love

and understanding have been a source of strength, and I couldn’t have done this without you.

To my daughter, thank you for your endless love and for your adorable curiosity about my work. Your fascination with my animal work taught me how to explain complex science in simple terms to a five-year-old. Explaining science to a five-year-old was sometimes the hardest part, but you made me better at it.

Author's Declaration

I declare that, except where reference is made to the contribution of others, this thesis is the result of my own work and has not been submitted for any other degree at the University of Glasgow or any other institution.

Signature:

Name: Rinter Karimi Kimathi

Definitions/Abbreviations

Abbreviation	Definition
ACPA	Anti-Citrullinated Protein Antibodies
AIDs	Autoimmune Diseases
AEA	Acute Experimental Arthritis
AIRE	Autoimmune Regulator
APC	Antigen Presenting Cell
BAFF	B Cell Activating Factor
CEA	Chronic Experimental Arthritis
CFA	Complete Freund's Adjuvant
CIA	Collagen Induced Arthritis
CIDRα	Cysteine-Rich Interdomain Region 1 Alpha
EBV	Epstein-Barr Virus
ELISA	Enzyme Linked Immunosorbent Assay
DMSO	Dimethyl Sulphoxide
FACs	Fluorescence-Activated Cell Sorting
FIB	Fibrinogen
HRP	Horseradish Peroxidase
ICOS	Inducible T Cell Costimulator
IgG	Immunoglobulin Gamma

IgM	Immunoglobulin Mu
MFI	Mean Fluorescent Intensity
OVA	Ovalbumin
PAD	Peptidylarginine Deaminase
PCR	Polymerase Chain Reaction
PBS	Phosphate Buffered Saline
PD1	Programmed Death Protein 1
RA	Rheumatoid Arthritis
RF	Rheumatoid Factor
REP	a-Enolase
SLE	Systemic Lupus Erythematosus
SIMs	Systems Immunology for Malaria Susceptibility
T-bet+	T-Box Expressed in T Cell
Tfh	T Follicular Helper
Th1	T Helper 1
TNC5 C	Tenascin C5 peptide
Treg	Regulator T Cell
VIM	Vimentin

1 Chapter 1- Introduction

1.1 Chapter overview

The overall aim of this thesis is to investigate the potential link between autoimmunity and *Plasmodium* infections. While malaria, a disease caused by *Plasmodium* species, has been linked to autoimmunity by the induction of anti-self-antibodies, the role of the increased levels of autoantibodies remains unclear.

For instance, elevated levels of autoantibodies have been linked to severe malaria [1-3], including the association of specific autoantibodies with severe malaria anaemia, acute kidney injury and post-discharged mortality [2-4]. However, contrasting findings from a longitudinal study suggest that increased levels of autoantibodies prior to a malaria season correlated with better clinical outcomes [5]. Notably, this study further indicated that these autoantibodies were functional with the ability to inhibit parasite growth *in vitro* [5].

Together, these findings suggest that autoantibodies could play a critical role in immune protection from malaria. However, the association of high levels of autoantibodies with severe malaria is hard to interpret as it could either indicate an epiphenomenon or a role in immunopathology. Nonetheless, their contribution to the development of autoimmune diseases [6-8] and their role in conferring protection in clinical malaria remains poorly understood and debatable.

The association between *Plasmodium* infections and autoimmunity is historical, with classical evidence from experimental mouse models reporting that infection with *P. falciparum* delays the onset of lupus-like autoimmune disease in mice [9]. Additionally, evidence from observational studies conducted in humans at the time also suggested that autoimmune diseases like SLE were relatively uncommon in Nigerian hospitals [10], further supporting the hypothesis that increased parasitic infections may be associated with a lower incidence of autoimmune diseases [10]. Nonetheless, recent evidence has challenged this idea, with reports of similar autoimmune disease incidences in malaria-endemic areas to those reported in the Western world [11-13].

My research, therefore, seeks to gain insights into the potential effect of increased levels of autoantibodies in adults living with endemic exposure to the malaria parasite, *P. falciparum*, and further explore the potential role of these autoantibodies in conferring protection from malaria during the acute phase of infection.

This chapter, therefore, will focus on a detailed literature review on autoimmune disease occurrence, pathogenesis, and prevalence in sub-Saharan Africa. Next, I will introduce the concept of the association between infection and autoimmunity. This will then be followed by a general summary of *Plasmodium* infections and an additional review of the literature on the link between malaria and autoimmunity. Finally, I will outline the research justification and the research hypothesis and define the key objectives of my PhD research.

1.2 Types of autoimmune diseases causes and consequences

Autoimmune diseases affect 5-8% of the world's population [14] and are known to occur due to a misguided immune response against the host, leading to damage in various organs [15,16]. While the underlying causes of autoimmune diseases are multifactorial, several factors such as genetic predisposition, infections, environmental exposures and hormonal factors are known to contribute to the aetiology of autoimmune diseases [17].

Notably, the prevalence of some autoimmune diseases is higher in females than in males, with a 10:1 ratio reported in SLE [18,19]. Additionally, ethnicity is considered a significant factor in the manifestation of autoimmune diseases, with certain conditions reported to occur at higher incidences in particular ethnic groups. For example, SLE is considered to occur more frequently in people of African ancestry compared to those of European ancestry [20,21].

Another important feature of autoimmune disease is the presence of autoantibodies, which are antibodies targeting self-antigens and often appearing long before the clinical manifestations of disease [22]. Autoantibodies serve not only as diagnostic markers but are also essential for disease classification and correlate with disease severity [23,24].

More than 80 different autoimmune diseases (AIDs) have been identified [25] and are further categorised depending on whether these self-reactive antibodies are directed at an individual organ (organ specific) or the antibodies are directed against a wide range of autoantigens that act throughout the body (systemic) [16,26]. For example, organ-specific autoimmune diseases such as autoimmune thyroid disease usually result explicitly in attacks on the thyroid gland [27]. On the other hand, systemic autoimmune diseases are characterised by immune dysregulation and immune-mediated damage of multiple organs [28] and include AIDs such as SLE, Sjögren's syndrome, autoimmune haemolytic anaemia, multiple sclerosis, and rheumatoid arthritis.

While the aetiology of AIDs is not clear, they are thought to occur through several phases, involving first the initiation [29]; at this phase, no clinical symptoms are

exhibited, and certain factors, such as genetic traits such as single gene mutations (e.g., AIRE mutation) [30] and environmental triggers such as Epstein Barr virus and smoking [31] are considered to trigger their onset.

Following initiation, the next phase occurs through self-perpetuated inflammation and tissue damage [29]; this involves a continuous cycle in which the immune system mistakenly attacks the host antigens due to the occurrence of a dysregulated immune system being triggered, initially in the secondary lymphoid organs and then spreading to areas that have an abundance of the specific autoantigen [32], most patients present with clinical disease in this second phase.

The last phase, which is resolution, occurs through the activation of inhibitory pathways and a regulatory mechanism that helps limit the effector response; at this phase, most patients tend to suffer from relapse and remitting disease as a consequence of a defect in maintaining a balance between the effector pathogenic responses and regulation [33]. However, failure of the regulatory mechanism to limit the pathogenic responses may result in chronic autoimmune disease [34].

1.3 Mechanisms of immune tolerance

To avoid the occurrence of autoimmune disease, the immune system maintains a delicate balance between effective immune responses towards foreign antigens and immune tolerance towards self [35]. This complex process is mediated by two mechanisms: central or peripheral [36], with the central mechanism initiated in the thymus and bone marrow for T and B cells, respectively while the peripheral tolerance occurs in the circulation. Furthermore, the loss of immune regulation through this mechanism results in the presence of circulating autoreactive lymphocytes [35]. Here, I will detail the immune mechanism for both T and B cells.

1.3.1 T cell immune tolerance

Central tolerance for T cells occurs in the thymus, where the development of T cell receptors (TCRs) involves the random rearrangement of V (Variable), D (Diversity), and J (Joining) genes [37], a process that is inherently error-prone, often resulting in receptors that recognise self-antigen. While receptor diversity is key

in preventing infections as the wide range of foreign peptide recognition depends on the high receptor diversity of the patrolling immune cells, this mechanism also increases the risk of producing immune cell receptors that react towards the host's own peptides consequently resulting in autoimmune diseases [35,36,38]. Therefore, to prevent potential damage to the host, the immune system has evolved mechanisms to eliminate self-reactive lymphocytes within central lymphoid organs [38–40].

T cells undergo positive and negative selection in the thymus as part of this central tolerance [39]. This process has recently been reviewed [38,39]: and occurs when T cell precursors migrate to the thymus from the bone marrow and undergo differentiation and maturation before selection [38]. This selection process occurs when thymocytes encounter self-peptides presented by major histocompatibility complex (MHC) molecules, where the fate of thymocytes largely depends on the degree of complementarity between their T-cell receptors (TCR) and the MHC molecules presenting self-peptides. Thymocytes with TCRs that do not complement the self-MHC/peptide complex then undergo "death by neglect," a form of spontaneous apoptosis [41].

While thymocytes whose TCRs are fully complementary to the MHC/peptide complex are negatively selected through "clonal deletion" or "central tolerance," where they die by antigen-induced apoptosis [42]. Conversely, thymocytes with TCRs that recognise MHC molecules but not the cognate peptides are positively selected, surviving and continuing development.

Furthermore, the MHC class determines their differentiation with the recognition of MHC class I, resulting in CD8 lineage differentiation [43], while recognition of MHC class II results in CD4+ lineage differentiation [44,45].

Notably, this process is still imperfect, given a fraction of autoreactive T cells escape central tolerance and enter the periphery. Peripheral tolerance mechanisms provide additional ways of eliminating autoreactive lymphocytes through mechanisms such as anergy, also referred to as hypo-responsiveness, where T cells that recognise self-antigens in the absence of proper costimulatory signals becoming non-functional [46]. Peripheral deletion is another mechanism,

where autoreactive T cells are eliminated if they encounter their specific antigen on inappropriate cells that either do not provide appropriate signals for T cell activation or are not APCs [43]. In addition, CD4+CD25^{+}FOXP3^{+} T regulatory (Treg) cells are essential in keeping autoreactive T cells in check and preventing their activation and autoreactive proliferation [47] by dampening autoreactive T cells that have evaded central elimination, as well as T cells that recognise self-antigens due to molecular mimicry during infections [48].

1.3.2 B cell immune tolerance

B cells play a central role in initiating the onset of multiple autoimmune diseases, including rheumatoid arthritis and SLE [49]. The presence of autoantibodies and the association between these autoantibodies and the pathogenesis of B cell-mediated autoimmune diseases highlights the crucial role B cell tolerance plays in preventing autoimmunity [50].

After immature B cells mature in the bone marrow, they express unique and randomly generated B cell receptors (BCRs). This process is error-prone and results in self-reactive naive B cells, potentially posing a risk of initiating an autoimmune response. In order to prevent this, central tolerance mechanisms are triggered and primarily involve processes such as clonal deletion, anergy, and BCR editing [36].

Remarkably, if the BCR is bound to the self-antigen with high affinity, this B cell undergoes 'clonal deletion' [51] and is removed from the immune repertoire. If the affinity is lower, the B cell might be inactivated or become anergic but not deleted [50,52].

Moreover, approximately 20 per cent of immature B cells that are found to carry a self-reactive receptor will undergo receptor editing to change their antigen-binding specificity, sparing them from deletion. If editing does not occur, these autoreactive B cells may undergo apoptosis [53]. Thus, through the central tolerance mechanisms, the frequency and functionality of autoreactive B cells are reduced.

In the peripheral tissues, a subset of B cells referred to as regulatory B (Breg) cells are responsible for effectively maintaining peripheral tolerance by curtailing

ongoing pathological immune responses and restoring immune homeostasis [54]. This is supported by evidence from multiple studies that consistently show Breg cells can suppress pathology caused by detrimental inflammatory responses in the context of autoimmunity [55].

1.4 Pathogenesis of autoimmune diseases

1.4.1 Role of autoantibodies in autoimmune diseases

Autoantibodies are frequently detected in healthy individuals, at a prevalence ranging from 0.3% to 4.6% and up to 10% cumulatively [56]. Notably, the prevalence of autoantibodies increases with age, plateauing around adolescence [57]. While several autoantibodies, such as anti-nuclear and anti-smooth muscle antibodies (ANA and ASMA, respectively), are common in healthy adults [58]. Interestingly, natural autoantibody responses, mainly IgM, have been suggested to play a role in immunological homeostasis and protect against pathogens [59].

While it is well known that autoantibodies can contribute to autoimmune diseases, their general presence is not predictive of a higher risk of developing autoimmune disease[24,60,61]. Therefore, the relationship between the presence of autoantibodies in healthy individuals and the development of disease remains complex and not fully understood.

Notably, autoantibodies in the serum serve as a crucial indicator of the dysregulation of either central or peripheral tolerance mechanisms [50], where the dysregulation allows for the maturation of B cells, producing autoantibodies and their differentiation into plasma cells that secrete these antibodies [62]. At the same time, autoantibodies are established as significant drivers of autoimmune diseases, with multiple mechanisms already established on how they contribute to pathology [63]. For example, pathogenic autoantibodies may exert direct toxic effects through receptor stimulation, blocking neural transmission, altered signalling, microthrombosis, cell lysis, neutrophil activation and inflammation [63].

Importantly, several factors are known to contribute to the pathogenicity of autoantibodies. For example, studies in mouse models suggest that different IgG subclasses have varying degrees of pathogenic potential, with IgG2a and IgG2b

being the most pathogenic in lupus nephritis owing to their ability to activate Fc receptors and complement, respectively [64].

Autoantibody specificity is another crucial contributor to pathogenicity; in particular, autoantibodies targeting cell surface or extracellular antigens tend to be more pathogenic [65]. Extracellular autoantibodies, binding to membrane receptors and secreted molecules, are directly pathogenic, disrupting normal protein function and contributing to disease onset shortly before diagnosis [65]. In contrast, intracellular autoantibodies, which typically do not directly access their targets, serve mainly as biomarkers of abnormal immune activity [66]. Thus, intracellular autoantibodies can be detected for years or even decades before clinical symptoms arise, indicating a prolonged subclinical phase that may lead to irreversible tissue damage [66].

Additionally, the type of autoantibody may also impact treatment. For instance, autoimmune diseases that are driven by extracellular autoantibodies can often be treated by targeted therapies such as rituximab, while autoimmune conditions that involve intracellular autoantibodies may be more challenging to treat because of the involvement of T-cell-mediated damage and other components of the immune system [65]. Lastly, the glycosylation pattern of IgG autoantibodies can influence their pathogenicity, with galactosyl glycoforms being more pathogenic in some cases [67].

Given the wide array of autoimmune diseases, in this chapter I will focus on the pathogenesis of rheumatoid arthritis (RA) and systemic lupus erythematosus (SLE), as they both exemplify the complex interplay of autoantibodies and specific immune responses likely to occur as a result of a dysregulated immune system and more importantly, they are also known to occur as a result of the interplay between infections and genetics.

1.4.2 Rheumatoid arthritis

Rheumatoid arthritis (RA) is a multifactorial autoimmune disease characterised by chronic inflammation and joint destruction [68]. The aetiology of RA involves genetic predisposition, environmental agents [69–72], and dysregulation of both the innate and adaptive immune responses [73]. Other aetiological factors, such as smoking,

industrial pollutants and changes in the microbiota, can also affect the course of RA onset [74].

RA affects approximately 58 million people globally [75], with factors such as age and sex influencing its prevalence. Notably, women aged over 60 years are six times more likely to be affected than younger women [76]. Furthermore, research suggests that the genetic risk for RA accounts for about 15% of cases [71] and is particularly associated with specific alleles on chromosome 6, such as HLA-DR1 and HLA-DR4.

Environmental factors like viral infections (e.g. Epstein-Barr virus and parvovirus B19); tobacco use [77]; and other nonspecific triggers such as trauma and infections also contribute to RA development. Smoking increases the risk of developing anti-citrullinated protein autoantibodies (ACPA) [78,79], while Human Leukocyte Antigen Shared Epitope (HLA-SE), is more closely linked to the progression toward inflammatory arthritis [80]. Anti-citrullinated protein antibodies (ACPA) are autoantibodies that target a non-essential amino acid (citrulline) generated after arginine is post-translationally modified by peptidylarginine deiminase (PAD) enzymes [81]. ACPA can be detected years before clinical signs of RA and serve as specific early detection biomarkers [82].

The oral infectious agent *Porphyromonas gingivalis* is another significant contributor to RA [83] as it induces citrullination by expressing its own PAD enzymes, generating neo-antigens, that activate T cells resulting in the ACPA generation [84]. Moreover, *P. gingivalis* mediates inflammation through IL-17 signalling, thereby promoting the erosion of bone and cartilage [85,86]. This is evidenced by higher frequencies of *P. gingivalis* observed in the oral microbiomes of ACPA-positive individuals, suggesting its crucial role in RA onset [87]. Other infectious agents, such as *Aggregatibacter actinomycetemcomitans,* are known to induce citrullination of a wider array of antigens through the release of toxins that result in PAD activation; these pathogens have been isolated in RA patients and are considered a contributor to RA through these mechanisms [88]. In contrast, *Mycobacterium tuberculosis* has been shown to trigger the production of ACPA [89]. However, this response occurs against both the native and citrullinated peptides and has not been directly linked to the development of RA [90].

Although smoking and periodontitis are both associated with low levels of ACPA, the pathogenesis of RA occurs in the presence of both HLA-SE and ACPA, leading to more severe disease with more joint destruction [83,91]. Notably, ACPAs can activate myeloid cells and intensify joint inflammation, particularly when combined with other pathogenic antibodies or additional triggers [92,93].

The earliest sign of immune dysregulation in RA is often the presence of circulating ACPAs, which are frequently associated with elevated cytokine levels [91] and can be detected several years prior to the appearance of joint symptoms, suggesting that the initial pathogenic mechanisms are likely to have occurred outside the synovial compartment.

Importantly, the presence of both Rheumatoid Factor (RF) and ACPA [94] is considered a hallmark feature of RA, with ACPA considered highly specific to RA and is often associated with more aggressive disease [95], evidenced by its correlation with more joint and bone damage [96]. Moreover, several factors contribute to ACPA's pathogenicity, such as they are primarily of IgG and IgA isotypes and, therefore, have undergone extensive affinity maturation in germinal centres, resulting in high-affinity, highly N-glycosylated antibodies [97,98]. In contrast, RF are mainly of the IgM isotype and have undergone a simpler maturation process and, therefore, have limited glycosylation, impacting their pathogenic role.

Together, several factors, including genetic susceptibility, environmental triggers, and immune responses, possibly explain the complex mechanism underlying the pathogenesis of RA.

1.4.3 Detection of anti-citrullinated protein antibodies (ACPA) in Rheumatoid arthritis

The diagnostic role of ACPA is well established, with several detection assays developed and widely used in the clinical diagnosis of RA, particularly the first commercial detection methods was initially based on the detection of a single cyclic citrullinated peptides (CCP1) produced by filaggrin [99]. Subsequent generations of these assays, such as CCP2 and CCP3, have been developed and are

shown to significantly improve both the sensitivity and specificity of RA diagnosis [100,101]. More recently, assays targeting non-cyclic citrullinated peptides (ACPA) have also been developed, [102–104] providing a broader diagnostic accuracy by detecting a wider spectrum of ACPA.

Intriguingly, while citrullinated peptides have been vital in RA diagnostics, a recent study investigating rheumatoid arthritis-associated interstitial lung disease (RA-ILD) demonstrates that the inclusion of anti-native protein antibodies, alongside ACPAs, improves the prediction of RA-ILD [105]. While these findings need validation, they underscore the importance of incorporating both the native and citrullinated peptides to improve the diagnostic accuracy and clinical outcome predictions in RA.

1.4.4 Pathogenies of SLE

SLE primarily affects women and occurs as a result of the immune system mistakenly targeting nearly all organs, further resulting in symptoms such as arthritis, skin issues, blood disorders, and kidney damage [106]. Notably, a higher prevalence of SLE in the USA is reported in the African, Asian, Hispanic and Native American populations, where higher mortalities have also been reported [107,108].

The pathogenesis of SLE is complex and multifactorial, characterised by genetic predisposition [109], immune dysregulation [110] and various environmental triggers [110,111]. Furthermore, autoantibodies, particularly anti-double stranded DNA (dsDNA), are a hallmark of SLE and may indicate an ongoing pathogenic process [94]. Interestingly, the complexity of SLE is further exemplified by the wide array of autoantibodies detected in individuals with SLE, with over 200 distinct types identified, targeting a wide variety of molecules, such as nucleic acids, lipids, native proteins or proteins with post-translation modifications, organelles, different cell types, plasma proteins, and tissues [112].

Recent discoveries have also greatly improved our understanding of SLE pathogenesis [113,114]. For instance, more than 100 genetic variants associated with immune signalling pathways have been identified using genome-wide association studies [115]. Among these, signal transducer and activator of transcription 4 (STAT4) [116], which encodes for a transcription factor involved in the interferon signalling

pathway, has the strongest association with SLE. Additionally, the apolipoprotein L1 gene [117] is common in people of African ancestry and may increase predisposition to more severe end-organ manifestations.

Moreover, the pathogenesis of SLE reflects a dysregulation of both the innate and adaptive immune responses, which are further characterised by the involvement of several immune cell types [118]. Central to this, dysregulation is the impaired clearance of cell debris resulting in a loss of self-tolerance, and dysregulated type 1 interferon pathways further contribute to chronic inflammation [118].

Renal injury is the most common and serious form of tissue damage in SLE, and it often involves immune-complex deposition, inflammation and scarring in the kidneys [119]. Moreover, apoptosis has been indicated in the pathogenies of SLE via the release of autoantigens in apoptotic blebs [120,121], which serve as a source of nucleic acids, [122] resulting in the activation of immune cells. Thus, these autoantigens can break immune tolerance, inducing autoimmunity by priming autoreactive T cells [123]. Notably, specific autoantibodies, including anti-dsDNA, anti-blood cell, and anti-phospholipid antibodies, are directly related to SLE injuries, including nephritis [124].

1.5 Prevalence of autoimmune diseases in sub-Saharan Africa

Although once considered rare in Africa [13], autoimmune diseases are now increasingly reported at incidences similar to those in Western countries [11,12]. For instance, the prevalence estimates of RA in Africa from systematic analyses conducted in 2010 reported an RA estimate of 0.42% [125,126], which was comparable to that in Southern Europe of 0.33% [127]. Moreover, recent evidence based on an analysis of studies conducted between 1975 and 2014 estimates RA to occur at a prevalence ranging from 0.06 to 3.4% (Figure 1-1) [128].

SLE, another autoimmune disease that's been understudied in Africa, was reported to occur at a prevalence of 12.2 per 100,000 among South African blacks [20], which is comparable to the incidence of SLE in Brazil is 8.7 per 100,000.

Notably, while there is emerging evidence on RA and SLE prevalence, there is still limited data on other autoimmune diseases [129], which could mainly be attributed to challenges in the diagnosis and treatment, consequently resulting in significant underreporting [125]. For example, extensive underreporting has been noted in hospital-based versus population-based studies for RA in sub-Saharan Africa, with a 6 to 10-fold reduction in hospital reports [125]. Thus, although unsurprising, the true incidence of autoimmune disease in sub-Saharan Africa may be masked and could be considerably higher than currently inferred. Given this, there is an urgent need for increased improved diagnostic capabilities and awareness of autoimmune diseases in Africa [129].

Another important consideration is the selective pressure exerted by the *Plasmodium* parasite, which not only shaped human genes related to immune responses [130] but also resulted in the presence of several shared genetic variants between malaria and SLE [7,131]. Therefore, it remains unclear whether infections caused by the *Plasmodium* parasite can trigger autoimmune diseases in individuals with autoimmune-susceptible genes. Particularly given that *Plasmodium* infections are known to induce the production of autoantibodies commonly associated with autoimmune conditions [8,132,133]. Thus, the need for studies investigating the potential link between *Plasmodium* induced autoantibodies and autoimmune conditions like the current study.

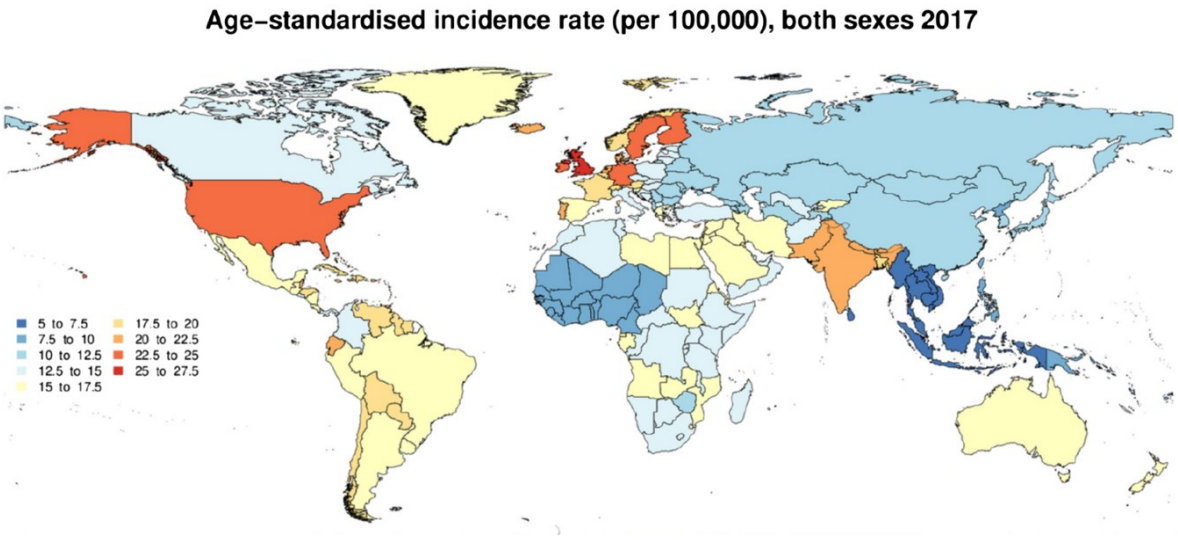

Figure 1-1: Age-standardised prevalence rate of RA (per 100,000), both sexes, 2017 by country.

Reproduced with permission from the Global Burden of Disease Study (Institute for Health Metrics and Evaluation, 2017), published in the Annals of the Rheumatic Diseases. University of Glasgow, License #5874841184215. https://doi.org/10.1136/annrheumdis-2019-215920 [75]

1.6 Infections and autoimmunity

A wide array of infections have been linked to the induction and pathogenesis of autoimmune disease as outlined in (Figure 1-2) [17,134-137]. However, it is well known that infections alone are insufficient to cause autoimmunity and that a combination of certain genetic traits and hormonal and environmental factors is required [138,139]. Additionally, it is worth noting that the "high burden of infections" from childhood, rather than a single pathogen, may be responsible for the induction of autoimmune diseases [136].

Several mechanisms that contribute to an autoreactive immune response, including molecular mimicry, bystander activation and epitope spreading, have been elucidated [136,138]. For example, Parvovirus B19 and Epstein-Barr virus have been associated with various autoimmune diseases through mechanisms such as molecular mimicry, bystander activation and others [140,141].

Notably, during inflammatory infectious such as malaria and COVID-19, there is an association between the clinical manifestation of the disease and the appearance of autoantibodies, suggesting that the presence of autoantibodies in such patients might contribute to pathology [6].

In the next section, I will focus my discussion on the link between *Plasmodium* infections and autoimmunity, which is the subject of my thesis.

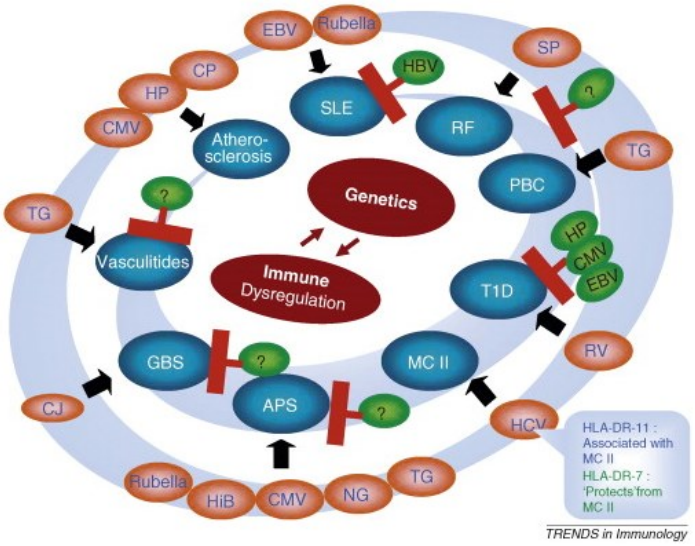

Figure 1-2: Illustration of the interplay of infections and autoimmune diseases.

This diagram illustrates how certain infections are associated with the induction of autoimmune diseases (orange circles), while other infections are known to ameliorate/prevent the development of autoimmune diseases (green circles). Abbreviations: CJ, *Campylobacter jejuni*; CP, *Chlamydia pneumoniae*; HiB, *Haemophilus influenzae*; HP, *Helicobacter pylori*; NG, *Neisseria gonorrhoeae*; SP, *Streptococcus pyogenes*; RV, Rotavirus; TG, *Toxoplasma gondii*.

(Figure reproduced [136]**)**

1.7 Overview of *Plasmodium* infections

In this and the following sections, I will discuss the literature on *Plasmodium* infections and further provide evidence for an association between the complex interplay between *Plasmodium i*nfections and autoimmunity.

In the unexposed individual, malaria is a life-threatening infectious disease caused by the protozoan *Plasmodium* parasite. Despite the disease being curable and preventable, the incidence of *Plasmodium* infections worldwide is estimated at 249 million cases, with 94% occurring in sub-Saharan Africa and approximately 608,000 deaths reported annually [142]. Notably, the global incidence of malaria has declined by 37% between 2000 and 2015 [143]; however, progress in disease control has recently stalled due to several factors such as increased insecticide resistance in vector populations, the emergence of artemisinin-resistant parasites, and

challenges related to inadequate funding and access to quality care [144,145]. Nonetheless, with the recent rollout of the first to be approved malaria vaccine, RTS, S, and now the approval for R21/Matrix M, there is renewed hope that preventative vaccination will reduce malaria mortality by 30% [146]. Nonetheless, none of these vaccines have achieved the WHO efficacy target of 90%, and their effectiveness at improving control will also depend on many other factors, including the level of funding and implementation programmes.

More than 200 *Plasmodium* species are known to exist, but only five cause human malaria: *P. falciparum*, *P. vivax*, *P. malariae*, *P. ovale*, and *P. knowlesi* [147]. Among these, *P. falciparum* and *P. vivax* pose the most significant public health threats, with *P. falciparum* being the most prevalent in sub-Saharan Africa and the deadliest species, accounting for nearly all malaria mortality [148]. In contrast, *P. vivax* is associated with less severe disease and has the widest geographical distribution [149]. It is also worth noting that prior to the 1970s, *P. falciparum* distribution was prevalent worldwide [150]; however, through intensive insecticide spraying and environmental engineering, it has been eradicated in Europe, which currently only experiences imported cases of malaria [151].

1.8 *Plasmodium* life cycle

All five *Plasmodium* species that infect humans and mammals are transmitted by mosquitoes of the genus *Anopheles*, whereas the transmission of parasites infecting birds and reptiles is associated with a different mosquito genus [152]. *Plasmodium* species life cycle is particularly complex, as the parasite alternates between two different hosts and involves multiple stages (Figure 1-3).

The pre-erythrocytic liver stage, which is the first stage in the human host, begins when an infected female mosquito injects an average of 10-100 sporozoites under the dermis during a blood meal, along with saliva that has anticoagulant properties [153,154]. The sporozoites are infective and motile at this stage, and this allows approximately 70% of the sporozoites to enter the bloodstream and rapidly migrate to the liver, invading the hepatocytes [154,155], with the remaining 30% invading the lymphatic vessels [156].

Once in the liver, the sporozoite invades the hepatocytes by traversing through multiple hepatocytes and ultimately transitioning from an invasive to a productive stage [157,158] through the formation of a parasitophorous vacuole. Notably, this marks the first phase of asexual reproduction known as schizogony, which produces thousands of merozoites from a single sporozoite [159].

The released merozoites then invade RBC within 30-70 seconds, [160] producing 8-64 merozoites within 24-72 hours, depending upon the *Plasmodium* species [161]. At the same time, some merozoites undergo gametocytogenesis, producing male and female gametocytes that circulate in the blood, thus increasing the chances of transmission when the next mosquito takes a blood meal [162]. Male gametocytes are then activated, leading to cell division and the production of eight motile gametes within 15 minutes [161]. Following activation, a female gametocyte forms a macrogamete, while male gametocytes produce eight motile microgametes. These male and female gametes then fertilise to form the zygote that elongates to become a motile ookinete that penetrates the midgut wall to form an oocyst within 24 hours.

Hundreds to thousands of sporozoites then develop within each oocyst over the next 10-15 days [163]. The oocyst eventually bursts, releasing the sporozoites into the mosquito's body (haemocoel) [164,165], where the circulating haemolymph carries them to the salivary glands and awaits transmission during the next blood meal [166].

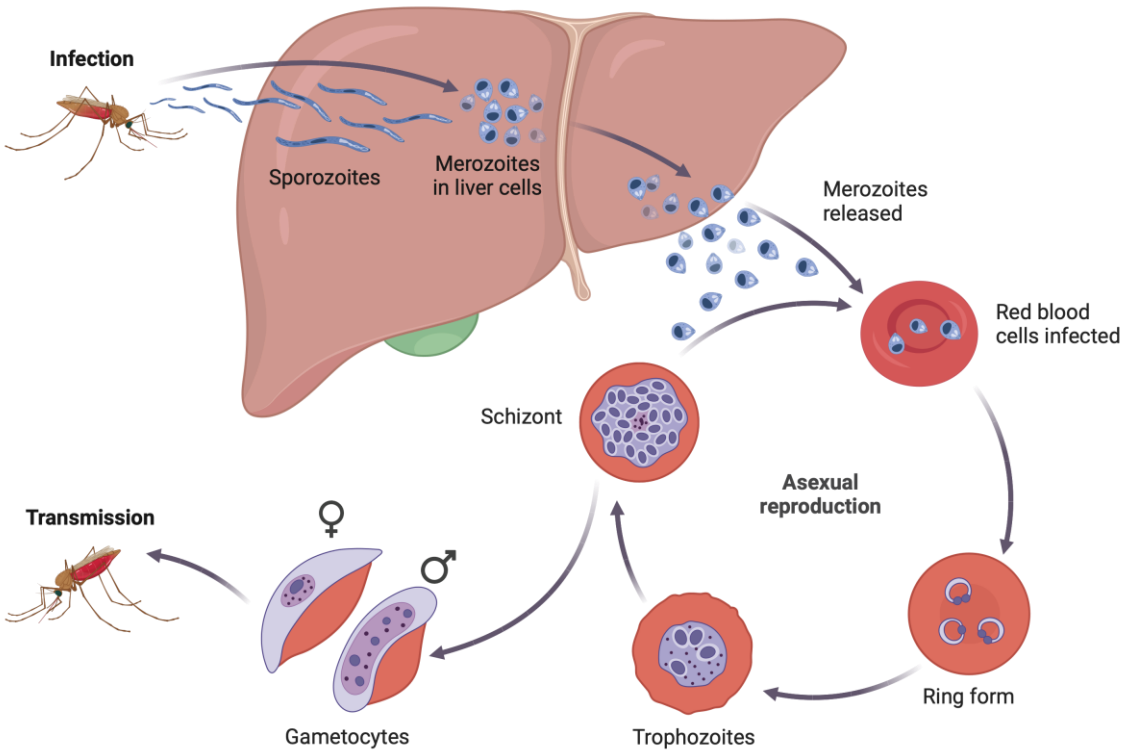

Figure 1-3: The life cycle of *Plasmodium* parasite (Image retrieved from Biorender)

1.9 Clinical manifestations of *Plasmodium falciparum*

The spectrum of clinical outcomes following *Plasmodium falciparum* exposure ranges from asymptomatic infection, mild, self-limiting fever and flu-like symptoms to severe complications, including cerebral malaria and severe anaemia [167]. While uncomplicated malaria is characterised by the presence of fever, chills, headache, myalgia, nausea, vomiting, fatigue, anaemia and jaundice in the absence of organ damage [168]. These cases, however, can progress quickly to more severe complications such as cerebral malaria, renal impairment and pulmonary issues [169]. Importantly, the wide spectrum of clinical outcomes is influenced by several factors, including the age and history of exposure to the parasite for the host and variation of adhesive molecules expressed on blood-stage parasite [170,171]. Our understanding of these complex interactions is crucial for predicting clinical outcomes and developing effective interventions [172].

1.10 Immunity to malaria

Immunity to *Plasmodium falciparum* requires a complex interplay between innate and adaptive immunity [173]. The oft-cited classical study by Cohen et al [174] provided evidence of the crucial role of antibodies in controlling parasitaemia and malaria symptoms. In this study, antibodies from immune adults were transferred to children suffering from severe malaria, resulting in a significant reduction in parasitaemia and alleviation of malaria symptoms. While this study provides strong evidence for humoral immunity in malaria infection, our understanding of immunity to *P. falciparum* remains limited due to the parasite's complex life cycle, antigen diversity, and the fact that immunity is often acquired over time and depends on the frequency of exposure [175].

1.11 Adaptive immune response

1.11.1 Naturally acquired immunity (NAI)

Additional evidence for naturally acquired immunity (NAI) was demonstrated through studies conducted in two regions of Java in Indonesia with varying malaria intensity, where immunity was closely linked to ongoing exposure to the parasite [176].

Known factors influencing NAI development include the intensity of *Plasmodium* parasite transmission, age, frequency of exposure, host genetic factors, and parasite genetic diversity [176]. Furthermore, the frequency of exposure to *Plasmodium spp*. is also essential for NAI development, as repeated infections can gradually increase immunity [177,178]. Genetic factors have also been shown to affect susceptibility and variability in immune responses across human populations [179]. In addition, reduced parasite diversity can also facilitate more rapid NAI development. Together, all these factors contribute to the dynamics of NAI.

1.11.2 Acquisition and maintenance of humoral immune response

Antibodies play a vital role in conferring protection against malaria; this was first demonstrated through the passive transfer of immunoglobulin G (IgG) from immune adults to children with severe malaria, resulting in significantly reduced

disease severity [174]. Several immuno-epidemiological studies have supported this key finding, linking antibodies to protection from clinical malaria episodes [177].

Importantly, malaria-specific antibodies mediate their function and limit the growth of blood-stage parasites through various mechanisms, including blocking erythrocyte invasion [180,181] opsonising infected erythrocytes via phagocytosis [180,182,183], growth inhibition, [184], antibody-dependent cellular killing [185], and promoting complement-mediated lysis[186].

Notably, immuno-epidemiological studies also indicate that antibody responses to malaria are short-lived [187,188], quickly diminishing without ongoing parasite exposure. For instance, following an acute malaria episode, antibodies specific to *Plasmodium* antigens can decline to very low or undetectable levels within months or even weeks despite an initially strong response [189]. Moreover, children living in areas of intense transmission have increased antibodies to numerous *P. falciparum* antigens [190,191], but the breadth and intensity of this response decreases during dry seasons when there is little malaria transmission. Thus, indicating that the robust antibody response observed during peak transmission may be driven by short-lived plasma cells.

Furthermore, the parasite antigens directly interact with B cells via the cysteine-rich interdomain region 1 alpha (CIDRα), impacting the host B cell activating factor (BAFF), thus hindering the development of long-lived memory B cells [192]. While studies emphasise the significance of antigenic variation and allelic diversity in the immune response to *Plasmodium falciparum* [193] there is also evidence suggesting that chronic exposure to the parasite induces alterations in B cell responses that might be responsible for the immune evasion mechanisms of *P. falciparum* [194].

1.11.3 B cells in *P. falciparum* infections

In the acute phase of malaria infections, naive B cells are stimulated and undergo differentiation, leading to an increase in memory B cells [195] and atypical B cells [196]. However, the resulting polyclonal humoral response rarely reaches protective threshold levels, and it is only after repeated exposures to the parasite that individuals in malaria-endemic areas develop protective immunity [176].

Several factors contribute to this suboptimal response, including the preferential activation of Th1-polarised Tfh cells, which are less effective in assisting B cells, thereby leading to inadequate antibody production [197,198]. Atypical memory B cells, which expand during chronic malaria exposure, exhibit diminished B cell receptor signalling and reduced effector function [199]. Additionally, elevated plasma BAFF (B-cell activating factor) levels during acute malaria may influence B-cell differentiation and the maintenance of antibody levels [200].

Moreover, certain parasite antigens have been identified to be critical for the induction of hypergammaglobulinemia during malaria infection; for example, the C1DR1a domain of the *Plasmodium falciparum* erythrocyte membrane protein 1 (PfEMP1) [201,202], a major blood-stage antigen, and a significant virulence factor of the parasite, is released in the bloodstream and preferentially activates and expands memory B cells (MBCs).

Thus, the associations between hypergammaglobulinemia and autoimmunity in malaria, as well as the appearance of autoantibodies characteristic of autoimmune disease, support the idea that some parasite antigens may cross-react [203] with human autoantigens, resulting in cross-reactive immune responses. For example, serum from patients with systemic lupus erythematosus (SLE) and no history of exposure to *Plasmodium* infection, was found to react with *P. falciparum* antigens [204], suggesting a potential risk for autoimmune complications.

Therefore, it is necessary to characterise antigen-specific B cell responses against malaria, which may give rise to targets for vaccine or therapeutic design that will optimise efficacy and avoid autoimmune responses.

1.11.4 Atypical B cell production in *Plasmodium* infections

Atypical B cells are associated with autoimmune diseases, with their depletion correlated with reduced autoantibody levels [205]. However, given recent evidence, these cells are now considered part of normal immune responses to infection and vaccination [206]. Moreover, atypical B cells are a common phenomenon in malaria infections [196], with higher levels associated with increased parasite exposure [207] and broader antibody responses and function [208].

Unlike classical memory B cells, atypical B cells lack expression of CD21 and CD27 and have increased expression of CD11c, Tbet, CXCR3, and inhibitory markers such as FCRL3 and FCRL5 [209]. This altered expression leads to reduced B cell receptor signalling and decreased responsiveness, resulting in a diminished capacity to become antibody-secreting cells [210,211]. Consequently, atypical B cells are often considered exhausted or unresponsive to stimulation.

Interestingly, conflicting evidence also suggests that atypical B cells from individuals exposed to *P. falciparum* exhibit a strong response to high-affinity membrane-associated antigens while displaying a markedly reduced response to low-affinity antigens. Thus, limiting the activation of atypical B cells by low-affinity antigens, such as autoantigens [212].

Notably, recent evidence sheds light and provides further clarification through the indication that atypical B cells (CD21-CD27-) are present as three distinct subsets with different functions[213]. One subset is anergic (non-responsive), with a high activation threshold, high CD11c expression (+++), and no CD86 expression (-), similar to atypical B cells in SLE. Another subset develops from memory B cells and rapidly differentiates into antibody-secreting cells upon stimulation. This activated subset exhibits high somatic hypermutation (+++), minimal CD11c expression (+), and no CD86 expression (-). The third subset functions as an antigen-presenting subset, requiring additional signals to mature into antibody-secreting cells. It upregulates HLA and CD86, has high somatic hypermutation (+++), and expresses CD11c (+++) and CD86 (+++) [213]. These findings, therefore, clarify the diverse roles of atypical B cells in immune responses and show that their composition adapts to changing levels of pathogen exposure [213].

1.11.5 CD4+ T cells in *P. falciparum* infections

The role of CD4+ T cells in clinical malaria is well-established in both mouse models and human malaria [214]. During malaria infection, the immune response is orchestrated by different subsets of CD4+ T cells, each playing distinct roles against the *Plasmodium* parasite [215]. $CD4^+$ T Helper 1 (Th1) cells, for example, promote the production of interferon-gamma (IFNγ), which is critical for activating macrophages [216] and enhancing CD8+ T cell cytotoxicity [217] necessary

for the direct elimination of *Plasmodium*-infected erythrocytes in the bloodstream.

Mature Tfh cells are characterised by the expression of the transcription factors BCL-6, CXCR5 and PD1 [218], which, upon infection, promote the maturation of *Plasmodium*-specific germinal centres [218]. Thus, the ability of T follicular helper (Tfh) cells to generate a robust antibody response and establish long-term immunity is crucial for protection from reinfection, particularly in regions where repeated exposure to malaria is common [219].

Moreover, individuals in malaria-endemic areas consistently show an expansion of Treg populations during blood-stage malaria, with lower Treg frequencies linked to lower parasite loads and more favourable disease outcomes [215,220]. Importantly, Tregs are vital in the malaria immune responses as they maintain immunologic tolerance and prevent hyper-inflammatory responses that can lead to tissue damage [221].

1.12 Possible link between *Plasmodium* infections and autoimmunity

While the presence of autoantibodies following *P. falciparum* infection is known [1,5,6,8] ; these autoantibodies have varied specificity, with some autoantibodies targeting smooth muscle, single-stranded DNA, double-stranded DNA, ribonucleoproteins (RNPs), as well as other autoantibodies targeting the brain antigens such as dendrite [222], Immunoglobulin E Autoantibody to 14-3-3 ε Protein [132], and RBC [1,223].

Notably, unlike some viral and bacterial diseases, where a single infection exposure confers lifelong protection, immunity to malaria is slow to acquire and develops with repeated exposure to the parasite [176]. The slow acquisition of immunity has been associated with antigenic variation of the parasite [224] and alterations in the B cell compartment [192]. Therefore, the frequent repeat *P. falciparum* infections are known to gravely dysregulate the immune system, with B cells overactivation and the production of autoantibodies, particularly with evidence indicating that T-bet+ B cells, are linked to autoantibodies against phosphatidylserine on erythrocytes [3,4].

In addition to the B cell dysfunction, *Plasmodium* infection also impairs dendritic cell function, contributing to immune dysregulation [225]. For example, *in vitro* studies using monocyte-derived DCs, when exposed to *P. falciparum*-infected red blood cells, showed a marked decrease in the expression of crucial maturation markers such as CD40, CD80, CD86, and CD83 [226]. In addition, both *in vitro* and *in vivo* studies have reported the presence of reduced expression of MHC on DC exposed to infected red blood cells [227]. Furthermore, there is evidence of reduced expression of HLA-DR and CD86 on DCs from malaria-infected children, which consequently affects their ability to process and present antigens [228,229].

While neutrophils are essential for pathogen clearance during severe malaria, the inflammatory response is known to lead to excessive tissue damage due to the release of toxic granules and ROS [230]. In addition, neutrophils produce Neutrophil Extracellular Traps (NETs) [231] that play a critical role in limiting *Plasmodium* infections; however, they are also known to contribute to inflammation and tissue damage [231,232]. Notably, NETs and antinuclear antibodies have been observed in *P. falciparum*-infected children, suggesting potential autoimmune mechanisms [233].

Collectively, this evidence suggests that *Plasmodium* infection significantly disrupts the immune system, contributing to both B cell and dendritic cell dysfunction, as well as promoting inflammatory responses through neutrophils, potentially driving autoimmune processes.

1.13 Mechanism of autoantibodies production in *Plasmodium* infection

Several mechanisms, such as molecular mimicry, bystander activation and epitope spreading, have been implicated in autoantibody production [234]. However, little is known about the mechanisms that trigger autoantibody production during malaria infection.

1.13.1 Molecular mimicry

Molecular mimicry is an immune evasion mechanism used by pathogens that results in shared immunoreactive epitopes between the host and the parasite [234].

This phenomenon was initially described using mouse models in *Streptococcus pyogenes*, where the M protein, a virulence factor and host myosin were found to be cross-reactive, potentially inducing rheumatic heart disease [235]. Moreover, molecular mimicry is also linked to other autoimmune diseases like multiple sclerosis (MS) [234] and Graves' disease [236].

Molecular mimicry by *P. falciparum* has been documented in several studies. For instance, the parasite's translationally controlled tumour protein (pfTCTP) has been shown to mimic human histamine-releasing factor (HRF) [237]. Similarly, PfEMP1 is reported to contain similar domains to human proteins like vitronectin [238]. Additionally, approximately 19 *P. vivax* proteins share sequence similarities with human red blood cell proteins such as ankyrin, actin, and spectrin [239]. While these similarities are based on sequence similarity, recent evidence indicates that approximately 7% of *P. falciparum* proteins have structural similarities with human proteins at the tertiary level, with about 44 potential mimicry interactions [203]. Thus, this high sequence and structural similarity between host and pathogen increases the risk of autoimmune diseases in genetically susceptible individuals.

1.13.2 Bystander activation

Bystander activation is a process in which T cells are activated independently of T cell receptor stimulation, typically through the binding of soluble and membrane-bound particles to other receptors [240]. *P. falciparum* has been shown to induce CD4+ T cell activation and proliferation independently of pathogen load, which can lead to tissue damage and severe disease, compared to *P. vivax* [241]. Additionally, the digestive vacuole of *P. falciparum*, released following parasite rupture, has also been shown to activate complement on bystander cells, contributing to malarial anaemia [242].

1.13.3 Epitope spreading

Epitope spreading refers to the process of expanding the range of epitopes targeted by the immune system from the initial dominant and focused response towards less prominent or hidden epitopes on the same protein [243]. Although other factors may initiate the induction of autoimmune diseases, epitope spreading enables autoantigen presentation by APC, which activates autoreactive

lymphocytes [244]. Moreover, evidence suggesting immune evasion by *P. falciparum* through epitope spreading has been reported in studies on the thrombospondin-related anonymous protein (TRAP) family, where immune responses were induced to the entire length of TRAP protein, instead of specific immunodominant areas [245].

1.13.4 B cell Polyclonal activation

Abnormal B cell responses are associated with autoimmune diseases such as SLE [246]. Similarly, *P. falciparum* infection is known to induce polyclonal B cell activation, resulting in the occurrence of hyper-gammaglobulinemia in malaria-infected individuals [201,202]; a phenomenon mediated by the parasite's erythrocyte membrane protein 1 (PfEMP1) CIDR1α domain [201,202].

Additionally, parasite DNA has also been shown to activate T-bet+ B cells (atypical B cells) through TLR9 and IFN-γ signalling, contributing to severe malaria anaemia [3]. These T-bet+ B cells have been shown to contribute to the pathophysiology of malaria-induced anaemia through the production of antiphospholipid antibodies [3].

1.14 Role of *Plasmodium* induced autoantibodies in inducing pathology

While *Plasmodium* infections are known to induce increased autoantibodies with a wide range of specificity [6,8], their role in malaria pathogenesis, however, remains unclear. Notably, high levels of anti-phosphatidylserine and anti-DNA antibodies have been reported in children with severe malaria [1,2,8], and recent studies suggest these autoantibodies could serve as potential biomarkers of disease severity [247]. Here, I will review the current literature on the association between autoantibodies and malaria-related pathologies like anaemia, cerebral malaria, and renal dysfunction.

The presence of increased autoantibodies in severe malaria anaemia suggests that they could be important in the pathogenesis of severe malaria anaemia [1,223,239]. Moreover, recent evidence from mouse models has elucidated molecular mechanisms underlying the pathogenies of anaemia [3,4]. Specifically, antibodies to phosphatidylserine (PS), which is highly expressed in RBCs, were found to increase

the clearance of uninfected erythrocytes and contributed to anaemia in a mouse model [1,3]. Interestingly, the production of these anti-phosphatidylserine antibodies was also shown to be induced by *Plasmodium* DNA activating TLR9 and IFN-γ receptor signalling via T-bet+ B cells [3,4].

While autoantibodies to erythrocyte surface antigens are present across malaria-endemic areas [223,239,248,249]. An inverse relationship between atypical B cell levels and levels of haemoglobin exists, suggesting that atypical B cell expansion could be driving increased autoantibodies and anaemia [1,4]. Similar findings have been reported for *P. vivax*-infected individuals, where higher autoantibody levels were observed in anaemic compared to non-anaemic individuals [8,223,239].

Cerebral malaria (CM), caused by *P. falciparum* parasites, is a neurovascular syndrome that can result in decreased consciousness, coma, [250] and seizures. Moreover, cerebral malaria is known to account for about 90% of malaria deaths and predominantly affects children in sub-Saharan Africa [251]. The sequestration of infected RBCs within the brain microvasculature underlies cerebral malaria's pathogenesis [250]. Notably, evidence of high levels of IgG autoantibodies to brain antigens correlated with increased TNF-α levels and poor outcomes in cerebral malaria [133]. Thus, autoantibodies could be important in the pathogenesis of cerebral malaria. In addition, higher levels of autoantibodies to voltage-gated calcium channels have been reported in Kenyan children with cerebral malaria [252], with recent evidence of the increased presence of pro-thrombotic autoantibodies against platelet factor 4/polyanion has also been suggested as one of several mechanisms that contribute to the development of CM [253]. However, it remains unclear whether these autoantibodies play a pathological role in cerebral malaria or are simply a consequence of tissue damage.

Acute kidney injury (AKI) refers to a sudden and significant decline in kidney function, which is a common complication in severe malaria [254]. AKI occurs in around 40% of severe *P. falciparum* infections, particularly affecting children and adults in low-transmission areas [255]. Several mechanisms for the induction of this pathology have been proposed, including parasite sequestration, microvascular obstruction, and intravascular hemolysis, which are known to amplify the damaging effects of the host inflammatory response [254]. Furthermore, recent

studies have correlated high levels of anti-DNA antibodies with severe malaria, specifically AKI, in children [2]. Thus, these findings suggest an immune-mediated pathway, similar to those observed in SLE nephritis, could be involved in malaria-associated AKI, though further research is needed.

Overall, these data suggest that malaria-induced autoantibodies play a pathological role in severe malaria. However, it remains unclear whether these autoantibodies arise from severe tissue damage or actively contribute to the development of severe disease.

1.15 Autoantibodies play a protective role against malaria infection

Contrary to the common knowledge that autoantibodies are associated with pathology, there is evidence indicating a protective role for autoantibodies in malaria infection [8]. Importantly, autoantibodies from patients with autoimmune diseases like SLE have also shown reactivity against *Plasmodium* proteins and can suppress *P. falciparum* growth *in vitro*, suggesting a protective effect [204].

Moreover, experimental evidence suggests a protective role for anti-DNA antibodies in malaria, as their depletion has been associated with higher mortality rates [256]. Additionally, studies have also shown that RF levels are negatively correlated with age and parasitaemia in children from Côte d'Ivoire [257], and elevated levels of Immunoglobulin E autoantibody to 14-3-3 ε protein have also been reported in asymptomatic individuals compared to those with severe malaria [132]. Further supporting this idea, higher levels of anti-self-antibodies have been detected in children with asymptomatic malaria compared to those with mild malaria [133].

Interestingly, ssDNA-binding IgM autoantibodies peak seven days post-infection, and ssDNA-binding IgG autoantibodies peak at 14 days, indicating that these antibodies are specifically elicited in response to infection [256], suggesting that the autoantibodies could be appearing as a consequence of infection.

However, while previous evidence was initially based on observational studies conducted at a single point in time, a more robust and recent study measured

autoantibody levels prior to a malaria season and correlated the levels to clinical outcomes. This study found that higher antinuclear antibody (ANA) reactivity in healthy children before a malaria season was associated with a reduced risk of clinical malaria [5]. Notably, these autoantibodies bound to *P. falciparum* proteins involved in erythrocyte invasion and blocked parasite growth in vitro [5], suggesting they were functional and most likely mediating the parasite clearance.

Collectively, this provides evidence that autoantibodies are protective during malaria infection. However, their role is still debatable, and well-designed studies are necessary to clarify their function and potential benefits.

1.16 Effect of *Plasmodium* infection on the population's genetic susceptibility to autoimmunity

Plasmodium parasite is known to exert selective pressure on the human genome to enhance survival against severe malaria, as evidenced by the extremely high frequency of sickle-cell traits in areas of high malaria prevalence [258] and the presence of very rare, highly protective, blood groups like Dantu [259]. However, while these genetic adaptations confer advantages in malaria resistance, they can also lead to other consequences, such as sickle cell disease. Notably, certain genetic variants that enhance immune responsiveness, and thus reduces susceptibility to malaria such as FcγRIIB, may increase the risk of developing autoimmune diseases [7,260]. For example, mice deficient in FcγRIIB, a condition that increases susceptibility to SLE, were found to be more protected against experimental cerebral malaria [261].

Additionally, TNF gene polymorphisms are associated with either susceptibility or resistance to malaria, with specific mutations (e.g., TNF G-308A and TNF G-238A) linked to severe malaria and high parasitaemia [262,263]. These same TNF polymorphisms are also implicated in the development of SLE, indicating a possible connection between malaria and autoimmune diseases [264].

Interestingly, while RA in Europeans is linked to HLA-DR1 or HLA-DR4, there is limited data on whether people of African descent acquire HLA gene polymorphisms that offer protection or increase susceptibility due to malaria. For instance, in West Africa, individuals with HLA Class I Bw53 and HLA Class II

DRB11302-DQB10501 were more protected from severe malaria [265]. Conversely, HLA-DR0401, which increases RA risk [266], has been associated with increased malaria susceptibility [267]. This suggests that chronic *Plasmodium* infections may have driven the selection of specific HLA genes in these populations resulting in heightened susceptibility to autoimmune diseases.

Taken together, the likelihood of an increased reservoir of genetic risk factors associated with autoimmune diseases in malaria-endemic regions and the lack of reliable data on the true incidence of autoimmune diseases in sub-Saharan Africa underscores the need to develop more robust studies to provide a clearer understanding of this association.

1.17 Malaria murine models

Mouse models are extensively used to study malaria pathogenesis and immune responses, leveraging various *Plasmodium* species to replicate different aspects of human malaria [268]. Although no single model perfectly replicates human malaria, comparative transcriptomics indicates that *P. yoelii* 17XL infection most closely mirrors the gene expression changes observed in severe human malaria syndromes [269]. Additionally, *P. berghei* ANKA infection in C57BL/6J mice is a widely utilised model for severe malaria, as it mirrors many symptoms of human cerebral malaria [269].

For my research, applying the *Plasmodium chabaudi* rodent malaria model provides valuable insights into autoimmunity and immune regulation. Particularly given that *Plasmodium chabaudi* model closely replicates many of the pathological and immunological characteristics of human malaria infections,[270] making it an invaluable tool for advancing our understanding of the disease. For example, *P. chabaudi* mirrors key features of *P. falciparum*, such as cyclical fever episodes, immune response dynamics, and the development of anaemia; these similarities provide critical insights into host-parasite interactions [270]. Notably, *P. chabaudi* induces chronic infections, making it helpful in studying anti-*Plasmodium* immunity, a key aspect for my study [270]. Moreover, *P. chabaudi* has been reported to reduce circulating immune complexes and improve histopathological changes in various organs in lupus-prone mice [271]. Together, these suggest that these

parasites play a critical in modulating autoimmune responses, making them a valuable model for studying autoimmunity in the context of infectious diseases.

1.17.1 Life cycle of *P. chabaudi*

The *Plasmodium chabaudi* life cycle, similar to *P. falciparum*, begins during a blood meal when the mosquito injects sporozoites into the rodent host, which migrate to the liver and infect liver cells. In the liver, they multiply and release merozoites into the bloodstream, invading red blood cells and undergoing a 24-hour replication cycle. The cells then burst, releasing more merozoites, perpetuating the cycle [272].

Some merozoites then transform into gametocytes, which mosquitoes ingest during subsequent blood meals, completing the life cycle [272]. Notably, the life cycle in *P. chabaudi* is tightly synchronised with the host's circadian rhythms, which enhances the parasite's survival and transmission [272].

1.17.2 Drawbacks of the *P. chabaudi* model

While this model is useful, one of the key limitations is that sequestration of the parasites occurs in the liver, [273] rather than the brain as observed with severe human malaria [274]. Moreover, the circulating parasitaemia required to induce pathogenic symptoms [270] in mice is much higher than in human infections, reducing its translational applicability. Furthermore, mice exhibit hypothermia as a clinical symptom, contrasting with the fever commonly associated with human malaria [275].

1.18 Study justification

Although autoantibodies are common in individuals residing in malaria-endemic areas, their role remains controversial [6,8]. Additionally, *Plasmodium* infections are known to drive the selection of genes that are protective against severe malaria, but these same genes are associated with an increased risk of autoimmune disease [7]. The mechanisms underlying this association still remain unclear. These findings, therefore, raise important questions, such as whether *Plasmodium* infection could increase predisposition to autoimmune disease, particularly given the lack of reliable data on the prevalence of autoimmune disease in sub-Saharan Africa.

Another key issue is understanding the potential benefits of these autoantibodies: is there an advantage to increased autoimmunity? While my research aims to clarify this, a recent publication [5] released as I completed my PhD suggests that increased autoimmunity, particularly before a malaria season, is predictive of better clinical outcomes. However, this raises concerns about whether increased autoimmunity might come at a price, especially since most autoimmune diseases increase with age, and residents of malaria-endemic areas may be at genetic risk for autoimmunity.

My study, therefore, seeks to address this research gap by employing mouse models and established cohorts of individuals living in a malaria-endemic area in Kilifi, Kenya. Using mouse models allowed for the investigation of the effect of increased autoimmunity resulting from malaria infection on the development of experimental arthritis. Moreover, these models were then used to study whether autoimmunity could contribute to the pathogenicity of clinical malaria.

Extending these findings to humans, I used established cohorts of individuals living in areas with different malaria transmission to investigate whether persistent exposure to malaria causes autoimmunity. Furthermore, by examining cohorts of children with varied clinical outcomes, specifically those with uncomplicated versus severe malaria, I investigated the role of autoimmunity in acute infection.

1.19 Research hypothesis

I hypothesise that *P. falciparum* infection leads to the production of low-affinity binding autoantibodies that play a protective role in acute malaria; however, this might increase the risk of developing autoimmune disease later in life as illustrated in (Figure 1-4).

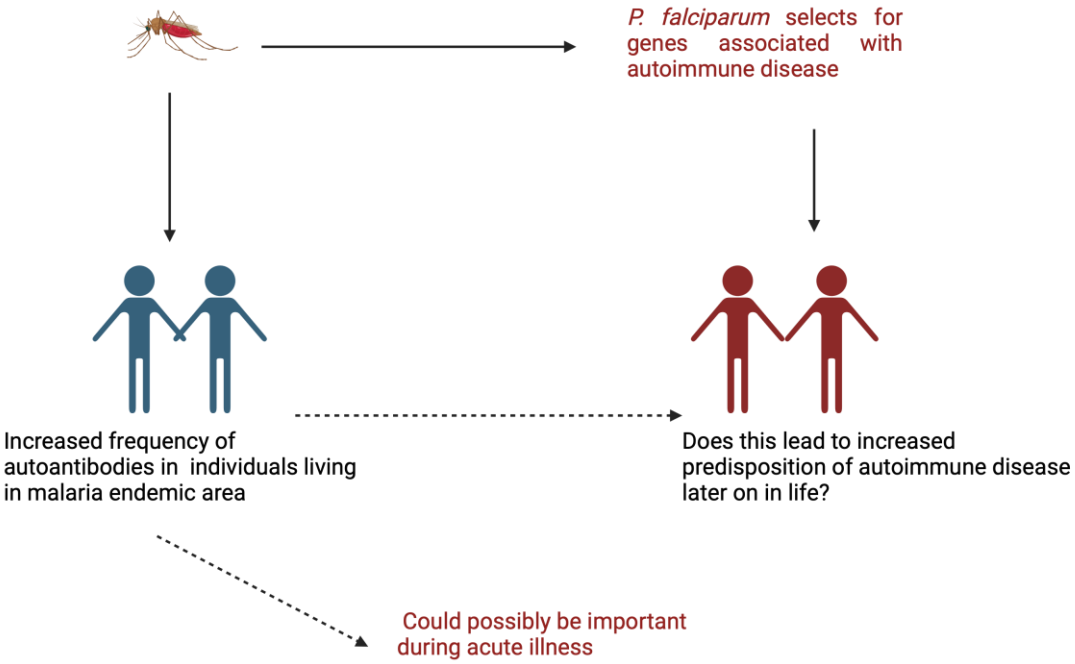

Figure 1-4: Illustration of the research hypothesis.

Solid lines represent established relationships that have been confirmed by existing research, while dashed lines indicate hypothesised associations that I proposed to investigate in this research. Figure created with BioRender.com

1.20 Thesis study aims

1.20.1 Project aim and objectives

The aim of this project is to investigate the associations between *Plasmodium* infections and autoimmune diseases using murine models of human RA and *P. chabaudi* infection, and further screen for the presence of autoimmune markers in individuals living in a malaria endemic area in Kenya.

1.20.1.1 Specific objectives

1.20.1.2 Murine Studies

1. To characterize ACPA responses, as well as antibody responses to corresponding native peptides, during *P. chabaudi* infection.

2. To investigate the effect of *P. chabaudi*-induced ACPA responses and antibody responses to corresponding native peptides on the development of experimental arthritis in mice.

3. To evaluate whether ACPA, as well as antibody responses to corresponding native peptides elicited from an experimental arthritis model, confer protection against *P. chabaudi* infection.

1.20.1.3 Clinical Studies

1. To assess the prevalence of known autoimmune markers, including ACPA and antibody responses to their corresponding native peptides, in adults living in malaria-endemic regions.

2. To examine immunological phenotypic differences in individuals with varying antibody responses to both citrullinated and corresponding native peptides in malaria-endemic areas.

3. To investigate the presence and levels of ACPA and antibody responses to corresponding native peptides in children with varied clinical outcomes.

2 Chapter 2- Material and methods

This chapter is structured into two components: the first section outlines the methods utilised in the application of animal models, while the second section details the methods used in analysing human samples from individuals living in a malaria endemic area in Kilifi, Kenya.

2.1 Section 1: Animal section

2.1.1 Animals

Seven- to eight-week-old male mice C57BL/6 were purchased from Envigo (UK), and OT-II TCR transgenic mice, genetically engineered to express CD4+ T cells specific to chicken OVA 323-339 (OT-II TCR), within the context of MHC II molecule I-A^b [276] were bred in-house for this research. All the mice were maintained in a specific pathogen free facility at the University of Glasgow, with all experiments performed under UK home office licence PP9595420 and approved by the local ethics committee.

2.1.2 *P. chabaudi* infections

Plasmodium chabaudi AS parasites (acquired from a collaborators lab in Edinburgh*)* were maintained as frozen stabilate, in liquid nitrogen and subsequently thawed and passaged by infecting one mouse via intraperitoneal (i.p.) injection. Once a parasitaemia of 5-10% was reached the passage mouse was euthanised by terminal anaesthesia, and blood was harvested via cardiac bleed. 1X10^5 parasitised red blood cells (pRBCs) resuspended in PBS were then injected i.p. for all *P. chabaudi* infection experiments.

In some experiments, to eliminate chronic infections, 20 mg/kg of chloroquine diphosphate salt (Sigma-Aldrich, Poole, UK) was administered subcutaneously (s.c) [277,278]. Naive controls were included in all experiments and throughout the infection period the mice were monitored daily for changes in weight and any signs of distress, while adhering to the limits outlined in the licence.

2.1.3 Assessment of parasitaemia

Parasitaemia in the infected mice was monitored using blood smears, which were prepared by pricking the mouse tail vein and placing a drop of blood on a microscope slide and allowing it to dry for 30 seconds. The blood smears were then fixed using 100% methanol (ThermoFisher) for 30 seconds and initially stained with Hemacolor® Rapid staining of blood smear (Sigma-Aldrich) for 7 seconds, followed by immediate rinsing in tap water, which was followed by a 30-second dip in Giemsa stain (Sigma-Aldrich) [279] and a final rinse with tap water. The slides were then allowed to dry, and immersion oil was applied on the slide for parasitaemia assessment using bright-field microscopy with a 100x objective. Parasite count was determined by calculating the percentage of infected red blood cells relative to the total observed red blood cells [280].

2.1.4 Assessment of autoantibody kinetics following *P. chabaudi* infection

In this study, I included a group of naive mice (n=6), and two groups of mice infected with *P. chabaudi* parasite (n=6), as illustrated in (Figure 2-1). In the *P. chabaudi* groups, one group was treated with chloroquine on day 15 to model an acute infection, while the other group was left untreated to model chronic infections. Tail bleeds were collected periodically over 63 days for the assessment of autoantibodies using ELISA.

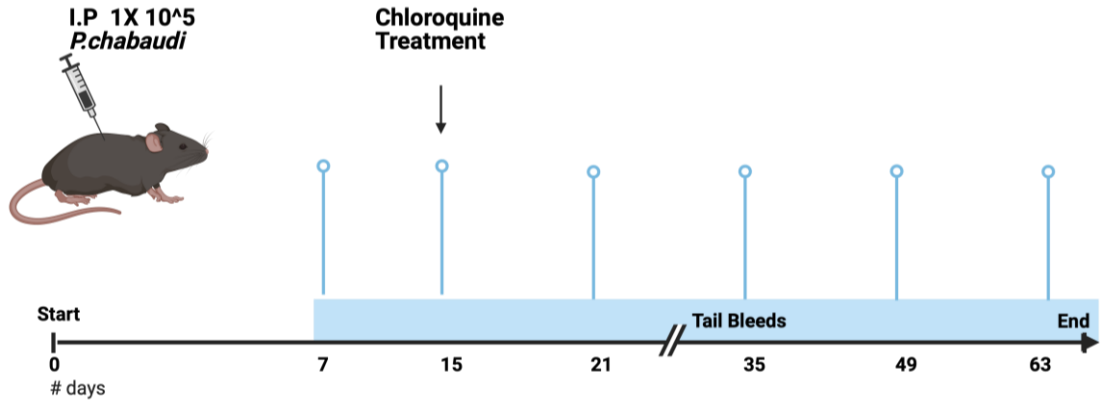

Figure 2-1: *P. chabaudi* infection study timeline for the assessment of autoantibodies kinetics.

Illustration of *P. chabaudi* infection timeline, where C57BL/6 male mice were infected with *P. chabaudi* parasite; one group of mice (n=6) was chloroquine treated on day 15 while the other was left untreated (n=6), naive were also included (n=6). Tail bleeds were taken periodically for ELISA over a 63-day period for assessment of autoantibody kinetics. The mice were then culled on day 63 and blood was harvested by cardiac puncture spleen and liver was harvested for flow cytometry and PCR assays respectively.

2.1.5 Inhibition of peptidyl arginine deiminase (PAD) enzymes in *P. chabaudi* infected mice using BB-Cl-amidine

Two groups of mice (N=16) were infected with *P. chabaudi* to investigate the effect of inhibiting peptidylarginine deiminase (PAD) enzymes. One group (n=8) was treated daily with BB-Cl-Amidine (Cayman chemical, #17079), a pan-PAD inhibitor that blocks all PAD isoforms activity, while the other group (n=8) received the vehicle control (1% DMSO in PBS), as outlined in (Figure 2-2). BB-Cl-amidine a pan-peptidylarginine deiminase (PAD) inhibitor [281], was administered intraperitoneally at a dosage of 1 mg/kg/day [281] dissolved in 1% DMSO in PBS at 10 mL/kg.

Additionally, two naive control groups were included (n=8), one treated with the drug and the other with the vehicle. During the infection period blood was drawn on day 7 for ELISA and tail pricks were taken daily to determine parasitaemia. Mice were also weighed daily and culled on day 14 where blood was harvested for ELISA.

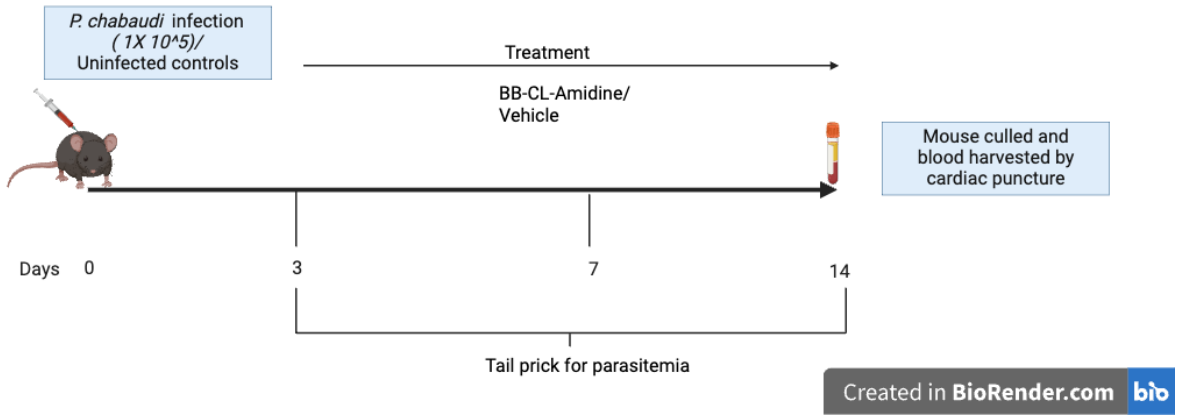

Figure 2-2: Illustration of the *P. chabaudi* infection and PAD inhibition study timeline

C57BL/6 male mice (n=8) were infected with 1 × 10^5 *P. chabaudi*-infected RBCs; one group of mice was treated with BB-Cl-Amidine, while the other group was left untreated. Naive mice were also included as controls. Tail bleeds were taken on day 7 for ELISA while tail pricks were taken daily to determine parasitemia. Daily measurement for weights were also taken and on day 14 mice were culled and blood harvested.

2.1.6 *P. chabaudi* infection followed by induction of acute experimental arthritis (AEA)

Mice were first infected with *P. chabaudi*, followed by the induction of AEA as outlined in (Figure 2-3) as previously described [282]. For this experiment, the mice were divided into groups (n=8). The following steps were carried out to induce acute experimental arthritis: (a) Harvesting OTII T cells from TCR transgenic mice, (b) Differentiating these T cells into a Th1 phenotype, (c) Preparation of OVA antigen and HAO antigen and (d) Subsequent adoptive transfer of the OTII T cells.

2.1.6.1 Harvesting of OTII T cells

Spleens and lymph nodes were harvested from OTII TCR transgenic mice. Single-cell suspensions were separately prepared from both spleen and lymph node by gently mashing and passing through a cell strainer using the 2 mL BD PlastiPak™ Luer Slip Syringe without Needle (Fischer Scientific), followed by rinsing with PBS buffer. The cells were then transferred into a 50 mL centrifuge tube (Corning®) and centrifuged at 400x g for 6 minutes. For the spleen-derived single-cell suspension, an additional step was performed to eliminate red blood cells. Specifically, 5 mL of red blood cell lysis buffer (eBioscience) was added and incubated for 5 minutes on ice. The cells were then rinsed in 5 mL PBS, centrifuged for 5 minutes at 4°C at 400x g, and counted using a hemocytometer. CD4+ T cells were then isolated using the MACS negative selection (Miltenyi CD4+ Isolation Kit, #130-104-454) according to the protocol. The resulting positive fraction was retained and utilised as antigen-presenting cells.

2.1.6.2 T cell differentiation into a Th1 phenotype

Differentiation of T cells into a Th1 phenotype was done as previously described [283]. APCs from the positive fraction were treated with mitomycin C (50 µg/mL) and incubated for 1 hour at 37°C, followed by subsequent washing and counting. Th1 polarisation was induced by culturing the isolated CD4+ T cells with mitomycin C-treated antigen-presenting cells in a 1:1 ratio in the presence of OVA323-339 (Sigma), interleukin-12 (IL-12: PeproTech), and anti-IL-4 monoclonal antibody (R&D Systems). The cells were then cultured in 75 cm^2 vented flasks (Corning), maintained at a tilt, and incubated at 37°C with 5% CO2 for 72 hours. Following

this incubation period, the percentage of Th1-polarised cells was determined using flow cytometry analysis.

2.1.6.3 Preparation of OVA antigen and HAO antigen

The OVA antigen (Code OAC – Worthington Biochemicals) was prepared as previously described by [282,284] by dissolving tissue culture grade OVA at a final concentration of 1 µg/µL in complete Freund's adjuvant (CFA). Specifically, the emulsion was generated by quickly mixing the OVA in PBS with CFA using a 1 mL syringe (Fisher Scientific) and the presence of a stable pellet without observable oily waves upon immersion in water or PBS confirmed its readiness.

Following the preparation of the OVA antigen, heat aggregated OVA (HAO) was generated as previously described [285]. Briefly, chicken ovalbumin (Sigma), was initially diluted in PBS to achieve a concentration of 20 mg/mL, followed by incubation at 100°C for 2 hours in 1.5 mL centrifuge tubes, each containing 200 µL volume. Following this, centrifugation at 17,000x g for 5 minutes was performed, and the supernatant was carefully aspirated. The resulting pellet underwent resuspension in 500 µL of PBS, and this centrifugation-aspiration cycle was repeated to ensure optimal purification; the final pellet was resuspended in 200 µL of PBS, which was then stored frozen.

For subsequent experiments, the required aliquots were thawed and thoroughly mixed in 1800 µL of PBS in GentleMACS c-tubes (Miltenyi Biotec) using a Miltenyi GentleMACS dissociator (program HAP), a customised program. The samples underwent multiple runs on the dissociator until optimal dissociation was guaranteed. The resulting mixture was then passed through a 26-gauge (26G) needle, ready for injection.

2.1.6.4 Adoptive transfer of OTII TCR transgenic CD4+ T cells to induce acute experimental arthritis (AEA)

2x10^6 Th1-polarised OTII TCR transgenic CD4+ T cells were transferred to C57BL/6 mice [283] via subcutaneous injection. One day following the transfer of OTII TCR transgenic CD4+ T cells, these mice also received a subcutaneous injection of 100 µg OVA emulsified in CFA. After ten days, these mice were footpad

challenged with 50 µL containing 100 µg of heat aggregated OVA (HAO) or PBS as control and sacrificed a few days later [282,286].

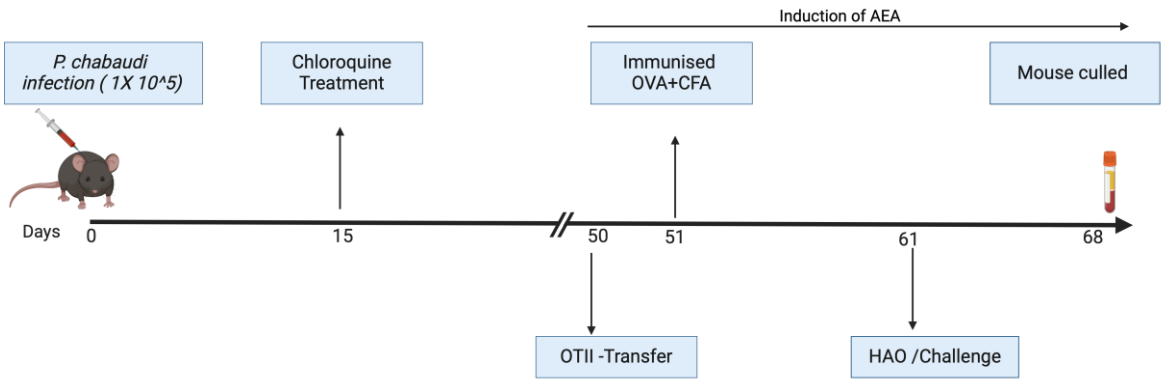

Figure 2-3: Illustration of prior *P. chabaudi* infection + acute experimental arthritis model.

In this model, male C57BL/6 mice were initially infected with *P. chabaudi* before the induction of AEA. This procedure involved several steps: first, OTII T cells were isolated from transgenic mice, followed by induction of a Th1 phenotype in CD4+ T cells. Subsequently, the Th1-polarised CD4+ T cells were transferred into recipient mice and the next day, OVA antigen was prepared and administered to the mice. Ten days after, the mice underwent a footpad challenge with HAO or PBS to initiate breach of tolerance and induction of experimental arthritis before being sacrificed a few days after the challenge. During the study period tail bleeds were taken periodically for assessment of autoantibodies kinetics using ELISA.

2.1.7 *P. chabaudi* infection followed by induction of chronic experimental arthritis (CEA)

The induction of chronic experimental arthritis (CEA) is a two-step process involving the initial induction of acute experimental arthritis (AEA) as described earlier (section 2.1.6.1-2.1.6.4). After AEA was induced, mice were infected with *P. chabaudi* on day 20, followed by the induction of CEA on day 41, as illustrated in (Figure 2-4).

To induce CEA, mice previously immunised and challenged with heat aggregated OVA antigen (HAO) underwent a rechallenge with HAO, as outlined by [286]. Specifically, 30 days after the initial HAO challenge, the mice received a local subcutaneous injection of 50 µL containing 100 µg of HAO in Freund's incomplete adjuvant (IFA), administered on the same foot that was initially challenged with HAO. Control animals received a 50 µL injection of PBS alone.

Additionally, one of group in the *P. chabaudi*-infected mice were treated with 20 mg/kg of chloroquine diphosphate salt (Sigma-Aldrich, Poole, UK) administered subcutaneously (s.c.).

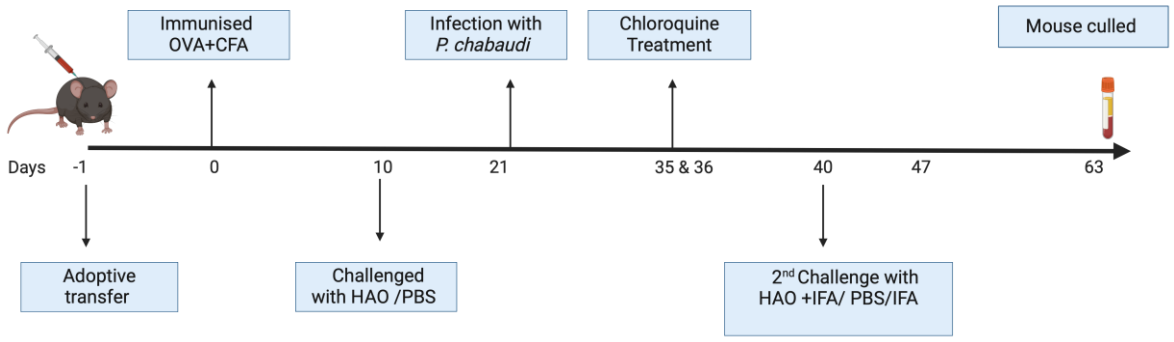

Figure 2-4: Induction of Chronic Experimental Arthritis (CEA) following *P. chabaudi* Infection

The induction of chronic experimental arthritis (CEA) is a two-step process involving the initial induction of acute experimental arthritis (AEA). OTII T cells were isolated from transgenic mice and induced to differentiate into a Th1 phenotype. These Th1-polarised CD4+ T cells were then transferred into recipient C57BL/6 mice (n=8) and one day later, OVA antigen was prepared and administered to the mice. Ten days post-immunisation with the OVA antigen, the mice underwent a footpad challenge using either heat aggregated OVA antigen (HAO) or PBS. This was then followed by *P. chabaudi* infection 3 weeks later and treated with chloroquine on days 35 and 36. To induce CEA, mice previously immunised and challenged with (HAO) underwent a rechallenge with HAO thirty days after the initial HAO challenge. Specifically, mice received a local subcutaneous injection of 50 µL containing 100 µg of HAO in Freund's incomplete adjuvant (IFA), administered in the same foot initially challenged with HAO. The control group received a 50 µL injection of PBS alone. The mice were then culled on day 63.

2.1.8 Induction of chronic experimental arthritis (CEA) prior to *P. chabaudi* infection

Induction of CEA model was performed as described above this was then followed by *P. chabaudi* infection as illustrated in (Figure 2-5).

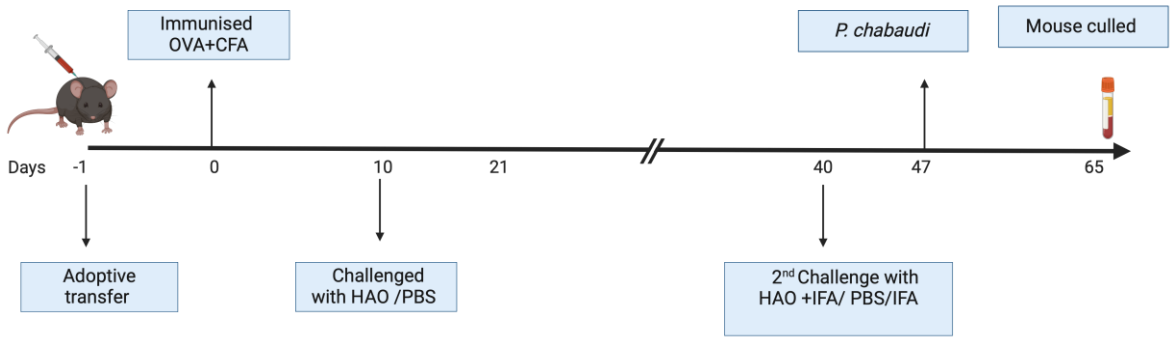

Figure 2-5: Chronic Experimental Arthritis Model (CEA) followed by *P. chabaudi* Infection at day 47.
This figure illustrates the induction of CEA followed by *P. chabaudi* infection on day 47. Initially, the AEA was induced, as described previously. Subsequently, a CEA model was initiated. To induce CEA, mice previously immunised and challenged with (HAO) underwent a rechallenge with HAO thirty days after the initial HAO challenge. Specifically, mice received a local subcutaneous injection of 50 µL containing 100 µg of HAO in Freund's incomplete adjuvant (IFA), administered in the same foot initially challenged with HAO. The control group received a 50 µL injection of PBS alone. *P. chabaudi* infection was then done on day 55 following induction of CEA.

2.1.9 Assessment of arthritis in the AEA and CEA experimental arthritis.

The assessment of arthritis in both AEA and CEA experimental models involved daily monitoring of mice for any signs of arthritis. Disease progression, including observation for erythema, swelling, or loss of function, was evaluated as detailed by [286]. Signs of arthritis in each paw were assessed on scale from 0 to 4, indicating ascending severity: 0 = no reaction; 1 = mild, with definite redness and swelling of the ankle/wrist or apparent redness and swelling limited to individual digits, regardless of the number of affected digits; 2 = moderate to severe redness and swelling of the ankle/wrist; 3 = redness and swelling of the entire paw, including digits; and 4 = maximally inflamed limb with involvement of multiple joints [287]. Paw thickness, serving as a measure of swelling, was assessed in millimetres using dial callipers (Kroeplin, Munich, Germany) [288].

2.1.10 Archived serum samples from a (CEA) model

Samples previously collected from a chronic experimental arthritis (CEA) experiment conducted by (Shaima Mazin Jawad Al Khabouri) (a previous PhD student in the lab) [284] with timepoints at days 42 and 48 archived at −80°C were used for ELISA.

2.1.11 Tissue isolation and sample processing

Spleens and lymph nodes were harvested at the end of the experiment, and single-cell suspensions were prepared as described above (section 2.1.6.1). The samples were then ready for staining for flow cytometry.

2.1.11.1 Flow Cytometry

Single-cell suspensions obtained from the spleen and lymph nodes were prepared and stained with a cocktail of conjugated antibodies see (Table 2-1), diluted at 1:200, and incubated for 20 minutes at 4°C. To differentiate the live cells from dead cells, staining of dead cells was done using the fixable viability dye eFluor 506 (ThermoFisher) for 20 minutes at 4°C. The samples were then fixed with 2% PFA washed and resuspended in FACS buffer (PBS/2% FCS/2 mM EDTA). The samples were then acquired using BD LSR Fortessa and analysed using FlowJo software version 10.8.1.

Table 2-1: B and T flow cytometry cell staining panel

Marker	Fluorochrome	Clone	Company
GL7	Alexa Fluor 488	GL7	BioLegend
CD44	PerCP Cy5.5	IM7	eBioscience
CD19	APC	eBIO1D3	eBioscience
CD62L	APC-eFluor 780	MEL-14	eBioscience
CD11c	PE-Dazzle	N418	BioLegend
CD278 (ICOS)	PE-Cy7	C398.4A	BioLegend
FAS(CD95)	PE	Jo2	BD Biosciences
B220	eFluor 450	RA3-6B2	eBioscience
CD279(PD1)	BV711	29F.1A12	BioLegend
CD3	BV785	17A2	BioLegend
CD4+	BUV395	GK1.5	BD Biosciences
Viability	eFluor 506		eBioscience

2.1.12 ELISA for the detection of antibody responses to native and citrullinated peptides

Following the end of each experiment, mice were humanely euthanised via terminal anaesthesia followed by cervical dislocation. Blood samples were then collected via cardiac puncture. Subsequently, these blood samples underwent two rounds of centrifugation at 17,000x g for ten minutes, and the plasma was harvested and promptly frozen. ELISA, as previously described [289], was used to detect and quantify antibodies to well-characterised native peptides and their corresponding citrullinated peptides (Table 2-2). Briefly, 96-well plates (Costar) were coated with 50 µL/well of 10 µg/mL peptide in bicarbonate buffer. The plates were washed three times using PBS/0.05% Tween 20 (PBST) (Sigma-Aldrich), followed by blocking with 100 µL of 5% BSA/ PBST at room temperature for 2 hours (hr). Murine plasma samples were diluted at 1/20 in 50 µL of 0.1% BSA/ PBST overnight. After the incubation, the plates were washed three times with PBS 0.05% Tween 20, followed by incubation with horseradish peroxidase-conjugated rabbit anti-mouse murine IgG at room temperature for 1.5 hr. This was then followed by further washing using PBST and incubation with 100 µL of O-Phenylenediamine Dihydrochloride (OPD) at a final concentration of 0.4 mg/mL (Sigma). The plates were then stopped with 50 µL of 2 M H_2SO_4, and absorbance was read at 492 nm using a Tecan Sunrise plate reader (Tecan).

A standard curve was established by titrating mouse IgG to quantify antibody titers in ng/mL for all samples. Additionally, where the standard curve was not available, antibody levels were reported as fold changes relative to a positive control. The fold change was determined by normalising the absorbance (OD) of each test sample to that of the positive control, thus allowing for relative comparisons of antibody levels without absolute quantification.

2.1.13 Native (un-citrullinated) and citrullinated peptide

Native peptides and their corresponding citrullinated peptides were bought from Pepceuticals (UK). These proteins studied in here are highly conserved between mice and humans, thus allowing for reliable cross-species comparisons in this research [290–293].

Table 2-2: Human Native (Un-citrullinated) and Citrullinated Peptides

Native (Un-citrullinated)	**Citrullinated**
Fibrinogenb (FIBb) (CNEEGFFSARGHRPLDKKC)	cFIB b (fibrinogenb) (CNEEGFFSA-cit-GHRPLDKKC)
Tenascin C5 peptide (TNC5) (CEMKLRPSNFRNLEGRRKR)	cTNC5 (tenascin-C5 peptide) (CEMKL-cit-PSNF-cit-NLEG-cit-cit-KRC)
Vimentin (VIM) *CKIHAREIFDSRGNPTVEC*	cVim (Vimentin) *CKIHA-cit-EIFDS-cit-GNPTVEC*
Alpha-enolase REP *(CVYATRSSAVRLRSSVPC)*	CEP *(CVYAT-cit-SSAV-cit-L-cit-SSVPC)*

2.1.14 PCR for the detection of *P. chabaudi* parasite

DNA was extracted using (Qiagen DNA extraction kit) from 10 μL of blood taken from the tail bleeds of all the mice. For PCR, primers targeting the conserved 18S rRNA were developed. Specifically, FWD 5' CCTAACATGGCTTTGACGGG 3' and RVS 5'GTGCCCTTCCGTCAATTCTT 3' primers were used to detect the presence of *P. chabaudi* parasite using (Biorad S1000 Thermal Cycler). PCR products were resolved on 1% agarose gel electrophoresis, stained with SYBR™ Safe DNA Gel Stain and visualised on a GelDoc system (BioRad, Hertfordshire, UK).

2.1.15 Bioinformatics: Sequence analysis

To identify sequence similarity between *P. falciparum* and human proteins, specifically Tenascin-C, Fibrinogen, Vimentin, and Enolase, BLASTp was used to align each of the protein sequences obtained from UniProt to *Plasmodium* sequences from the *Plasmo*DB database. The sequences for the human proteins were retrieved from UniProt and aligned against the *P. falciparum* proteome in *Plasmo*DB to determine potential homology and functional similarities. The alignment parameters were set to default values according to blastp parameters

on NCBI website [294,295]. Additionally, to explore the potential presence of peptidylarginine deiminase (PAD) enzymes within the *P. falciparum* genome, sequences of human PAD isoforms (PAD1-6) were also retrieved from UniProt and aligned against the *P. falciparum* proteome available in *Plasmo*DB.

2.1.16 Sample size calculation

Using G*Power software version 3.1.9.6. power calculations were performed and based on previous preliminary studies I estimated that 6 mice per group would provide 80% power to detect significant differences (α<0.05) for the *P. chabuadi* infection studies, while for the experimental arthritis mouse models, inferring from previous pilot studies, I estimated 8 mice per group will provide 80% power to detect significant differences (α<0.05).

2.1.17 Statistical analysis

Data generated were analysed using Prism software version 9.0 (GraphPad). Variations between groups were assessed using one-way ANOVA followed by appropriate post hoc tests, including Tukey's multiple comparisons test or Dunnett's test, as indicated in the figure legends. For non-parametric data, the Mann-Whitney U test or Kruskal-Wallis test was used. In all figures, significance is denoted as follows: *p < 0.05; **p < 0.01; ***p < 0.001; ****p < 0.0001.

2.2 Section 2: Human section

2.2.1 Human cohort studies

This section details the methods and materials utilised to analyse clinical samples obtained from individuals residing in a malaria-endemic area in Kenya. Expanding upon findings from the mouse studies, I extended the research by utilising archived historical samples at the KEMRI-Wellcome Research Programme, Kilifi, Kenya.

2.2.2 Ethical approval

Approval for participation in these cohort studies was granted by the Kenya Medical Research Institute Ethics Review Committee ref:(KEMRI/SERU/CMR-C/022/3149) and the research was conducted adhering to the principles outlined in the Declaration of Helsinki. Specifically, this involved obtaining informed consent from participants in their local language before any study procedures. Written informed consent for participation in this study was provided by the parents of the children involved.

2.2.3 Children cohorts - study design and participants.

To gain insights into the role of autoantibodies produced following *Plasmodium* infections, I utilised well-established children's cohort at the KEMRI Wellcome Trust in Kilifi, Kenya. Specifically, two distinct children's cohorts were employed: the Kilifi County Hospital admissions cohort, which included children hospitalised for severe forms of malaria, and the Systems Immunology Cohorts (SIMs) cohort, which enabled the collection of longitudinal samples from children under weekly surveillance for uncomplicated malaria in malaria-endemic areas. Further details about each of these cohorts will be described below.

2.2.3.1 Kilifi County Hospital admissions cohort

This study comprises a retrospective cohort investigation involving children residing within the Kilifi Health and Demographic Surveillance System (KHDSS) study area and were admitted to Kilifi County Hospital between January 2018 and December 2018. The hospital has established a regular clinical surveillance system

wherein trained clinicians evaluate children upon admission and discharge. Laboratory tests that involved a complete blood count, malaria blood film, and blood culture were performed on children admitted to the hospital. Following these procedures, samples obtained from this surveillance system are archived and stored at -80°C.

This study's inclusion criteria were children under 14 years admitted with severe malaria. Severe malaria was defined as admission to a hospital with detectable parasites by microscopy and the presence of at least one of the following symptoms:

- Cerebral malaria (defined as a Blantyre coma score of <3)
- Severe malaria anaemia (defined as a haemoglobin concentration of less than five g/dL)
- Respiratory distress (defined as deep breathing as assessed by a clinician).

Additionally, given that asymptomatic parasitaemia is common in malaria-endemic regions and clinical features of severe malaria may overlap with other common causes of admission, therefore a parasite threshold was incorporated to enhance specificity, where the inclusion criteria were restricted to parasitaemia above 2500 parasites/µL [296].

2.2.3.2 Systems immunology cohorts (SIMs)

The study participants were recruited from a community-based cohort in Junju and Ngerenya villages along Kenya's coastal region [297,298]. These cohorts aim to evaluate malaria immunity in children by continuously monitoring them from birth to a maximum of 15 years. Participants undergo weekly malaria surveillance, yearly cross-sectional bleeds, and active clinical surveillance. Junju experiences moderate to high *P. falciparum* transmission, while Ngerenya has seen a significant reduction in malaria incidences since 2005 to very low [299].

Notably, *P. falciparum* episodes are typically diagnosed during weekly active surveillance conducted by a field worker in the same village as the child. During these visits, the field worker records auxiliary body temperature and recent fever history. If a child is febrile, a blood sample is collected for a *Plasmodium*

falciparum specific rapid diagnostic test (RDT) and blood smears. Clinical malaria episodes are identified by a body temperature exceeding 37.5°C and 2,500 parasites per microliter of blood. Additionally, an annual cross-sectional survey precedes Kilifi's main malaria transmission season. During these surveys, 5 mL of venous blood is collected for immunological studies, and blood smears are performed to determine cross-sectional *Plasmodium falciparum* densities and prevalence.

2.2.4 Adult cohorts - Study design and participants

2.2.4.1 Cross-sectional Adult Bleed Adult Samples

In this study, I included individuals aged 18-60 living in a malaria-endemic area in Kilifi, Kenya. These participants were part of an ongoing annual cross-sectional bleed conducted in two villages, Ngerenya and Junju, which are approximately 20 km apart. Junju, located on the southern side, experiences continuous moderate to high malaria transmission, with *Plasmodium falciparum* prevalence of 30% during the dry period (January to May), increasing to 70% during the high transmission seasons (May to August and October to December). In contrast, *Plasmodium falciparum* transmission has significantly diminished in Ngerenya since 2005. In 1998, Ngerenya had a parasite prevalence of 40% and a transmission intensity of 10 infective bites per person per year. However, since 2005, transmission has dropped to negligible or very low levels in this village [299] .

2.2.5 ELISA for detection of antibody responses to the native and citrullinated peptides

ELISA, as previously described [289] was used to detect and quantify antibodies to four well-characterised native peptides and their corresponding citrullinated peptides (Table 2-2). Briefly, 96-well plates (Costar) were coated with 50 μL/well of 12.5 μg/mL in coating buffer (Carbonate-Bicarbonate Buffer -Sigma). The plates were washed three times using PBS/0.05% Tween (Sigma), followed by blocking with 5% BSA/PBS at room temperature for 2 hours (hr). Human plasma samples (archived and stored at -80°C) were retrieved from -80°C and left to thaw, diluted at 1/50, and incubated overnight. After the incubation, the plates were washed three times with PBS 0.05% Tween (Sigma), followed by incubation with horseradish peroxidase-conjugated rabbit anti-mouse murine ELISA and rabbit

anti-human IgG diluted at 1/5000 (Dako), at room temperature for 1.5 hr. This was then followed by further washing using PBS 0.05% Tween (Sigma) and incubation with 100 µl of O-Phenylenediamine Dihydrochloride (OPD) at a final concentration of 0.4 mg/mL (Sigma). The plates were then stopped with 50 µl of 2 M H2SO4, and absorbance was read at 492 nm using a microplate reader. A standard curve was prepared to determine the relative antibody titres in arbitrary units for all the samples.

2.2.6 Schizont ELISA

The antibody response to the schizont extract was determined as previously described [300,301]. Schizont extract from *Plasmodium falciparum* 3D7 strain was prepared and coated on high absorbance ELISA plates (Costar) in coating buffer (Carbonate-Bicarbonate Buffer -Sigma-Aldrich). Briefly, 96-well plates (Costar) were coated with 100 µL/well of schizont extract diluted 1:10,000 in the coating buffer and incubated overnight at 4°C. Following this, the plates were then washed three times using PBS/0.05% Tween (Sigma), followed by blocking with 200 µL of 5% BSA/PBS at room temperature for 2 hours. Plasma from human samples was diluted at 1:1000 in 1% BSA/PBS and added to the plates, followed by incubation overnight at 4°C. In addition, malaria immune globulin (MIG) generated from a pool of plasma samples from individuals residing in an area of high malaria transmission was titrated on each plate, serving both as a positive control and providing values for a standard curve to convert optical density (OD) readings into concentration. Following incubation, the plates were washed three times with PBS/0.05% Tween (Sigma), followed by incubation with horseradish peroxidase-conjugated rabbit anti-mouse and rabbit anti-human IgG, diluted 1:5000 (Dako), at room temperature for 1.5 hours. The plates were then washed six times with PBS/0.05% Tween (Sigma) and incubated with 100 µL of O-Phenylenediamine Dihydrochloride (OPD) at a final concentration of 0.4 mg/mL (Sigma). The reaction was then stopped with 50 µL of 2 M H2SO4, and the absorbance read at 492 nm using Tecan Sunrise plate reader (Tecan).

2.2.7 Flow cytometry

2.2.7.1 B cell extracellular staining

Frozen Peripheral Blood Mononuclear Cells (PBMCs) were thawed in a 37°C water bath until pea-sized ice crystals remained. In a biosafety cabinet, 1 mL of pre-warmed RPMI 1640, supplemented with Penicillin/Streptomycin, L-Glutamine, and Fetal Calf Plasma (FCS), was gently added dropwise to the thawed cells. The cells were then transferred to a 15 mL tube with 10 mL of the RPMI media followed by centrifugation at 440x g for 7 minutes. Following this, the cells were washed once with RPMI buffer and rested at 37°C for 2 hours before undergoing two additional washes with 10 mL RPMI buffer followed with centrifugation at 440x g for 7 minutes. After washing, cell viability was assessed using trypan blue staining. With a minimum of 1 million cells per sample surface stained using an antibody mix primarily targeting B cells (Table 2-3) in the dark for 30 minutes. Subsequently, the cells were washed twice in FACS buffer (PBS + 2 mM EDTA + 2% FBS) and stained with a viability dye at a 1/1000 dilution for 15 minutes at room temperature in the dark.

2.2.7.2 B cell intracellular staining

For intracellular staining of T-bet and FCRL5, B cells were initially stained for surface markers as described above. Subsequently, cells were fixed and permeabilised using the FoP3 buffer staining kit as per the manufacturer's instructions (Thermo Fisher Scientific). After washing, cells were stained with the respective antibodies (Table 2-4) for 30 minutes at room temperature, followed by another round of washing before acquisition on a 5-laser BD LSR Fortessa flow cytometer. Gating was performed using FlowJo software version 10.4.2. (FlowJo LLC, Ashland, OR, USA).

Table 2-3 : B cell extracellular flow cytometry cell staining panel

Marker	Fluorochrome	Clone	Dilution	Company
CD19	APC R700	HIB19	1/40	BD
IgD	BV421	IA6-2	1/40	BD
CD10	APC	HI10a	1/20	BioLegend
CD20	BV711	2H7	1/40	BioLegend
CD21	FITC	BU32	1/40	BioLegend
CD27	BV650	O323	1/20	BioLegend
CD14	BV605	M5E2	1/20	BioLegend
CD11c	BV786	BLY6	1/20	BD
Viability	BV510		1:1000	BD

Table 2-4: B cell intracellular flow cytometry cell staining panel

Marker	Fluorochrome	Clone	Dilution	Company
FCRL5	PE	509F6	1/20	BioLegend
TBET	PE-Cy7	4B10	1/20	BioLegend

2.2.7.3 T cell extracellular flow cytometry staining

Frozen Peripheral Blood Mononuclear Cells (PBMCs) were thawed in a 37°C water bath until pea-sized ice crystals remained and processed as described above. A minimum of 1 million cells per sample underwent surface staining using an antibody mix primarily targeting T cells, as outlined in (Table 2-5). After staining, the cells were washed twice in FACS buffer (PBS + 2mM EDTA + 2% FBS) and treated with a viability dye at a 1/1000 dilution for 15 minutes at room temperature in the dark.

2.2.7.4 Intracellular staining of T cells

For intracellular staining of FOXP3, cells were initially surface stained as described in section 2.2.7.1. Subsequently, the cells were fixed and permeabilised using the FOXP3 Fix/Perm staining kit (eBiosciences) following the manufacturer's instructions. After washing, the cells were stained with antibodies (Table 2-6) for 30 minutes at room temperature in the dark, followed by another round of washing before acquisition on a 5-laser BD LSRFortessa flow cytometer. Gating was performed using FlowJo software version 10.4.2. (FlowJo LLC, Ashland, OR, USA).

Table 2-5: T cell extracellular flow cytometry cell staining panel

Marker	**Fluorochrome**	**Clone**	**Dilution**	**Company**
CD20	FITC	2H7	1/40	BioLegend
CD14	FITC	M5E2,	1/20	BioLegend
CD19	FITC	HIB19	1/20	BioLegend
CD4+	PerCP/Cyanine 5.5	RPA-T4	1/40	BioLegend
CD3	BV605	OKT3	1/20	BioLegend
CD45RA	BV650	HI100	1/20	BioLegend
CD25	BV786	M-A251	1/40	BioLegend
Viability	BV510		1/1000	BD

Table 2-6: T cell intracellular flow cytometry cell staining panel.

Marker	Fluorochrome	Clone	Dilution	Company
FOXP3	AF647	206D	1/20	BioLegend

2.2.8 Autoantibody profiling using the OmicsArray

Antibody responses to known autoantigens were analysed using the OmicsArray™ Antigen Microarray Profiling Services by GeneCopoeia (Rockville, Md). The plasma samples were initially pre-processed through digestion with DNASE I enzyme, with a 30-minute incubation period. Following this step, slides were carefully assembled onto the hybridisation cassette and sealed using 16-well silicone gaskets to create leak-proof individual wells. 100 µL of wash buffer was then added to each array, followed by shaking at 0.181x g for 5 minutes using VWR® high-speed microplate shake. After incubation, the wash buffer was discarded using a pipette, and then the slides were incubated with 100 µL of block buffer at room temperature for 1 hour on a shaker. Following the blocking process, the slides were washed twice with PBST (100 µL for each well), with each wash step lasting 5 minutes on the shaker.

The plasma samples initially digested with DNASE I were further processed by adding 90 µL PBST into each digested plasma sample or control. These samples were added to each well on the slide (100 µL) and incubated at room temperature for 1 hour on the shaker. After sample incubation, arrays were washed with PBST, followed by blocking buffer, and then PBST once more, each with a 5-minute incubation on the shaker. Following the washing steps, anti-human IgG (Cy3-conjugated) antibodies (diluted 1:1000 in PBST) and Cy5 anti-human IgM (diluted 1:1000 in PBST) were added and incubated at room temperature for 1 hour in a shaker. Following the incubation, arrays were washed with 100 µL PBST (3x) per well, with a 5-minute incubation for each wash. The slides were carefully disassembled from the hybridisation cassettes, rinsed with 45 mL of PBS (2x) with a 5-minute incubation on the shaker, and finally with 45 mL of nuclease-free water (2x), each for 5 minutes with incubation on the shaker per wash. The slides were dried by centrifugation at 300x g for 5 minutes using a combiSlide adapter (Eppendorf).

2.2.9 Acquisition of array images and subsequent data processing

For array image capture and data processing, fluorescent signals were acquired using the GenePix 4300A microarray scanner. The 532 nm channel was used to scan Cy3 fluorescence, allowing the detection of IgG and the 647 nm channel was

used for Cy5, allowing the detection of IgM. Raw data, including foreground, background signals and the signal-to-noise ratio (SNR), were obtained by extracting the fluorescent signals using GenePix™Pro v7.0 software.

2.2.10 Statistical analysis for protein microarray data

Data generated using the protein microarray assay was analysed using protGear v1.3.31, [302], a pre-processing suite integrated into R v4.3.1 and allows for background correction, quantification of within-sample variation, normalisation, and batch correction that is specific for protein microarray.

3 Chapter 3- Characterisation of anti-citrullinated protein antibodies (ACPA) and corresponding native protein antibodies following *P. chabaudi* infection in a murine model

3.1 Introduction

Autoimmune disease incidence is on the rise, with a global prevalence of 12.5 % worldwide [303,304], and a greater fraction of this increase is attributed to environmental exposures and other lifestyle changes [304]. While the induction of autoimmune disease is driven by the complex interaction of genetics and environmental factors [305], the aetiology of most autoimmune diseases is still considered to be either "complex" or "multifactorial".

Importantly, infections which are considered environmental factors have been implicated in the pathogenesis of autoimmunity [136], with several pathogens, such as viruses, bacteria, and parasites, including HIV, tuberculosis, and malaria, reported to trigger autoimmunity [136,138]. Additionally, it is well-known that infections such as malaria and COVID-19 that induce an acute inflammatory response often results in elevated levels of autoantibodies targeting diverse host antigens, including nucleic acids, membrane proteins, carbohydrates, as well as phospholipids [6,306]. While some of these infection-induced autoantibodies are known, the role that they play in infection-induced pathogenesis is only beginning to be elucidated.

Malaria, a disease caused by *Plasmodium* species, was linked to autoimmunity by the induction of anti-self-antibodies, and the presence of anti-self-antibodies was associated with increased disease severity in children [1,2,253]. Importantly, while antibodies elicited following *Plasmodium* infections are essential for protection from clinical malaria, a phenomenon that was first demonstrated by the seminal experiments of S. Cohen [174], intriguingly, only a small fraction of antibodies produced in *P. falciparum* infections recognise parasite antigens; some of these antibodies target host antigens, while others produce polyreactive antibodies [307]. Moreover, while the presence of autoantibodies during *Plasmodium* infections is a well-known phenomenon, the association between malaria and autoimmune disease was first observed by Greenwood [9,10] through historical studies, reported

that systemic lupus erythematosus (SLE) was rarer in Nigeria and further proposed [10], that parasitic infections might possibly provide some degree of protection against SLE.

Furthermore, experimental data from mice also supported this idea, with mice infected with *P. yoeli* observed to be protected from severe autoimmune nephritis (the hallmark of SLE), in both the SLE-prone NZB/NZW mice [9] or FcyR2B-deficient mice [261]. Although both the epidemiological studies and experimental evidence suggest that *Plasmodium* infections are able to modulate the immune system to alleviate autoimmune severity, there is a need to give consideration to the fact that the true incidence of autoimmune disease in sub-Saharan Africa has remained debatable, with the current evidence suggesting that autoimmune diseases could be occurring at similar prevalence rate to those reported in more developed countries [11]. Thus, necessitating the need to revisit this association between malaria and autoimmunity.

Rheumatoid arthritis (RA), like SLE, is an autoimmune disease that occurs as a result of a complex interplay between genetic predisposition and environmental triggers and is driven by continuous inflammation affecting peripheral joints, leading to swelling, stiffness, pain, and progressive joint destruction [308]. An essential feature of RA is the formation and presence of autoantibodies against modified antigens known to occur through the conversion of peptidyl arginine to peptidyl citrulline, which is referred to as citrullination [309].

This process is catalysed by Peptidylarginine deiminase (PAD) enzymes which play a critical role of catalysing the citrullination of arginine residues, converting them into citrulline, a modification linked to autoantibody production in inflammatory conditions [310]. In humans these enzymes are encoded by five genes (PAD1–PAD4 and PAD6) located on chromosome 1 [311]. While, in mice, these enzymes are encoded by four genes (*Padi1*, *Padi2*, *Padi3*, and *Padi4*), located on chromosome 4 [311].

Interestingly, citrullination targets several proteins such as type II collagen, fibrinogen, a-enolase, filaggrin, histones, and vimentin [312], and is considered a normal physiological process involved in numerous biological functions such as

brain development and cell death; it is however, been reported to be overrepresented in inflammation-related diseases such as RA, multiple sclerosis, and Alzheimer's disease [313]. While citrullination is a normal response at inflammation sites, anti-citrullinated antibodies, which precede the onset of symptoms in RA and are associated with poor outcomes and joint destruction, serve as RA diagnostic markers, and it's detected in two-thirds of patients with a specificity of 98% [314]. Several of these citrullinated peptides, including fibrinogen, vimentin, enolase, type II collagen, and tenascin C, are recognised in RA and are crucial in the diagnoses of clinical RA [315].

Thus, in this chapter, using mouse models, I investigate whether antibody responses to the native and citrullinated peptide antigens that are relevant to the diagnosis of RA occur in the setting of *Plasmodium* infections. In addition, I use a chronic *Plasmodium* infection to gain insights into the kinetics of autoantibody production, using *P. chabaudi* infection (a mouse *Plasmodium* parasite that closely resembles the human *P. falciparum*).

3.1.1 Study rationale

The rationale for examining the presence of anti-citrullinated protein antibodies (ACPA) and corresponding native protein antibodies in *P. chabaudi*-infected mice was twofold: first, our laboratory had access to an experimental arthritis mouse model already established [282]; second, ACPA is an important diagnostic biomarker for RA used in a clinical setting [314]. Furthermore, the broader aim of the project was to evaluate whether elevated production of autoantibodies as a consequence of *Plasmodium* infections would lead to increased susceptibility to autoimmune disease later in life. Thus, applying a pre-existing RA mouse model in our laboratory aligned with the overall goal of this project of testing the hypothesis that infectious diseases such as malaria might contribute to the triggering or exacerbation of autoimmune responses such as rheumatoid arthritis.

Thus, here I report the induction of antibody responses to the native and citrullinated peptide antigens, in the context of *Plasmodium* infection by a rodent malaria parasite, *P. chabaudi*. While previous research has demonstrated that *Plasmodium* infection does induce autoantibody production, the production of antibody responses to the native and citrullinated peptide antigens in *Plasmodium*

infections is yet to be studied. Thus, the research presented here adds new knowledge and improves our understanding of antibody responses to the native and citrullinated peptide antigens production in *Plasmodium* infections, therefore providing further insights into the kinetics of antibody responses to the native and citrullinated peptide antigens and immunological triggers of autoimmunity, particularly the contribution of environmental triggers.

3.1.2 Chapter aims and summary

This chapter aims to investigate the complex interplay between *Plasmodium* infection and autoantibody production. First, I compared the levels of ACPA and corresponding native protein antibodies between an acute *P. chabaudi* infection model (Figure 3-1) and mice in the chronic experimental arthritis (CEA) model group (Figure 3-2). Next, I investigated the kinetics of antibody responses against both the native and citrullinated antigens during a chronic *P. chabaudi* infection. Lastly, I assessed whether the production of these autoantibodies was specific to *Plasmodium* infections and further explored the potential mechanisms underlying their production, including the role of PAD enzymes through PAD inhibition studies.

3.2 Results

3.2.1 Establishing assays to detect ACPA and corresponding native protein antibodies

To establish whether *P. chabaudi* infection elicited the production of ACPA and corresponding native protein antibodies, I conducted a series of experiments using female mice. Initially, the mice were infected with *P. chabaudi*, and chloroquine-treated 5 days later as depicted in (Figure 3-1). Unfortunately, due to the mice developing severe anaemia, the mice had to be euthanised early in the experiments for humane reasons. Additionally, given that ACPA production is associated with rheumatoid arthritis (RA), I next investigated if the levels of antibody responses to both the native and citrullinated peptides induced in the *P. chabaudi* infection model would be comparable to those produced in acute experimental arthritis (AEA) and chronic experimental arthritis (CEA) mouse model.

Therefore, I set up ELISA assays using samples from the acute *P. chabaudi* infection model and archived serum samples detailed in (section 2.1.10) from mice from an "acute" and "chronic" experimental arthritis model of RA (EA), outlined in (Figure 3-2). The samples from the RA model were initially part of research conducted by a previous PhD student in our lab (Shaima Mazin Jawad Al Khabouri) [284]. ELISA assays [289] were then performed to assess immune responses to both the native and citrullinated Tenascin-C5 peptide (c-TNC5) and Fibrinogen (c-FIB) in the *P. chabaudi* group and the mice in the experimental arthritis groups.

These results indicated that mice infected with acute *P. chabaudi* elicited comparable levels of antibody responses to both the native and citrullinated peptides, similar to the responses observed in both the "acute" and "chronic" experimental arthritis groups (Figure 3-3 A-H).

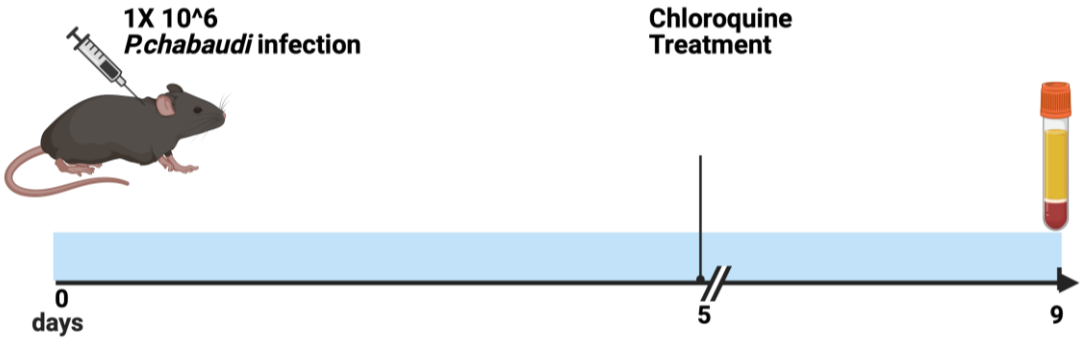

Figure 3-1: Acute *P. chabaudi* infection model - Initial timepoint for assay establishment. This figure illustrates the initial stages of establishing the acute P. chabaudi experimental protocol. 6- 8-week-old female mice (n=5 per group) were injected intraperitoneal (I.P.) with 100 µL of 1x10^6 P. chabaudi infected RBC and parasitaemia was monitored daily by thin blood smears stained with Giemsa's stain. Mice were then treated with 20 mg/kg of Chloroquine diphosphate salt (Sigma-Aldrich, Poole, UK) I.P. 5 days post infection to clear the infection. The mice were then left to rest for four days, following which they were placed under terminal anaesthesia; blood was drawn by cardiac puncture and used for further experiments. Image created with BioRender.com

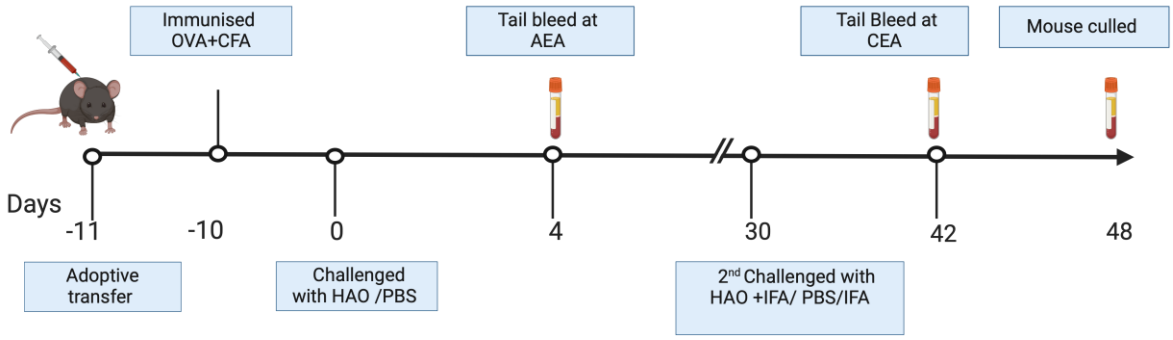

Figure 3-2: Experimental outline of the "acute" or "chronic" experimental arthritis model in mice.

To induce either the "acute" or "chronic" experimental arthritis in mice, OTII T cells were first isolated from transgenic mice and were subsequently induced to differentiate into a Th1 phenotype. These Th1-polarised CD4+ T cells were transferred into recipient C57BL/6 mice (n=5). One day following the transfer, OVA antigen was prepared and administered to the mice, and ten days post-immunisation with the OVA antigen, the mice were subjected to a footpad challenge using either heat aggregated OVA antigen (HAO) or PBS. Mice in the AEA groups were culled four days later. For the CEA group, mice that had been previously immunised and challenged with HAO were rechallenged with HAO 30 days later through subcutaneous injection of 50 µL containing 100 µg of HAO in incomplete Freund's adjuvant (IFA) into the same foot that had initially been challenged. The control group received a 50 µL injection of PBS alone. A tail bleed was performed on day 42 to collect serum samples, and the mice were euthanised 5 days later. Image created with BioRender.com

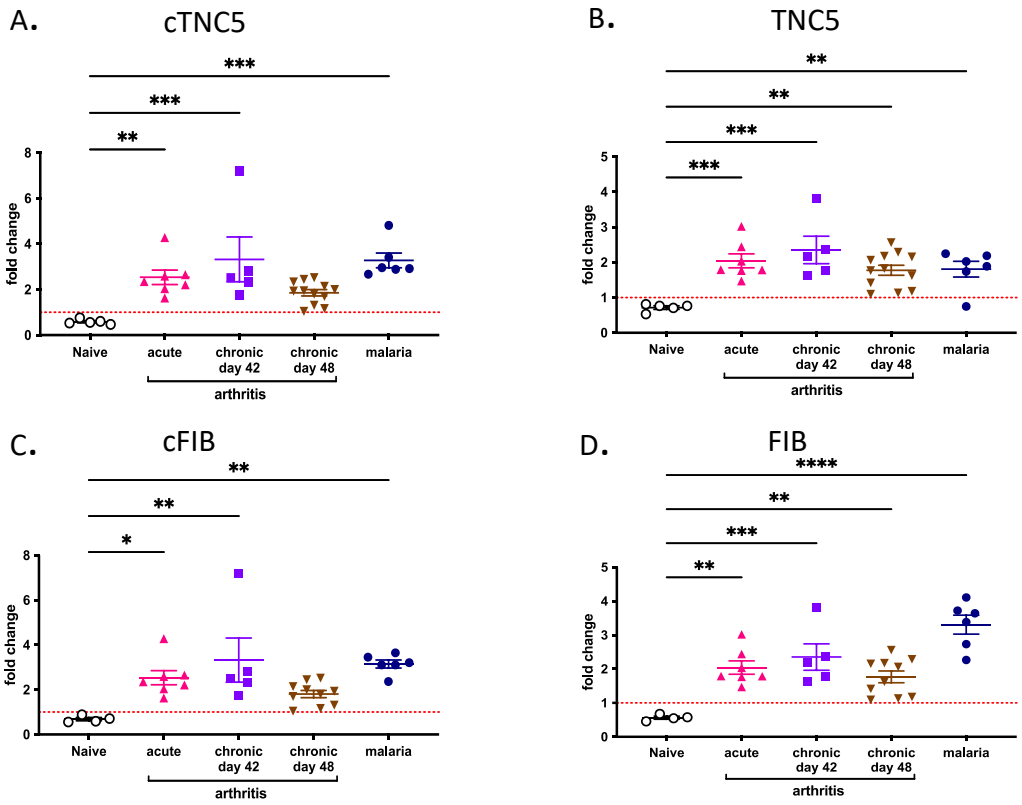
A.
cTNC5
***
***
**
fold change
Naive
acute
chronic day 42
chronic day 48
malaria
arthritis
B.
TNC5
**
**
***
***
fold change
Naive
acute
chronic day 42
chronic day 48
malaria
arthritis
C.
cFIB
**
**
*
fold change
Naive
acute
chronic day 42
chronic day 48
malaria
arthritis
D.
FIB
****
**
***
**
fold change
Naive
acute
chronic day 42
chronic day 48
malaria
arthritis

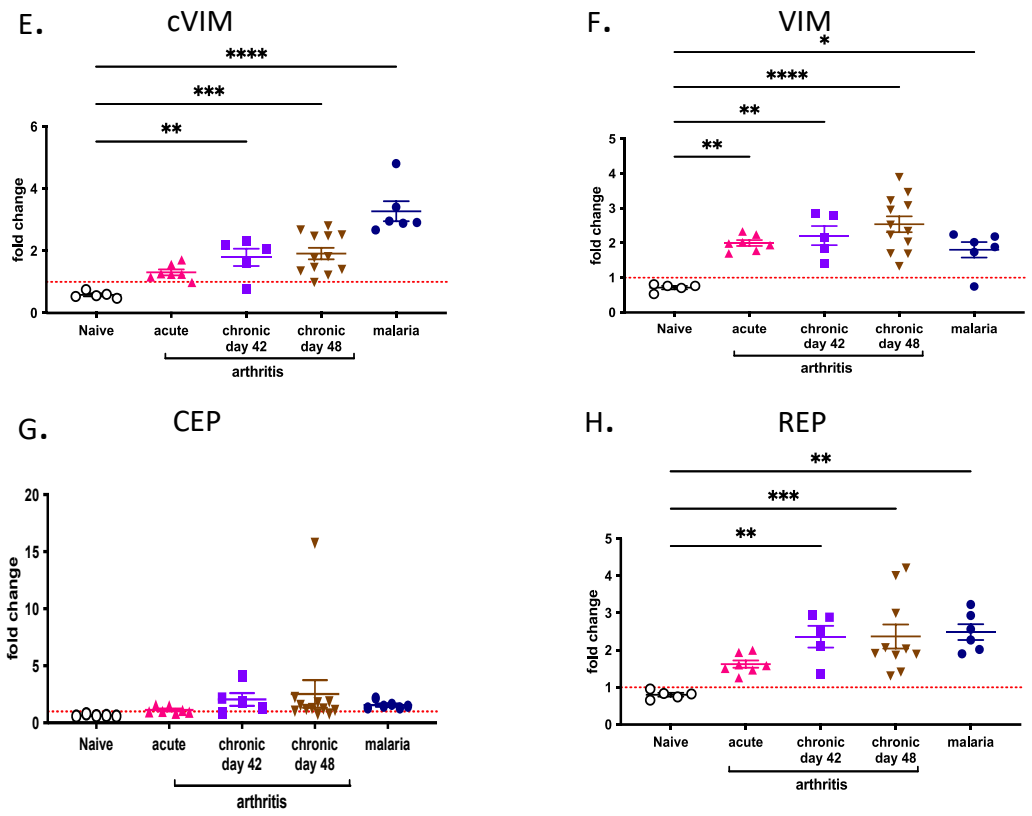

Figure 3-3: Increased autoantibody responses to both citrullinated and corresponding native peptides following *P. chabaudi* infection.

Female C57BL/6 mice, ages 6–8 weeks, were infected with P. chabaudi and culled nine days later. Serum samples were obtained from the P. chabaudi-infected mice (P.C) (blue) as well as from mice in the experimental arthritis group, including the "Acute EA" (pink), "Chronic EA D42" (purple) and "Chronic EA D48" (brown). ELISA was then performed to determine the IgG levels against the citrullinated and native forms of tenascin C5 peptide (panels A and B), fibrinogen (panels C and D), vimentin peptide (panels E and F) and a-enolase (panels G and H). Graphs represent mean values with standard error of the mean (SEM). A one-way ANOVA with Dunnett's multiple comparisons test was performed (* p <0.05, **p<0.005, ***p<0.0005).

3.2.2 Induction of varying levels of cFIB/FIB and cTNC5/TNC5 autoantibodies in mice infected with *P. chabaudi*

Next, having established that *P. chabaudi infection* induced the production of antibody responses to the native and citrullinated peptide antigens, I set up experiments to understand the kinetics of these autoantibodies during chronic *P. chabaudi infection*. I therefore set up a time course experiment using three groups of mice: naive control mice (n=6) and two groups of mice that were infected (n=6) with *P. chabaudi*. While one group of the infected mice was treated with chloroquine to model an acute infection, the other group was left untreated to model chronic infections as outlined in the experimental outline (Figure 3-4 A). Tail bleeds were then taken periodically over 63 days, and ELISA was used to determine the levels of antibodies to two native peptides, Tenascin C5 peptide (TNC5) and Fibrinogen (FIB), and their corresponding citrullinated peptides (cTNC5 and cFIB). Parasitaemia was also monitored using Giemsa staining over this time course. Antibodies to cTNC5/TNC5 and cFIB/FIB peptides were observed to peak at week 2 (Figure 3-4 B-E), one week following the peak parasitaemia of 20–35% observed between days 7–9 (Figure 3-4 F): which was then followed by a decline in the level of autoantibodies. Notably, the levels of antibody responses to the native and citrullinated peptide antigens observed at the later time points were still higher than the baseline levels observed in the naive group. Thus, our results show that peak antibody responses to the native and citrullinated peptide antigens production is driven by parasite presence, and that they persist at low levels post-parasite clearance, providing valuable insights into when and how these autoantibodies are produced.

A.

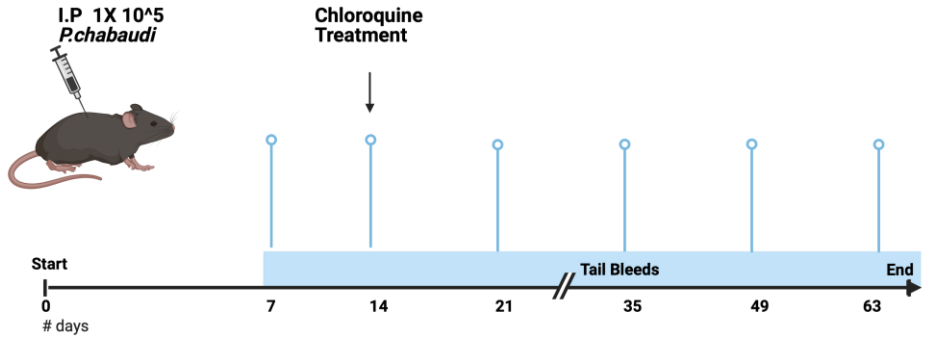
I.P 1X 10^5
P.chabaudi
Chloroquine
Treatment
Start
Tail Bleeds
End
0
7
14
21
35
49
63
days


P.C +Chloro
P.C
Naive

B.

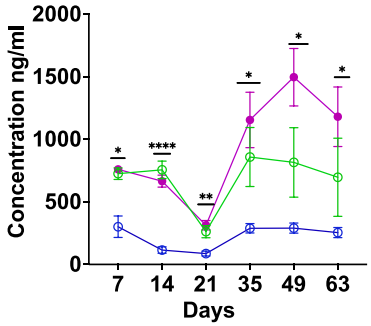
Anti-cFIB
Concentration ng/ml
2000
1500
1000
500
0
7
14
21
35
49
63
Days

C.

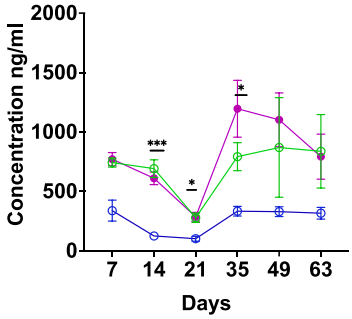
Anti-FIB
Concentration ng/ml
2000
1500
1000
500
0
7
14
21
35
49
63
Days

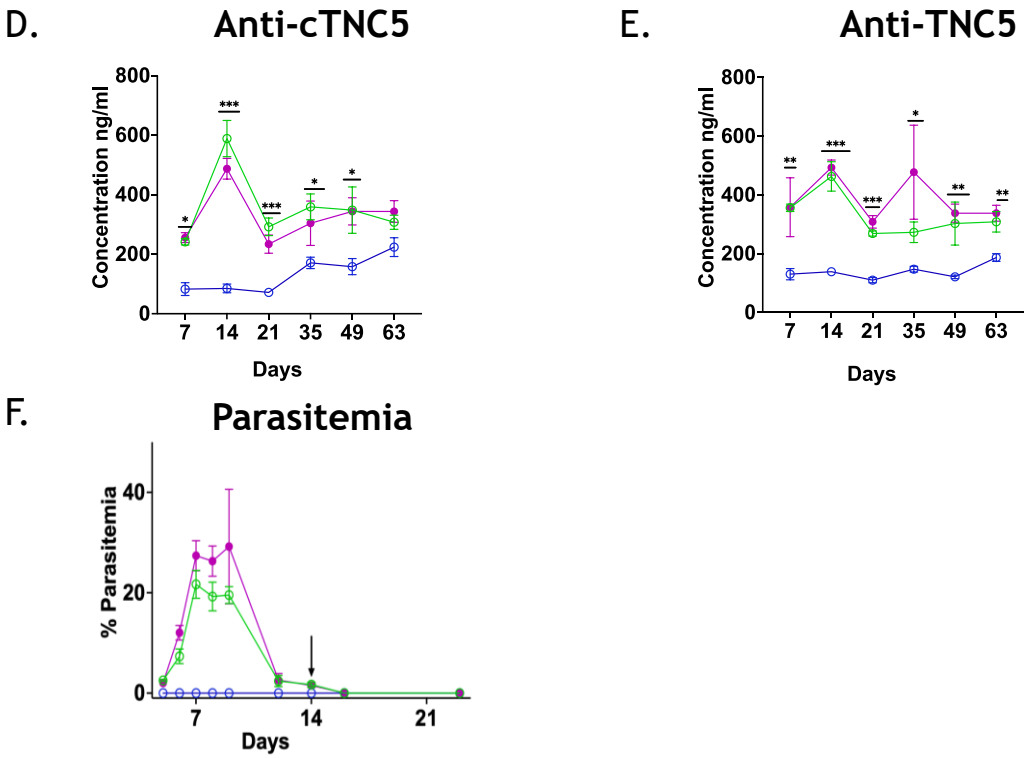

Figure 3-4: Autoantibody kinetics following *P. chabaudi infection* in treated and untreated malaria-infected mice.

A.) *P. chabaudi infection* model for the autoantibody kinetics. 7–8-week C57BL/6 male mice (n=6) were infected with 1 X 10^5 *P. chabaudi* infected RBC; one group of mice was chloroquine treated while the other was left untreated, and naive mice were also included as control. Tail bleeds were taken periodically for ELISA and over a 63-day period, as highlighted by the various time points on the outline. A time-course of the autoantibody response to cTNC5 and cFIB and the corresponding native peptides TNC5 and FIB was determined using ELISA in the infected chloroquine treated (green), infected+ untreated mice (pink) and in the naive mice (blue). (B) Anti-cFIB. (C) Anti-Fib, (D) Anti-cTNC5, (E) Anti-TNC5 autoantibody response. The levels of parasitaemia were also determined using microscopy over the course of the infection. (F) Percentage parasitaemia over a several days with arrow indicating timepoint for chloroquine treatment. Graphs show the mean with SEM, Tukey's multiple comparisons test was performed (* p <0.05, **p<0.005, ***p<0.0005).

3.2.3 Persistent B and T Cell activation following infection with *P. chabaudi* at day 63

The exact mechanism driving the break of self-tolerance against citrullinated antigens remains unknown; however, there is recent evidence suggesting that ACPA immune response in RA are first initiated by a 'hit' of low-level ACPA production resulting from either genetic or environmental factors, which is then followed by a 'second hit' of increased arthritogenic factors leading to higher ACPA levels and a more mature inflammatory autoimmune response [316]. While the presence of antibody responses to the native and citrullinated peptide antigens has now only been reported in the context of *Plasmodium* infections in this study, the production of other autoantibodies induced by *Plasmodium* infections has been linked to various mechanisms such as molecular mimicry, bystander activation, epitope spreading or B-cell hyperactivation [8]. Here, I evaluate potential immune mechanisms influencing the production of antibody responses to the native and citrullinated peptide antigens in mice infected with *P. chabaudi*. The aim was to identify changes in the proportions of immune cells correlated with the increased levels of these autoantibodies at the end of 63 days, when the parasites are all cleared, but the levels of antibody responses to the native and citrullinated peptide antigens, though produced at lower levels, are still higher than the naive.

I conducted experiments to evaluate changes in humoral immune responses. Specifically, I assessed the activation status of CD4+ T cells and germinal centre B cells at 63 days post-infection. T follicular helper (Tfh) cells are known for their crucial role in promoting antibody production by activating B cells within the germinal centres and thus, are important in generating high-affinity, class-switched antibodies necessary for effective pathogen defence [317]. Activated CD4+ T cells were therefore identified using specific markers (Figure 3-5). Herein, increased CD44+ CD4+ T cells and PD1+ ICOS+ CD4+ T cells were elevated in the treated and untreated *P. chabaudi* experimental groups compared to the naive group (Figure 3-6 A-B). Notably, given that *Plasmodium* infections have been linked to immune perturbations [192], particularly B cell dysregulation, I next focused on germinal centre B cells. A significant increase in the percentage of

germinal centre B cells was observed in the *P. chabaudi*-infected experimental groups compared to the naive group (Figure 3-6 C).

In addition, the percentage of atypical B cells reported to be associated with chronic complications in malaria, HIV and autoimmunity [318] were also assessed in both the treated and untreated mice after *P. chabaudi* infection (Figure 3-6 D) and a higher percentage CD11c B cells were observed in both treated and untreated mice infected with *P. chabaudi*. These findings further suggest that *P. chabaudi* induces an enhanced humoral immune response during *Plasmodium* infections, with the activation of CD4+ T cells resulting in an increase in germinal centre B cells and the presence of atypical B cells.

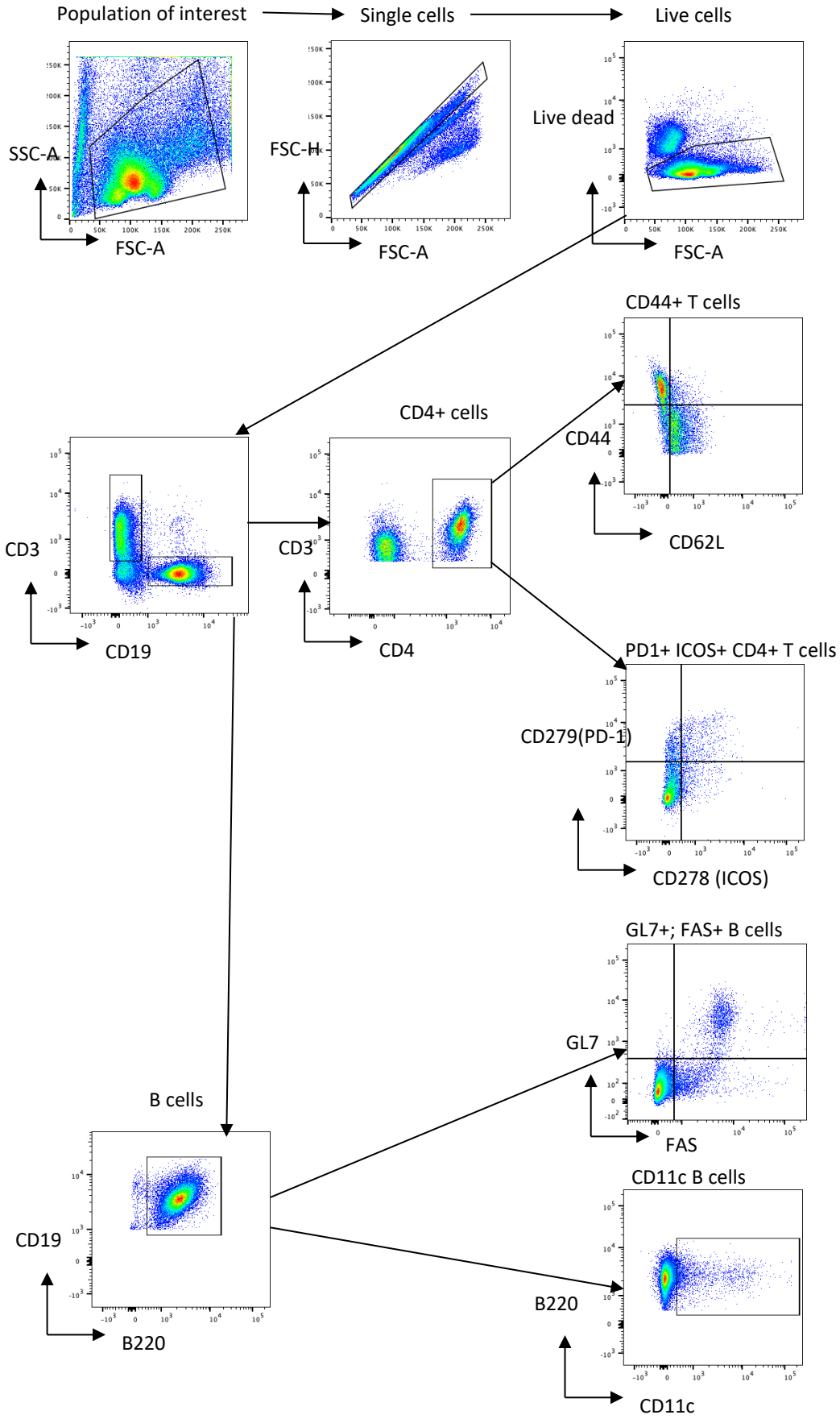
Population of interest
Single cells
Live cells
SSC-A
FSC-A
FSC-H
FSC-A
Live dead
FSC-A
CD44+ T cells
CD4+ cells
CD44
CD62L
CD3
CD19
CD3
CD4
PD1+ ICOS+ CD4+ T cells
CD279(PD-1)
CD278 (ICOS)
GL7+; FAS+ B cells
GL7
FAS
B cells
CD19
B220
CD11c B cells
B220
CD11c

Figure 3-5: Gating strategy to identify activated CD4+ T cells and B cells from spleen of infected mice.

Illustrates the flow cytometry gating strategy for identifying activated CD4+ T cells and B cells from the spleens of infected mice. Initially, splenocytes were isolated and stained according to methods detailed in the method section. Activated CD4+ T cells were identified by gating on lymphocytes, single cells, and live cells, followed by the selection of CD3+ CD19- cells and the CD4+ marker. CD4+ T cells were then identified based on the CD44 (CD44hi) and CD62L markers, along with other markers such as ICOS and PD-1. For B cells, after gating on lymphocytes, single, and live cells, I isolated CD3- CD19+ cells. Germinal centre B cells were further identified within the CD19+ B220+ population using GL7 and FAS markers, and an additional marker, CD11c, was also used to identify CD11c B cells.

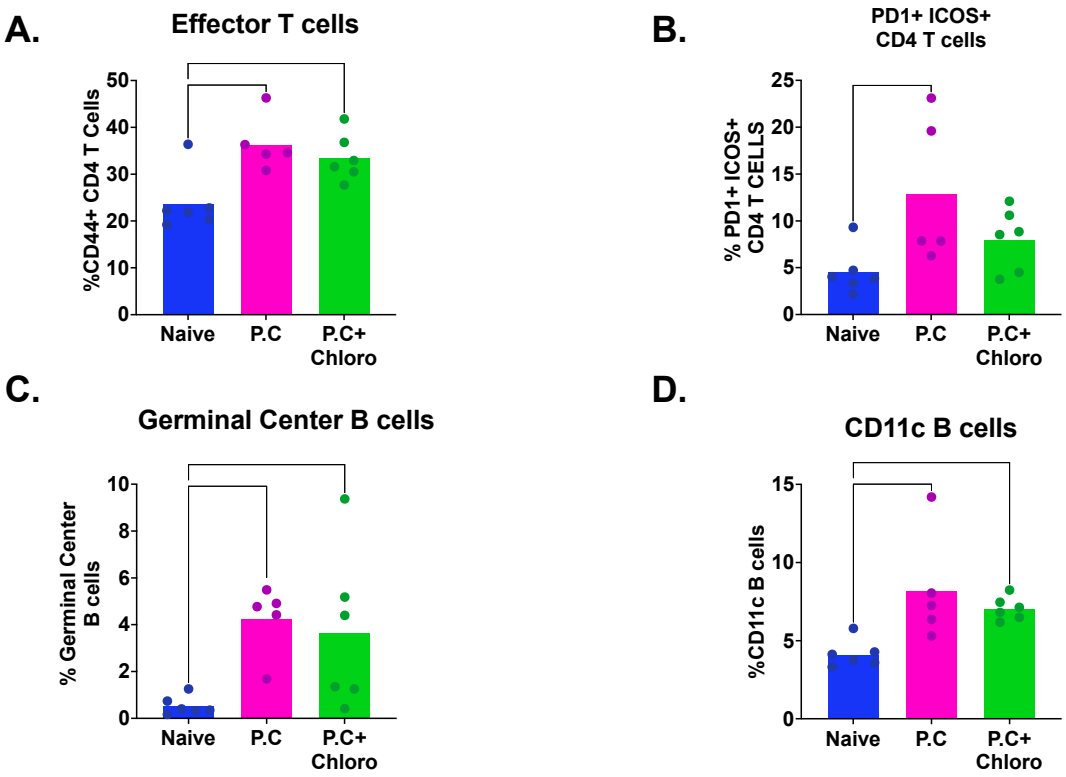

Figure 3-6: Persisting T and B cells activation status following parasite clearance.

Mice were infected with *P. chabaudi;* one group was chloroquine treated while the other group was left untreated. Spleen was harvested 63 days post-infection for flow cytometry analysis. A.) Bar chart showing the percentage of CD44+ CD4+ T cells. B.) Percentage of PD1+ ICOS+ CD4+ T cells C.) Percentage of GL7+ FAS+ B cells D). Percentage of CD11c B cells from the spleen of chloroquine treated (green), untreated(pink), and (Blue) naive mice. Statistical analysis one-way ANOVA with Dunnett's multiple comparisons test ns: not significant * p-value of < 0.05; **: p<0.01.

3.2.4 Increased activation of B and T cells on day 7 post- *P. chabaudi* infection: A timepoint associated with peak antibody responses to the native and citrullinated peptide antigens

To further understand the immune profile associated with increased antibody responses to the native and citrullinated peptide antigens , specifically at week 2. I set up an experiment where mice were infected with *P. chabaudi and* culled 7 days post infection (Figure 3-7 A). The spleens were harvested, and flow cytometry was performed. This timepoint was important as it aligned with the peak parasitemia (Figure 3-4 F) and the anticipated peak in the levels of antibodies to the native and citrullinated peptide antigens at the two-week point (Figure 3-4 B-E). This approach was based on the understanding that both the germinal centre reaction and T cell response would precede the elevated antibody responses to the native and citrullinated peptide antigens observed in the second week.

At this time point mice in the *P. chabaudi* group showed increased levels of CD44HI CD4+ T cells and ICOS+PD1+ CD4+ T cells (Figure 3-7 B-C) compared to the naive. A similar trend was also observed with both cells germinal centre B cells and the CD11c B cells (Figure 3-7 D-E). These findings, therefore, underscore the significant immune activation induced by *P. chabaudi* infection, that correlated with the critical period of increased antibody responses to the native and citrullinated peptide antigens.

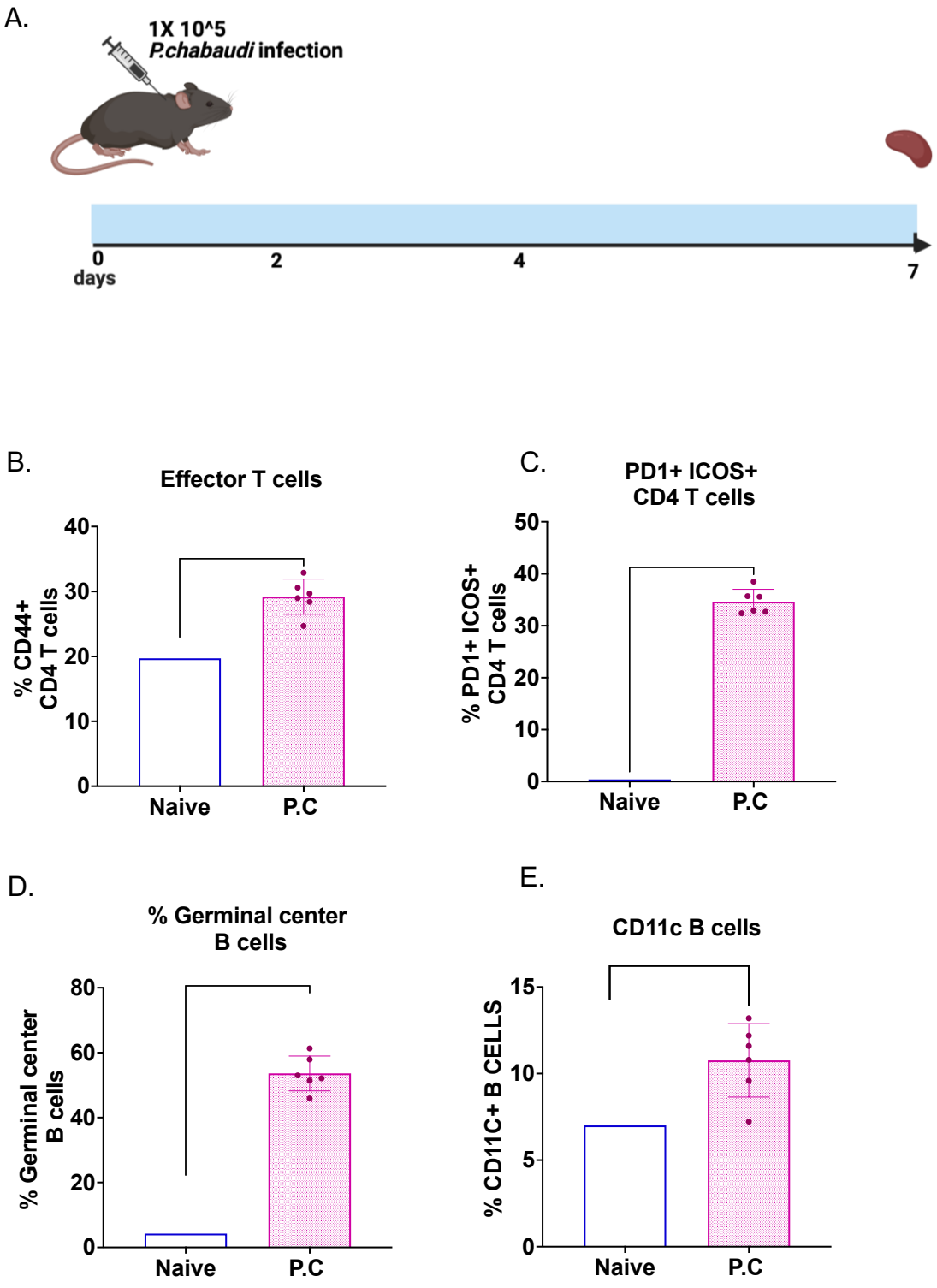

Figure 3-7: Increased B and T cell activation at 7 days post-infection.

C57BL/6 male mice, aged 7-8 weeks (n=6), were infected with 1X 10^5 *P. chabaudi* parasites; a control group of naive mice was also included in the study. Seven days following *P. chabaudi* infection, terminal anaesthesia was performed, blood was drawn via cardiac puncture for subsequent experiments, and spleens were harvested for flow cytometry analysis. The data is presented as bar charts: B) the percentage of CD44+ CD4+ T cells, C) the percentage of PD1+ CD4+ T cells, D) the percentage of GL7+ FAS+ B cells, and E) the percentage of CD11c B cells. The immune cell populations were compared between *P. chabaudi* -infected mice (pink) and naive mice (blue), with statistical significance determined using unpaired T tests. * p-value of < 0.05; **: p<0.01.

3.2.5 *P. chabaudi* is not detected by PCR 63 days post infection.

To confirm that the persistent production of antibody responses to the native and citrullinated peptide antigens at later stages (day 63) wasn't a result of the continued parasite presence, I performed PCR assays to evaluate the levels of the parasite in the mice on day 7 an early point expected to show parasite presence and on day 63, a later stage. As expected, I observed the presence of parasites by PCR on day 7 post infection (Figure 3-8 A). However, by day 63, all mice, including both those infected with *P. chabaudi and* treated with chloroquine and those infected but untreated, showed no presence of *P. chabaudi* in the blood, as indicated in (Figure 3-8 B).

A. 7 days post infection

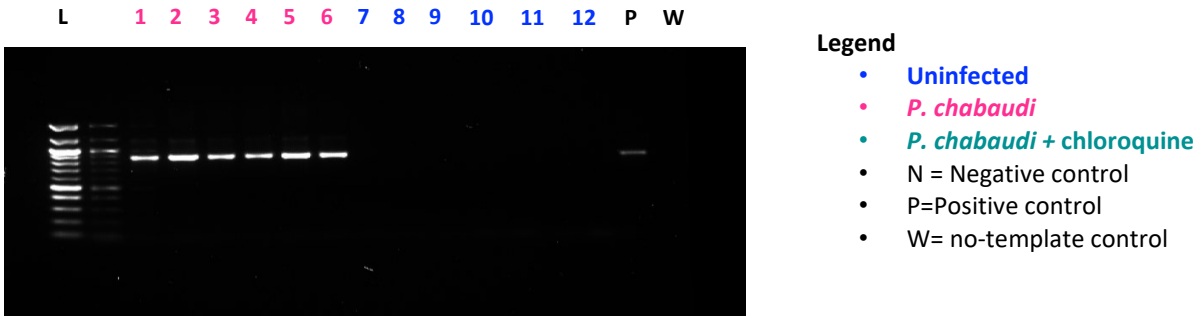

B. 63 days post infection

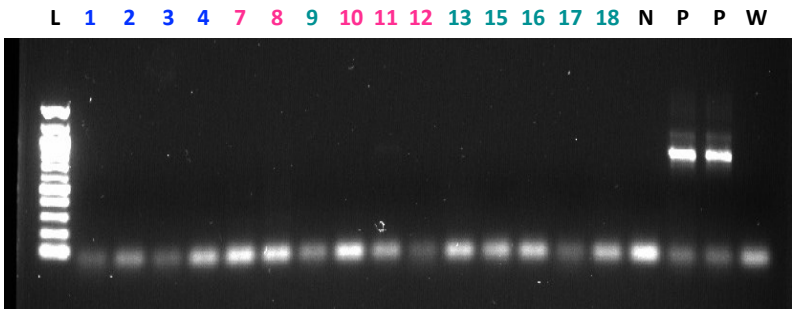

Figure 3-8: Agarose gel electrophoresis (1% agarose) of PCR amplified products using *P. chabaudi specific* PCR primer sets.

Agarose gel electrophoresis (1% agarose) was used to analyse PCR products amplified using *P. chabaudi* specific primers. Samples were obtained from experimental mice at two distinct post-infection time points: day 7 (early) and day 63 (late). Gel lanes are color-coded to represent different experimental groups: blue (naive), (pink) infected + untreated mice; and green (infected mice + chloroquine treatment). Other controls included 'n' for negative, 'p' for positive, and 'w' for non-template controls. A molecular weight ladder, with 100 base pair increments, was used to estimate the size of the PCR products.

3.2.6 *P. chabaudi* and *Trypanosoma brucei* induce elevated levels of antibody responses to the native and citrullinated peptide antigens

Next, I aimed to expand our understanding of how *P. chabaudi* infections, in comparison to other infections, trigger the production of antibody responses to both native and citrullinated peptides. Serum was obtained from mice infected with *P. chabaudi*, *Escherichia coli*, influenza A virus, *Clostridium difficile*, and *Trypanosoma brucei* was analysed for autoantibodies targeting native and citrullinated peptides of Tenascin C5, Fibrinogen, and α-enolase.

The samples were generously provided by our collaborators: *E. coli* samples were collected after a 4-day infection period (Dr. Gillian Douce's Lab); influenza A virus samples were obtained after a 2-week experiment (Dr. Megan Macleod's Lab); *C. difficile* samples were collected following a 40-day experiment (Dr. Gillian Douce's Lab); *T. brucei* samples were collected on days 9 and 12 post-infection (Prof. Annette MacLeod's Lab); and *Plasmodium* and naive samples were obtained from a 14 day experiment. The timing of these samples was dictated by the respective collaborators' experimental design and the availability of samples from their studies. All mice were housed and maintained in a specific-pathogen-free facility at the University of Glasgow. All experiments were conducted under the authority of a UK Home Office license and were approved by the local ethical review committee, ensuring adherence to institutional guidelines.

Interestingly, I found that mice infected with *P. chabaudi* and *T. brucei* had significantly higher levels of antibody responses to the native and citrullinated peptide antigens in relation to those infected with the other pathogens (Figure 3-9 A-F). This suggests that *P. chabaudi* infections and *T. brucei* infections, both eukaryotic pathogens with complex life cycles, have a more substantial impact on triggering autoantibody production than the other infections and certain mechanisms unique to these pathogens could be driving the production of these autoantibodies.

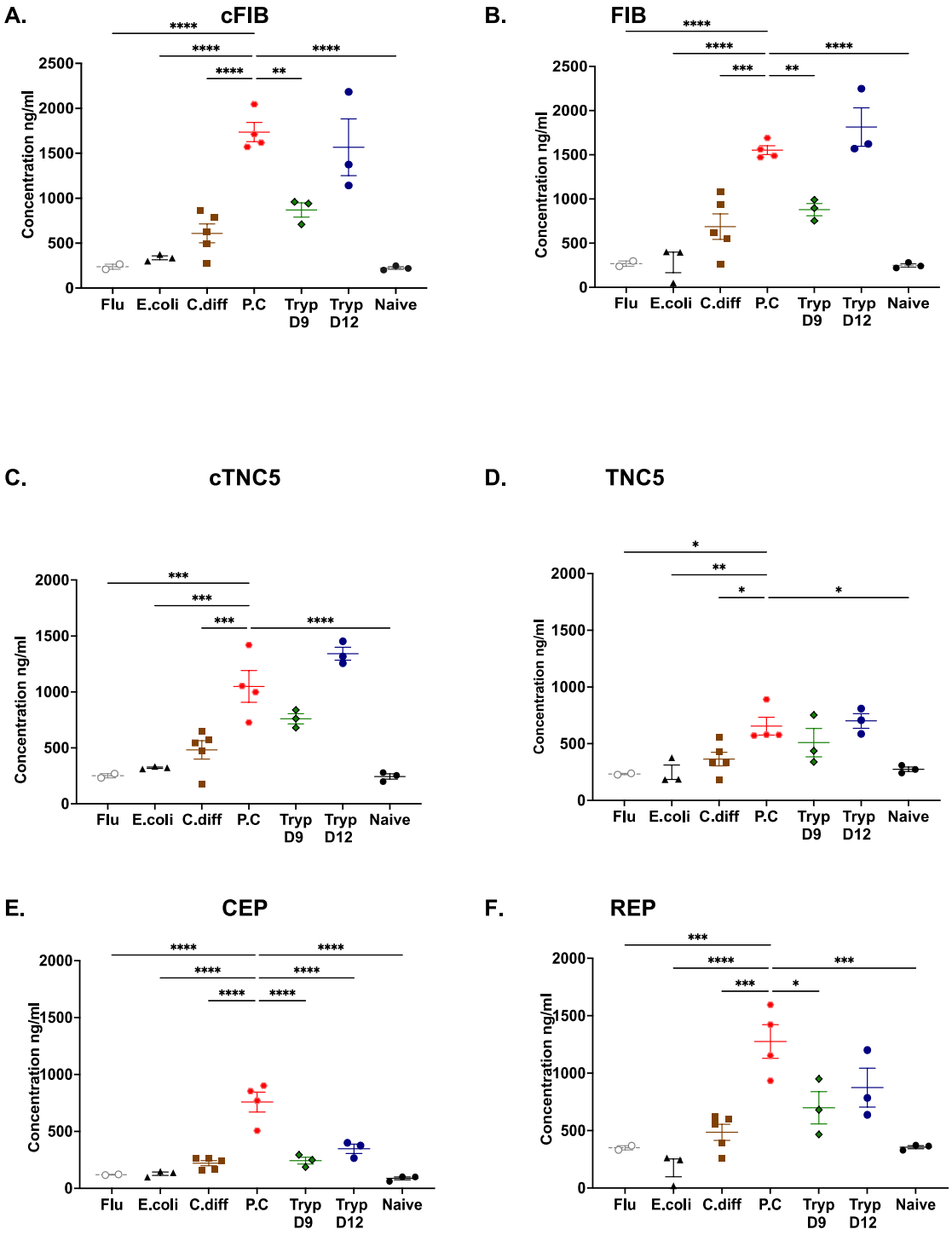

Figure 3-9: *P. chabaudi* and *Trypanosoma brucei* induces elevated levels of antibodies against native and citrullinated peptides compared to other infections.

Serum samples were obtained from collaborative laboratories that conducted research on mice infected with various pathogens, including influenza virus, *E. coli*, *Clostridium difficile*, *Trypanosoma brucei*, as well as naive and *P. chabaudi*-infected mice from my study. The ELISA method was employed to quantify IgG autoantibody responses to both the citrullinated and their respective native peptides: cFIB and FIB in panels (A and B), cTNC5 and TNC5 in panels (C and D), and CEP and REP in panels (E and F). Statistical analysis was performed using one-way ANOVA with Dunnett's multiple comparisons test, comparing all groups to the *P. chabaudi* group. ns: not significant * p-value of < 0.05; **: p<0.01.

3.2.7 Impact of drug-induced PAD inhibition on the production of antibodies against native and citrullinated peptides in *P. chabaudi*-infected mice

Next, given the established role of peptidylarginine deiminase (PAD) enzymes in the citrullination of proteins and their association with autoantibody production [310] as well as the known impact of PAD4 on neutrophil trafficking in malaria [319]. I investigated whether PAD enzyme activity contributes to the generation of antibodies against native and citrullinated peptides during *P. chabaudi* infection.

Specifically, BB-Cl-Amidine, a pan-PAD inhibitor [281] that irreversibly inhibits PAD1–PAD4 was employed in this study. Notably, it has previously been used effectively in mouse models to reduce neutrophil extracellular trap (NET) formation without impairing reactive oxygen species (ROS) production [281], thus highlighting its potential to modulate PAD activity without disrupting essential immune functions.

To test this in the context of *Plasmodium* infections, mice were infected with *P. chabaudi* and drug treated daily from day 3 post infection with BB-Cl-Amidine to inhibit the PAD enzyme activity as outlined in (Figure 3-10 A). While one group of mice received treatment with BB-Cl-Amidine, the other *P. chabaudi* infected group received the vehicle. Additionally, two naive control groups were included, one treated with the drug and the other with the vehicle. Blood was drawn on day 7 for ELISA during the infection period, and tail pricks were taken daily to determine parasitemia. Mice were also weighed daily and culled on day 14, with blood harvested for ELISA.

Using serum collected on days 7 and 14, ELISA was performed. On day 7 (Figure 3-10 B-J), no significant differences were observed between the drug-treated group and the infected vehicle group. However, by day 14 (Figure 3-11 A-H), cFIB levels were seen to be significantly elevated in the infected vehicle compared to the infected drug treated group, suggesting that the drug had some subtle effects, but these were not enough to completely inhibit PAD activity.

Parasitaemia and weight loss were also compared between the two groups; however, the drug did not appear to have any significant impact on parasitaemia

(Figure 3-12 A) or weight loss (Figure 3-12 B). Lastly, a search for PAD enzyme homologues was conducted in the *Plasmodium* database using the human PAD1-6 protein sequences derived from UniProt. As indicated in the (Table 3-1) this data did not indicate the presence of any PAD homologous sequences.

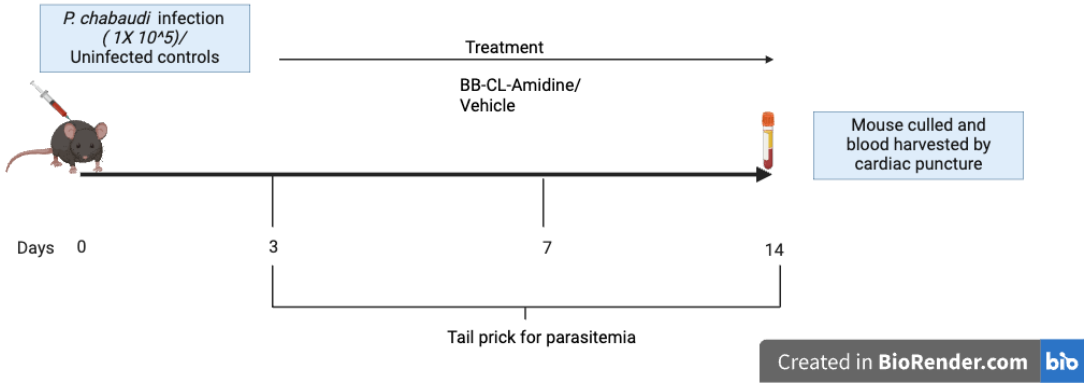

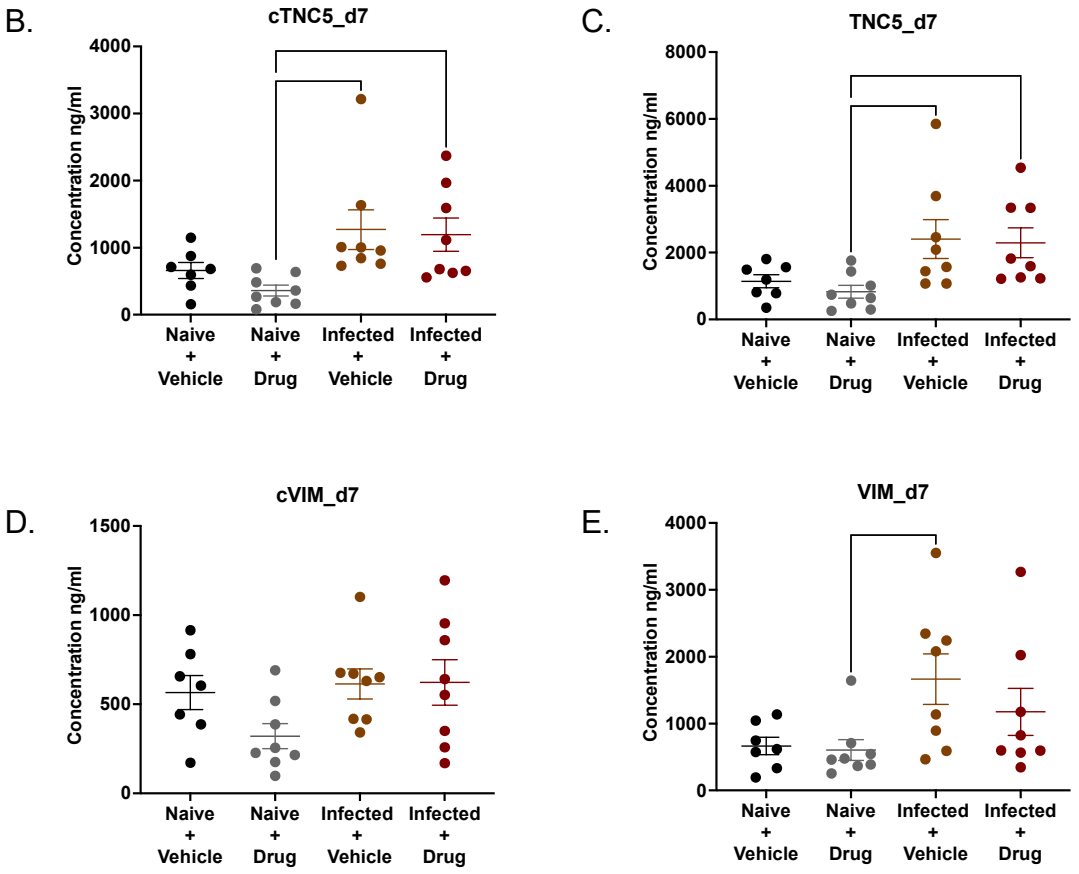

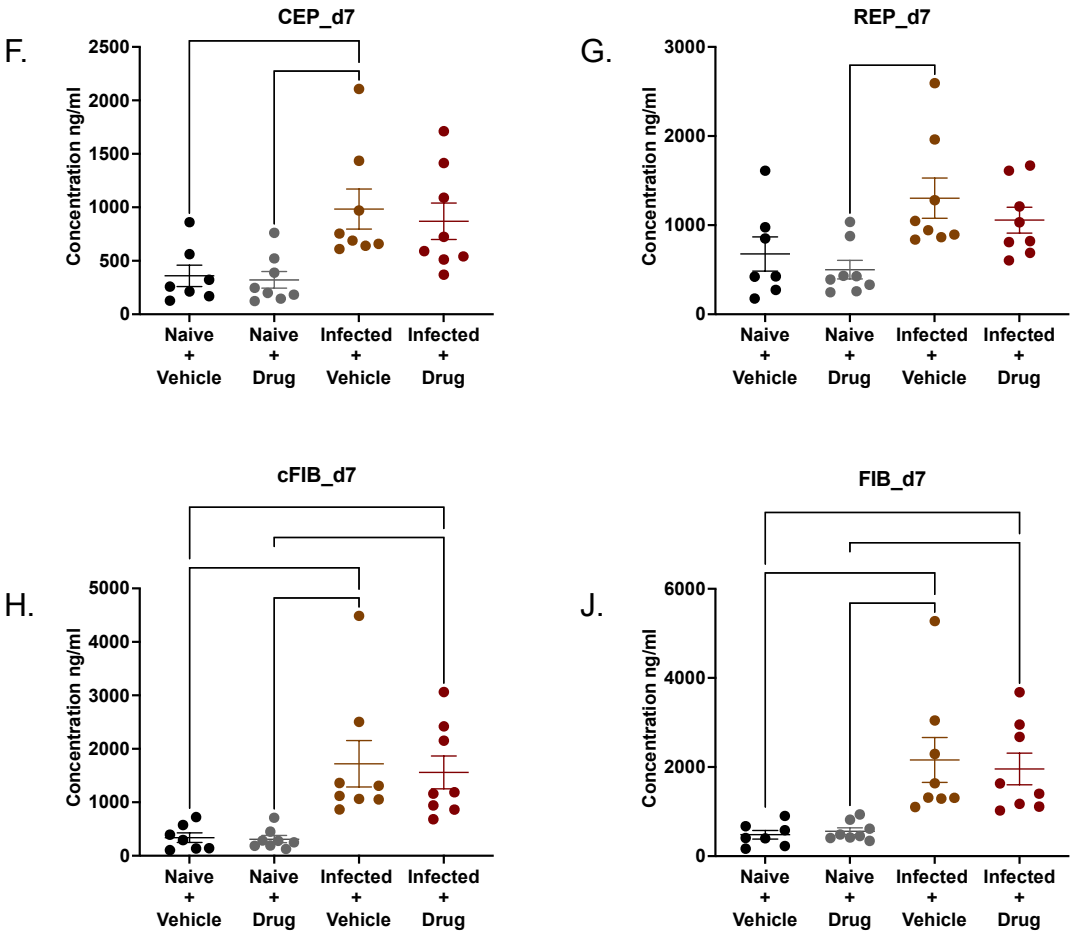

Figure 3-10: No significant difference in autoantibody levels was observed on day 7 between the infected mice and drug-treated groups compared to the infected control groups.

(A) *P. chabaudi* infection model for PAD4 inhibition. C57BL/6 male mice (n=8) were infected with 1 × 10^5 *P. chabaudi*-infected RBCs; one group of mice was treated with BB-Cl-Amidine, while the other group was left untreated. Naive mice were also included as controls. Tail bleeds were taken on day 7 for ELISA while tail pricks were taken daily to determine parasitaemia. Autoantibody responses to citrullinated and corresponding native peptides were determined using ELISA in the following groups: naive + vehicle (black), naive + drug (grey), infected + vehicle (brown), and infected + drug-treated (red) mice. (B) Anti-cTNC5, (C) Anti-TNC5, (D) Anti-cVIM, (E) Anti-VIM, (F) Anti-CEP, (G) Anti-REP, (H) Anti-cFIB, and (I) Anti-FIB autoantibody responses. Graphs show the mean with SEM. One-way ANOVA with Tukey's multiple comparisons test was performed (*p < 0.05, **p < 0.005, ***p < 0.0005).

A.

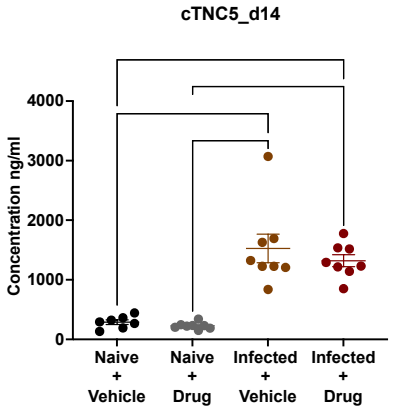
cTNC5_d14
Concentration ng/ml
4000
3000
2000
1000
0
Naive + Vehicle
Naive + Drug
Infected + Vehicle
Infected + Drug

B.

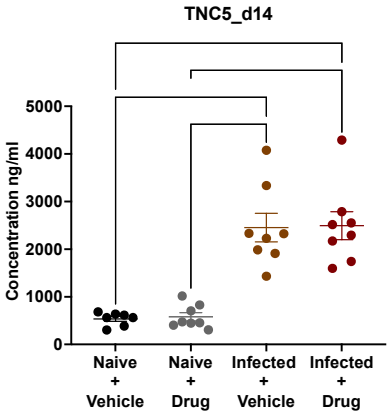
TNC5_d14
Concentration ng/ml
5000
4000
3000
2000
1000
0
Naive + Vehicle
Naive + Drug
Infected + Vehicle
Infected + Drug

C.

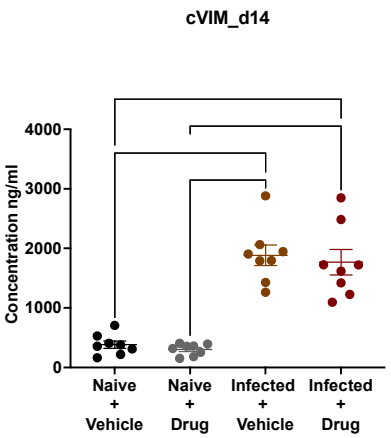
cVIM_d14
Concentration ng/ml
4000
3000
2000
1000
0
Naive + Vehicle
Naive + Drug
Infected + Vehicle
Infected + Drug

D.

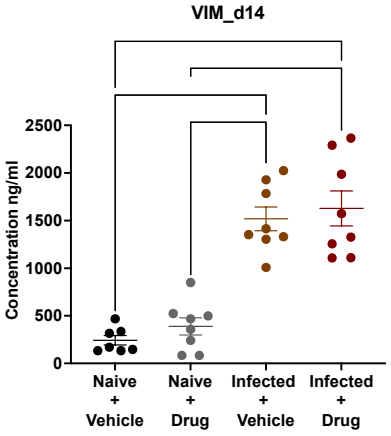
VIM_d14
Concentration ng/ml
2500
2000
1500
1000
500
0
Naive + Vehicle
Naive + Drug
Infected + Vehicle
Infected + Drug

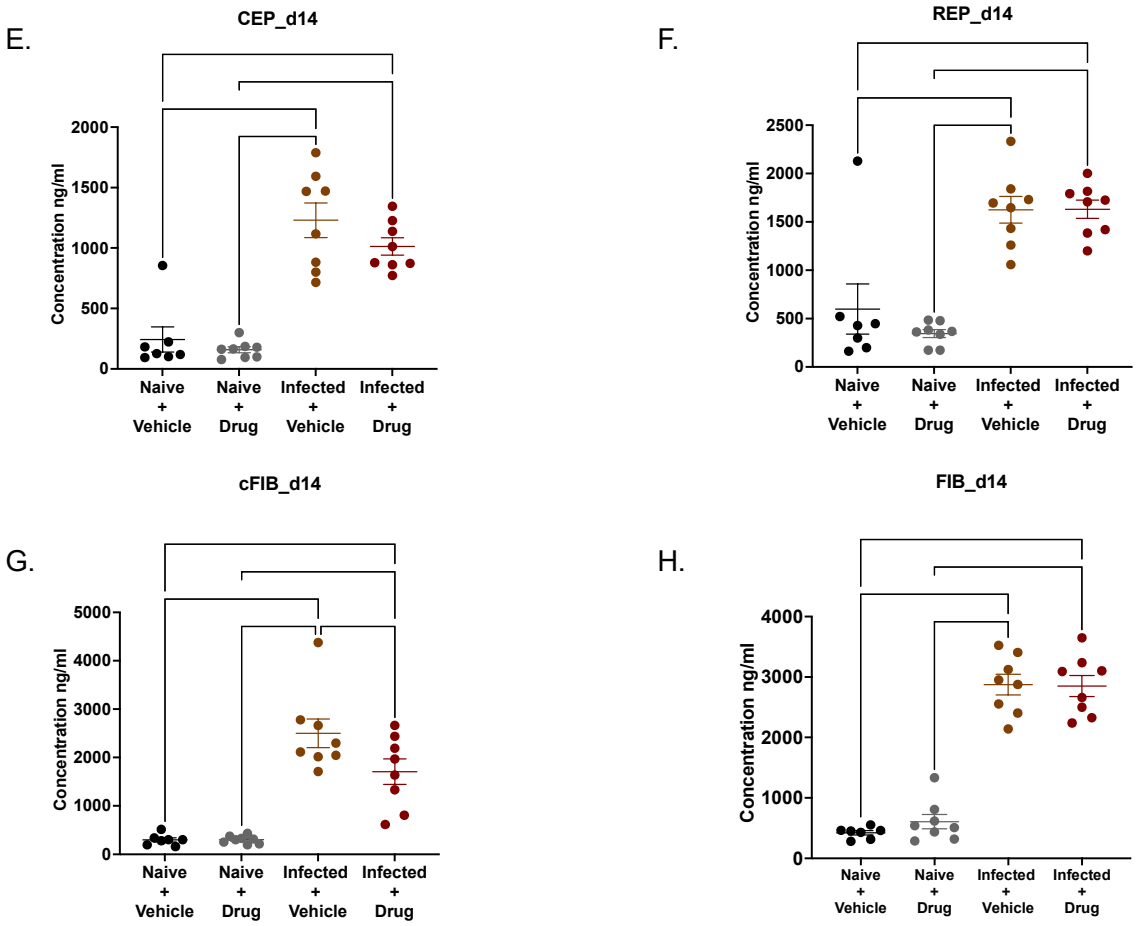

Figure 3-11: Increased cFIB levels were observed on day 14 in the infected + vehicle mice compared to the infected + drug treated group.

Autoantibody responses to citrullinated and corresponding native peptides were determined using ELISA in the following groups: naive + vehicle (black), naive + drug (grey), infected + vehicle (brown), and infected + drug-treated (red) mice. (A) Anti-cTNC5, (B) Anti-TNC5, (C) Anti-cVIM, (D) Anti-VIM, (E) Anti-CEP, (F) Anti-REP, (G) Anti-cFIB, and (H) Anti-FIB autoantibody responses. The mice's weights and parasitaemia levels were also monitored throughout the infection period. Graphs show the mean with SEM. One way ANOVA with Tukey's multiple comparisons test was performed (*$p < 0.05$, **$p < 0.005$, ***$p < 0.0005$).

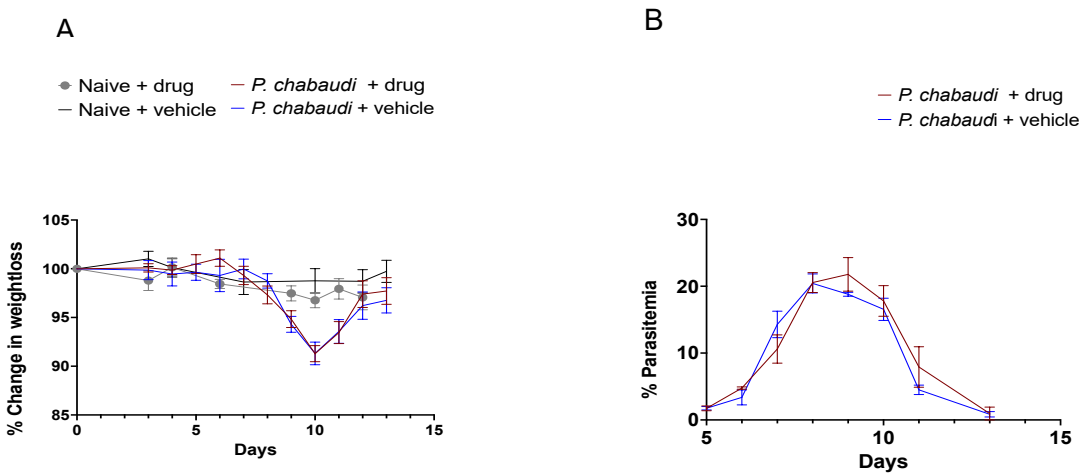

Figure 3-12: PAD inhibition has no influence on the development of clinical *P.chabaudi* infection

Two groups of mice were infected with 1 × 10^5 *P. chabaudi*-infected RBCs; one group of mice was treated with BB-Cl-Amidine, while the other group was left untreated. Naive mice were also included as controls. Tail pricks were taken daily to determine parasitaemia and weights measurements were taken daily. **A.**) Change in weight shown as percentage of initial weight (**B.**) percentage parasitaemia over several days. Graphs show the mean with SEM.

Table 3-1: Human PAD sequence search for PAD Homologues in the *Plasmodium* Proteome Database

GeneID	Organisms	Score	E-value	Product description	Search Weight
PF3D7_1002000.1	*Plasmodium falciparum 3D7*	37	0.021E0	*Plasmodium* exported protein (hyp2), unknown function	0
PCHAS_0725000.1	*Plasmodium chabaudi chabaudi*	33.9	0.2E0	ubiquitin carboxyl-terminal hydrolase 13, putative 0	0
PF3D7_1465800.1	*Plasmodium falciparum 3D7*	32.7	0.55E0	dynein beta chain, putative	0
PCHAS_1011900.1	*Plasmodium chabaudi chabaudi*	30.8	2.4E0	conserved *Plasmodium* protein, unknown function	0
PCHAS_1450500.1	*Plasmodium chabaudi chabaudi*	30.4	2.7E0	asparagine/aspartate rich protein, putative	0
PF3D7_1327300.1	*Plasmodium falciparum 3D7*	30.4	2.6E0	subpellicular microtubule protein 3	0
PCHAS_0900051.1	*Plasmodium chabaudi chabaudi*	30	4.2E0	reticulocyte binding protein, putative	0
PCHAS_0415100.1	*Plasmodium chabaudi chabaudi*	30.8	0.84E0	CS domain-containing protein, putative	0
PF3D7-0615600.1	*Plasmodium falciparum 3D7*	28.5	6.2E0	zinc finger protein, putative	0
PCHAS_0919700.1	*Plasmodium chabaudi chabaudi*	31.6	0.57E0	RAP protein, putative	0
PF3D7-1132500.1	*Plasmodium falciparum 3D7*	28.1	8.2E0	Amino acid transporter, putative	0
PF3D7-0611600.1	*Plasmodium falciparum 3D7*	27.7	8.6E0	Basal complex transmembrane protein 1	0
PCHAS_0212800.1	*Plasmodium chabaudi chabaudi*	28.5	5E0	AP2 domain transcription factor AP2-L, putative	0
PCHAS_0315200.1	*Plasmodium chabaudi chabaudi*	28.5	4.2E0	Vacuolar protein sorting-associated protein 45, putative	0
PCHAS_1035100.1	*Plasmodium chabaudi chabaudi*	28.1	6.1E0	AP2 domain transcription factor AP2-G2, putative	0
PCHAS_1239800.1	*Plasmodium chabaudi chabaudi*	31.2	1.2E0	50S ribosomal protein L12, apicoplast, putative	0
PCHAS_1213200.1	*Plasmodium chabaudi chabaudi*	29.6	5.3E0	*Plasmodium chabaudi chabaudi* merozoite surface protein MSA180, putative	0

PF3D7_1435300.1	*Plasmodium falciparum 3D7*	29.3	6E0	glutamate synthase (NADH), putative	0
PCHAS_0403600.1	*Plasmodium chabaudi chabaudi*	28.9	7.9E0	inner membrane complex protein 1e, putative	0
PCHAS_1010400.1	*Plasmodium chabaudi chabaudi*	28.9	9.4E0	glutamate synthase (NADH), putative	0
PCHAS_1366300.1	*Plasmodium chabaudi chabaudi*	28.5	3.7E0	conserved *Plasmodium* protein, unknown function	0

3.3 Discussion

Here, I demonstrate that acute *P. chabaudi* infection induces the production of antibody responses to both the native and citrullinated peptide antigens at levels similar to those found in mice in the CEA group. Moreover, using a chronic *P. chabaudi* infection model, I further demonstrate that the levels of these autoantibodies peak in the second week of infection and decline as the infection resolves but remain at levels higher than those in uninfected controls at 63 days post-infection. These findings thus provide evidence that *P. chabaudi* infection induces the generation of antibody responses to the native and citrullinated peptide antigens.

In this study, I examined antibody responses to citrullinated and corresponding native peptides in acute *Plasmodium chabaudi* infection and compared the responses to those of mice in the experimental arthritis group. Increased antibody responses to citrullinated and native peptides were observed in both the *P. chabaudi*-infected mice and CEA groups. While antibody responses to the native and citrullinated peptide antigens have not previously been reported in the context of *Plasmodium* infections, existing research links *Plasmodium* infection to an increase in autoantibodies in mice and human malaria [1,223,248,256].

Notably, other infections that trigger increased ACPA production, such as the bacterial pathogen *Porphyromonas gingivalis*, have been associated with the pathogenesis of RA due to its ability to induce citrullination, particularly given that *P. gingivalis* has its own PAD enzymes, a key factor implicated in the disease's pathology [320]. However, sequence analysis of the *P. chabaudi* proteome indicates a lack of homologous PAD enzymes, suggesting that the observed autoantibody responses are likely driven by host immune mechanisms rather than the pathogen itself.

Importantly, antibody responses to native and citrullinated peptides have also been observed in other infections, such as tuberculosis (TB), without evidence of RA development [89,90]. Given these observations, ACPA presence in infections may, therefore, reflect a broader immune activation with an altered immune system. Intriguingly, a recent study reported that the inclusion of antibodies targeting citrullinated and corresponding native peptides enhanced the diagnostic accuracy

of rheumatoid arthritis associated interstitial lung disease RA-ILD [105]. While these observations suggest a key role of ACPA and antibody responses to native peptides in the diagnosis of RA, this also raises important questions about how infection-induced ACPA production and corresponding native peptide recognition might contribute to breach in self-tolerance mechanisms, a phenomenon that should be explored in future studies.

Next, I examined the kinetics of antibodies directed against native and citrullinated peptide antigens in a chronic *P. chabaudi* infection. Mice infected with *P. chabaudi* had peak levels of autoantibodies at week 2, and these autoantibodies seemed to decline with most of the parasites cleared by day 14. Thus, this suggests that parasite infection drives the production of antibodies directed against native and citrullinated peptide antigens. However, despite parasite clearance, the levels of these autoantibodies were maintained at levels above the naive controls. Similarly, peak autoantibodies that target host un-infected RBC have been reported in mice infected with *Plasmodium yoelii* 17XNL, with the levels declining with parasite clearance [1]. Additionally, similar studies using the *P. chabaudi* infection model have also reported increased IgG autoantibodies to nuclear antigens that remained elevated for at least two weeks after the parasite was cleared, suggesting a sustained immune response even post-infection [321].

Given the peak levels of antibodies directed against both the native and citrullinated peptide antigens are observed at week two and sustained levels are maintained following parasite clearance, I next examined the immune cell phenotype, particularly CD4+ T cells and germinal centre B cells correlating with these time points. On days 7- and 63-days post-infection, I report increased CD4+ T cell activation, with CD44HI and PD1+ICOS + CD4+ T cells elevated. As expected, I see increased germinal centre (GC) B cell activation on day 7 and prolonged expansion of the GC 63 days post-infection. Similar findings using a *P. chabaudi* model reported sustained GC B cells 60 days post-infection [322]. Although these findings suggest a non-impaired immune response, it is well known that malaria induces a significant polyclonal B cell response, especially in the acute phase of the infection [323,324]. Notably, the presence of sustained production of antibodies against native and citrullinated peptides in *P. chabaudi* has not been reported

previously, and whether their production at this time point is associated with the polyclonal B cell overactivation still needs to be studied.

In addition, given the presence of atypical B cells ($CD21^{-}CD27^{-}CD11c^{+}T\text{-}bet^{+}$) in the context of chronic infection and autoimmune disease, I also assayed for B cells expressing CD11c marker. Herein, I report an increase in B cells expressing CD11c in the malaria-infected mice compared to the naive. It is well noted that chronic infections with *Plasmodium* is associated with an impaired B cell response, leading to the accumulation of atypical B cells [211,318]. Importantly, there is evidence demonstrating that atypical B cells expressing FcRL5, and T-bet are associated with the production of autoantibodies that target uninfected RBC [3,4]. However, given the scope of this study, I could not ascertain if the increase in these CD11c B cells were directly associated with the production of ACPA.

Next, to establish if the presence of antibodies against native and citrullinated peptide antigens was unique to *Plasmodium* infections, I compared the levels of these antibodies generated during *P. chabaudi* infection with those associated with other inflammatory infections, including *E. coli, influenza, Clostridium difficile, P. chabaudi*, and *T. brucei*. While the levels of these autoantibodies were lower in the other infections, both mice infected with *P. chabaudi* and *T. brucei* displayed significantly higher levels of antibodies against native and citrullinated peptides than those infected with other pathogens, suggesting that *P. chabaudi* and *Trypanosoma brucei* infections have a more substantial impact on triggering autoantibody production than other infections. However, it is important to acknowledge that the timing of sample collection may have influenced these findings. The samples were pre-collected, with *E. coli* and *C. difficile* samples obtained at 4- and 40-days post-infection, respectively, influenza A virus samples collected at 2 weeks, *T. brucei* at 9 and 12 days, and *P. chabaudi* during the second week of infection. While these time points reflect sample availability based on our collaborators predesigned experiments, the variability in sampling timing across infections could contribute to observed differences. Similarly, antibodies against native and citrullinated peptides have also been detected in patients with active pulmonary Tuberculosis [89,90], *Porphyromonas gingivalis* [325,326], *Aggregatibacter actinomycetemcomitans* [88]. While the bacterial pathogens named above are linked to production of such antibodies, it is important to note the

bacteria tested in this study did not seem to induce high levels, suggesting that unique, pathogen-specific mechanisms may be involved in the induction of antibodies against native and citrullinated peptides.

While the mechanisms that trigger ACPA production in infections are not fully described, I hypothesized that neutrophils could be key players as they express PAD4 and release them during netosis [327], moreover PAD4 polymorphism are associated with RA [328,329]. To explore the role of PAD enzymes in this process, I examined the effect of PAD inhibition on antibody production. My findings indicate that inhibition of PAD using BB-Cl-Amidine did not seem to have an impact on the production of antibodies against native and citrullinated peptide antigens, with similar levels of these autoantibodies observed in mice infected and treated with the drug and mice that were infected and not treated. However, an exception to this trend was cFIB, which was significantly decreased in the *P. chabaudi* drug treated group compared to the *P. chabaudi* vehicle group on day 14. This suggests that while PAD inhibition using BB-Cl-Amidine wasn't effective, using PAD-deficient mouse models might provide more pronounced results. Notably, PAD4 inhibition has been shown to alter liver pathology, with markedly reduced pathology and neutrophil trafficking [319], which may explain the reduced cFIB levels observed in the PAD-inhibited mice.

Moreover, PAD4 inhibition did not appear to affect the overall course of infection, as both mouse weight (a clinical feature) and parasitemia levels were not significantly different between the vehicle-treated and drug-treated groups. Similar observations have been reported in other studies [319]. Thus, PAD4 inhibition may have more subtle effects on antibodies against native and citrullinated peptide antigens production and immune response during infection rather than directly influencing the course of the disease.

Taken together, the interplay between infections such as *Plasmodium,* ACPA production, and immune activation provides possible underlying mechanisms that could contribute to the breakdown of self-tolerance, with implications for understanding autoimmune disease pathogenesis. Furthermore, these findings indicate the complexity of the immune response elicited during *P. chabaudi* infection and the need for a better understanding of infections in the context of autoimmunity.

4 Chapter 4- Assessment of the impact of *P. chabaudi* induced elevated antibody responses to both the native and citrullinated peptides on experimental arthritis development

4.1 Introduction

This chapter discusses the role of antibodies against native and citrullinated peptides that are generated during *P. chabaudi* infection in mice. Specifically, I aim to understand whether the increased antibodies against native and citrullinated peptides would exacerbate or inhibit the development of experimental arthritis. Additionally, I also explore the role of elevated responses to both the native and citrullinated peptides on the development and progression of *Plasmodium* infection.

While the aetiology of RA is poorly understood, several risk factors are known to be associated with RA, such as age, gender (female) and environmental factors such as exposure to silica, smoking and infectious agents [70,330]. For example, pathogens such as bacteria, parasites and viruses, through the initiation of mechanisms such as epitope spreading and molecular mimicry, can trigger an autoimmune response [331]. Furthermore, increasing evidence from both clinical and pre-clinical studies implicate infections such as *Porphyromonas gingivalis* [332-334], *Proteus mirabilis* [335], Epstein Barr virus [336] and Mycoplasma [337] as critical contributors to RA pathogenesis.

Although the association between *Plasmodium* infections and RA is long-standing, with classical studies reporting on the suppression of Freund's adjuvant arthritis in rats by *Plasmodium* parasites [338], recent studies continue to support these findings. For example, mice infected with *P. yoelii* at four weeks following the induction of collagen-induced arthritis (CIA) developed milder arthritis, indicating that the parasite conferred some protective effect [339]. However, despite current evidence indicating that *Plasmodium* infections do not exacerbate or worsen symptoms of experimental arthritis but rather play a role in protection, data from these same studies suggest that the protective effect depends on the parasite species and the timing of the infection. Specifically, one study [339] found that infection with *P. yoelii* at four weeks but not at one week conferred protection,

while previous studies by Greenwood [338] noted that only infections with *P. yoelii*, but not *P. berghei ANKA*, resulted in milder arthritis, thus suggesting that specific immune mechanisms are induced at these time points and by these species.

Thus, given my findings on the increased *P. chabaudi*-induced antibody responses to both the native and citrullinated peptides and considering the association of ACPA with severe RA and its strong predictive value for increased joint damage [340], exploring the role of *Plasmodium* induced antibodies against native and citrullinated peptides in the pathogenesis of RA was essential. Furthermore, evidence from a current study shows that the transfer of monoclonal ACPA from RA patients into mice resulted in pain-like behaviour and bone loss, which was further demonstrated to occur in a peptidylarginine deiminase-4 dependent manner [341]. Similarly, monoclonal antibodies specific to citrullinated fibrinogen derived from patients, and a well-known ACPA when transferred in mice, resulted in increased arthritis [93,103,342]; thus, necessitating the need for further investigation into the effect of *Plasmodium* induced antibodies against native and citrullinated peptides on the development of experimental arthritis in mice.

Therefore, in this study, in addition to the *P. chabaudi* infection model, I employed an antigen-induced arthritis model [282,286], that results in transient arthritis through the transfer of OVA-specific Th1 CD4+ T cells, followed by immunisation with OVA/CFA and subsequently challenged with heat aggregated OVA. The application of this model was important not only as it was established in the lab, but it is also known to mimic the clinical and pathological features of human RA, such as breach of tolerance to self-antigens, synovial hyperplasia, cellular infiltration and cartilage erosion [282,286]

4.1.1 Study Rationale

In clinical RA, the presence of ACPA is a predictor and a risk factor for joint destruction [102,343] ; therefore, while my findings suggest an increase in antibody responses to both the native and citrullinated peptides in mice infected with *P. chabaudi*, it was necessary to understand the potential impacts of *P. chabaudi*-induced antibodies against native and citrullinated peptides with a focus on the development of experimental arthritis (EA). Thus, using both the Acute experimental arthritis (AEA) and Chronic experimental arthritis (CEA) mouse

model, two infection time points were explored; first, I investigated if prior *P. chabaudi* infection impacted the development of AEA. This time point was critical as it best represented what would occur in real life, where individuals living in a malaria endemic area are first exposed to *Plasmodium* infections and aligned with the overall project hypothesis. Next, using an established CEA mouse model [286], I explored the second timepoint where AEA was first induced, followed by *P. chabaudi* infection, with subsequent induction of CEA model. This sequence of experiments was strategically selected to assess the impact of the timing of the infection, particularly whether *P. chabaudi*-induced elevated antibody responses to both the native and citrullinated peptides will influence the progression of CEA.

Lastly, given the controversial role of autoantibodies, some studies suggest their importance in conferring protection [5,204]; in contrast, high levels of anti-phosphatidylserine and anti-DNA antibodies were reported in children with severe malaria [2,4]. I, therefore, investigated if the presence of autoantibodies particularly of elevated levels to both the native and citrullinated peptides would contribute to protection against clinical symptoms of malaria. This aim aligned with our working hypothesis that *Plasmodium* infections induce the production of low-affinity binding autoantibodies that play a protective role in acute malaria-induced illness.

4.1.2 Chapter Aims

This chapter has two main aims: first, to investigate the impact of *P. chabaudi*-induced antibody responses to both the native and citrullinated peptides on the development experimental arthritis using both the acute (AEA) and chronic (CEA) experimental arthritis models in mice. Secondly, explore whether elevated levels of antibody responses to both the native and citrullinated peptides, generated through the induction of CEA, will confer protection during the acute phase of *Plasmodium* infection in mice by assessing its effects on parasitemia, inflammation, and associated tissue pathology.

4.2 Results

4.2.1 Prior infection with *P. chabaudi* does not affect the development of acute experimental arthritis (AEA)

To investigate the impact of the increased levels of *P. chabaudi* induced antibody responses to both the native and citrullinated peptides on the development of AEA, I combined the *P. chabaudi* infection model with the AEA mouse model as outlined (Figure 4-1). Additionally, several experimental groups were also included, as described in (Table 4-1). Among these groups, I particularly included chloroquine treated controls to ensure that the observed results were attributable to the experimental conditions only rather than chloroquine's known immunomodulatory effects in RA [344,345].

Following induction of acute experimental arthritis, paw measurements and clinical scores were taken daily as outlined in the protocol [346]. As expected, the greatest increase in paw measurement and clinical score were seen on day 2 in the AEA group (Figure 4-2 A, B), confirming that the model had worked as expected. Notably, increased paw measurement was observed in the AEA, Chloro-AEA, and P.C+ Chl+ AEA groups; however, no significant differences were observed between mice that had prior *Plasmodium* infection and those that didn't, suggesting that prior infection with *P. chabaudi* does not affect the development of AEA, which was in contrast to our research hypothesis that the increase in antibody responses to both the native and citrullinated peptides would exacerbate the development of arthritis. Notably, I did not observe any significant impact of chloroquine treatment on the development of acute experimental arthritis. Next, I analysed the kinetics of antibody responses to both native and citrullinated peptides to assess their levels prior to the induction of AEA. Consistent with my previous observations in chapter 3, mice infected with *P. chabaudi* prior to the induction of AEA showed an initial increase in antibody responses to both native and citrullinated peptides, which decreased as the infection cleared (Figure 4-2 C-F). Notably, subsequent induction of AEA following infection with *P. chabaudi* did not result in further increases in the levels of these autoantibodies in the P.C +Chl + AEA.

Lastly, I investigated whether antibody responses to both the native and citrullinated peptides following *P. chabaudi* infection were specific or a consequence of a broader, non-specific antibody response. An anti-OVA ELISA was therefore conducted across all experimental groups, and as expected, elevated anti-OVA antibody responses were observed in the AEA, Chloro-AEA, and P.C +Chl +AEA groups (Figure 4-2 G). This observation was expected as the induction of AEA involved immunisation with OVA antigen and followed by subsequent challenge with heat aggregated OVA as detailed in the methods sections (Chapter 2).

In contrast, no anti-OVA responses were detected in the *P. chabaudi*-only group at this timepoint, suggesting that *P. chabaudi* infection does not induce a generalised polyclonal antibody response. While this finding supports the specificity of increased antibody responses to both the native and citrullinated peptides, further confirmation would be required. For example, investigating earlier timepoints of *P. chabaudi* infection during active infection, as well as use of additional approaches, such as affinity purification or antigen-specific assays, would further confirm whether the observed ACPA levels are exclusively targeted against citrullinated autoantigens.

Table 4-1: Experimental groups

Group	Type	Treatment
Naive	Control	No treatment
Naive + chloroquine	Control	Chloroquine treatment at D15
P. chabaudi + chloroquine (P.C + Chl)	Control	*P. chabaudi* infection followed by chloroquine treatment at D15
P. chabaudi + Chloroquine + AEA (P.C+ Chl+ AEA)	Experimental group	*P. chabaudi* infection followed by chloroquine treatment (D15) and induction of AEA
Chloroquine + AEA (Chl + AEA)	Experimental group	Induction of chloroquine treatment at D15 followed by Acute Experimental Arthritis.
Acute Experimental Arthritis (AEA)	Experimental group	Induction of Acute Experimental Arthritis

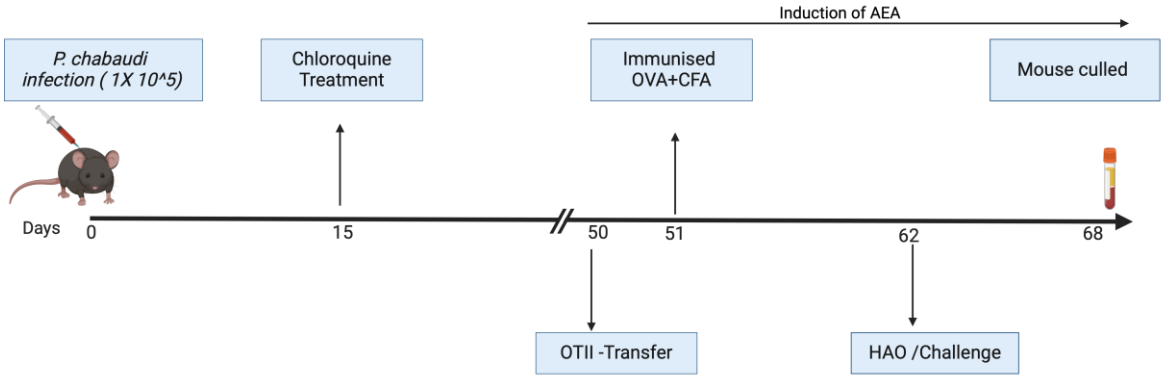

Figure 4-1: Illustration of the experimental outline for *P. chabaudi* infection and subsequent induction of AEA.

In this experiment, C57BL/6 mice (n=8) were initially infected with 1 X 10^5 parasitised RBCs. Fifteen days post-infection, the mice were treated with chloroquine. Subsequently, AEA was induced as outlined in Section 2.222 (Methods Section). Briefly, OTII CD4+ T cells were isolated from transgenic mice and induced to differentiate into Th1 phenotype. These Th1-polarised CD4+ T cells were then transferred into the *P. chabaudi* -infected mice and one day following the transfer, the mice were immunised with the OVA antigen, which was then followed by a footpad challenge using either heat aggregated OVA antigen (HAO) or PBS ten days later. Created in BioRender. Kimathi, R. (2024) BioRender.com/c71k02.

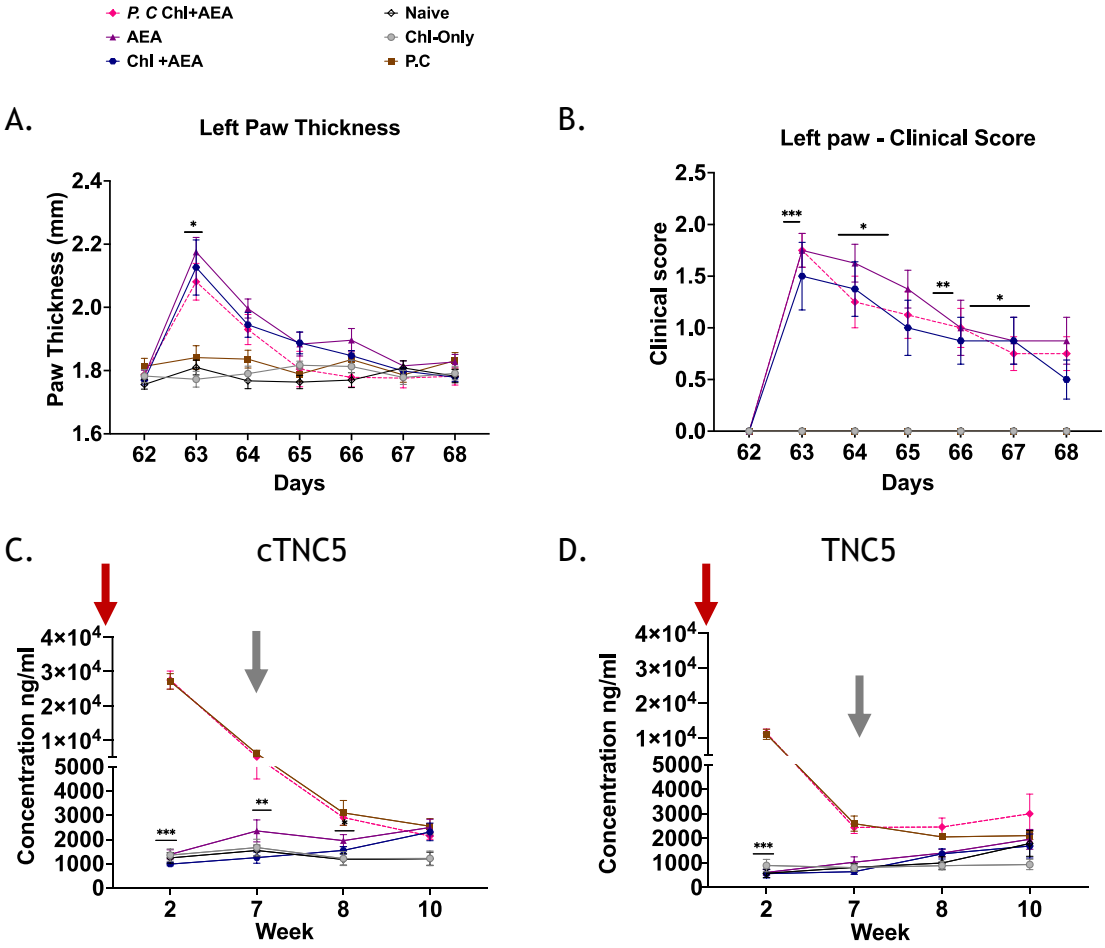

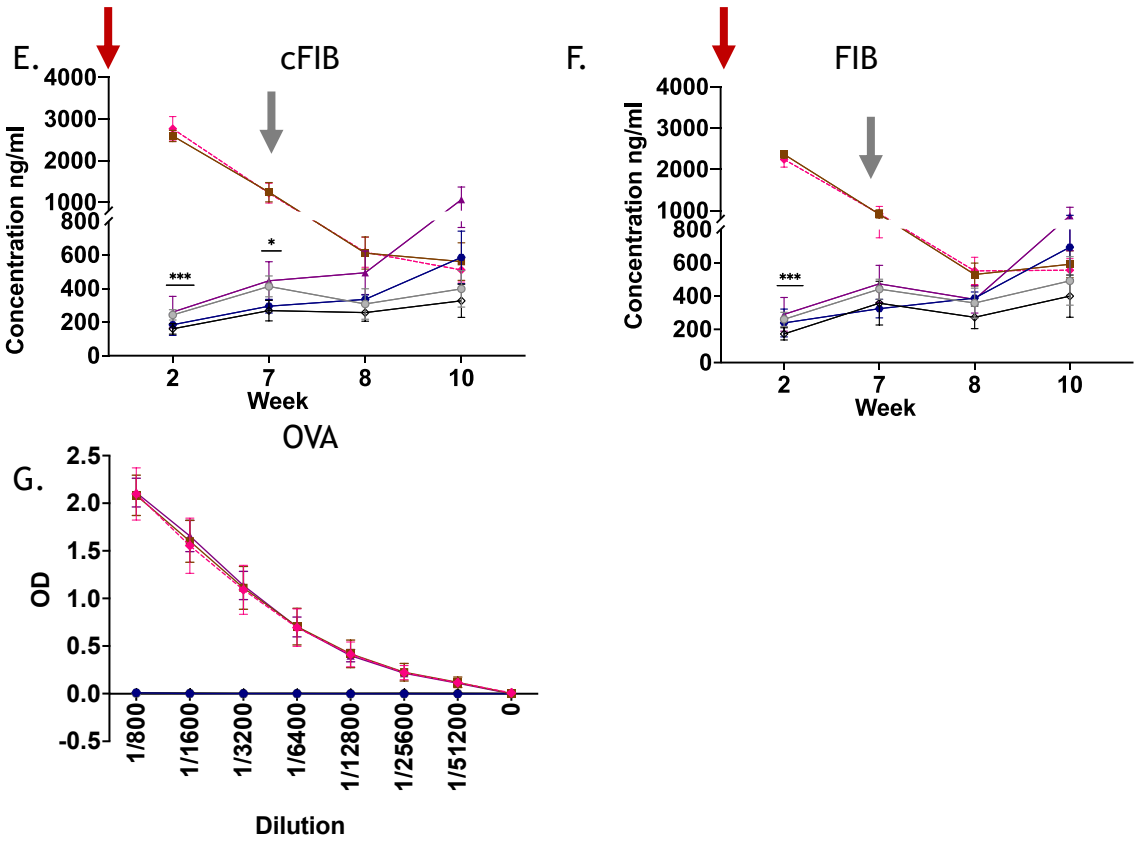

Figure 4-2: Prior infection with *P. chabaudi* does not affect the development of acute experimental arthritis (AEA) in mice.

Following the induction of Acute Experimental Arthritis (AEA) in mice, paw thickness and clinical scores were measured daily. A.) Graph showing the mean +/- SEM left hind paw thickness in mm B.) Graph showing the mean +/- SEM left hind paw clinical score. Blood samples were taken periodically for ELISA, with the key study timepoints denoted by a red arrow for the *P. chabaudi* infection and a grey arrow for the induction of AEA. C.) and D.) Graphs represent the autoantibody responses to cTNC5 and its native peptide TNC5, while E.) and F.) represent responses to cFIB and the native peptide FIB. G.) Represents the antibody responses to the OVA antigen determined by titration of serum by ELISA. Statistical analysis was performed using one-way ANOVA with Tukey's multiple comparisons test, with significance indicated as ns (not significant), *p < 0.05, **p < 0.01, ***p < 0.001, ****p < 0.0001. indicated key comparisons made between the P.C+Chl+AEA and Chol-AEA group.

4.2.2 Increased CD11c B cells in the spleen of *P.C* +Chl + AEA group compared to the AEA group

Next, using flow cytometry I evaluated B and T cell phenotypes in the spleen using the gating strategy illustrated (Figure 4-3). This was crucial, especially considering the use of the OVA experimental arthritis model, which is initiated and maintained by Th1 CD4+ T cells [282] and additionally, given that *Plasmodium* infections are known to alter the immune system [347].

I, therefore, began by examining the activation status of CD4+ T cells, by assessing the expression of CD44 and CD62L on CD4+ T cells. A significant increase in effector T cells (CD4+ CD44HI, CD62L-) (Figure 4-4 A) was observed in the (P.C+ Chl+ AEA) group compared to naive controls, while memory T cells (CD4+ CD44+ CD62L+) were notably higher in the P.C group (Figure 4-4 B), with no significant differences between the (P.C+ Chl+ AEA) and (Chl + AEA) groups.

Next, I examined CD4+ T cells expressing PD1+ICOS+, which were increased in several groups, including AEA, Chloro-AEA, P.C+Chl+AEA, and P.C, with no significant differences between the P.C+Chl+AEA and Chl+ AEA groups (Figure 4-4 C). Similarly, I also evaluated B cells expressing FAS+GL7+, which represent germinal centre B cells, notably, the percentage of germinal centre B cells mirrored the patterns seen in PD1+ICOS+ CD4+ T cells (Figure 4-4 D).

Interestingly, CD11c B cells, which are often reported in chronic infections and autoimmune diseases were markedly increased in the P.C+Chl+AEA group compared to the AEA group (Figure 4-4 E), marking the only key difference observed between mice that had a prior *P. chabaudi* infection followed by induction of AEA.

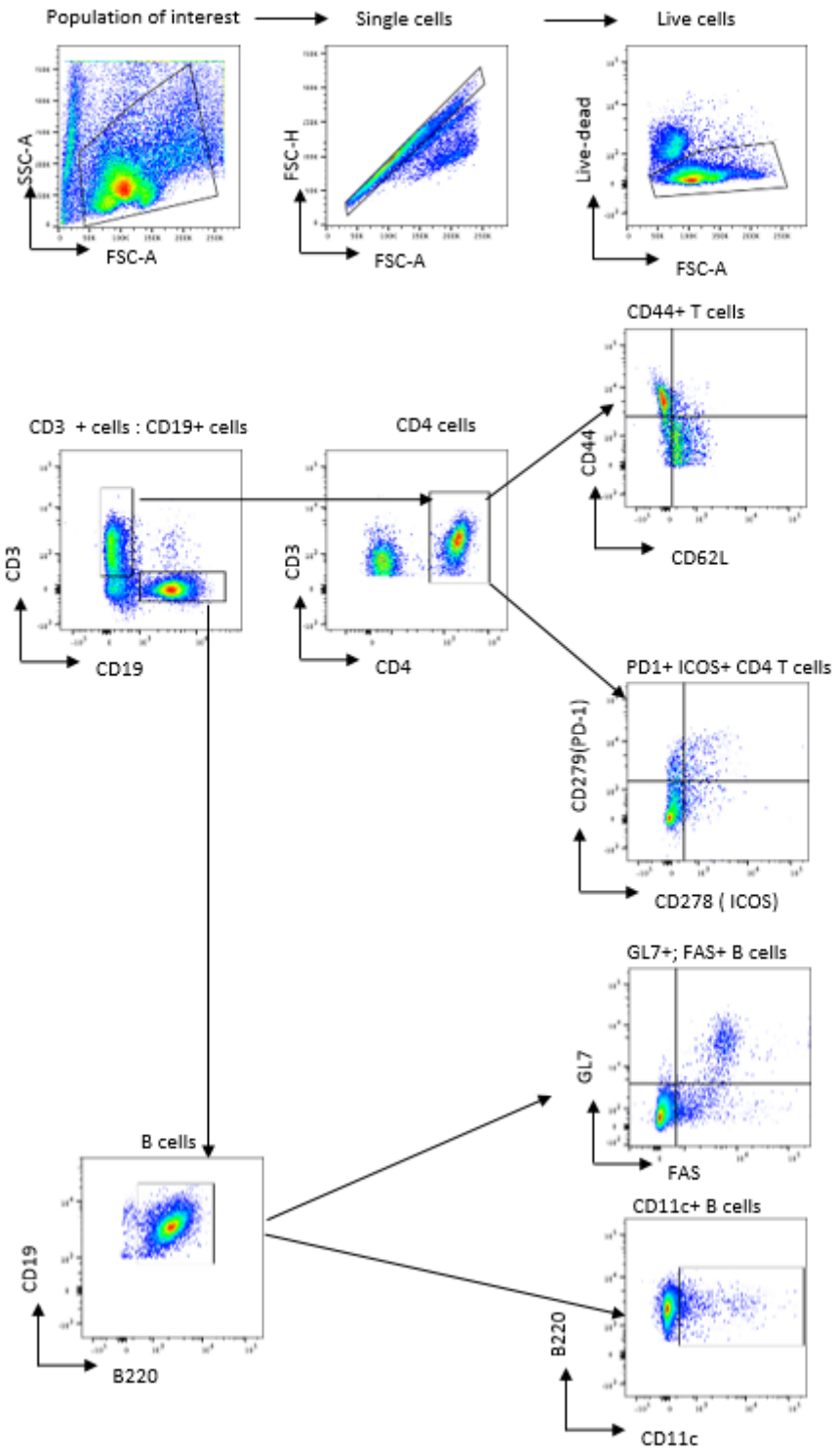

Figure 4-3: Gating strategy to identify activated CD4+ T cells and B cells

Illustrates the flow cytometry gating strategy for identifying activated CD4+ T cells and B cells from the spleens of infected mice. Initially, splenocytes were isolated and stained according to methods detailed in the method section. Activated CD4+ T cells were identified by gating on lymphocytes, single cells, and live cells, followed by the selection of CD3+ CD19- cells and the CD4+ marker. CD4+ T cells were then identified based on the CD44 (CD44hi) and CD62L markers, along with other markers such as ICOS and PD-1. For B cells, after gating on lymphocytes, single, and live cells, I isolated CD3- CD19+ cells. Germinal centre B cells were further identified within the CD19+ B220+ population using GL7 and FAS markers, and an additional marker, CD11c, was also used to identify CD11c B cell.

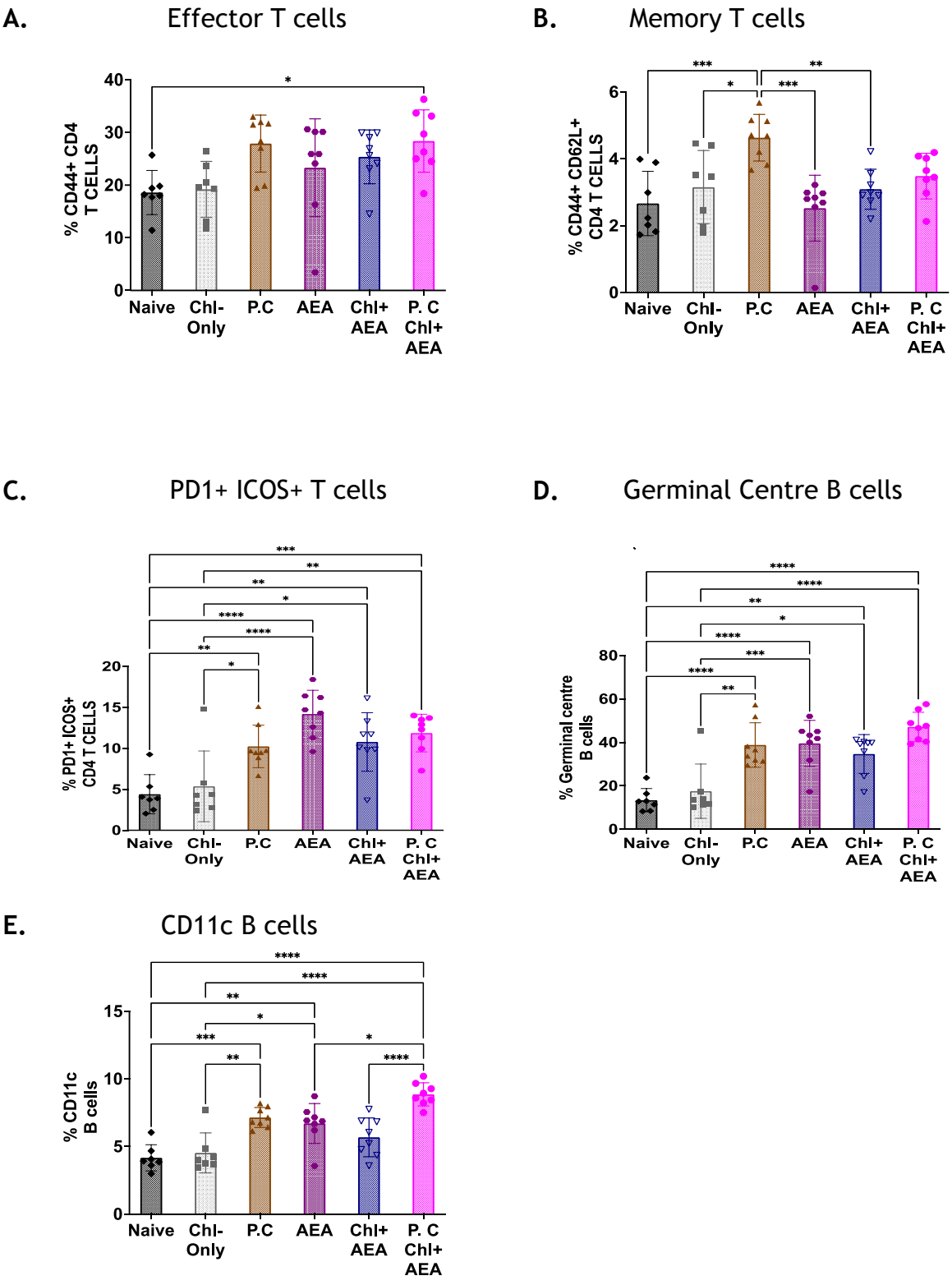

Figure 4-4: Increased CD11c B cells in the spleens of the P.C +Chl +AEA group compared to the Chl +AEA group

Spleen was harvested from all the experimental groups for flow cytometry. A.) Bar chart showing the percentage of effector T cells with mean +-SD (CD44+ CD4+ T cells.) B.) Percentage of memory CD4+ T cells (CD44+ CD62L+ CD4+ T cells) C.) Percentage of PD1+ CD CD4+ T cells D.) Percentage of GL7+ FAS+ B cells E). Percentage of CD11c B cells from the spleen of from the spleen of all the mice in the experimental groups. Statistical analysis one-way ANOVA with Tukey's multiple comparisons test comparisons test (ns: not significant * p-value of < 0.05; **: p<0.01).

4.2.3 Prior *P. chabaudi* infection doesn't impact the development of chronic experimental arthritis (CEA) model

Using the AEA model, I have shown that prior infection with *P. chabaudi* does not alter the course of the development of experimental arthritis in mice. However, given that the AEA model is a milder form of experimental arthritis model, I took advantage of an existing chronic experimental arthritis (CEA) model in our laboratory [286], particularly given that the CEA model is more applicable to human RA, as it results in a more aggressive form of disease with both an increased inflammatory response and extensive cartilage destruction in comparison to the AEA model [286].

Moreover, other studies have also reported on the impact of *Plasmodium* infection on the collagen-induced arthritis (CIA) model, which is a more aggressive form of experimental arthritis [348]. Notably, in one particular study the timing of *Plasmodium* infection was deemed crucial in the development of CIA [339]; specifically, infection with *P. yoelii* at four weeks rather than at one week prior to induction of CIA appeared to be protective and resulted in a milder form of arthritis [339]. Thus, given the significance of the use of a more aggressive experimental arthritis model and the impact of timing of infection, therefore in my study, I aimed to investigate the impact of prior infection of *P. chabaudi* on the development of CEA. Notably, this study was complex and involved several key steps, with the initial induction of AEA as outlined in (Figure 4-5), followed by *P. chabaudi* infection three weeks later and subsequent induction of CEA, several experimental groups were also included, as detailed in Table 4-2.

The development of CEA was assessed by daily measurements of paw thickness and clinical score. While increased paw measurements and clinical scores were observed across CEA, Chl+ CEA, and P.C+ Chl+ CEA, P.C.+ CEA groups (Figure 4-6 A-B), no differences were observed between mice that had prior infection with *P. chabaudi* suggesting that prior *P. chabaudi* infection did not alter the development of the CEA model.

Additionally, antibody responses to both the native and citrullinated peptides were also measured following *P. chabaudi* infection, particularly just before CEA induction. Notably, while *P. chabaudi*-infected mice exhibited increased antibody responses to both the native and citrullinated peptides (Figure 4-6 C-F), this did not exacerbate the development of CEA.

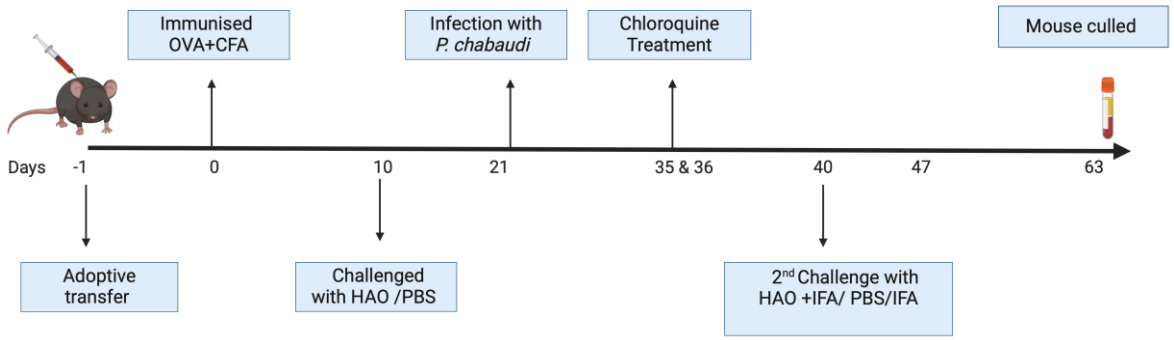

Figure 4-5: An outline of the experimental design that involved infection with *P. chabaudi* at three weeks and subsequent induction of CEA.

To induce CEA in mice, OTII T cells were isolated from transgenic mice and induced to differentiate into a Th1 phenotype. These Th1-polarised CD4+ T cells were then transferred into recipient C57BL/6 mice (n=8), and one day later, OVA antigen was prepared and administered to the mice. Ten days post-immunisation with the OVA antigen, the mice underwent a footpad challenge using either heat aggregated OVA antigen (HAO) or PBS. This was then followed by *P. chabaudi* infection three weeks later and treated with chloroquine on days 35 and 36. This was followed by subcutaneous injection of 50 µL containing 100 µg of HAO in Freund's incomplete adjuvant (IFA) into the same foot, while the control group received a 50 µl injection of PBS alone. The mice were then culled on day 62.

Table 4-2: Experimental groups

Group	Type	Treatment
Naive	Control	No treatment
P.C + Chl	Control	Mice infected *with P. chabaudi* followed by chloroquine treatment
CEA	Experimental group	Induction of chronic experimental arthritis (CEA)
P.C+ Chl+ CEA	Experimental group	Mice infected with *P. chabaudi* followed by chloroquine treatment and induction of CEA
P.C+CEA	Experimental group	Mice infected with *P. chabaudi*, followed by induction of CEA without chloroquine treatment

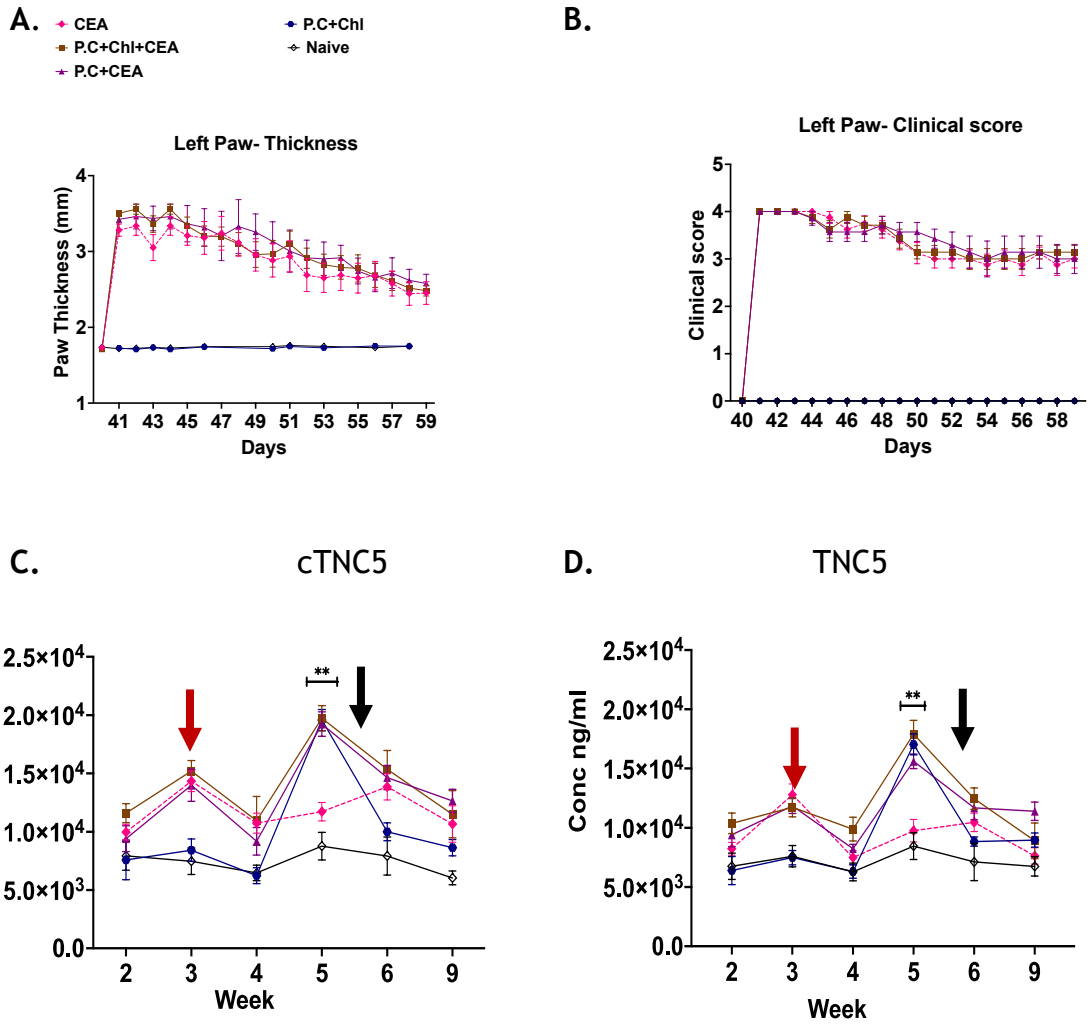
A.
CEA
P.C+Chl
P.C+Chl+CEA
Naive
P.C+CEA
Left Paw- Thickness
Paw Thickness (mm)
Days
B.
Left Paw- Clinical score
Clinical score
Days
C.
cTNC5
Conc ng/ml
Week
D.
TNC5
Conc ng/ml
Week

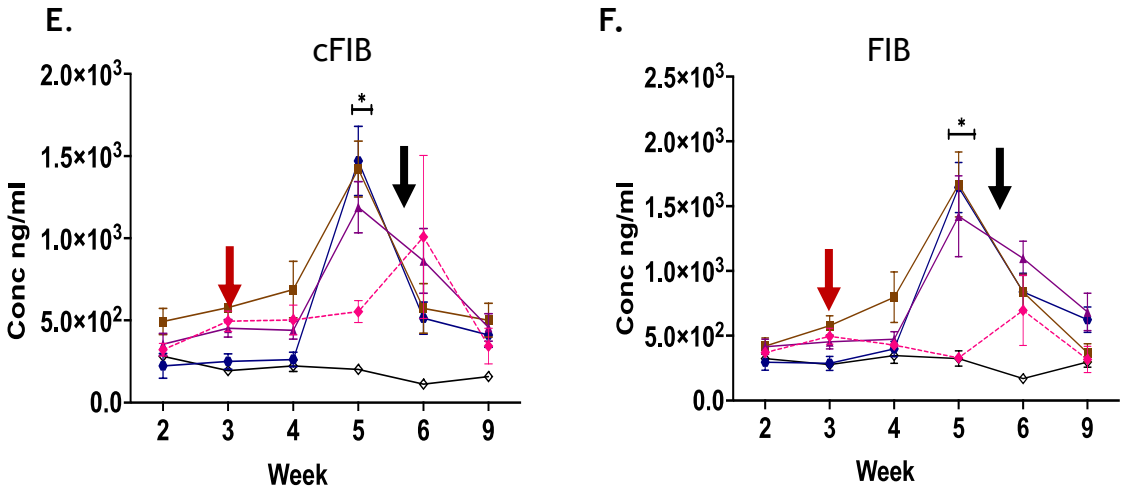

Figure 4-6: Prior *P. chabaudi* infection doesn't impact the development of chronic experimental arthritis (CEA) Model.

Following the induction of Chronic Experimental Arthritis (CEA) in mice, paw thickness and clinical scores were measured daily. A.) Graph showing the mean +/- SEM of left hind paw thickness in mm B.) Graph showing the mean +/- SEM of left hind paw clinical score. Blood samples were taken periodically for ELISA. The study timeline is delineated by arrows: red for when mice were infected with *P. chabaudi* infection, and black for CEA induction. Autoantibody responses to cTNC5 and cFIB, as well as their corresponding native peptides TNC5 and FIB, were evaluated using ELISA. C.) and D.) Graphs represent the autoantibody responses to cTNC5 and its native peptide TNC5, while E.) and F.) Represent responses to cFIB and the native peptide FIB. Statistical analysis was performed using one-way ANOVA with Tukey's multiple comparisons test, with significance levels marked as *p < 0.05, **p < 0.01, ***p < 0.001, ****p < 0.0001. Key comparisons indicated were made between the P.C+Chl+CEA and CEA group.

4.2.4 Increased activation of germinal centre B and T cells in the spleen of *P. chabaudi* CEA.

Next, I evaluated the activation status of B and T cells in the popliteal lymph node and the spleen, I will first discuss the data from the lymph node. Specifically, I examined the expression of CD44 and CD62L on these cells across all groups to identify effector T cells (CD4+ CD44HI, CD62L-) and memory T cells (CD4+ CD44+ CD62L+). No significant differences were observed in effector CD4+ T cells (CD44HI, CD62L-) across the groups (Figure 4-7 A); however, memory CD4+ T cells (CD44+ CD62L+) (Figure 4-7 B); showed a notable increase in the P.C+Chl+CEA group compared to the P.C+Chl group alone.

Next, I analysed PD1+ICOS+ CD4+ T cells these markers were used to identify T follicular helper (Tfh) cells, which play an important role in promoting the production of high-affinity, class-switched antibodies by driving B cell responses within germinal centres, crucial for effective immune defence [317]ce [317]. These cells were significantly increased in the P.C+Chl group only compared to CEA and P.C+ Chl+CEA (Figure 4-7 C). Additionally, I also assessed B cells expressing FAS+GL7+ markers to identify germinal centre B cells. An increase in germinal centre B cells was observed only in the P.C+Chl+CEA group compared to the naive group (Figure 4-7 D). In addition, the percentage of atypical B cells a sub-set of B cells identified by CD11c marker were also assessed. No significant differences in CD11c B cells were observed across all the groups (Figure 4-7 E).

Notably, flow cytometry was also performed on the spleen, a crucial lymphoid organ in mounting immune responses against *Plasmodium* infections. An increased percentage of effector T cells in the P.C+Chl +CEA group compared to the CEA and naive groups was observed (Figure 4-8 A). ICOS+ PD1+ CD4+ T cells were also higher in the P.C+Chl+CEA than in all other experimental groups (Figure 4-8 C), and a similar trend was observed with germinal centre and CD11c B cells (Figure 4-8 D-E).

Overall, an activated immune phenotype was observed in the spleen compared to the lymph node, with increased levels of PD1+ICOS+ CD4+ T cells, germinal centre B cells, and CD11c B cells in the P.C+Chl +CEA group compared to the CEA groups.

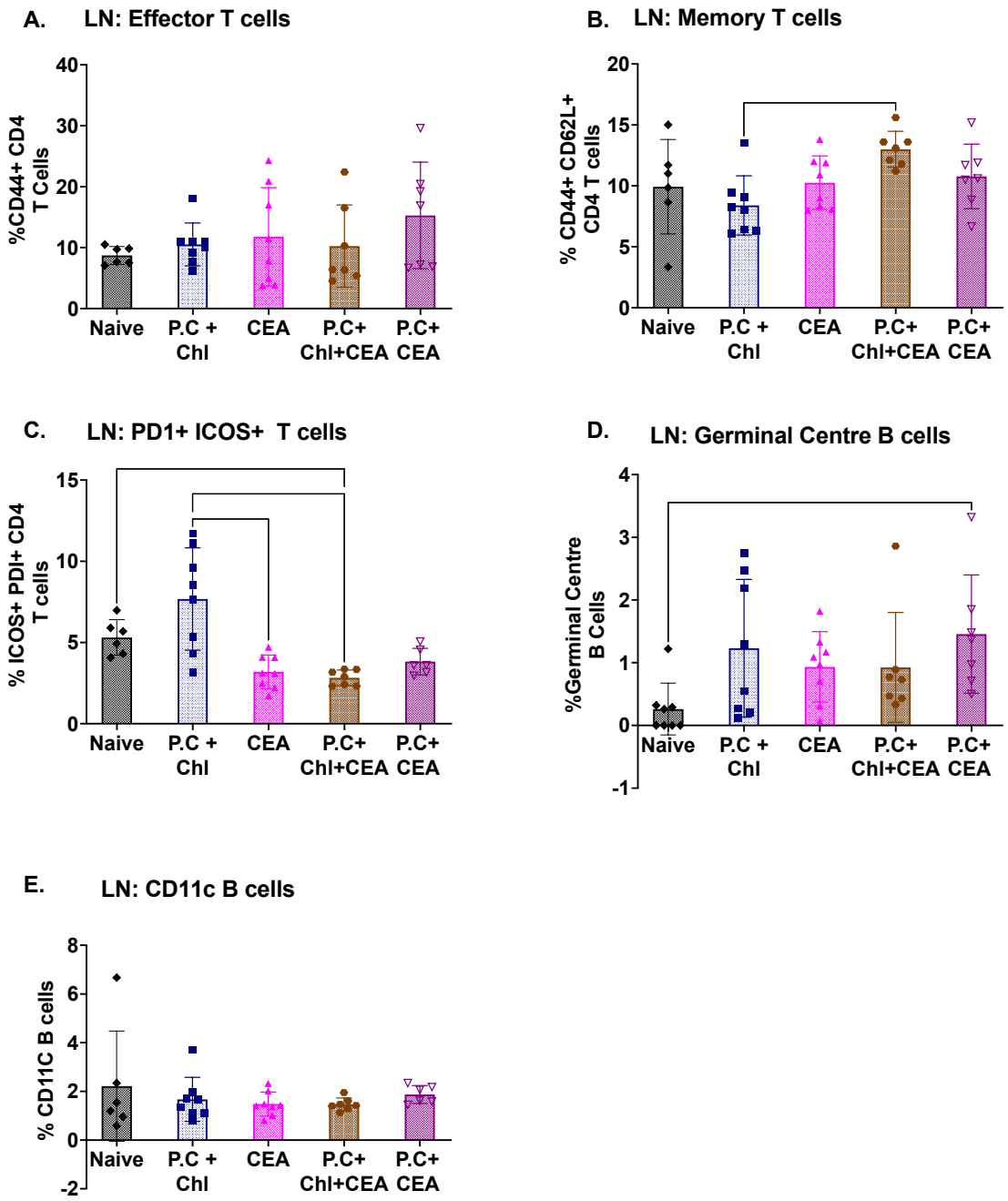

Figure 4-7: No significant differences in B and T cell activation in the lymph node

Following infection with *P. chabaudi*, and the subsequent induction of CEA as outlined in Figure 4-5. Cells were obtained from the left popliteal lymph node and flow cytometry was performed. A.) Bar chart showing the percentage of effector T cells (CD44+ CD4+ T cells.) B.) Percentage of memory CD4+ T cells (CD44+ CD62L+ CD4+ T cells) C.) Percentage of PD1+ CD4+ T cells D.) Percentage of GL7+ FAS+ B cells E). Percentage of CD11c B cells from the left popliteal lymph node in all the experimental groups. Statistical analysis was performed using one-way ANOVA with Tukey's multiple comparisons test comparisons test (* p-value of < 0.05; **: p<0.01).

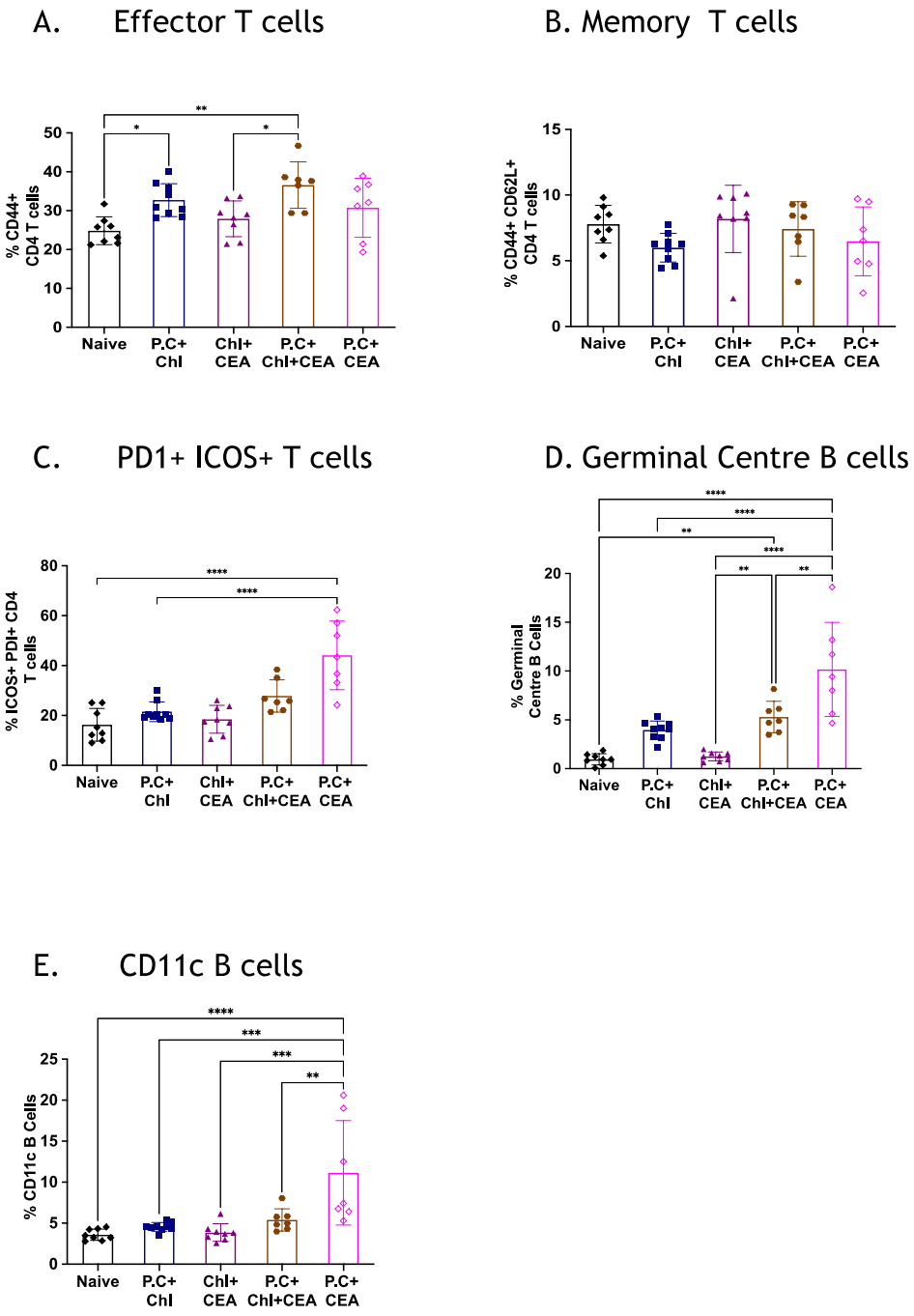

Figure 4-8: Increased activation of both germinal centre B and T cells in the spleen of *P. chabaudi* CEA group.

Following infection with *P. chabaudi*, and subsequent induction of CEA as outlined in Figure 4-4 Cells were obtained from the spleen and flow cytometry was performed. A.) Bar chart showing the percentage of effector T cells (CD44HI CD4+ T cells.) B.) Percentage of memory CD4+ T cells (CD44+ CD62L+ CD4+ T cells) C.) Percentage of PD1+ ICOS+ CD4+ T cells D.) Percentage of germinal centre B cells E). Percentage of CD11c B cells from the spleen of all the mice in the experimental groups. Statistical analysis was performed using one-way ANOVA with Tukey's multiple comparisons test comparisons test (ns: not significant * p-value of < 0.05; **: p<0.01).

4.2.5 *P. chabaudi* infection and pathology is not ameliorated by increased antibody responses to native and citrullinated peptides

In the sections above, I have examined the impact of *P. chabaudi* infection on the development and progression of experimental arthritis, with the focus of determining whether the heightened production of antibodies against native and citrullinated peptides exacerbates arthritis. While these antibodies do not seem to play a crucial role in the development of both AEA and CEA, it is vital to explore whether they play a key role in protection, particularly given evidence of the role of autoimmunity in clinical malaria protection [5]. Thus, it was crucial to explore and set up experiments that would shed light on the potential protective role of these antibodies in the acute phase of *Plasmodium* infection. This approach therefore aims to provide a deeper understanding of the dual role of these antibodies in both experimental arthritis and *Plasmodium* infection contexts.

As detailed above, the role of *Plasmodium* induced autoantibodies is controversial, with several studies suggesting that they play a protective role [204,307]; specifically, autoantibodies have been shown to have an inhibitory effect of on parasite growth in vitro [5,204], while other studies also report the potential contribution of autoantibodies to the severity of the disease [1,222].

To gain insights into the role of antibodies against native and citrullinated peptides in, I tested the hypothesis that autoantibodies produced during *Plasmodium* infection could be significant in conferring protection from the disease. Herein, I induced chronic experimental arthritis in mice to stimulate the production of antibodies to native and citrullinated peptides and subsequently infected the mice with *P. chabaudi* to observe the impact of these autoantibodies on disease progression as outlined in (Figure 4-9 A). Appropriate controls, such as P.C and naive groups, were also included.

At day 49, prior to *P. chabaudi* infection, increased levels of autoantibodies above the naive were observed for some of the peptides tested (Figure 4-9 B-E), with *P. chabaudi* infection resulting in a further increase in the levels of antibodies to native and citrullinated peptides. However, no differences in parasitaemia or weight loss between the CEA+ P.C and P.C groups were observed (Figure 4-9 F-G).

Therefore, my findings suggest that while elevated antibodies to both native and citrullinated peptides are produced during *Plasmodium* infection, they may not necessarily provide protection against the disease or substantially impact pathology.

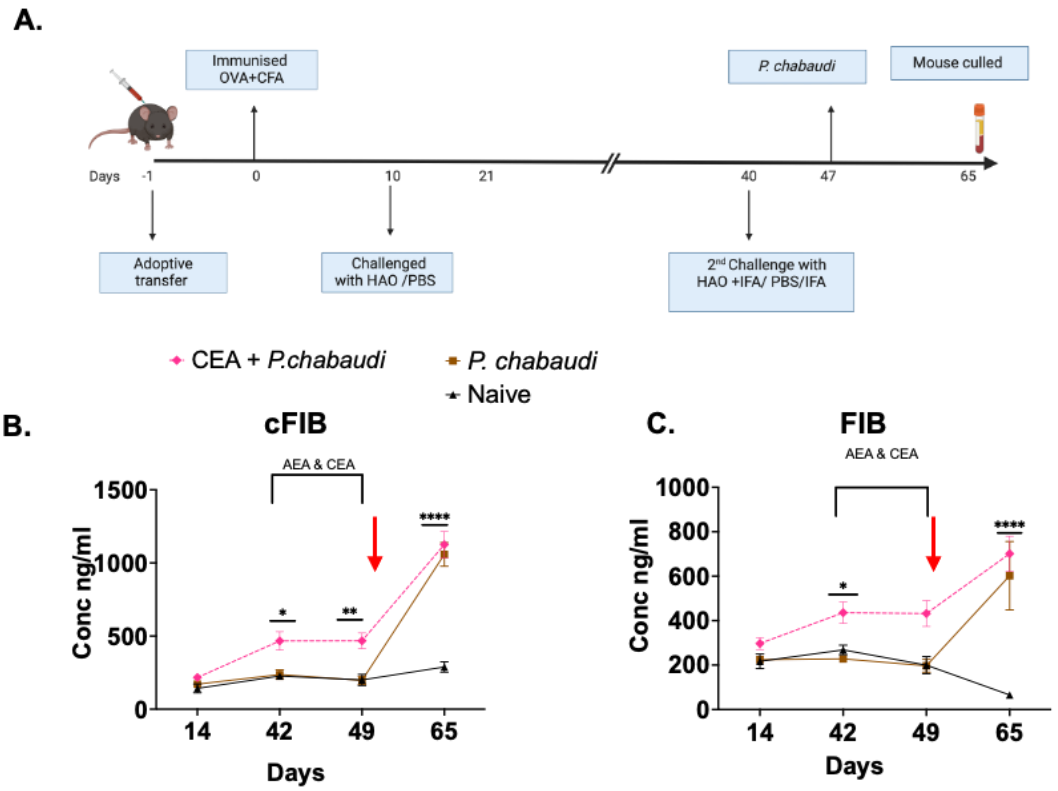

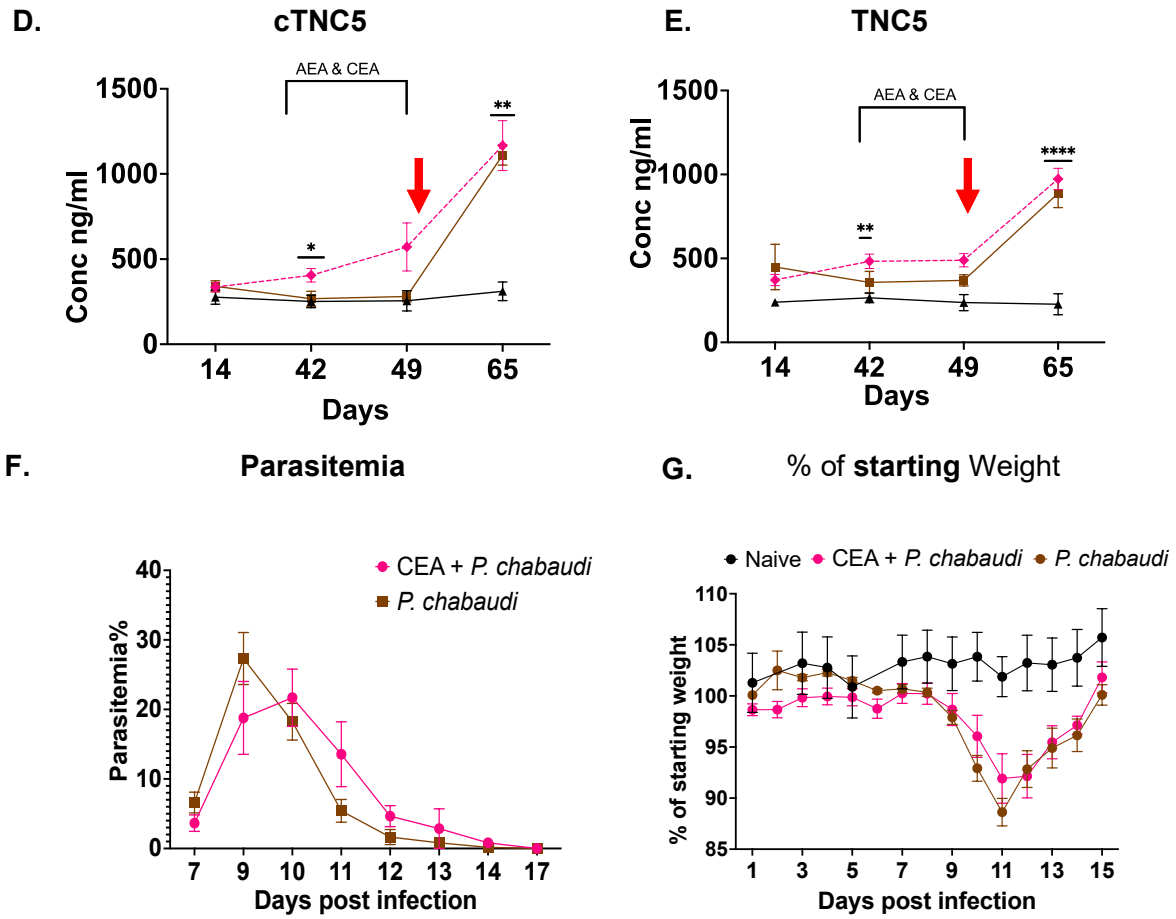

Figure 4-9: Prior experimental arthritis does not ameliorate *P. chabaudi* infection or pathology.

Experimental arthritis was induced in a group of naive male C57BL/6 mice followed by infection with *P. chabaudi* (PC+EA group), while another group of mice, were only infected with *P. chabaudi* (P.C). Appropriate naive controls were included. Mice were weighed daily and parasitaemia was determined daily via tail bleed. (A) An outline of the experimental design. Tail bleeds were taken periodically for ELISA over a 65-day period with the red arrow indicating when the *P. chabaudi* infection was performed. A time-course of the autoantibody response to cTNC5 and cFIB and the corresponding native peptides TNC5 and FIB was determined using ELISA (B) Anti-cFIB. (C) Anti-Fib, (D*)* Anti- cTNC5, (E) Anti-TNC5 autoantibody response. The levels of parasitaemia and weight were also determined over the course of the infection. (F) parasitaemia (percentage of infected red blood cells) and (G.) Percentage change in weight in the *P. chabaudi* infected mice. Graphs show mean with SEM, with Tukey's multiple comparisons test ns: not significant * p-value of < 0.05; **: p<0.01.

4.3 Discussion

While the presence of ACPA is a key feature of rheumatoid arthritis (RA) and has been shown to be associated with aggressive bone and joint destruction [102], the role of *Plasmodium*-induced antibodies against native and citrullinated peptides has not been explored. Particularly given that presence of these autoantibodies in the context of *Plasmodium* infections has only now been reported in this thesis (ref chapter 3). In this chapter, I, therefore, discuss the impact of heightened antibodies to both native and citrullinated peptides on the development of both the AEA and the CEA models and further investigate whether increased levels of these antibodies could confer protection during acute *Plasmodium* infection in mice.

To investigate the impact of *Plasmodium* infections on the development of experimental arthritis, I took advantage of the two experimental arthritis models available in our lab. In the first experiment, mice were infected with *Plasmodium chabaudi* prior to the induction of AEA, which resulted in increased antibodies to both native and citrullinated peptides levels Figure 4-2; however, these did not result in any significant effect on acute experimental arthritis progression, as the experimental groups AEA, Chloro-AEA, and P.C+Chl+AEA groups had similar clinical scores and paw measurements.

Next, I explored a second approach, which involved prior infection with *P. chabaudi* followed by subsequent induction of the CEA. This model is known to result in more aggressive arthritis, and its features mimic the human RA; thus, would provide a platform to gain insights into the role of antibodies to both native and citrullinated peptides using a more chronic model. While increased levels of these autoantibodies were observed as a consequence of *Plasmodium* infection, prior to induction of CEA (Figure 4-6), all mice developed arthritis irrespective of prior *P. chabaudi* infection, without any significant differences across the key groups (P.C+CEA groups and CEA). Therefore, these data suggest that although the levels of antibodies to both native and citrullinated peptides were increased in the (P.C+CEA groups) compared to the CEA, this didn't alter the progression of CEA. One possible explanation is that the ACPA levels induced by *P. chabaudi* infection did not exceed a critical threshold needed to impact disease progression. Particularly, given that, the antibody responses to citrullinated peptides may have

been comparable to those against native peptides, failing to drive a stronger autoimmune response. Additionally, this data contrast evidence from several studies; for example, treating mice with anti-citrullinated vimentin has been shown to induce bone loss [349]; additionally, monoclonal antibodies derived from human RA, when injected into mice, has been shown to induce pain-like behaviour, bone loss, and inflammation, mimicking pre-clinical RA [341]. Conversely, there is also evidence suggesting that recombinant ACPA ameliorates disease symptoms [350], indicating that the role of ACPA is unclear.

Notably, *Plasmodium* infections have been shown to confer protection against experimental arthritis in mice [9,339]; however, this protective effect appears to vary depending on the arthritis model used, the timing of arthritis induction relative to the timing of *Plasmodium* infection [339], and *Plasmodium* species-specific [338,339], which possibly explains variation in the findings reported in my study.

B and T cell phenotypes were also examined, and a significant increase in CD11c B cells in the P.C+ AEA group compared to the AEA group were observed. Additionally, the second experimental outline where mice were infected with *P. chabaudi* followed by induction of (CEA), the P.C+CEA group exhibited an overall increased immune activation with higher levels of germinal centre B cells, CD11c B cells, and PD1+ICOS+CD4+ T cells compared to the CEA group. These pronounced differences in immune activation between the AEA and the CEA could be attributed to the use of a CEA model in the second experimental outline which is more chronic and severe. Additionally, and consistent with my findings, increased CD11c B cells which I also observed have previously been associated with the production of autoantibodies that target uninfected RBC [3,4]. However, given the scope of this study, my results indicated a correlation between the increase in CD11c B cells and the production of antibodies to both native and citrullinated peptides, but causation could not be established.

Lastly, while there is evidence supporting the role of autoantibodies in conferring protection from *Plasmodium* infections, specifically, higher levels of anti-self-antibody levels detected in children with asymptomatic malaria compared to those with mild symptomatic malaria [351]. Increased antibodies to both native and citrullinated peptides , prior to infection with *P. chabaudi*, did not alter the clinical disease progression or pathology, suggesting that while *Plasmodium*-

induced antibody responses to these peptides are present, they may not be crucial in providing protection.

In conclusion, these findings suggest that while *Plasmodium* infections induce elevated antibody responses to both native and citrullinated peptides, these antibodies do not affect the development of experimental arthritis, nor do they confer protection against clinical malaria. However, further research is needed to understand the complex interplay between the generation of these autoantibodies and *Plasmodium* infections. For example, future research could focus on the use passive transfer studies of specific monoclonal ACPA to evaluate their role in development of experimental arthritis and further determine the threshold above the native that would results in development of experimental arthritis. Importantly, to gain insights into the role of *P. chabaudi* induced antibody responses to both native and citrullinated peptides in conferring protection against *Plasmodium* infections, future studies could also employ the use of in vitro assays, such as growth inhibition assays, to further shed light on their protective effects against the *Plasmodium* parasite.

5 Chapter 5- Investigating the association between *Plasmodium falciparum* infections/disease severity and autoimmunity using samples from individuals residing in an endemic area in Kenya.

5.1 Introduction

Having reported on the induction of increased antibody responses to both native and citrullinated peptides in mice infected with *P. chabaudi* in chapters 3 and 4, I extended my investigations to human malaria using historical samples, initially collected for malaria immunology studies at KEMRI Wellcome Trust Research Programme in Kilfi, Kenya (KWTRP), to determine whether *P. falciparum* exposure and severe malaria are associated with increased autoimmune antibodies. These analyses involved samples from both adult and children cohort participants from Junju and Ngerenya in Kilifi County, Kenya. Importantly, while these two villages are only about 20 kilometres apart, they experience differential malaria transmission levels; with Junju experiencing moderate to high levels of *P. falciparum* exposure, while Ngerenya has seen a drastic reduction in *P. falciparum* exposure from 40% in 1998 to between very little and nil since 2000 [299]. The variability in malaria transmission between the two cohorts made them suitable for measuring correlations between levels of *P. falciparum* exposure and autoantibody levels.

Notably, *P. falciparum* transmission in Kilifi is seasonal with two distinct seasons annually: the primary season runs from May to July and coincides with the long rains, while the second season takes place in November, aligning with the short rains [297]. The adult samples used in this study were collected in 2017 and 2018 during an annual cross-sectional bleed in March, corresponding to a period of very low *P. falciparum* transmission.

In addition to the adult samples, I also used samples from children to determine the presence of autoantibodies in uncomplicated (mild) and severe malaria cases. The uncomplicated malaria cases came from Junju (SIMs) (moderate to high *P. falciparum* transmission), and the severe cases were from a hospital admission cohort. Samples from uninfected children from Ngerenya (very low transmission) were used as healthy uninfected controls.

In this chapter, through the application of the above samples I seek to further explore the association between malaria and autoimmunity. Although the presence of autoantibodies is a common feature of *Plasmodium* infections [6,132,239,249], the association between malaria infection and autoimmunity is still considered complex, with specific autoantibodies, such as anti-phosphatidylserine, associated with severe malaria anaemia as they recognise uninfected RBC, thus promoting their clearance [1]. In contrast, there is new evidence suggesting that increased autoantibodies in children before a malaria season has been associated with better clinical malaria outcomes [5,204], thus indicating that autoantibodies elicited during *Plasmodium* infections could be playing a dual role of protection and pathology.

Moreover, to add to the complexity of this association between *Plasmodium* infections and autoimmunity, chronic *Plasmodium* infections are known to drive the selection of certain genetic traits that increase susceptibility to autoimmune diseases such as systemic lupus erythematosus (SLE) [7]. For example, data from experimental studies indicate that genetic susceptibility to SLE appears to protect against cerebral malaria in mice [261], while, at the same time, evidence from population studies indicates the presence of increased frequencies of specific variants of genes such as FcγRIIB in individuals of African ancestry as well as patients with SLE [7,260]. Thus, suggesting that malaria could be driving the presence of genes that are associated with SLE [7,12].

Given the complex interactions between *Plasmodium* infections and autoimmune diseases there is need to better understand the association between *Plasmodium* infections and autoimmunity particularly by conducting studies in malaria endemic areas. Herein, I will focus on the presence of specific autoantibodies, such as such as antibodies to both native and citrullinated peptides, first observed in *P. chabaudi* infected mice as described in chapters 3 and 4. Furthermore, extending these findings to a clinical setting is crucial, particularly given that ACPA is also a key biomarker in the clinical diagnosis of RA [352].

To investigate this further, I take advantage of well-established adult and children's cohorts in Kilifi, Kenya with each cohort playing a distinct role in addressing the different aims of the study.

First using the adult samples, I establish the presence of antibodies to both native and citrullinated peptides in individuals exposed to *Plasmodium* infections. In addition, I phenotyped B and T lymphocytes in these adults' cohort to identify immune cells that could be linked to the production of these autoantibodies.

Second, to further enhance our understanding of the association between *Plasmodium* infections and autoimmunity, I also apply the use of the GeneCopoeia autoantigen protein microarray platform to screen a wider more comprehensive array of autoimmune markers. Thus, providing a clearer picture of whether chronic exposure to *Plasmodium* infection is associated with increased frequencies of autoantibodies similar to those observed in autoimmune diseases.

Lastly, aligning with my research hypothesis, where I hypothesised that increased autoantibodies could be playing an important role in the acute phase of the infection. I utilised samples from children with varied malaria outcomes. Specifically, I used a cohort of children residing in the same community, that is, Junju and Ngerenya, with varied malaria outcomes, that included, healthy children, children with uncomplicated malaria, and children with severe malaria to investigate the potential association of increased antibodies to both native and citrullinated peptides with the varied clinical outcome. Importantly, the rationale for using the child cohort is supported by the recent evidence of the association between increased autoimmunity and enhanced protection from severe malaria [5], due to the functional ability of the autoantibodies to inhibit parasite growth [5].

5.1.1 Research Hypothesis

I hypothesise that *P. falciparum* infection leads to the production of low-affinity binding autoantibodies that play a protective role in acute malaria; however, this might increase the risk of developing autoimmune disease later in life.

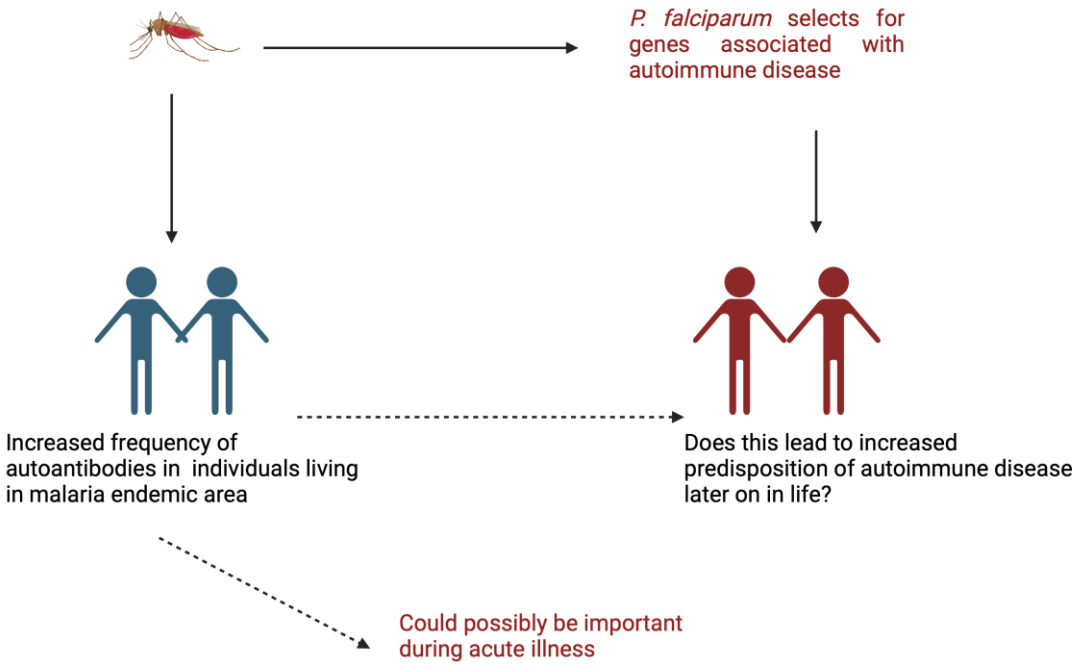

Figure 5-1: Illustration of the research hypothesis.

Solid lines represent established relationships that have been confirmed by existing research, while dashed lines indicate hypothesised associations that I proposed to investigate in this research. Figure Created with BioRender.com

5.1.2 Chapter Aims

1. To assess the prevalence of known autoimmune markers, including ACPA and antibody responses to their corresponding native peptides, in adults living in malaria-endemic regions.

2. Examine immunological phenotypic differences in individuals residing in a malaria-endemic areas with varied antibody responses to both the native and citrullinated peptides.

3. Investigate the presence of antibody responses to both the native and citrullinated peptides in children with varied clinical outcomes.

5.2 Results

5.2.1 Description of adult cross-sectional bleed study cohorts (2017 -2018)

For this research I used samples from a cross-sectional adult bleed, which is conducted yearly in two villages Junju and Ngerenya in Kilifi, Kenya. The total number of samples included in the study was 224, with the samples used drawn from two years, 2017 (n=71) and 2018 (n=153). The available epidemiological data included the participants' age and gender, as summarised in (Table 5-1).

Table 5-1: Description of adult samples cross-sectional study year 2017 and 2018

Location	Gender		Age range (Yrs)	Year_ 2017 (n=71)	Year_ 2018 (n=153)	Total samples
	F	M				
Junju	69	33	18-60	36	66	102
Ngerenya	69	53	17-69	35	87	122

5.2.2 Increased antibody responses to native and citrullinated peptides in adults living in high *P. falciparum* transmission (Junju)

To first demonstrate differences in the levels of *P. falciparum* exposure in the adult test samples, I used a *P. falciparum* parasite lysate (schizont extract) ELISA to assess the level of anti-parasite antibodies. Samples from Swedish donors with no prior exposure to *Plasmodium* parasite were included as negative controls. As expected, individuals from Junju exhibited significantly higher levels of antibodies to the *P. falciparum* extract compared to those from Ngerenya and the Swedish controls (Figure 5-2). Next, with the parasite exposure levels established in both cohorts, I proceeded to test for the presence of antibody responses to native and citrullinated peptides across the Junju and Ngerenya cohorts.

Interestingly, using ELISA increased levels of antibodies against citrullinated peptides (cTNC5, cFIB, CEP) and their corresponding native peptides (TNC5, FIB,

REP,) were observed in adults from Junju compared to those from Ngerenya, suggesting that *Plasmodium* infection might drive the production of elevated levels of antibodies to both the native and citrullinated peptides (Figure 5-3 A-F). Notably, cVIM was the only peptide whose antibody levels were similar between the two groups; however, antibody response to the native peptide VIM were increased in Junju compared to Ngerenya (Figure 5-3 G-H).

Moreover, the responses to citrullinated peptides seem to closely mirror the responses to the corresponding native peptides, such that adults with high responses to citrullinated peptides also tended to have high responses to native peptides, as shown in (Figure 5-4). Specifically, high Pearson's correlations were observed between cFIB and FIB (r = 0.76), cVIM and VIM (r = 0.63), CEP and REP (r = 0.51), and cTNC5 and TNC5 (r = 0.48). These correlations, therefore, suggest a strong association between responses to the native and citrullinated peptides, indicating that the immune response to the native peptides may precede those of citrullinated peptides or vice versa, however, further studies maybe required to establish the sequence of the immune responses.

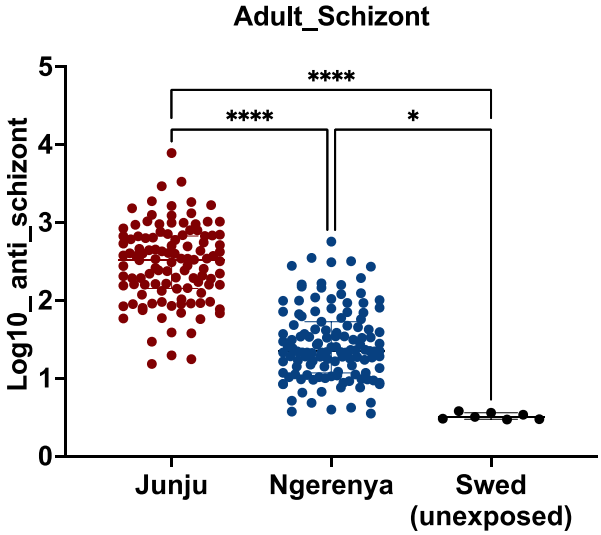

Figure 5-2: Significantly, higher levels of anti-schizont IgG antibody levels in Junju compared to Ngerenya.

Parasite exposure levels were measured using an anti-*P. falciparum* parasite lysate IgG ELISA (N=224). Comparisons of IgG antibody levels were made between samples individuals residing in Junju, Ngerenya, and a few malaria-naive controls (Swedish control). Kruskal-Wallis test followed by Dunn's test for multiple comparisons were performed, with error bars representing the median with interquartile range (*- p<0.05, **=<0.01, ***=<0.001).

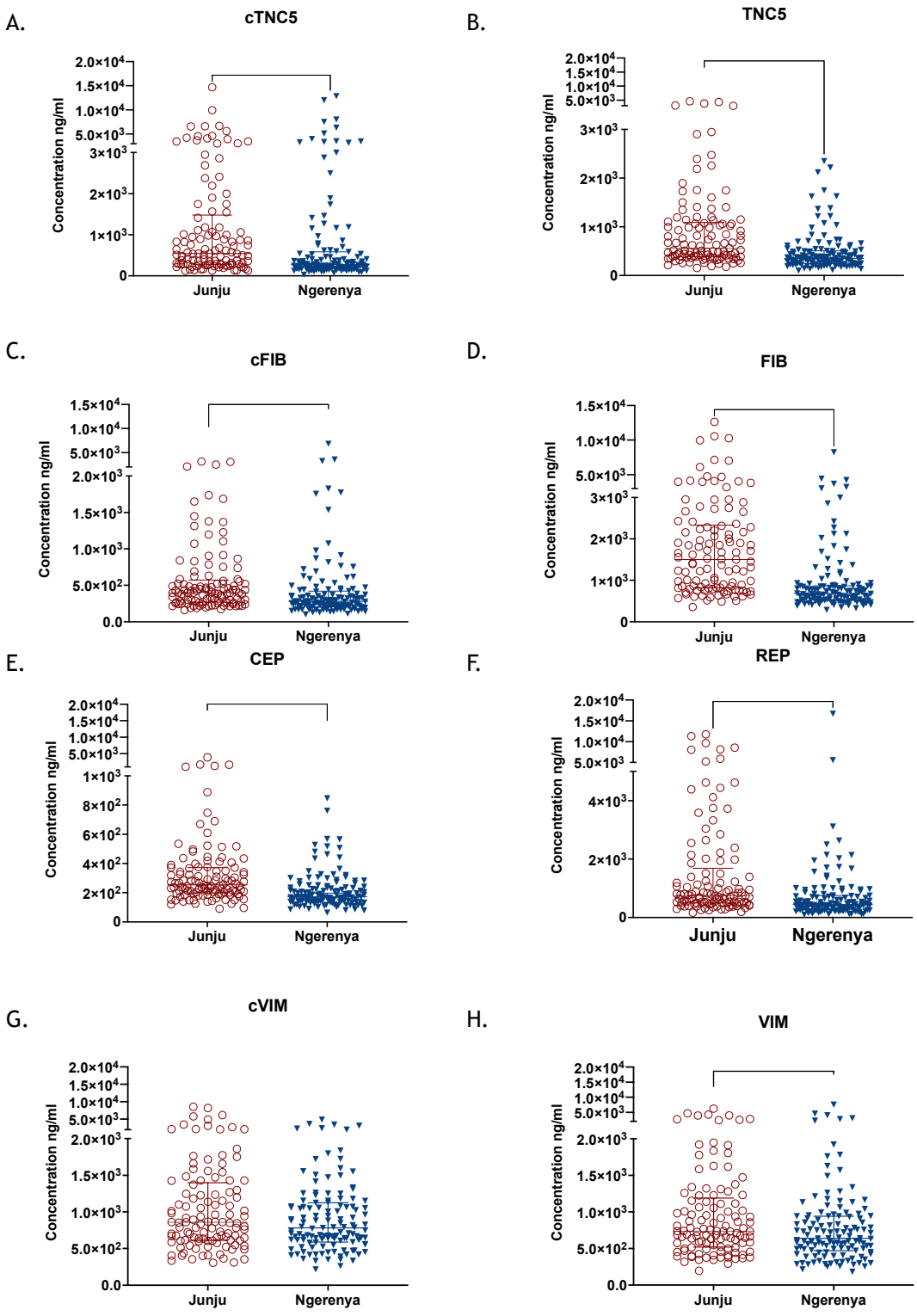

Figure 5-3: Significantly elevated levels of antibodies to native and citrullinated peptides responses in individuals from Junju

Antibody responses to citrullinated and corresponding native peptides were assessed in two adult cohorts from Junju and Ngerenya using ELISA. As represented using scatter plots as follows, cTNC5 and TNC5 in panels (A and B), cFIB and FIB in panels (C and D), CEP and REP in panels (E and F), and cVIM and VIM in panels (G and H). Error bars represent the median with interquartile range. Statistical analysis was performed using Mann-Whitney test. Statistical significance indicated: * $p<0.05$, ** $p<0.01$, *** $p<0.001$.

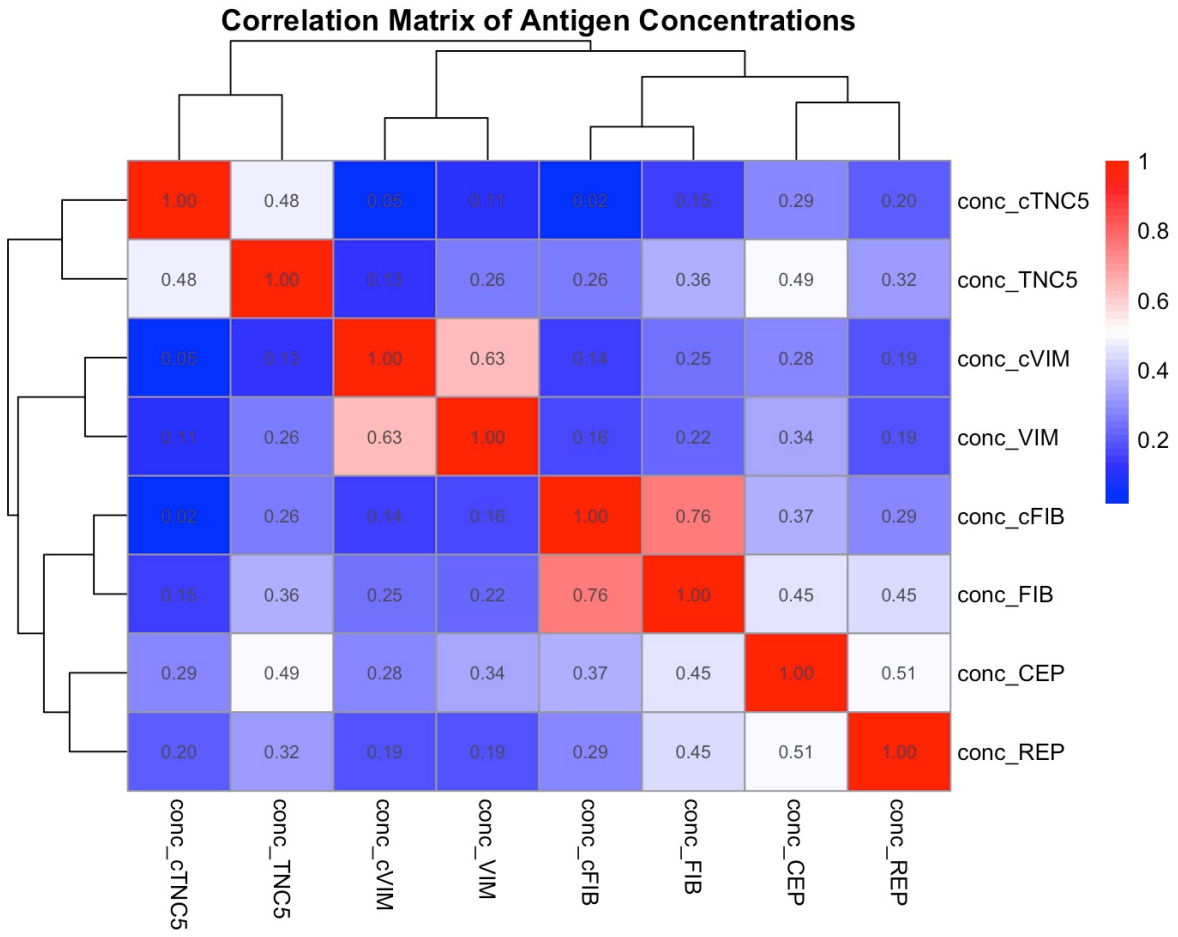

Figure 5-4: Antibody responses to citrullinated and native peptides were highly correlated.

A Pearson correlation matrix was used to visualise the correlation between citrullinated and native peptides ELISA data with the colour scale bar representing the correlation range, from 0.2 to 1, with red indicating a high correlation.

5.2.3 Gender and parasite exposure influence autoantibodies

While my data suggested that parasite exposure plays a role in shaping antibody responses to native and citrullinated peptides, I further analysed whether other factors such as age, sex, and schizont exposure (another marker of parasite exposure) impacted the levels of these autoantibodies. The correlation plots (Figure 5-5 A- D) indicated that being male and having higher parasite exposure were key contributors to increased autoantibodies levels. Specifically, representative plots for CEP, REP, and TNC5 (Figure 5-5 B, C, D) suggest that sex and parasite exposure influence autoantibody levels. However, for cTNC5 (Figure 5-5 A), these variables did not appear to have a significant effect. (see Supplementary Figure 7-1 for additional plots for cVIM, VIM, and cFIB, FIB responses).

A

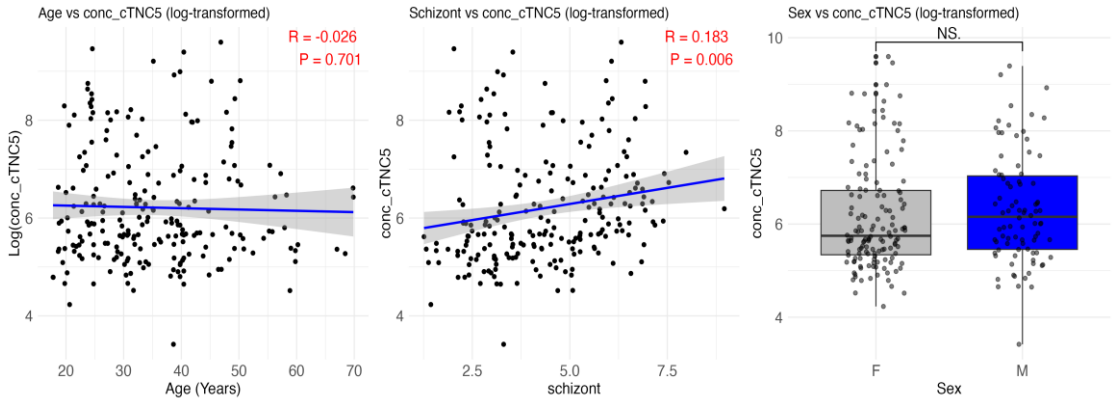
Age vs conc_cTNC5 (log-transformed)
R = -0.026
P = 0.701
Log(conc_cTNC5)
Age (Years)
Schizont vs conc_cTNC5 (log-transformed)
R = 0.183
P = 0.006
conc_cTNC5
schizont
Sex vs conc_cTNC5 (log-transformed)
NS.
conc_cTNC5
F
M
Sex

B

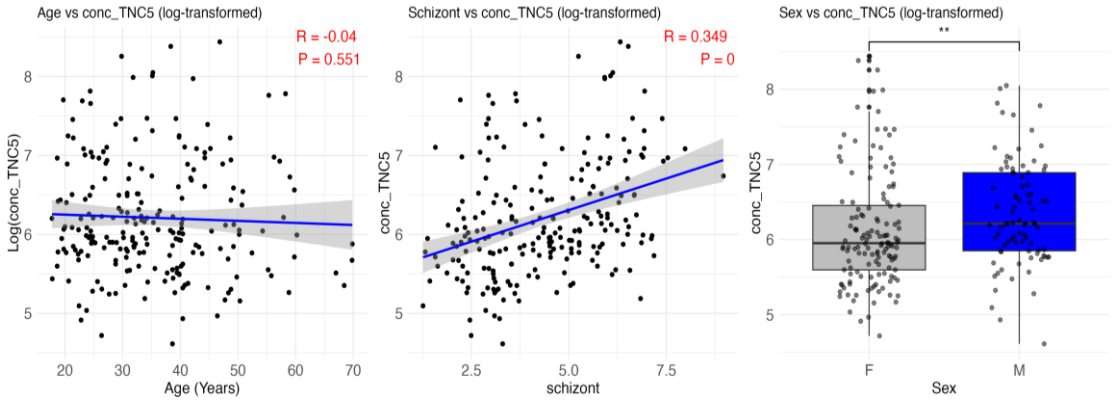
Age vs conc_TNC5 (log-transformed)
R = -0.04
P = 0.551
Log(conc_TNC5)
Age (Years)
Schizont vs conc_TNC5 (log-transformed)
R = 0.349
P = 0
conc_TNC5
schizont
Sex vs conc_TNC5 (log-transformed)
**
conc_TNC5
F
M
Sex

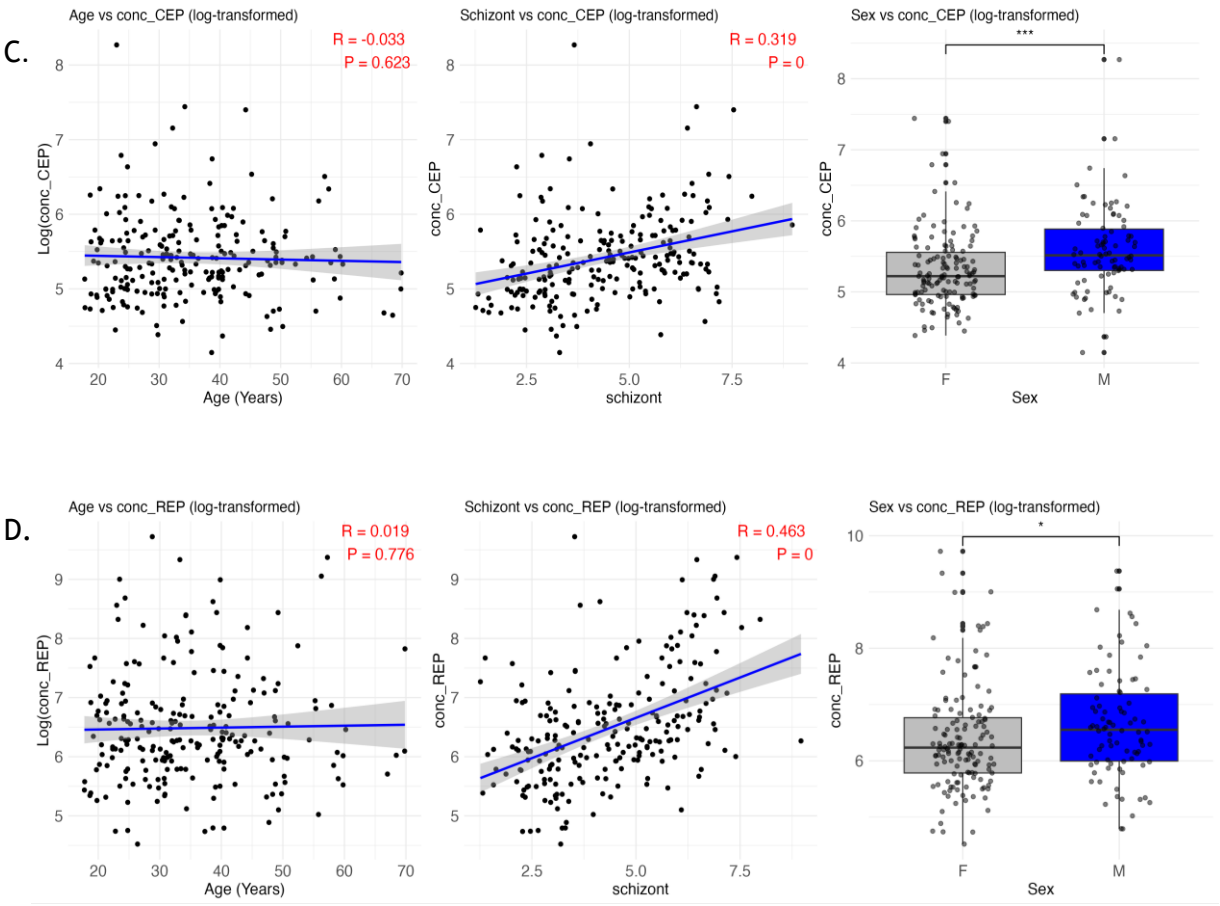

Figure 5-5: Sex and exposure to the parasite observed to influence antibody responses to both the native and citrullinated peptides.

Pearson correlation analysis was performed on log-transformed values, with correlation plots for age (left), schizont (parasite exposure) (middle), and boxplots for gender (right). Panel A) represents graphs for cTNC5, B) for TNC5, C) for CEP, and D) for REP. Pearson's correlation coefficient is shown along with significance levels: ns (not significant), * p<0.05, ** p<0.01, *** p<0.001.

5.2.4 Selection of samples for flow cytometry and protein microarray assays

Next, it was essential to be precise and objective in the selection of the adult samples for a more detailed and comprehensive analyses in the next set of experiments, which included flow cytometry and protein microarray platform, a high-throughput assay that allowed the screening of 120 autoantigens as outlined the experimental workflow (Figure 5-6). To identify the most suitable samples for the subsequent experiments, antibody responses to native and citrullinated peptides data for each antigen were first normalised by scaling, and the total antibody response for each individual was established and used to stratify the

individuals into high, medium, and low autoantibody responder groups using quantiles (Figure 5-7). This stratification was crucial for ensuring that subsequent analyses could effectively compare immune responses across these distinct groups.

Figure 5-6: Experimental plan for identifying adults with varied antibody responses to native and citrullinated peptides for subsequent assays

This figure outlines the experimental approach for identifying adults with varying levels of antibody responses to native and citrullinated peptides in a malaria-endemic region. Adults with varying antibody responses were then selected for subsequent experiments, that included flow cytometry and protein microarray experiments.

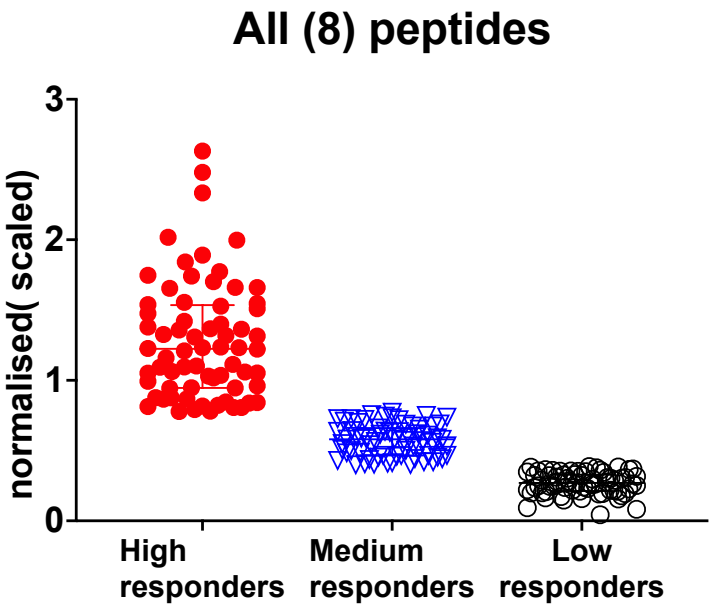

Figure 5-7: Identification of adults with varied antibody responses to native and citrullinated peptides for further analysis

Using ELISA antibody response data for native and citrullinated peptides were first normalised using scaling, and the total antibody response for each individual was established. The data were then stratified into high, medium, and low antibody responders based on total antibody levels using quantiles. These groups were selected for further experiments.

5.2.5 Differential B cell populations associated with varying levels of antibody responses to native and citrullinated peptides

Given that *Plasmodium* infections are known to cause significant alterations in the B cell compartment, particularly with the expansion of atypical B cells[196,199,209], it was crucial to examine B cells within the context of antibody responses to the native and citrullinated peptides. After stratifying the samples into high, medium, and low antibody responders, I next phenotyped B cells from a total of 39 adults, which included (n=22) individuals with high autoantibody responses and (n=17) low autoantibody responses. The selection of these samples was made with the aim of identifying any differential alterations in the immune cell profiles between individuals with high compared to those with lower auto-antibody levels.

First, using established B cell markers, I phenotyped the various B cell subsets as outlined in the gating strategy (Figure 5-8). Increased levels of activated memory B cells (CD21- CD27+) (Figure 5-9B) were observed in the high responders compared to the low responders. However, no significant differences were observed in the levels of resting B cells between the two groups (Figure 5-9 C).

Moreover, atypical B cells that are CD11c are commonly elevated in malaria-infected individuals; while their role remains unclear, there is evidence suggesting they may be associated with the production of anti-phosphatidylserine antibodies and are further involved in the development of severe malaria anaemia[3]. In this study, CD11c atypical B cells were also observed to be increased in the high responders compared to the low responders (Figure 5-9 D). With both CD11c T-bet+ B cells and CD21-T-bet+ B cells significantly elevated in the high responders compared to the low responders (Figure 5-9 F-G).

In contrast, naive B cells were more abundant in the low responders (Figure 5-10 A), while switched memory B cells were elevated in the high responders compared to the low responders (Figure 5-10 B). Although the findings from my research suggest that the observed increased levels of activated memory B cells and increased levels of atypical B cells linked to *Plasmodium* infections may influence generation of antibody responses to native and citrullinated peptides, further research is needed to clarify the role of atypical B cells as these observations may be largely due to the effects of chronic *Plasmodium* infection.

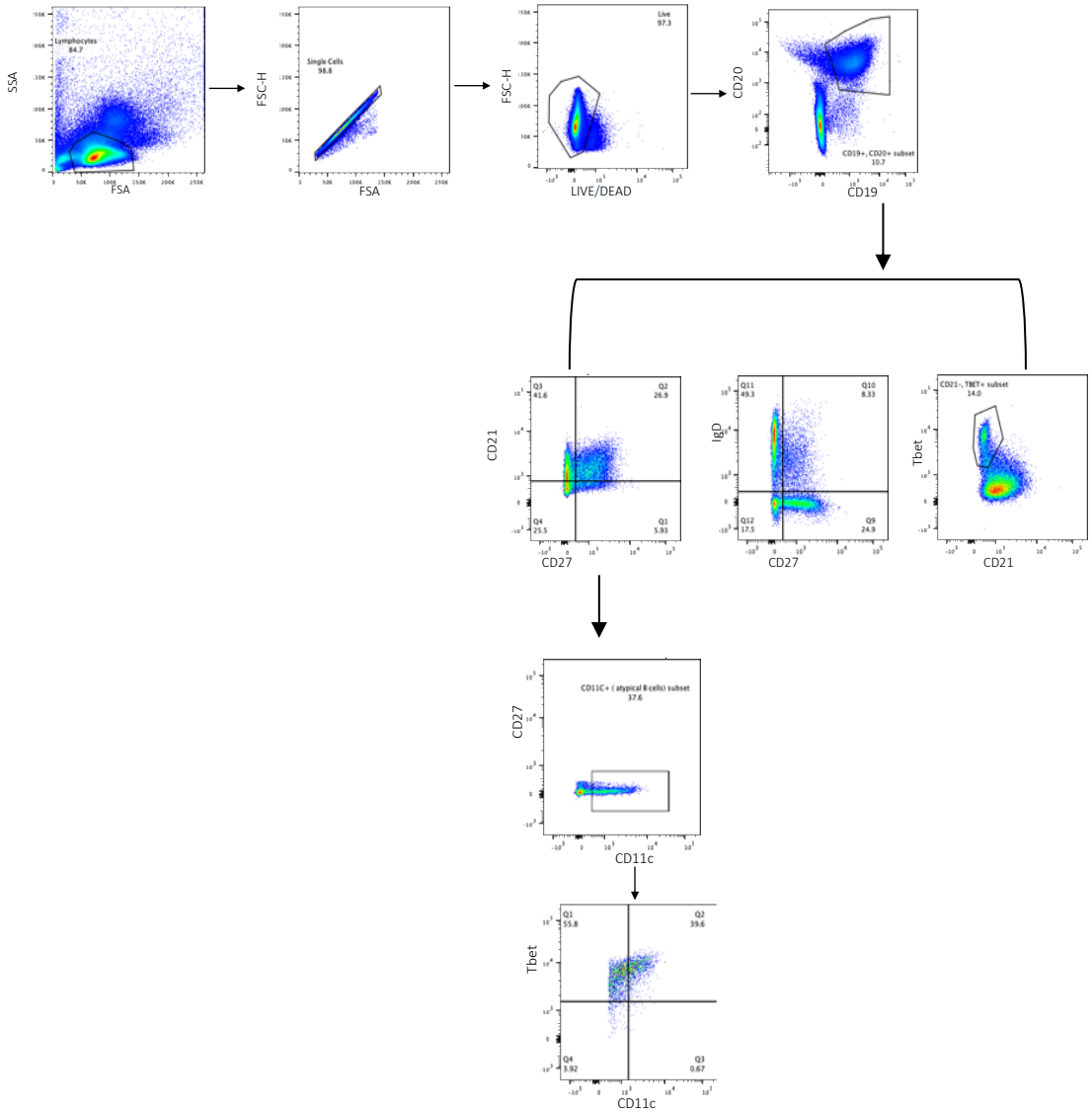

Figure 5-8: Gating strategy for B cells phenotyping and quantification of activated memory B cells, and atypical B cells that are CD11c.

Lymphocytes were gated based on FSC-A vs. SSC-A, followed by single-cell discrimination (FSC-H vs. FSC-A) to exclude doublets. Viable cells were identified using LIVE/DEAD staining. CD19+ CD20+ B cells were selected, and subsets were gated for memory B cells (CD21+ CD27+), activated memory B cells (CD21− CD27+), double-negative memory B cells/atypical B cells (CD21− CD27−), and (CD21− T-bet+). CD11c atypical B cells were further gated within the atypical B cell population.

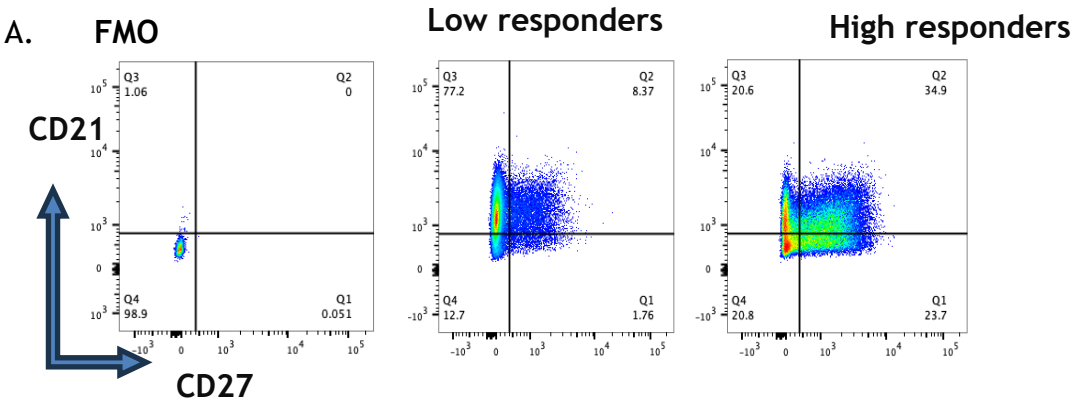

B. Activated Memory B cells

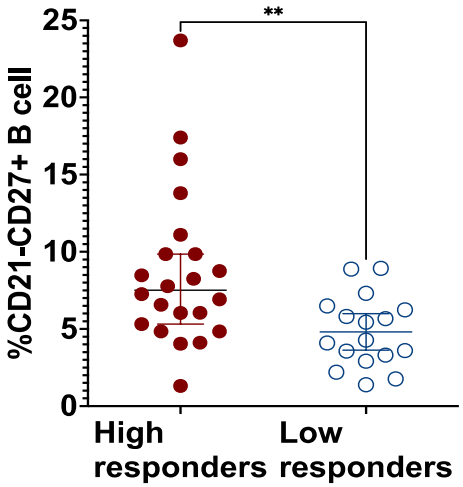

C. Resting Memory B cells

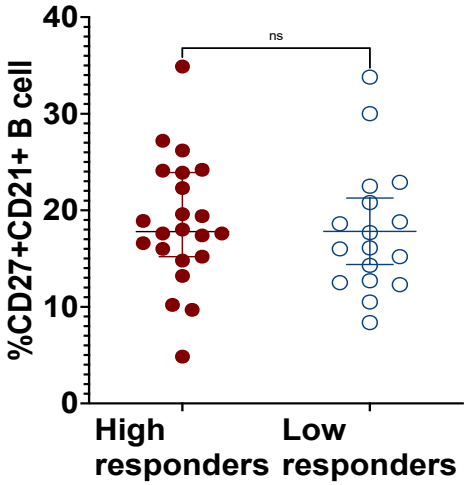

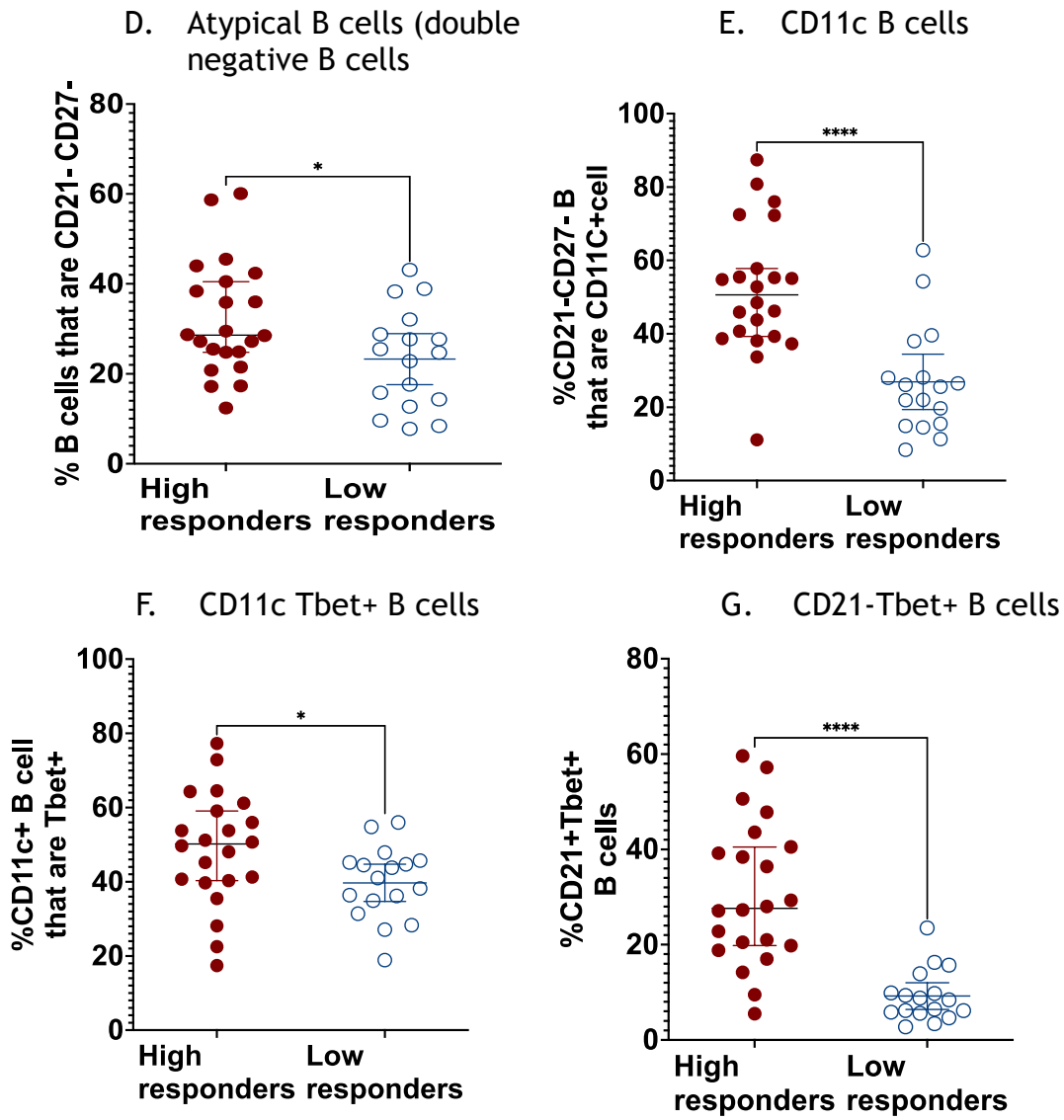

Figure 5-9: Increased frequencies of activated memory B cells and atypical B cells (Tbet+ CD11c) in the high antibody responders compared to the low antibody responders.

(A) Representative plots showing gating of B cells based on CD21 and CD27 markers in the low and high antibody responders. The percentage of the various B cells subsets were then plotted and as shown(B) Graph showing the percentage of activated memory B cells, (C) Graph showing the percentage of memory B cells, (D) Graph showing the percentage of double-negative atypical B cells, (E) Graph showing the percentage of CD11c B cells, (F) Graph showing the percentage of CD11c Tbet+ B cells, and (G) Graph showing the percentage of CD21- Tbet+ B cells. Statistical comparisons were performed using unpaired t-test, with error bars representing the mean ± SEM. Statistical significance is indicated as follows: * $p<0.05$, ** $p<0.01$, *** $p<0.001$, and **** $p<0.0001$.

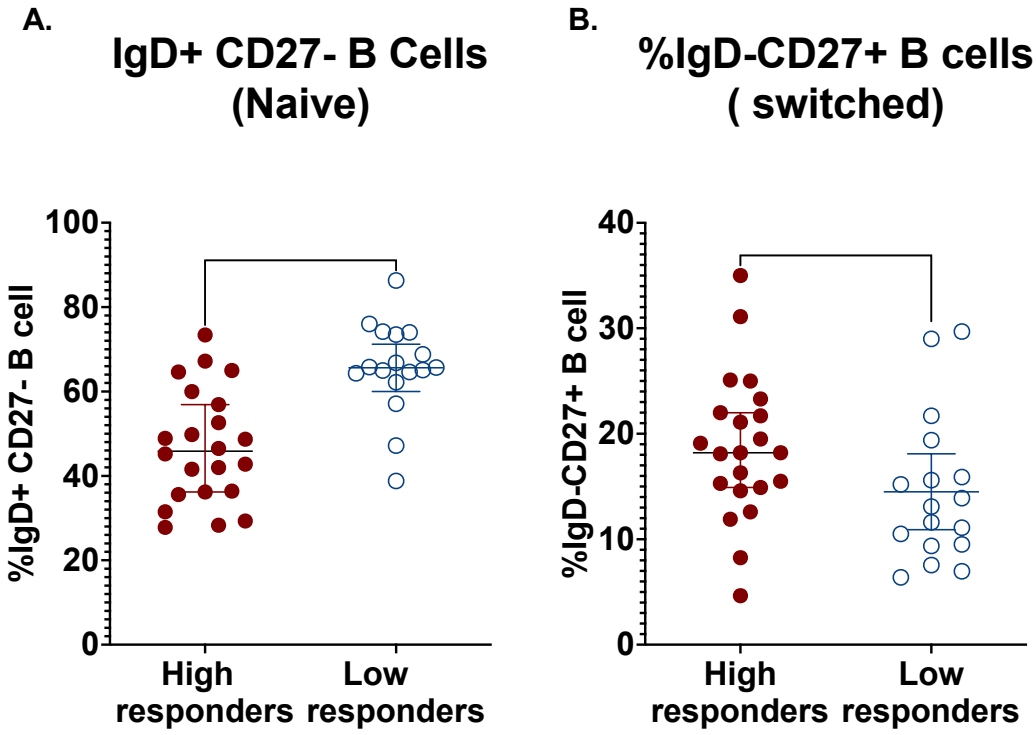

Figure 5-10: Increased frequencies of naive B Cells in the low responders group.

(A) Graph showing comparisons of the percentage of naive B cells (IgD+ CD27- B cells), and (B) graph showing the percentage of switched memory B cells (IgD- CD27+ B cells). Statistical comparisons were performed using unpaired t-tests, with error bars representing the mean ± SEM. Statistical significance is indicated as follows: * $p<0.05$, *** $p<0.001$.

5.2.6 The percentage of CD25+ FOXP3+ CD4+ T (regulatory T cells) cells were increased in the low responders group

Using flow cytometry, I also phenotyped a subset of regulatory T cells (CD25+ FOXP3+ CD4+ T cells), which are known to play a crucial role in mediating self-tolerance, thus preventing autoimmunity and maintaining immune homeostasis [353]. Using the gating strategy outlined in (Figure 5-11), I identified the proportion of CD25+ FOXP3+ CD4+ T cells. Interestingly, a comparison of the proportion of these cells in the high versus low responders revealed increased levels of CD25+ FOXP3+ CD4+ T cells in the low responders group compared to the high antibody responders' group (Figure 5-12 B).

In conclusion, our findings suggest that the increased regulatory T-cell levels in the low antibody responders' group possibly leads to a more effective suppression of autoreactive immune responses, resulting in lower autoantibody levels. However, further mechanistic studies are needed to fully understand this association.

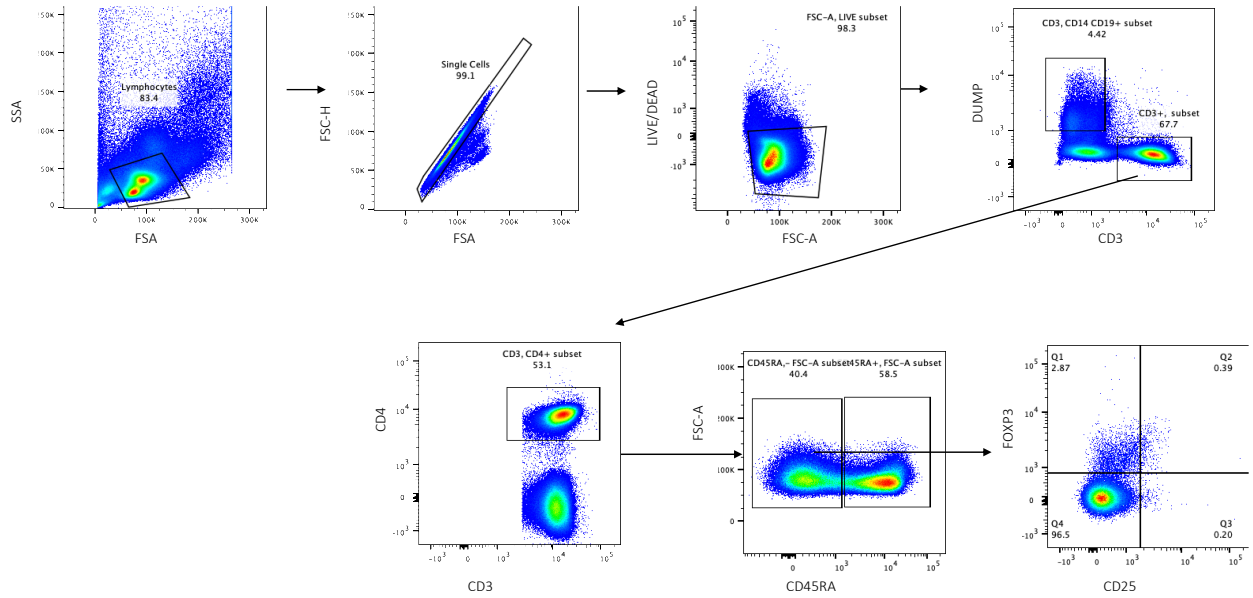

Figure 5-11: Gating strategy for T cells phenotyping and quantification.

Lymphocytes were identified using FSC-A vs. SSC-A, followed by single-cell discrimination with FSC-H vs. FSC-A to exclude doublets. Viable cells were then gated on using LIVE/DEAD staining, and CD3+ T cells were identified. CD4+ helper T cells were further gated, with subsets classified as naive (CD45RA+), effector/memory (CD45RA−), and regulatory T cells (CD25+ FOXP3+) within the effector/memory population.

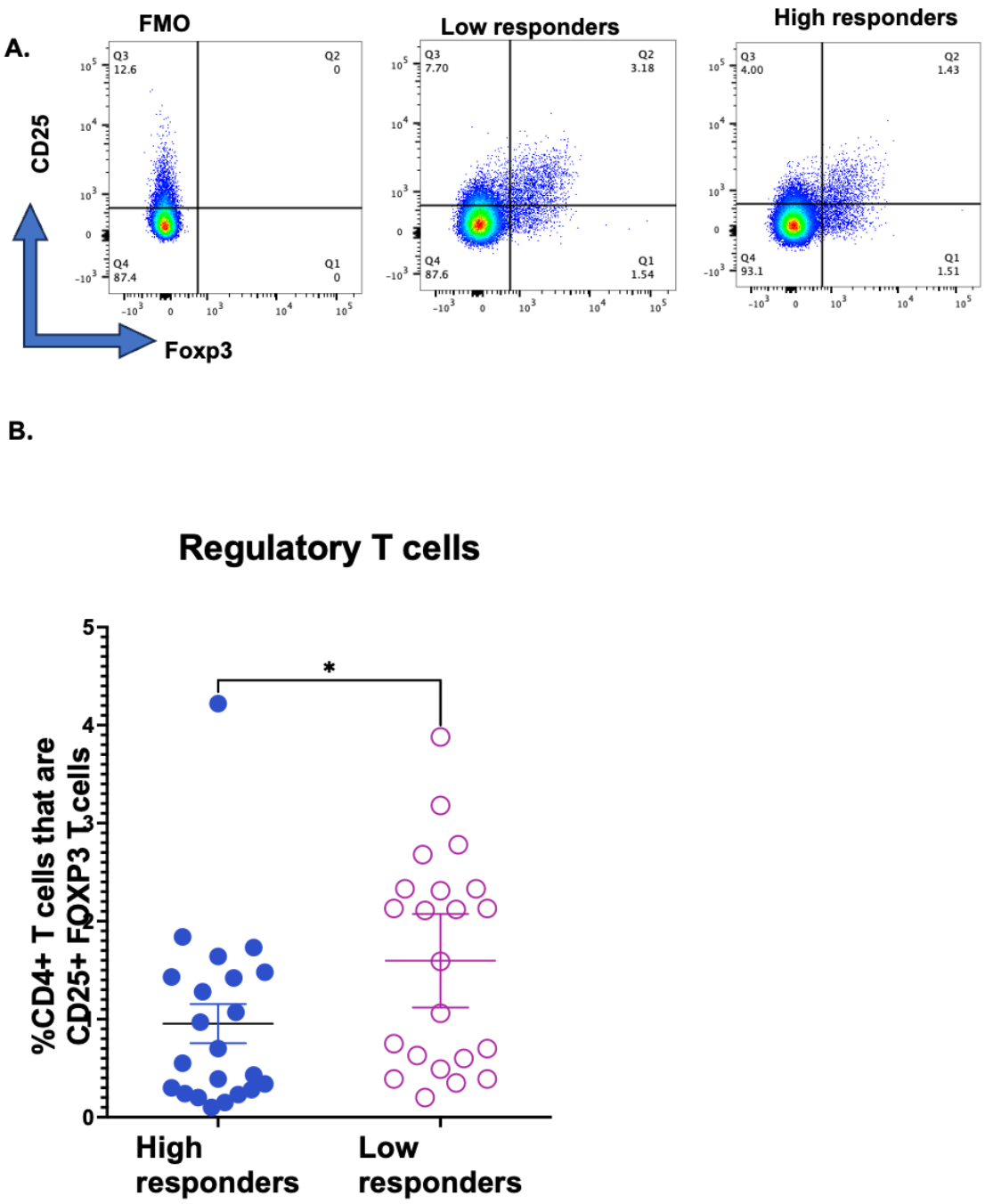

Figure 5-12: Increased frequencies of regulatory FOXP3+ CD25+ CD4+ T cells in the low antibody responders.

(A) Representative plots showing CD25 and FOXP3 markers in the low and high antibody responder groups. B) Graph showing the percentage of CD4+ that are CD25+FOXP3+ (regulatory T cells). Statistical comparisons were performed using Mann-Whitney test, with error bars representing the mean ± SEM. Statistical significance is indicated as follows: * $p<0.05$, ** $p<0.01$, *** $p<0.001$, and **** $p<0.0001$.

5.2.7 Protein microarray data cleaning and analysis pathway

A total of 127 samples from adults were selected for the protein microarray assay based on the criteria of whether they were high or low antibody responders, as shown in (Figure 5-6). These samples were then carried forward for further screening using the protein microarray platform, a high-throughput assay that allowed the screening of 120 autoantigens in a single well, as illustrated in (Figure 5-13 A). Furthermore, given the complexity and multi-dimensional nature of the data generated, robust data processing was essential to ensure high-quality results.

This was achieved by applying a protein microarray data processing suite, protGear, which includes a range of statistical functions organised within an R package, as outlined in (Figure 5-13 A) [302]. The first step in the process was background correction, which removes unwanted signals from sources other than the sample [354]. Notably, the protein microarray readout is the median fluorescence intensity (MFI) of the foreground, which also includes background intensity (unwanted signals). To determine the most appropriate background correction method, I plotted the foreground MFI against the background MFI (Figure 5-13 B) that served as a diagnostic plot essential in providing information for selecting the appropriate background correction method. For my dataset the lower foreground MFI values showed low background signals, while the higher foreground MFI values displayed a broader range of background levels suggesting variability in the background values thus, local background correction was applied.

Next, to normalise the data, an essential step that reduces the mean-variance dependence commonly seen in protein microarray data, which can obscure true biological variability, especially given the wide range of readouts, I first averaged the duplicates and applied the Variance Stabilisation Normalisation (VSN) method. This approach was particularly suited for my data, as shown in (Figure 5-14 A-B) because it handled negative values more effectively than traditional log transformation [355].

Lastly, since the samples were processed on different days, batch correction was necessary; this was done using the ComBat function from the SVA package, which

successfully minimised day-to-day variations, as demonstrated in (Figure 5-14 C-D).

Lastly, following data cleaning a total of 112 samples were carried forward for downstream analysis and visualisation. Precisely, the additional data cleaning processes involved the removal of duplicates and control samples, including blanks, Swedish sample, and a pooled serum from hyperreactive individuals from high malaria endemic regions, which served as the negative and positive controls respectively and had been included in each slide.

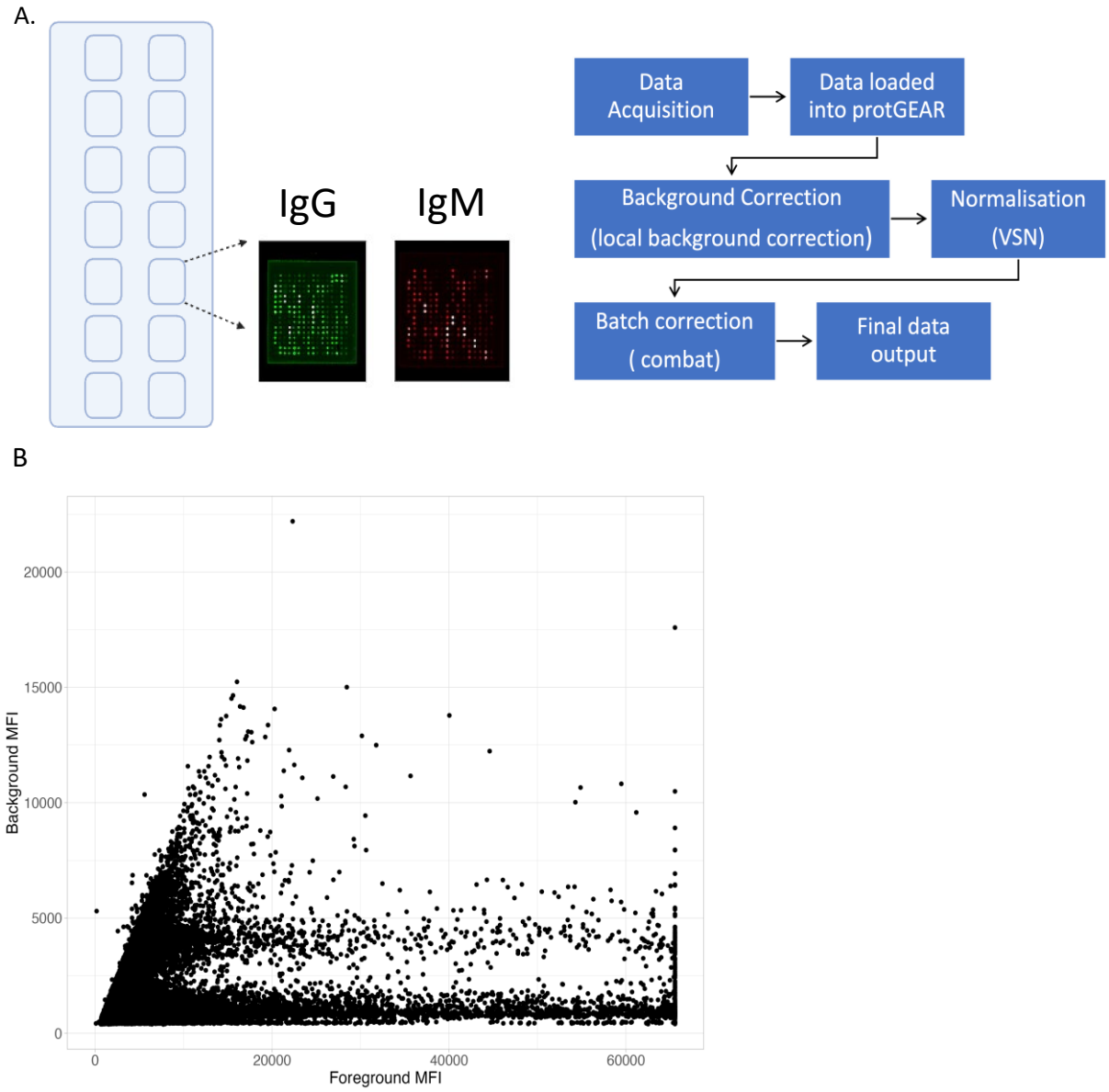

Figure 5-13: Data cleaning and quality control processes for protein microarray data performed by the application of the ProtGear.

A) An outline of the data acquisition and processing pipeline (protGear) used for the analysis. B) Scatter plot showing background MFI vs foreground MFI, serves as a diagnostic plot essential in providing information for selecting the appropriate background correction method.

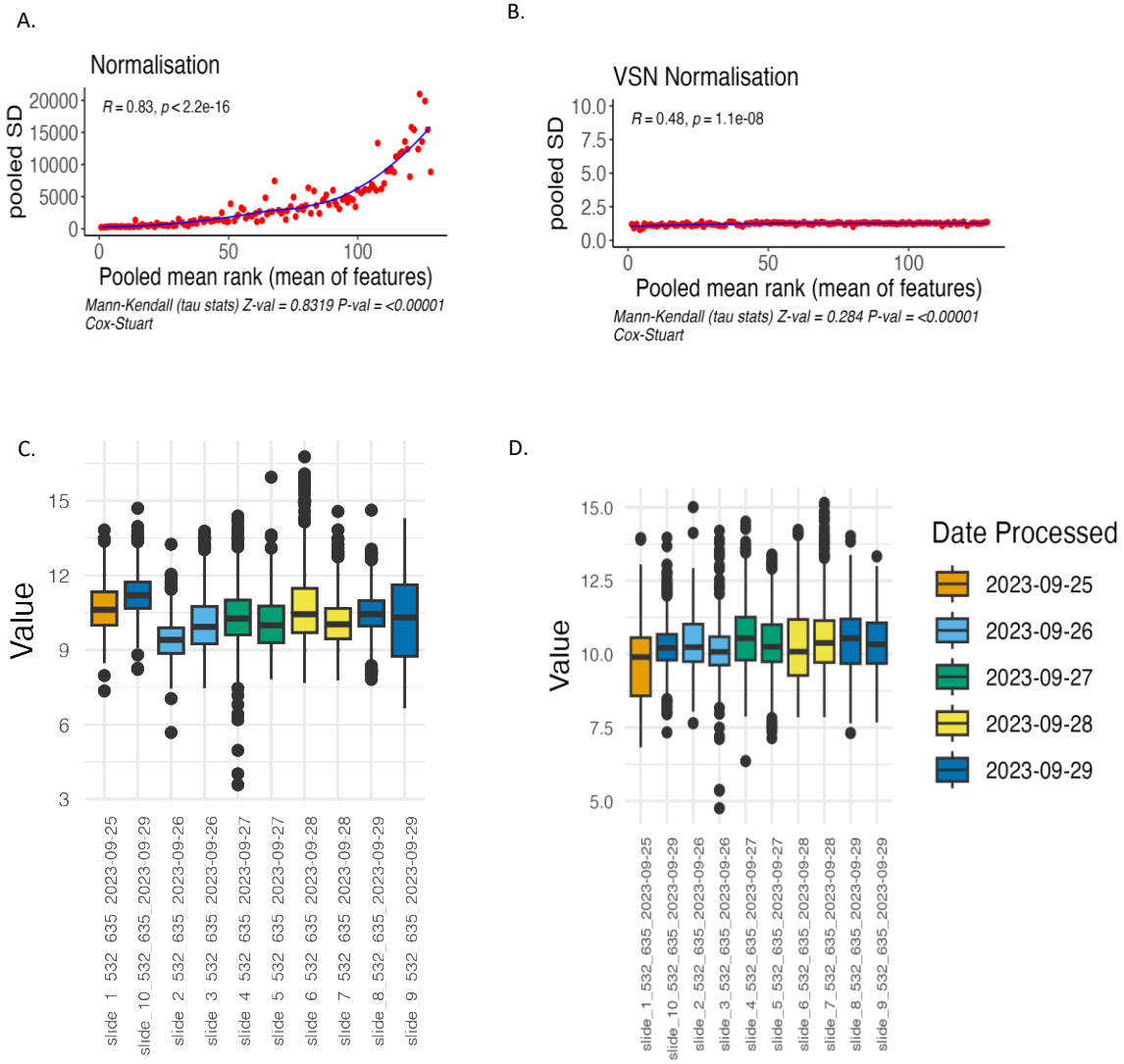

Figure 5-14: Data normalisation and batch correction processes for protein microarray data performed by the application of the ProtGear.

Following data cleaning, normalisation was performed using the VSN package in ProtGear, and batch correction was applied using the ComBat function from the SVA package. (A) and (B) show scatter plots of the data before and after normalisation, while (C) and (D) present boxplots of the data before and after batch correction, accounting for day-to-day variation.

5.2.8 Broad autoimmune responses in individuals chronically exposed to *Plasmodium* infections.

To generate a heatmap, the batch corrected raw data was first ranked, with the lowest value in each sample being assigned a rank of 1. Next malaria exposure data was integrated in the heatmap by arranging the ranked matrix based on schizont response levels which was grouped into 'High', 'Medium', 'Low', and 'No Exposure' categories. The heatmap was then generated with these annotations, with row clustering disabled to preserve the order of malaria exposure, while column clustering remained enabled to reveal patterns across variables, as shown in (Figure 5-15 A-B).

Notably, both IgM and IgG responses (Figure 5-5A-B)to the panel of autoantigens exhibited significant variation between individuals. While some individuals appeared relatively more responsive to a broader range of antigens, as indicated by the red circles, others displayed comparatively lower reactivity. However, it is important to note that these observations are based on ranked data, thus reflecting relative differences between individuals rather than absolute levels of response. Notably, a response here is referring to the ranked individual antibody levels.

Next, the batch corrected normalised data by VSN as described in (section 5.2.7) was matched with epidemiological data, including age, gender, and schizont antibody responses (*Plasmodium* parasite exposure). Both IgG and IgM responses were visualised using Principal Component Analysis (PCA) plots, as shown in (Figure 5-16 A-C) and (Figure 5-17 A-C), respectively. Although the heatmap indicated variability between the samples, this variability could not be explained by age, gender, or malaria exposure, as demonstrated in the PCA plots (Figure 5-16 A-C) and (Figure 5-17 A-C).

Furthermore, a comprehensive approach to data analysis was taken, by applying a Limma (Linear Models for Microarray Data). Limma is a widely used tool for analysing high-dimensional biological data, such as gene expression or protein levels and works by fitting a linear model to each protein (autoantigen) to estimate differences in immune response across groups. Additionally, the method also applies an empirical Bayes approach to stabilise variance estimates, making the analysis more reliable, especially when sample sizes are small. The log fold change (logFC) was calculated to determine how much higher or lower protein levels were between groups, P-values and adjusted p-values (q-values) were used to assess the significance of these differences, accounting for multiple comparisons.

However, even after adjusting the p-values, no significant associations were found between the antibody responses (IgG and IgM) and the variables of interest (age, gender, or schizont response), see Supplementary (Table 7-1, Table 7-2, Table 7-3, Table 7-4).

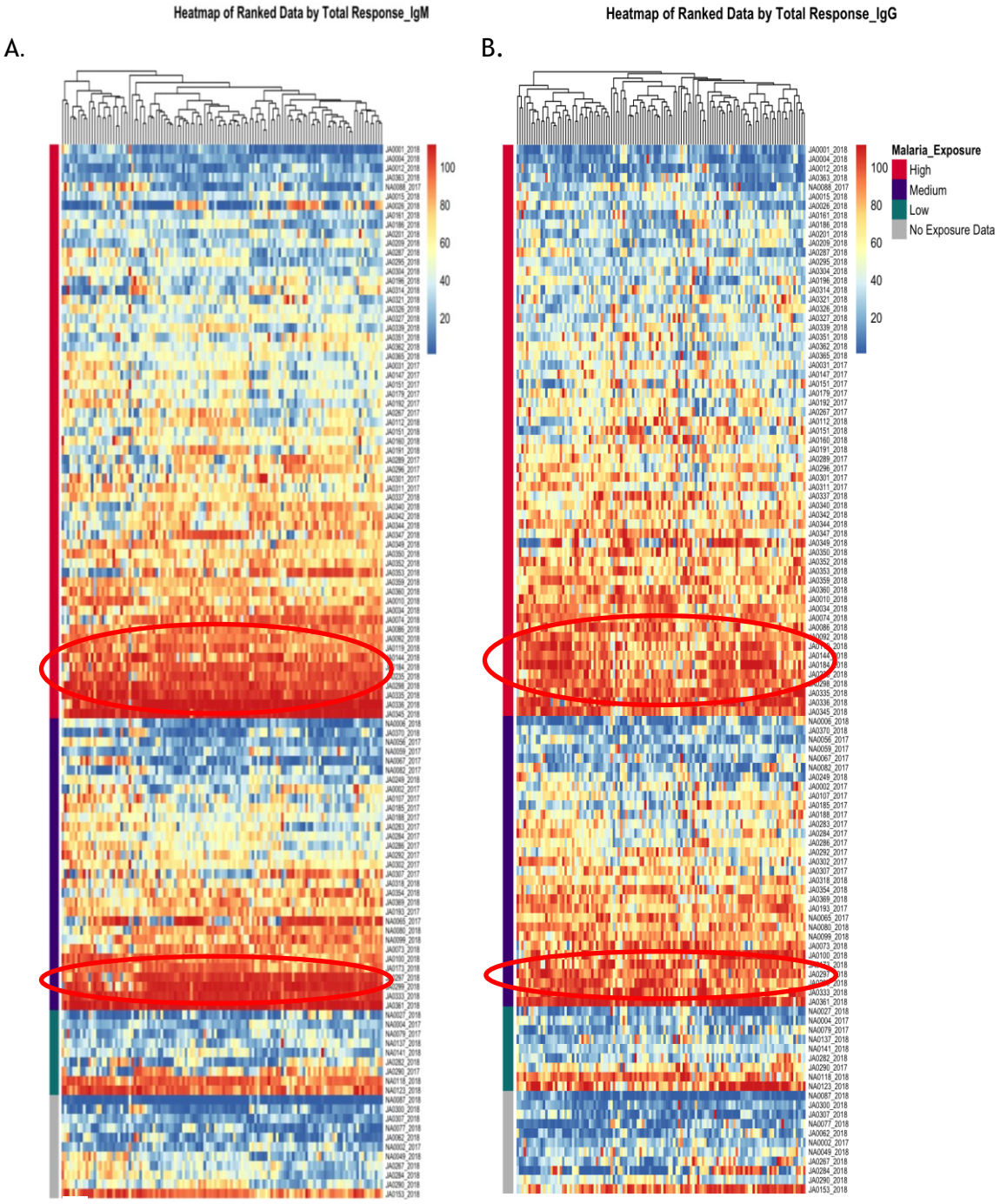

Figure 5-15: A wide array of autoantigen responses observed in malaria-exposed individuals

A total of 127 samples were profiled for both IgG and IgM autoantibodies to 120 autoantigens (GeneCopoeia). Following data cleaning, 112 samples were ranked and sorted by total overall responses, then visualised using heat maps: A) IgM, B) IgG. Red circles highlight individuals with higher reactivity to a broader range of antigens. The scale bar represents the range of rank scores, and the key indicates exposure to the parasite.

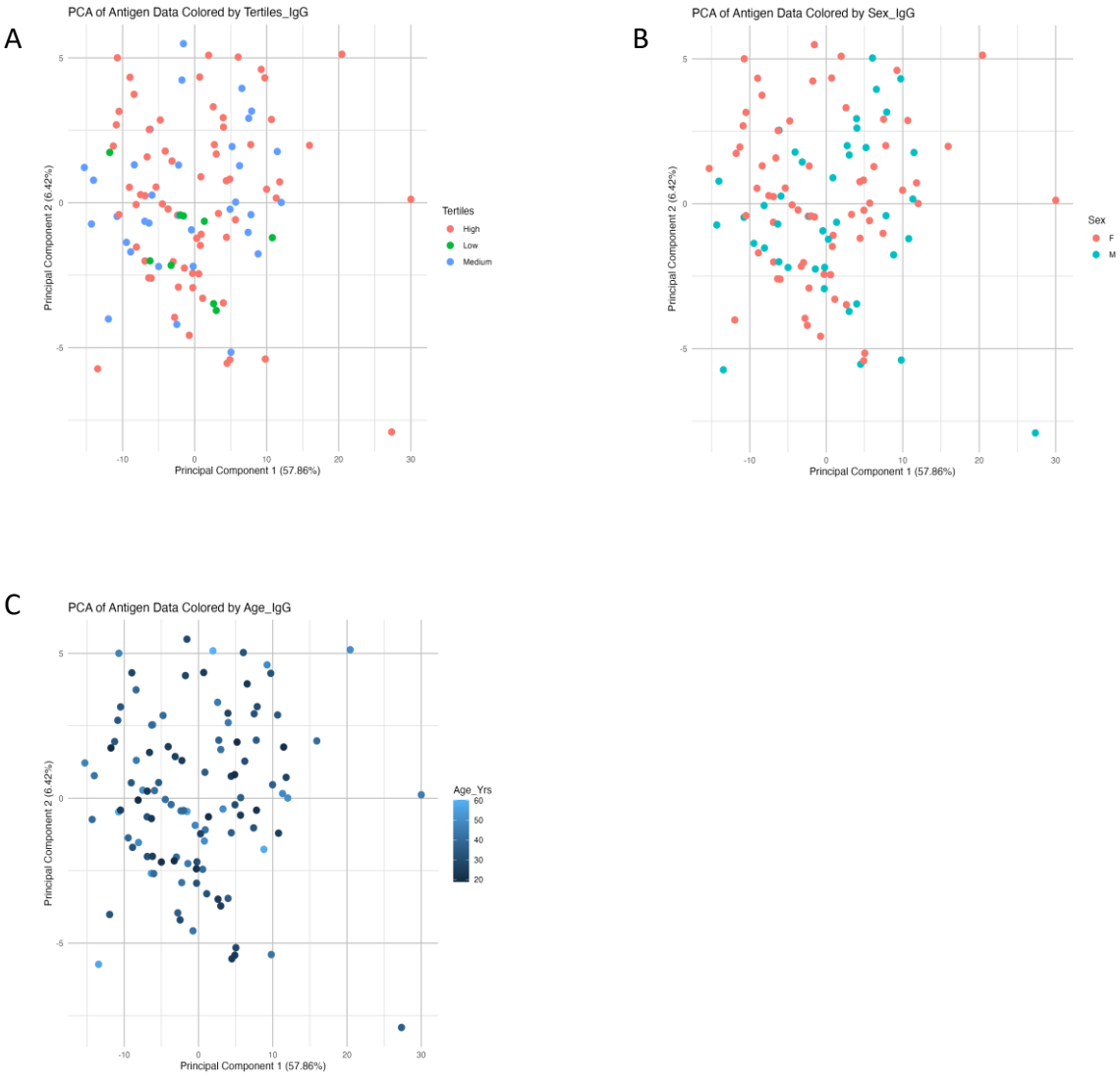

Figure 5-16: Lack of association between IgG autoantibody levels and available epidemiological data.

PCA plots were generated from 112 samples using the batch-corrected, normalised protein microarray data. The plots were labelled based on available epidemiological data: A) by parasite exposure grouped into tertiles, B) by gender, and C) by age. These analyses assess the potential associations between IgG autoantibody responses and epidemiological variables.

A.

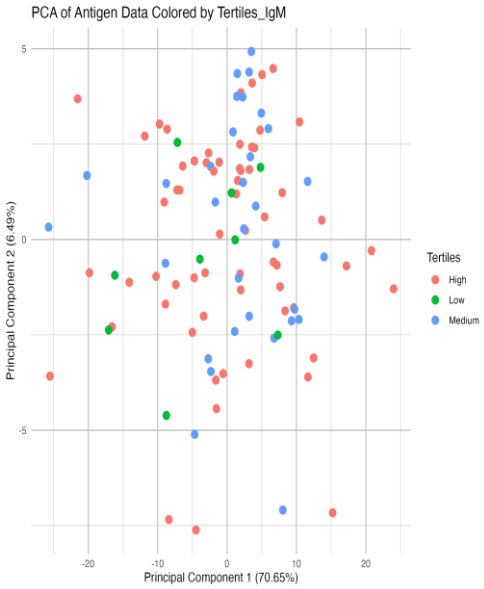

B.

C.

Figure 5-17: Lack of association between IgM autoantibody levels and available epidemiological data.

PCA plots were generated from 112 samples using the batch-corrected, normalised protein microarray data. The plots were labelled based on available epidemiological data: A) by parasite exposure grouped into tertiles, B) by gender, and C) by age. These analyses assess the potential associations between IgM autoantibody responses and epidemiological variables.

.

5.2.9 Identification of the top 20 autoantigens binding autoantibodies from adults with high *P. falciparum* exposure

Next, to identify the autoantigens from the protein microarray that most frequently bound their cognate autoantibodies from individuals with high *P. falciparum* exposure. First, the raw data was ranked based on MFI (mean fluorescent intensity) as previously described above in (section 5.2.8). The heatmap was then rearranged such that the rows represented autoantigens, ranked by their total immune response across all samples, from highest to lowest and columns represented individual samples grouped and ordered according to their malaria exposure categories (high, medium, low, and no exposure).

Although this ranking of the autoantigens by the total response allowed for the identification of autoantigens with the strongest responses, no specific autoimmune patterns were associated with exposure to *P. falciparum* parasites (Figure 5-18). However, an overall varied reaction to the autoantigens was observed, as highlighted in the heatmap for IgG (Figure 5-18).

The top 20 autoantigens eliciting the strongest responses were identified and listed in (Table 5-2), with, responses to common antigens such as EBNA1 (Epstein-Barr Nuclear Antigen 1) and LPS (lipopolysaccharide) serving as controls.

Amongst the top 20 autoantigens, responses to extracellular antigens like Calprotectin and Elastin and nuclear antigens like CENP-B, PCNA, and Ro/SSA were observed as the common autoantigens that bound their cognate antibodies. In addition, anti-phosphatidylserine antibodies, were also observed, an observation that was consistent with other studies, particularly given that anti-phosphatidylserine antibodies have previously been linked to the development of malaria-associated anaemia by targeting uninfected red blood cells and promoting their clearance [1,4].

Interestingly, responses to hemocyanin, an arthropod antigen used as a control for non-specific immune reactivity, were also observed. A similar profile of immune response patterns was seen with IgM responses, as shown in (Figure 5-19) and (Table 5-3). Overall, my findings show that chronic exposure to *Plasmodium* infection is associated with a wide range of autoantigen reactivity, indicating a

highly diverse and potentially dysregulated immune response profile in these individuals possibly due to chronic exposure to the parasite.

Table 5-2: Top 20 autoantigens IgG

A.)

B.)

AgName	category
EBNA1	Viral Antigen
CRP	Blood factor
Hemocyanin	Extracellular (non-human protein)
LPS	Bacterial (control)
CENP-B	Extracellular matrix
ssDNA	Nuclear antigen
Jo-1	Extracellular
GAD65/GAD2	Enzyme
AQP4	Membrane
Muscarinic receptor	Receptor
Elastin	Metrix
Calprotectin	Extracellular
B2glycoprotein1	Extracellular
PCNA	Nuclear antigen
KU(P70/P80)	Nuclear antigen
S100	Cytosolic
TTG	Enzyme
Ro/SSA(60Kda)	Ribonucleic
PL-7	tRNA Synthetase
Thyroglobulin	Glycoprotein

Figure 5-18: Top 20 autoantigens frequently observed bound to specific IgG autoantibodies from individuals with high exposure to *P. falciparum*

A total of 127 samples were profiled for both IgG and IgM autoantibodies against 120 autoantigens (GeneCopoeia). After data cleaning, 112 samples were carried forward for further analysis. The data was then ranked based on the total response for each autoantigen, and a heatmap was generated, displaying the autoantigens in order of their total response. Those with the highest overall response appear in ascending order: A) The heatmap represents IgG responses with a focus on identifying the autoantigens. The scale bar represents the range of rank scores, and the key indicates the level of parasite exposure. B) represents a table listing the top 20 autoantigens with the highest overall responses categorised by antigen type.

Table 5-3: Top 20 autoantigens IgM

A.)

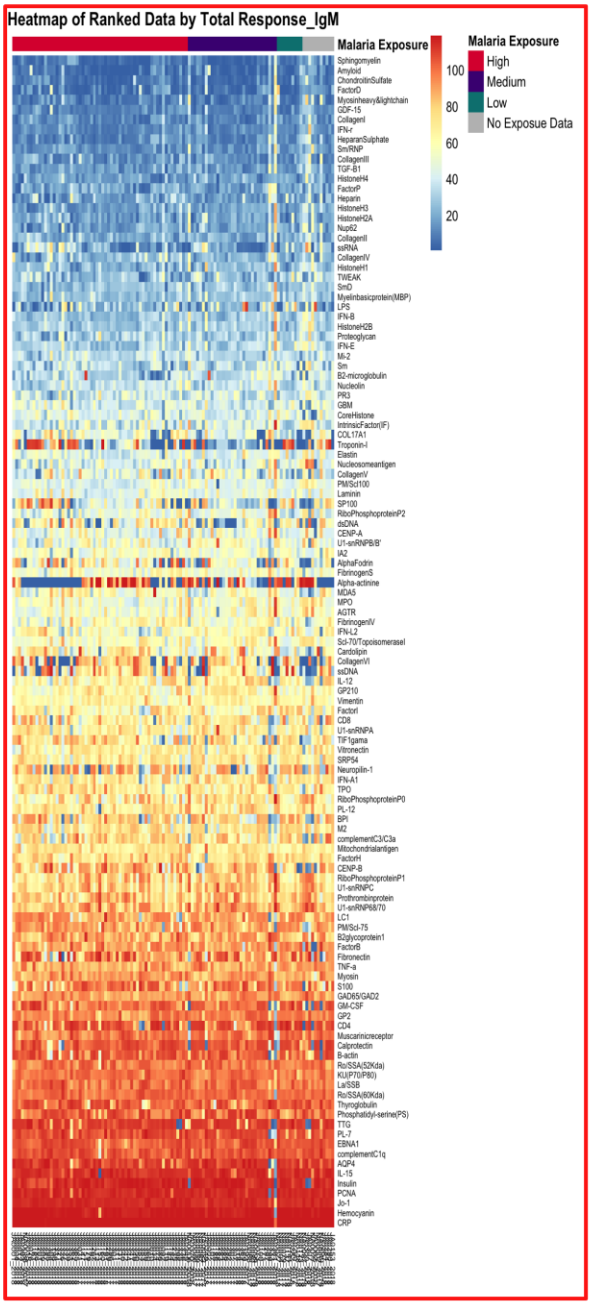

B.)

AgName	category
CRP	Blood factor
Hemocyanin	Extracellular (non-human protein)
Jo-1	Extracellular
PCNA	Nuclear antigen
Insulin	Hormone
IL-15	Cytokine
AQP4	Membrane
complementC1q	Complement
EBNA1	Viral antigen
PL-7	tRNA Synthetase
TTG	Enzyme
Phosphatidyl-serine(PS)	Phospholipids
Thyroglobulin	Glycoprotein
Ro/SSA(60Kda)	Ribonucleic
La/SSB	Nuclear antigen
KU(P70/P80)	Nuclear antigen
Ro/SSA(52Kda)	Ribonucleic
B-actin	Cytoskeletal
Calprotectin	extracellular
Muscarinic receptor	Receptor

Figure 5-19: Top 20 autoantigens frequently observed bound to specific IgM autoantibodies from individuals with high exposure to *P. falciparum*

A total of 127 samples were profiled for both IgG and IgM autoantibodies against 120 autoantigens (GeneCopoeia). After data cleaning, 112 samples were used for further analysis. The data was then ranked based on the total response for each autoantigen, and a heatmap was generated, displaying the autoantigens in order of their total response. Those with the highest overall response appear in ascending order: A) IgM. The scale bar represents the range of rank scores, and the key indicates the level of parasite exposure. B) represents a table listing the top 20 autoantigens with the highest overall responses categorised by antigen type.

5.2.10 Increased antibody responses to native and citrullinated peptides in children with severe and uncomplicated malaria

In this section, I will shift focus to the last aim of this research, which is to investigate whether the production of antibodies to native and citrullinated peptides is present and is associated with varied clinical outcomes, with key comparison being between healthy controls, Vs uncomplicated malaria Vs severe malaria in children.

Herein unlike the previous sections the samples analysed were from children. Specifically, I used samples from the hospital cohort (severe malaria), Junju cohort (uncomplicated malaria) and Ngerenya cohort (uninfected healthy controls). The rational for using this cohorts, is driven by the controversial role of autoantibodies in *Plasmodium* infections, where elevated autoantibody levels have been associated with severe malaria outcomes [2,248] and at the same time there is evidence of these autoantibodies playing a crucial role in conferring protection against clinical malaria [5,132].

5.2.10.1 Cohorts' demographics

5.2.10.2 First Cohort: Severe Malaria cases from hospital admissions

The first cohort comprised children with severe malaria, including those diagnosed with severe malaria anaemia and cerebral malaria. These children were hospitalised at the Kilifi County Hospital with confirmed malaria and admitted to the High Dependency Unit (HDU) for intensive monitoring. Severe *P. falciparum* malaria was defined according to the WHO criteria, which includes any of the following: cerebral malaria (Blantyre coma score of <3), severe malaria anaemia (hemoglobin concentration less than 5 g/dL), or other severe clinical syndromes[356].

5.2.10.3 Second Cohort: uncomplicated malaria cases from Junju

The second cohort involved children from the Junju cohort, a group under continuous weekly active surveillance for uncomplicated malaria (SIMs cohort). These children, residing in a rural subsistence farming villages on the Kenyan coast, were followed from birth and exit follow-up at 15 years of age. Junju, is a

region of moderate malaria transmission intensity, with a *P. falciparum* parasite prevalence of 30% during cross-sectional surveys conducted between January and May.

Uncomplicated malaria episodes were defined by home visits where field workers diagnosed malaria-related fevers characterised by an axillary temperature of ≥37.5°C and a *P. falciparum* parasite density exceeding 2,500 parasites per microliter of blood. For this study, I included samples from children with uncomplicated malaria and healthy uninfected controls (parasite negative) sampled from the cross-sectional bleed with demographics detailed on Table 5-4

5.2.11 Elevated levels of CEP, cFIB, Fib, and TNC5 in both severe and uncomplicated malaria cases.

Increased levels of CEP, cFIB, Fib, and TNC5 were observed in both the severe and uncomplicated malaria cases compared to healthy controls (Figure 5-20).

Table 5-4: Description of children samples 2018

Group	Age (Yrs)	Sample (size)	Temperature	Parasite density
Health Controls (Uninfected from Ngerenya)	2-9	20	35.7-37.1	0
Uncomplicated malaria (SIMs cohort)	0.5-9	51	35.4-38	2500-1648000 (ul)
Severe Malaria (Hospital admissions)	0.5-14	49	32.9- 39.7	2500- 999600(ul)

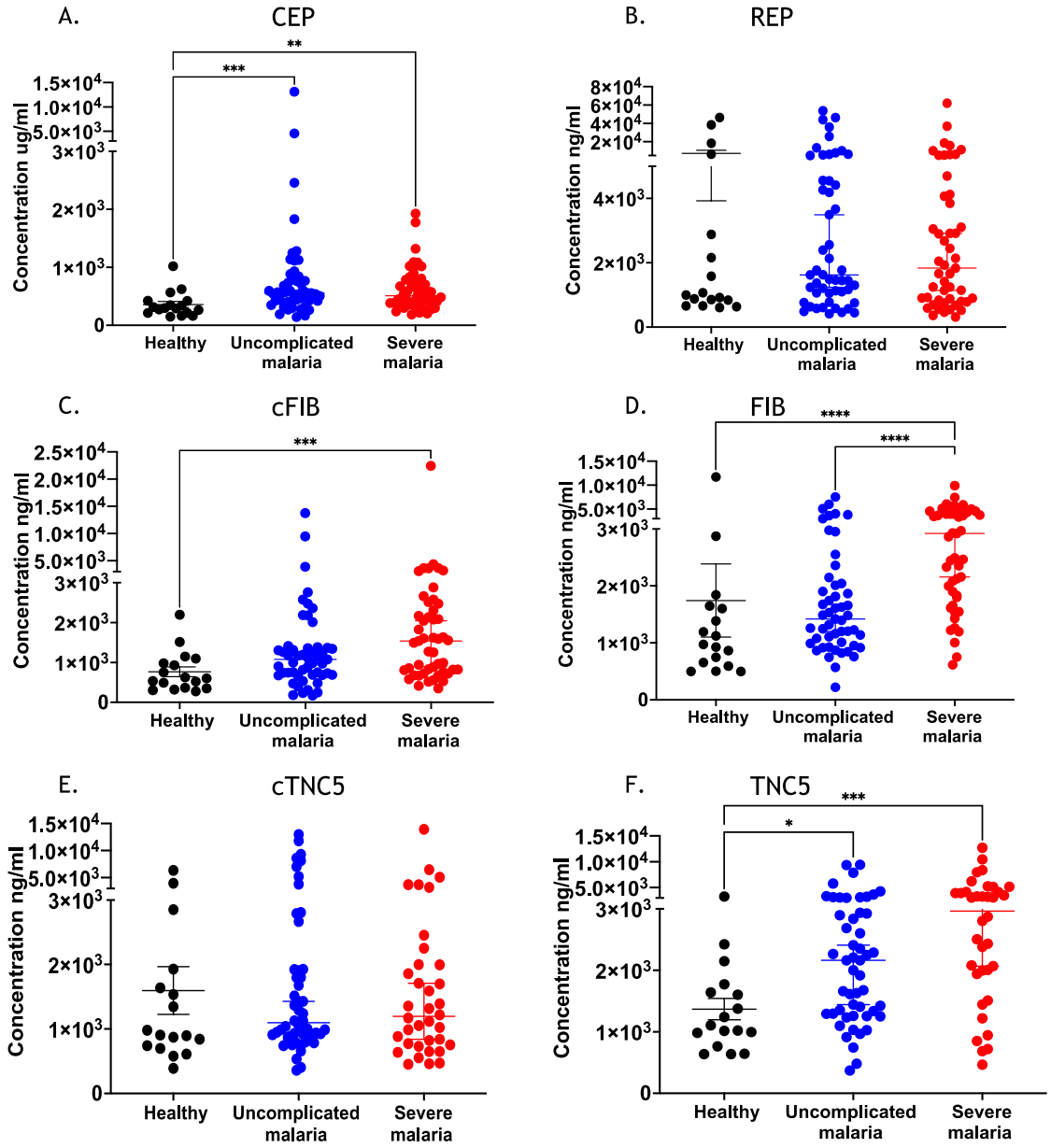

Figure 5-20: Increased antibody responses to native and citrullinated peptides in children with severe and uncomplicated malaria

Antibody responses to citrullinated and corresponding native peptides were assessed in the three groups: Healthy Controls (Ngerenya; uninfected), uncomplicated malaria (Junju), Severe malaria (Hospital admissions) using ELISA. The responses for CEP and REP are shown in panels (A and B), cFIB and FIB in panels (C). Statistical analysis was performed using a Kruskal- Wallis followed by the Dunn's multiple tests. Error bars represent the mean ± SEM. Statistical significance is indicated as follows: ns (not significant), * $p<0.05$, ** $p<0.01$, *** $p<0.001$.

5.3 Discussion

One of the aims of this chapter was to analyse the frequency of autoimmune antibodies in adults residing in Kilifi, Kenya, and further test the hypothesis that chronic *Plasmodium* exposure increases the risk for autoimmunity later in life. While the broader question of the possible contribution of chronic malaria exposure to autoimmune responses cannot be fully answered here, this study provides important insights that could be explored further.

Using mouse models (chapters 3 and 4), I demonstrated that *Plasmodium* infections induce the production of antibodies to native and citrullinated peptides [352]. Furthermore, extending these findings to humans with persistent exposure to *Plasmodium* parasites, I observed elevated antibodies to native and citrullinated peptides in individuals from Junju, a moderate to high *P. falciparum* transmission area, compared to those from Ngerenya, a low *P. falciparum* transmission area. Additionally, the correlation of these antibody levels with sex and parasite exposure further suggest that chronic *Plasmodium* exposure may drive their production.

Notably, the presence of antibodies to native and citrullinated peptides has not been extensively reported in the context of malaria, however, reports of other infections driving their production has been observed in periodontal infections. For example, *Porphyromonas gingivalis* [357] and *Actinobacillus actinomycetemcomitans* [333] are infections that are positively associated with ACPA IgG levels. In addition, other factors like smoking [78] and exposure to silica [358] are well-known triggers of citrullinated peptide production and, consequently, ACPA. However, while my research highlights the presence of antibodies to native and citrullinated peptides following *Plasmodium* infections further studies are required to understand if ACPA generated in the context of *Plasmodium* infections are pathogenic and drive the development of RA.

One potential mechanism driving ACPA production in RA is the presence of neutrophil extracellular traps (NETs), which release citrullinated antigens known to promote ACPA [359], therefore, in the context of *Plasmodium* infections NET formation could also be linked to ACPA production. Moreover, this idea is further

supported by the presence of elevated circulating ANAs and NETS in children with uncomplicated malaria [233]. Interestingly, recent evidence also shows that extracellular heme, a byproduct of *Plasmodium* infection, can trigger NET formation, however, this has been shown to occur independent of the PAD4 system and thus does not provide evidence of citrullination suggesting other mechanism could be triggering antibody production against native and citrullinated peptides production [231].

Next, given that *Plasmodium* infections are known to disrupt B cell compartments, leading to an increased proportion of atypical memory B cells expressing exhaustion markers [207,209,318,360], I assessed frequencies of several B cell phenotypes between the high and low antibody in the adult groups. Notably, an overall increase in activated B cells was observed in the high responders' group, indicating recent parasite infection. These findings are supported by Sundlings *et al* [196], who reported that activated memory B cells remained elevated three months post malaria exposure. Moreover, an increase in atypical B cells that were T-bet+ and CD11c was observed in the high responders group compared to the low responders, a phenomenon previously associated with increased anti-phosphatidylserine antibodies in both mice and human studies [1,4].

Thus, this observation raises important questions about the role of atypical B cells in malaria, which remains debatable. Interestingly, recent research has provided new insights by indicating that atypical B cells may exist in three distinct functional states, each with different roles in immune responses [213]. Thus, the presence of these atypical B cells in individuals with high antibody response levels suggests that they may play a role in their production, however, additional studies are necessary to determine whether these cells are indeed dysfunctional and contributing to the production of these antibodies.

In contrast to the observations made with the B cells, regulatory T cells (CD4+ FOXP3+, CD25+) were decreased in individuals with high levels of antibodies against native and citrullinated peptides compared to those with low levels, suggesting a potential regulatory effect of these T cells on the production of these autoantibodies. This is consistent with previous studies that have shown that Tregs decline in children with chronic exposure to malaria in high-transmission areas,

indicating that frequent *Plasmodium* exposure may alter regulatory immune responses [361,362]. Overall, these findings underscore the intricate relationship between malaria, immune dysregulation, and the potential development of autoimmunity.

Importantly, while the overarching goal of this study was to establish whether increased frequencies of autoantibodies would increase predisposition to autoimmune disease later in life, this research reports the presence of a wide array of autoantibodies, with certain individuals having broad reactivity to all antigens and minimal responses in others; however, the key variables, age, gender, or parasite exposure, were not linked to the variability.

This observation was likely attributable to the sample selection criteria, as most individuals included in the protein microarray analysis were selected based on their high antibody response levels against native and citrullinated peptide, with most of these individuals residing in Junju. Therefore, very few samples from individuals with little or no exposure to *Plasmodium* were included in the analysis. Additionally, age did not seem to influence the autoantibody levels in adults, findings that were consistent with previous studies that reported that the correlation between age and autoantibody levels increase with age but tends to plateau during adolescence [57].

Presence of high autoantibody levels against CRP, and a broad range of nuclear and extracellular antigens were also observed, alongside nonspecific responses to hemocyanin, suggesting potential immune dysregulation and hyperactivation. While similar findings of increased autoantibodies to extracellular and nuclear antigens have been reported previously, these studies were conducted on a smaller scale, screening a limited number of autoantigens [239,248,249,363,364]. In contrast, this research screened a broader array of 120 autoantigens associated with various autoimmune diseases in adults, providing a more comprehensive view of the potential immune dysregulation occurring. Notably, a similar array was also recently used, but the focus was on children [5].

Intriguingly, almost half of the screened autoantigens showed high reactivity, while the other half did not, indicating that immune-specific mechanisms may be

influencing these responses. One possible explanation for this pattern is molecular mimicry, particularly given that a recent study found approximately 7% of parasite antigens resemble host proteins [203]; for example, certain studies have reported on sequence similarity between *P. vivax* and human spectrin and as a consequence resulted in elevated levels of anti-spectrin antibodies [223]. For example, *P. falciparum* enolase and aldolase share structural or sequence similarities with their human counterparts, potentially leading to cross-reactive immune responses [365] . Such mimicry could disrupt immune tolerance, triggering the production of antibodies that target both parasite-derived and host antigens. Thus, this resemblance could be driving some of the elevated autoantibody responses observed in the study.

Lastly, it was crucial to investigate the presence of elevated antibody response against native and citrullinated peptide in children, particularly given the controversial role of autoantibodies in *Plasmodium* infections. While previous research has suggested that autoantibodies in malaria could play a dual role, contributing to both protection and pathology [8,204,223,239], more recent studies have added new insights. As I neared the completion of my PhD, a new study indicated that increased high levels of antinuclear antibodies ANA might confer protection in children against clinical malaria. Importantly, these autoantibodies were found to be functional, exhibiting growth-inhibitory activity [5].

However, the findings of my research contrast with that study, specifically given that increased antibody levels against native and citrullinated peptides were observed in children with both severe and uncomplicated malaria cases. Additionally, higher fibrinogen (Fib) antibody levels were mostly observed in children with severe cases.

This finding thus suggests a possible link between the production of antibodies against native and citrullinated peptides and parasite infections, with the potential for the native and citrullinated fibrinogen (cFib) antibodies to serve as biomarkers for severe malaria; nevertheless, larger studies are necessary for validation of this observations.

Notably, the differences in outcomes between my research and the recent study that provided evidence of increased autoimmunity and protection from severe malaria [5] could also be attributed to differences in study design, particularly because my research assessed antibody levels against native and citrullinated peptides at a single point in time, while the other study followed children over different malaria seasons, thus capturing a more dynamic immune response. Moreover, my study was focussed on screening for responses to specific antigens while this other study was more focussed on screening a group of broadly related antigens (ANA). Together, these findings suggest that the variety of autoantibodies elicited during malaria may have diverse, context-dependent roles.

In summary, this study reports that antibodies against native and citrullinated peptides are present in chronically malaria-exposed individuals. Although, antibodies against citrullinated peptides (ACPA) are specific for rheumatoid arthritis, it is not known whether their presence in the context of malaria is due to a breakdown in immune tolerance mechanisms due to chronic inflammation driven by *Plasmodium* infections. Furthermore, the presence of a wide array of autoantigen responses observed in this study indicate a shift towards increased autoreactivity in chronically malaria exposed adults, whether these autoantibodies are pathogenic and result in autoimmune diseases needs to be studied further.

6 Chapter 6 - Overall summary, general discussion and conclusions

6.1 Overview

The association between *Plasmodium* infections and autoimmune diseases has a historical basis, with observational studies carried out in West Africa by Greenwood *et. al.* in the 1970s, who noted that autoimmune conditions were rarer in sub-Saharan Africa [10]. Over the years, with the application of new technology, greater awareness of autoimmune diseases and research advancements, we now have a far better understanding than we did decades ago, at the time of Greenwood's report [303,304]. For instance, the true incidence of autoimmune diseases in sub-Saharan Africa wasn't apparent then but it is becoming more evident, with recent studies suggesting that their prevalence has been underestimated historically [11,12,129]. Notably, the prevalence of rheumatoid arthritis is now considered to occur at 0.36%, a prevalence rate similar to that in high income countries [75]. Similarly, the incidence of SLE is now estimated to occur at a prevalence of 1% in certain countries in sub-Saharan Africa [11]. Collectively, the reports above challenge the previously held idea that idea: that autoimmune diseases are rare in sub-Saharan Africa.

Interestingly, certain genetic traits linked to a predisposition to autoimmune disease, such as the FCYRII alleles driven by *P. falciparum* infections, have been reported in sub-Saharan Africa [7,260]. Additionally, recent evidence suggests that increased levels of pre- malaria season autoantibodies, may be protective against malaria in children during the ensuing season [5]. While this finding suggests a beneficial role for increased levels of autoantibodies in the context of malaria, it raises questions about the long-term consequences of chronic autoantibody production as a result of persistent *P. falciparum* infections. For example, does the presence of these autoantibodies increase the risk for the development of autoimmune diseases, and particularly in individuals with pre-existing genetic risk factors for autoimmune diseases?

Therefore, the overarching goal of my research was to examine the complex interplay between *Plasmodium* infections and the potential of developing autoimmune diseases. Thus, to answer these research questions, I applied the use

of both mouse models for malaria and RA, as well as human samples from individuals residing in malaria-endemic areas, to comprehensively measure correlations between *Plasmodium* parasite infections and levels of autoantibodies. Notably, the broader objectives of this research cannot be fully addressed within the scope of a PhD., as it would require a prolonged longitudinal cohort study following up individuals for decades. However, the data presented herein provides new knowledge that enhances our understanding of the complex relationship between *Plasmodium* infections and autoimmunity, particularly with the novel findings of the presence of antibodies against native and citrullinated peptides in chronically exposed malaria individuals.

6.2 Summary of the key findings

6.2.1 Increased levels of antibodies to native and citrullinated peptides, in individuals residing in a malaria endemic area

While infections, including Epstein-Barr virus (EBV) [31,141,336,366] have been implicated in the induction of autoimmune diseases, the association between *Plasmodium* infections and autoimmunity has been an ongoing debate. In this study, I observed that mice infected with *P. chabaudi* exhibited elevated levels of antibodies against native and citrullinated peptides, comparable to those seen in the chronic experimental arthritis (CEA) mice (chapter 3), suggesting that *Plasmodium* infection can equally induce an autoimmune response. Furthermore, other infections, such as *Porphyromonas gingivalis* (implicated in periodontal disease), have previously been linked to the production of these antibodies [83,87,357] and the induction of experimental arthritis. However, the presence of antibodies against native and citrullinated peptides in the context of *Plasmodium* infections represents a novel and unique finding of my research within this thesis.

Building on these results, I assessed the levels of these autoantibodies in individuals living in high versus low malaria transmission areas in Kilifi, Kenya and found significantly higher levels of antibodies against native and citrullinated peptides in individuals living in high malaria-endemic area (chapter 5), suggesting that chronic *Plasmodium* infections drive their generation. While the presence of antibodies against native and citrullinated peptides has not been reported in the context of *Plasmodium* infection in humans previously, other infections such as

Mycobacterium tuberculosis [367], *Porphyromonas gingivalis* [357,368], have been reported to induce the production of these autoantibodies.

Importantly, while ACPA is crucial for diagnoses of RA [316], presence of antibodies against native and citrullinated peptides in individuals exposed to *Plasmodium* raises important questions. For example, the presence of these autoantibodies in malaria-endemic populations may imply a link between chronic infection and potential autoimmune risk in the future. Moreover, smoking, a known factor influencing ACPA levels, is rare in this community, the use of firewood for cooking might be an important consideration influencing their production. Thus, this environmental factor could complicate the ability to definitively establish a relationship between *Plasmodium* exposure and production of antibodies against native and citrullinated peptides. Despite this, the consistency of the findings between the mouse and human data further strengthens the uniqueness and significance of this findings.

Following the observation of increased levels of antibodies against native and citrullinated peptides, I assessed the impact of *P. chabaudi* infection on acute and chronic experimental arthritis development. Notably, *Plasmodium* infection did not seem to significantly affect the development of experimental arthritis. While this observation contradicts our hypothesis, it's important to consider that the mice were only subjected to a single infection in comparison to individuals in malaria-endemic regions, where prolonged antigenic stimulation may lead to more pronounced and possibly pathogenic levels of ACPA over time.

In addition, interactions between *P. chabaudi-induced* antibodies against native and citrullinated peptides and genetic predispositions, such as HLA haplotypes, which are associated with a significantly increased risk of RA, are most likely to play a considerable role in the induction of an autoimmune response and autoantibody formation in humans [316]. Importantly, while my data indicates that *Plasmodium* infections can stimulate the production of antibodies against native and citrullinated peptides, the role of these autoantibodies in the context of human infection remains to be determined.

6.2.2 Broader spectrum of autoantibody profiles observed besides antibody responses to native and citrullinated peptides

In addition to antibody responses to native and citrullinated peptides, I assessed autoantibody profiles against 120 autoantigens commonly used as biomarkers in various autoimmune diseases using a protein microarray assay. This approach allowed me to explore whether adults with varying levels of these antibodies also exhibited differences in their broader autoantibody profiles. Among the 112 individuals screened, I observed a wide range of autoantibody reactivity, with some individuals exhibiting a strong reactivity to nearly all 120 autoantigens, while others showed little to no reactivity to any of them. Importantly, although there was variability across the samples, this observation could not be explained by known factors such as levels of parasite exposure, age, or gender, indicating that genetic or environmental factors may influence individual responses.

Although my data does not show an association between increased autoantibody levels and parasite exposure, this may be due to the fact that the samples used for the microarray were predominantly from Junju, a region with high *Plasmodium* infection transmission. As a result, I lacked an adequate comparison group of individuals not exposed to *Plasmodium* infections. It is worth noting that the initial screening for antibody responses to native and citrullinated peptides, included samples from both the high-transmission area (Junju) and the low-transmission area (Ngerenya); however, the low-transmission samples were excluded from the protein microarray analysis, as selection for the microarray assay was based on either high or medium levels of antibodies against native and citrullinated peptides. Therefore, the inclusion of matched samples from areas with no *Plasmodium falciparum* transmission would have provided a clearer understanding of the specific autoimmune responses driven by parasite exposure.

Additionally, several highly reactive autoantibodies, such as those targeting C-reactive protein (CRP), were detected in these cohorts, as well as autoantibodies against various extracellular antigens. While my findings of increased reactivity to a broad panel of autoantigens were consistent with other studies [10,248,369], a key difference is my study screened a more comprehensive panel of autoantigens. Notable this autoantibody responses were similar to patients with systemic lupus (SLE), [370–374] in which a wider autoantibody reactivity is very common, however,

it's challenging to conclude whether or not these was an indication of an on-going autoimmune disease or simply reflected a dysregulated immune system.

Interestingly, all participants exhibited a high response to EBN (Epstein-Barr Nuclear Antigen), indicating previous exposure to Epstein-Barr virus (EBV). Therefore, given that EBV has been implicated as a trigger for autoimmune diseases [366,375], future experiments should consider screening for the presence of this virus to further investigate the interplay of the EBV and *Plasmodium* infections and the combined contribution to immune dysregulation.

Lastly, this research highlights a link between *Plasmodium* infection and the induction of antibody responses to native and citrullinated peptides, supported by the strong evidence from both experimental and human studies. However, the implications of these findings in the field of autoimmune diseases still remain unclear. Further studies are therefore required to explore the long-term effects of chronic *Plasmodium* exposure on immune function and whether the observed autoantibodies are pathogenic [97,98] or simply a byproduct of immune activation in response to chronic infection. Moreover, the exact contributions of other factors, such as genetic and environmental factors, including smoking and other contributory HLA haplotypes [78–80,111], to these immune responses must be understood to better explain this complex association of *Plasmodium* infection and autoimmunity.

6.2.3 Elevated antibody levels against native and citrullinated peptides linked to increased atypical B cells and reduced T regulatory cells

Notably, as previously reported, chronic immune stimulation by repeated infections can lead to sustained activation of immune cells, such as B and T cells [194,209], resulting in a dysregulated immune system with the production of autoantibodies [1,6,8,249,369]

In addition, maintaining a proper balance between regulatory and effector mechanisms of the immune system is essential to preventing autoimmune diseases. In this study, I report an increased proportion numbers of regulatory T cells in participants with low antibody levels against native and citrullinated

peptides compared to the high responders' group, further demonstrating that chronic infections such as malaria can disrupt this balance by attenuating regulatory T cell function [362,376]. Moreover, the hyperstimulation of the immune system might be mediated through several mechanisms, such as chronic inflammation, molecular mimicry, bystander activation, or epitope spreading [8]. Thus, characterising such mechanisms could help understand how chronic *Plasmodium* exposure increases predisposition to autoimmunity.

I also report an increase in atypical B cells in the high responders. The presence of atypical B cells is a well-documented phenomenon in chronic infections [207–209,318,377,378] , including malaria, but their association with high antibody responders raise important questions. In the context of *Plasmodium* infections, atypical B cells have been associated with the production of anti-phosphatidylserine antibodies [4]. Similarly, in my study, while high antibody levels against native and citrullinated peptides were correlated with the presence of atypical B cells, it remains unclear whether these cells are directly responsible for their production. Moreover, recent evidence suggests that atypical B cells exist as three distinct subsets of atypical B cells in chronically exposed individuals. One subset is anergic (non-responsive), with a high activation threshold, similar to atypical B cells found in systemic lupus erythematosus (SLE); another subset develops from memory B cells and rapidly differentiates into antibody-secreting cells after stimulation, while the third subset requires an additional signal to fully mature into antibody-secreting cells[213]. Thus, raises the question of whether the atypical B cells observed in high responders are of the non-responsive subset, potentially contributing to immune dysregulation in this context.

Interestingly, non-specific autoantibodies were also observed in this study, for example hemocyanin, a foreign antigen found in arthropods [379], bound antibodies from the human plasma, suggesting that some of the observed immune reactivity might be non-specific. The fact that hemocyanin is not naturally present in humans yet there was a specific signal indicates the possibility that chronic infections may drive an overactive or dysregulated immune system, where the body reacts to both specific and non-specific antigens. Thus, it highlights the complexity of immune responses in individuals exposed to *Plasmodium* over

prolonged periods and raises important questions about the balance between protective immunity and the risk of developing autoimmunity.

6.2.4 Elevated antibody levels against native and citrullinated peptides in children with severe and uncomplicated malaria

Herein, I report increased levels of antibody levels against native and citrullinated peptides in children with severe malaria and uncomplicated malaria compared to healthy children. This is consistent with other studies that have reported evidence of increased autoantibodies correlated with severe malaria anaemia and acute kidney injury and thus suggests that these autoantibodies could be pathogenic [1-3]. In addition, anti-phosphatidylserine antibodies have been detected in children with severe malaria, and their role in enhancing the clearance of uninfected red blood cells [1,3] is well known.

By contrast, the role of autoantibodies in conferring protection has been indicated in several studies; specifically, in one study, increased levels of ANA before a malaria season were protective [5]. Moreover, these autoantibodies were also shown to be functional with the ability to inhibit parasite growth. Therefore, while my data and several other data suggest a pathogenic role for autoantibodies, there is need to study the kinetics of antibody levels against native and citrullinated peptides, and further gain insights into when they are produced, and whether they decline with parasite resolution.

6.2.5 Potential mechanism inducing antibody production against native and citrullinated peptides

Lastly, I next explored the potential mechanisms behind generation of antibody production against native and citrullinated peptides, such as molecular mimicry, which has previously been linked to the production of specific autoantibodies [8,203]. By analysing specific sequence similarity between the host's native peptide (e.g., fibrinogen, enolase, vimentin, and tenascin) and *P. falciparum* sequences, no significant matches were found, suggesting that molecular mimicry is not the primary mechanism behind their production in this context.

Additionally, given the crucial role of PAD enzymes, in citrullination [319,380], I also examined whether PAD activity was responsible for antibody production against native and citrullinated peptides in the context of *Plasmodium* infection. This was tested by administering a pan-PAD inhibitor targeting PAD1–PAD4 to *P. chabaudi*-infected mice and assessing its impact on autoantibody production. While the levels of most antibody responses against native and citrullinated peptides were unaffected, the decreased levels of cFIB antibody in the PAD-inhibited group compared to the control suggest that PAD enzymes contribute to the production of antibodies against citrullinated fibrinogen (cFIB). However, the inhibition achieved was insufficient to alter the levels of other antibodies targeting native or citrullinated peptides. Thus, these findings underscore the need for further validation through experimental studies using PAD knockout mice to fully elucidate the role of PAD enzymes in this process.

6.3 Conclusion

Although the presence of antibodies against native and citrullinated peptides and other autoantibodies indicates an ongoing autoimmune response, it does not necessarily mean that this leads to the development of clinical autoimmune disease [381]. Particularly given that autoimmune disease development is considered multifactorial, arising from genetic predispositions, environmental factors, and the complex immune system dynamics [137,382,383]. For example, genetic predispositions such as specific HLA haplotypes might increase an individual's susceptibility to developing autoimmune disease in the presence of environmental triggers such as infections and smoking, which might exacerbate this risk by inducing molecular changes in immune cells that break up immune tolerance [136] .

Therefore, in the context of *Plasmodium* exposure, it is essential to clarify how exposure to *Plasmodium* infections (an environmental trigger) interacts with genetic traits; for example, are RA-susceptible individuals at an increased risk for developing RA when chronically exposed to malaria due to the synergistic effects of genetic predisposition and immune hyperactivation? Moreover, does the protective genetic traits that evolved in malaria-endemic regions to reduce the risk of malaria traits some of which are linked to autoimmune disease susceptibility, increase the risk of autoimmunity in the presence of chronic *Plasmodium* infection [7].

Therefore, while my research, provides new insights into the complex interplay of chronic exposure to *Plasmodium* and autoimmune disease, a multifaceted approach is needed to fully understand this relationship, which can be achieved through long-term cohort studies incorporating genetics, environmental, and immunological factors are more likely to shed light on the contribution of chronic *Plasmodium* exposure to autoimmune disease development.

6.3.1 Outstanding questions

Importantly several questions stem from this study such as follows:

- Could the criteria for diagnosis of Rheumatoid Arthritis (RA) in malaria-endemic areas need revisiting, considering this data suggests that antibodies against native and citrullinated peptides might reflect a response to chronic *Plasmodium* exposure rather than RA-specific pathology?

- Furthermore, while recent research indicates that increased autoantibodies, particularly, might offer some protection against clinical malaria [5]. One of key question is what is the cost of autoimmunity, particularly are the autoantibodies produced in response to *Plasmodium* infections pathological, and if so, what are the long-term consequences of chronic autoantibody production?

6.3.2 Study limitations and future directions

Although, this study enhances our understanding of the association between *Plasmodium* infections and autoimmunity, it has limitations. For instance, the inclusion of matched samples from areas with no malaria transmission would have given a clearer picture of the specific immune response driven by parasite exposure, particularly for the protein microarray data.

Another limitation stems from the lack of sufficient data on the incidence and prevalence of autoimmune disease Africa, especially in malaria-endemic regions [11,12,129]. Therefore, future studies are needed to determine the prevalence of autoimmune diseases in these populations, which will enhance and improve our

understanding of the impact of increased autoimmunity following prolonged *Plasmodium* exposure. Importantly, as healthcare facilities improve in sub-Saharan and autoimmune conditions are becoming increasingly well-recognised, therefore the clinical thresholds of autoantibodies that predict increased susceptibility to autoimmune diseases in individuals exposed to *Plasmodium* need to be defined.

Moreover, future research directions should also include a more detailed analysis of whether these autoantibodies are pathogenic by investigating their glycosylation patterns, as glycosylation influences the pathogenicity of autoantibodies, such as ACPA [97,98]. Importantly, characterising the genetic traits of individuals with an overall increased autoimmune reactivity compared to individuals with less hyper-reactivity reactivity to the autoantigens but with similar parasite exposure levels will provide further insights into potential mechanism influencing autoantibody production in some individuals.

Therefore, the application of a more holistic approach to determining whether the autoantibodies identified in individuals chronically exposed to *Plasmodium* infections are pathological and further understanding the genetic and molecular mechanisms driving their production will greatly improve our understanding of the complex interplay between chronic exposure to *Plasmodium* infection and autoimmune disease. Additionally, the application of mouse models could provide additional insights into the role of ACPA through the application of passive transfer studies.

7 Appendices

7.1 Supplementary figures and tables for Chapter 5

A.

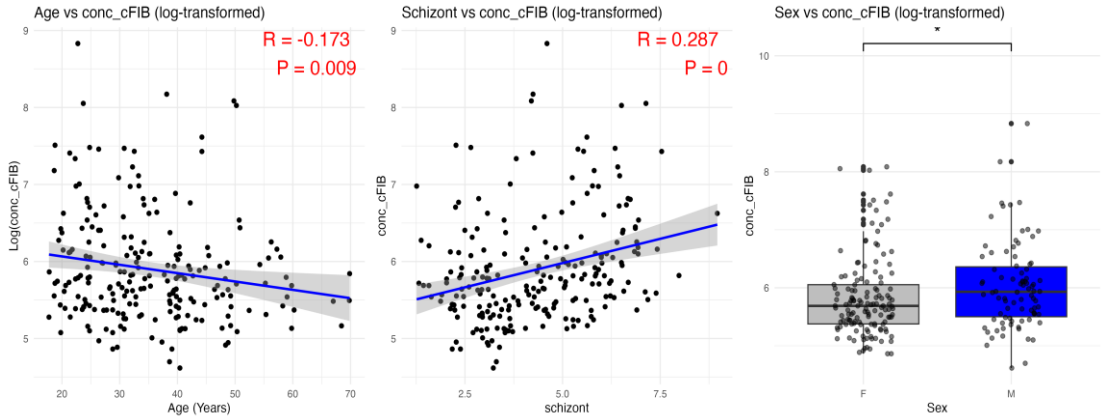

B.

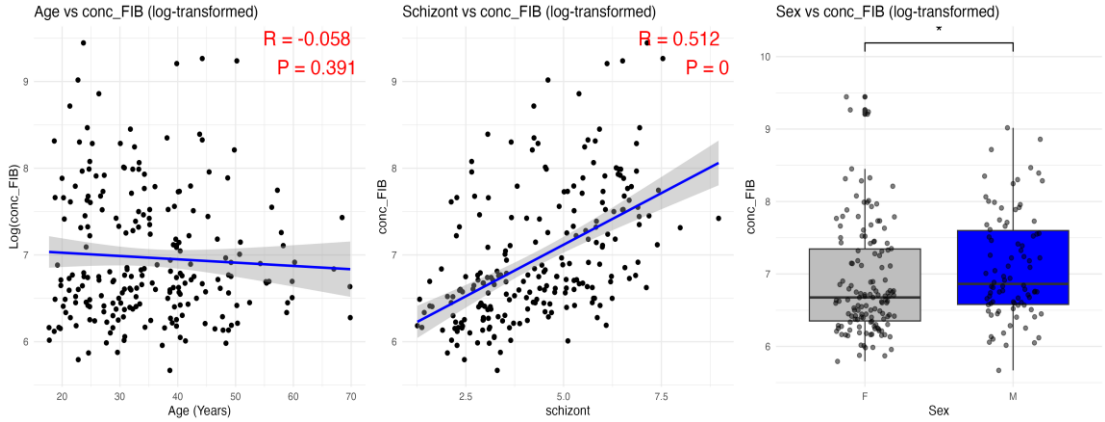

C.

D.

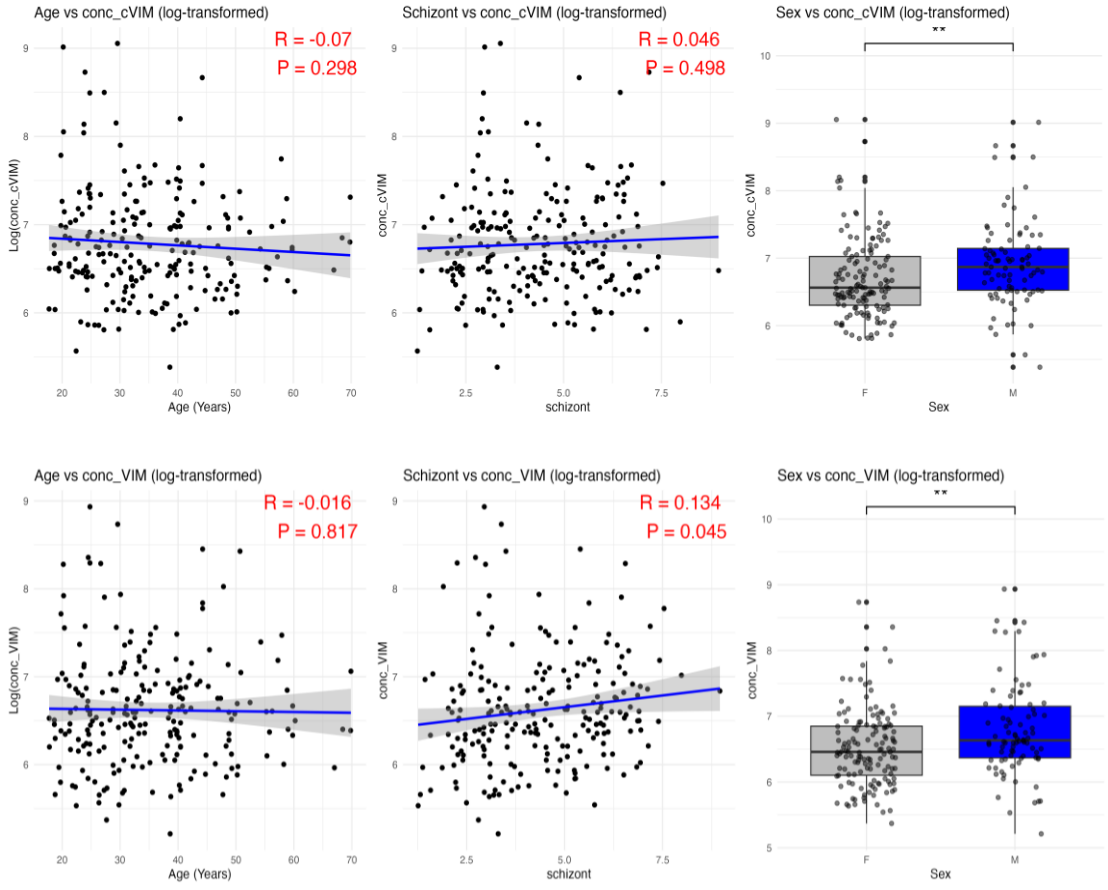

Figure 7-1: Sex and exposure to the parasite were observed to influence the levels of antibodies against native and citrullinated peptides

Pearson correlation analysis was performed on log-transformed values, with correlation plots for age (left), schizont (parasite exposure) (middle), and boxplots for gender (right). Panel A) represents graphs for cFIB, B) for FIB, C) for cVIM, and D) for VIM. Pearson's correlation coefficient is shown along with significance levels: ns (not significant), * p<0.05, ** p<0.01, *** p<0.001.

Table 7-1: Log2 Fold Change and Adjusted P-Values for Differential IgG Expression Across 120 Autoantigens in Females vs. Males

ID	log2fold	p	p.adj
LC1	-0.473376979785237	0.0382333193076223	1
Jo-1	-0.419250050891613	0.0482178324523463	1
CRP	-0.348962348402304	0.06360099367562	1
Thyroglobulin	-0.389292169424906	0.0794121584223788	1
SRP54	-0.408802857105217	0.0810185400626866	1
B-actin	-0.377810744311103	0.084116632429482	1
TPO	-0.336489264136002	0.0996365248812595	1
Vitronectin	-0.347239958544048	0.101734966331987	1
Prothrombin protein	-0.377176156233878	0.102966558502898	1
CENP-A	-0.317823513171089	0.114397051076782	1
ComplementC1q	-0.269201115409949	0.140631848543803	1
AQP4	-0.307190443195674	0.144840517700825	1
PL-7	-0.296320319796129	0.159146163070243	1
dsDNA	-0.26651020600481	0.180036051774004	1
Collagen V	-0.257137574851605	0.19595990771303	1
Myosin	-0.248819055965016	0.200930952890323	1
COL17A1	-0.278367330148853	0.201811516227641	1
Ro SSA 60Kda	-0.250242660492899	0.205114034307033	1
Neuropilin-1	-0.287993659918437	0.205244036804374	1
Chondroitin Sulfate	-0.29247652695092	0.213062772992645	1
LPS	0.247822124016474	0.216398735251592	1
Complement C3 C3a	-0.271318768560223	0.229775442736577	1

Collagen IV	-0.246701573437437	0.24016898314096	1
S100	-0.254475409294569	0.240589894830211	1
CENP-B	-0.241538957265854	0.247050559137489	1
AGTR	-0.216878113215345	0.249314981666493	1
Calprotectin	-0.251115818964894	0.249692679107952	1
Scl-70 Topoisomerasel	-0.235577537363154	0.252903877126333	1
Elastin	0.265008270357766	0.254657245652602	1
SP100	-0.267148132790665	0.26086682075516	1
KUP70P80	-0.247905164337721	0.265880374948493	1
Phosphatidyl-serine PS	-0.25842112278849	0.268321227072097	1
Alpha-actinine	0.207114760315476	0.272297096715158	1
Alpha Fodrin	-0.242094142196966	0.28170675338742	1
Collagen VI	-0.211050928325152	0.2841942832886	1
Muscarinic receptor	-0.228005683620231	0.284456941146429	1
Vimentin	-0.226603908641365	0.294538772184508	1
IL-15	-0.230829361587188	0.298003618162791	1
PCNA	-0.259644218308436	0.299621348103642	1
TNF-a	-0.211027073521421	0.321860625705971	1
B2 glycoprotein1	-0.185115545952696	0.326668132969116	1
LaSS B	-0.193087572323575	0.328160888466982	1
Factor H	-0.193478590661456	0.344851937260851	1
GP2	-0.196920725184701	0.345305784477146	1
ssDNA	-0.16087715481314	0.347485310604292	1
CD4+	-0.207295012328903	0.370339138650741	1

U1-snRNPC	-0.180381265367612	0.37329807064374	1
GP210	-0.194025487703431	0.391782728221294	1
U1-snRNP6870	-0.19616359745561	0.394322421247153	1
Fibrinogen IV	-0.173252405282176	0.403756841661268	1
Hemocyanin	-0.158141461522982	0.41939900824691	1
U1-snRNPA	-0.192625390316576	0.419951280423549	1
GDF-15	-0.183042681848774	0.426396732582734	1
MPO	-0.156742909068121	0.434060335744764	1
Ro SSA 52Kda	-0.132632880111539	0.449513933497456	1
Amyloid	-0.149594414712298	0.450839008054024	1
Fibrinogen S	-0.154004254890908	0.457768972353312	1
M2	-0.163911794702341	0.46851231181072	1
IL-12	-0.16395783646815	0.479379599306648	1
TTG	-0.153052480147078	0.486245725218045	1
BPI	-0.173838066759496	0.490539624426952	1
PMScl-75	-0.15920820745388	0.496341693763934	1
Aggrecan	-0.138570443791691	0.507251413849042	1
GM-CSF	-0.155358840850026	0.515204291493237	1
Core Histone	-0.152627869665447	0.516381331784008	1
PM Scl 100	-0.144239022962861	0.528641534090084	1
GBM	-0.137486713904411	0.531471371814486	1
Sphingomyelin	-0.132907225241116	0.532259238494835	1
Factor D	-0.118302700442335	0.57536438565098	1
Cardolipin	-0.124870467305382	0.593780471257631	1

Insulin	-0.105046610119306	0.611141335946022	1
IFN-A1	-0.116189393472916	0.630619495242775	1
HistoneH3	0.105051129014935	0.635675327356719	1
Myosin heavylight chain	0.0971748972383536	0.645069069869325	1
Ribophosphoprotein P0	0.0872600962515565	0.645860478736036	1
Histone H2A	0.10895986691679	0.649899460514166	1
RiboPhosphoprotein P1	-0.0837763875679464	0.651737969750752	1
B2-microglobulin	-0.0949322219002689	0.666166292145586	1
HistoneH1	0.107013256536827	0.666537851759436	1
SmD	-0.0932510878492719	0.669038039165256	1
IFN-L2	-0.104160699646663	0.669051726386727	1
IFN-r	-0.0943582907537243	0.684750906014641	1
Heparin	0.103087331637975	0.688204713288138	1
TIF1gama	-0.0826123519526948	0.702979023054471	1
Mi-2	-0.0710066244612476	0.71594251441285	1
ssRNA	-0.0830423969251254	0.716933953975285	1
HistoneH2B	-0.0864741930922839	0.722420189570862	1
TWEAK	-0.0842650625734179	0.72281721403852	1
GAD65GAD2	-0.0726531960993447	0.723690564933208	1
FactorB	-0.0735280149176841	0.729964638037165	1
SmRNP	0.0769839405591298	0.732754477440579	1
Nucleosome antigen	-0.0746861613205315	0.734778711512027	1
EBNA1	-0.0627554134017623	0.739030696971041	1

Factor P	-0.073652249018979	0.739119776898745	1
PR3	-0.0744133615445942	0.747763436381627	1
Collagen II	-0.0744889457090595	0.74985851266268	1
Fibronectin	-0.0679444840254784	0.749987415548704	1
Collagen III	-0.0754409862674849	0.750167556711902	1
TGF-B1	-0.0694827714174945	0.751790307215876	1
PL-12	-0.0683121646016925	0.753186595771389	1
Nucleolin	-0.0588390783341227	0.764681686228652	1
RiboPhosphoprotein P2	-0.0628337454595235	0.766783902932675	1
MDA5	0.0460761631531889	0.82510613874587	1
Myelinbasicprotein MBP	-0.0493382331373044	0.83341769149972	1
IA2	0.0515163835640285	0.837139332045743	1
IFN-E	-0.0384529375171753	0.861186822165022	1
Sm	-0.0374290561708472	0.865408022043157	1
Collagen I	-0.0354026341950106	0.869471204102284	1
U1-snRNPBB	-0.0352373001486206	0.871718211748508	1
Nup62	0.0336250052818064	0.873232195778254	1
CD8	0.0380224427622945	0.874991053624786	1
Intrinsic Factor IF	-0.0344393531067027	0.874999694350823	1
Troponin-I	-0.0296607487056456	0.89603075762009	1
Mitochondrial antigen	-0.0236133967893362	0.912266891000922	1
Proteoglycan	-0.0223208012039129	0.926391512249747	1
Factor I	-0.0193866265322264	0.934662824919711	1

Histone H4	0.0181626704619618	0.939706192006962	1
Heparan Sulphate	-0.0147132233460139	0.948697748570388	1
IFN-B	-0.00840748745311986	0.971095251939573	1
Laminin	0.000497077171984151	0.998310236144528	1

Table 7-2: Log2 Fold Change and Adjusted P-Values for Differential IgM Expression Across 120 Autoantigens in Females vs. Males

ID	log2fold	p	p.adj
LaSSB	-0.461417532544243	0.0498008799882577	1
Myosin	-0.432060487331539	0.065442771363441	1
Myelin basic protein MBP	-0.45045097645107	0.0667994765043786	1
Laminin	-0.435134085682469	0.068005407804148	1
B2 microglobulin	-0.439346476212923	0.0687299596383047	1
Fibrinogen S	-0.431224843862462	0.0691918472962255	1
Fibrinogen IV	-0.430735832980142	0.0694147868933382	1
IFNA1	-0.433752179602369	0.0726556378667983	1
CD8	-0.434317154092147	0.0737921552920724	1
IFNE	-0.408683861469296	0.0778121895517261	1
Jo1	-0.408017049217743	0.0782170735916159	1
Elastin	-0.422382344722418	0.0805628937812234	1
GP2	-0.408958383757379	0.08064298919286	1
Collagen IV	-0.4140809405998	0.080865933691554	1
EBNA1	-0.390179627722052	0.0907255484650838	1
CD4+	-0.382151222629253	0.0933653865485963	1

IL15	-0.391935261266646	0.0941120490147971	1
Calprotectin	-0.387768838922128	0.0983434992778137	1
AQP4	-0.391573689047546	0.099284438849442	1
Phosphatidylserine PS	-0.379152325667117	0.0993498876805231	1
GAD65GAD2	-0.381369114383503	0.101002867587606	1
CENPA	-0.389956319975248	0.101327640868378	1
Factor H	-0.385958087890015	0.10453738862889	1
Hemocyanin	-0.36124045565365	0.104709766563816	1
TNFa	-0.372325207362605	0.104727132954389	1
Collagen VI	-0.383947855128345	0.104903252330262	1
LC1	-0.390007391844129	0.105731800938155	1
IL12	-0.381587014630992	0.108727705736834	1
dsDNA	-0.373196261857976	0.110729702108452	1
Ro SSA 60Kda	-0.36717408361886	0.118373103523709	1
Vimentin	-0.381085961949182	0.118778108662225	1
SRP54	-0.37808692987709	0.121721142613716	1
Neuropilin1	-0.355886685473326	0.129950935596274	1
Bactin	-0.359231573144469	0.130147894379351	1
B2 glycoprotein1	-0.357518636926077	0.132390392926406	1
M2	-0.366673524274786	0.134062992645018	1
MDA5	-0.355820488579678	0.136692063555879	1
BPI	-0.354288603960642	0.138111662012408	1
Factor I	-0.338330643829952	0.13932080578293	1
KU P70 P80	-0.351613895565354	0.141316431736927	1

Vitronectin	-0.339554610666824	0.149546317291894	1
Complement C1q	-0.334069230558852	0.149835757445524	1
Thyroglobulin	-0.339457245531208	0.151548920181493	1
TTG	-0.337405650401631	0.153130166141182	1
GDF 15	-0.334876755354745	0.153336677899444	1
U1 snRN PA	-0.352037915322077	0.155694209187041	1
PCNA	-0.331740687690071	0.156502564317248	1
IFNB	-0.325675523280926	0.161883155896413	1
Factor B	-0.324468815295027	0.162866688521612	1
Mitochondrial antigen	-0.336821534084628	0.164394020820606	1
PL7	-0.326690148976524	0.166394946975228	1
Muscarinic receptor	-0.318226517257393	0.168828596508924	1
Core Histone	-0.333334472200354	0.170054700900354	1
GP210	-0.317842136113728	0.177757187847302	1
Mi2	-0.316248912574873	0.187890915820741	1
SmD	-0.309219981149253	0.190240905787486	1
Nucleolin	-0.301408680254901	0.195574499330815	1
IA2	-0.318160158951243	0.198849405934039	1
CRP	-0.273376522547083	0.200399100127316	1
Alpha Fodrin	-0.319912820826269	0.20190114841451	1
Complement C3 C3a	-0.300176179218157	0.202945270276231	1
IFN r	-0.290040564569799	0.209092287984758	1
GBM	-0.306170204607818	0.217305925922487	1
Scl70 Topoisomerasel	-0.294477690050667	0.218027164186047	1

PL12	-0.295828435284229	0.218115083260151	1
IFNL2	-0.296147890581527	0.22014388521306	1
TPO	-0.297801146570978	0.220943764884389	1
U1snRNP6870	-0.289502406769237	0.22384333247267	1
HistoneH2B	-0.292855825407265	0.224663132313269	1
ssDNA	-0.281508253092622	0.226717723949624	1
GMCSF	-0.2801136645289	0.238054127153631	1
S100	-0.262009025479487	0.240866690619694	1
MPO	-0.259286903559159	0.261707693310599	1
Collagen III	-0.261392339319374	0.26244538013795	1
Heparan Sulphate	-0.242339037313244	0.275137204707547	1
RoSSA52Kda	-0.258900771928383	0.277924549970019	1
PMScl100	-0.266281868894334	0.289115287124152	1
HistoneH2A	-0.232137445351438	0.323264801439995	1
TWEAK	-0.226763412791111	0.326257038995195	1
TIF1gama	-0.242072287626301	0.328673758507227	1
COL17A1	-0.225756222244964	0.346704863944998	1
TroponinI	-0.234924671054896	0.347186942455353	1
Sm	-0.214293967219318	0.349209108595756	1
PMScl75	-0.227272238819161	0.352030112852869	1
U1snRNPC	-0.217524402832628	0.354083617533954	1
Factor D	-0.203946113275725	0.365057692267868	1
Collagen V	-0.193638639780107	0.378766570494614	1
Prothrombin protein	-0.211635332162637	0.384043942711982	1

Aggrecan	-0.196261817751928	0.387808422463992	1
Cardolipin	-0.209135377492569	0.388591306074193	1
HistoneH3	-0.198445820815851	0.408059387319649	1
Amyloid	-0.172327663258223	0.417812298126505	1
SP100	-0.199027154706325	0.419668377487825	1
Insulin	-0.172303024619704	0.444544640632704	1
Alphaactinine	0.156231828632602	0.446972200890482	1
Heparin	-0.180577713541679	0.451566301390613	1
Fibronectin	-0.157797607227986	0.486924416500693	1
PR3	-0.159478937326047	0.495541791467628	1
Proteoglycan	-0.152126171927867	0.511342350152491	1
Nup62	-0.146675678461615	0.522674653042128	1
AGTR	-0.147988708321688	0.53296113130476	1
Intrinsic Factor IF	-0.132638615021578	0.535768168009448	1
Ribo Phosphoprotein P0	-0.126233289308254	0.559011224322034	1
Ribo Phosphoprotein P1	-0.123013125910166	0.568316962665422	1
Collagen I	-0.124302786188473	0.574768592696692	1
SmRNP	-0.121659747191175	0.583877044719197	1
Collagen II	-0.125776490155346	0.584945500409592	1
Ribo Phosphoprotein P2	-0.119642004853888	0.613603880917694	1
CENPB	-0.112550870058496	0.627744053113859	1
U1sn RNPBB	-0.113526007985881	0.630779749437358	1
LPS	-0.115772597122217	0.637580550351676	1

Factor P	-0.103693233946587	0.650413528851018	1
Histone H1	-0.0965007661440498	0.672235563436975	1
ssRNA	-0.0896679586476101	0.701941761748331	1
Histone H4	-0.0867356615701458	0.720760462153605	1
Myosinheavy light chain	0.0651212903776003	0.77215109401188	1
Chondroitin Sulfate	-0.0624938079051586	0.7792165615131	1
Sphingomyelin	-0.0618298690009271	0.785082784432038	1
TGFB1	0.00679315002770044	0.976003426357902	1
Nucleosome antigen	0.000671882738921216	0.997629950577537	1

Table 7-3: Log2 Fold Change and Adjusted P-Values for Differential IgG Expression Across 120 Autoantigens Based on Schizont Levels

ID	log2fold	p	p.adj
Core Histone	0.751666291166045	0.0705130908812977	1
IFN-E	0.700099346805829	0.0904977477378341	1
IFN-B	0.66997702437651	0.10781879334436	1
RiboPhosphoprotein P2	-0.624627278287742	0.128523785303498	1
Heparin	0.6260907688644	0.132208644501981	1
B2-microglobulin	0.606220880779482	0.14292393905733	1
Laminin	0.598471343612643	0.151657332657447	1
COL17A1	-0.577700035521751	0.164766747248766	1
CD8	0.560890247762254	0.183239713128155	1
Hemocyanin	0.535894440530326	0.187891793101834	1
Fibrinogen S	0.535178590534756	0.190715469916727	1

SmRNP	0.535036538301947	0.193951128511554	1
Sphingomyelin	0.525632929540716	0.200690874581501	1
Sm	0.499487103416065	0.221580137959722	1
TGF-B1	0.498824348006287	0.225469513783431	1
Histone H1	0.507598269576503	0.230666821463797	1
Nucleosome antigen	0.491302954215993	0.232243891777936	1
Factor I	0.491329740638999	0.234225419866645	1
Proteoglycan	0.494229454544803	0.237072689640611	1
AGTR	0.476447218081022	0.241669098438147	1
ssRNA	0.486433732881653	0.244847931940262	1
Elastin	0.472970597200441	0.251658875739595	1
GDF-15	0.476549181073504	0.253365586353145	1
Collagen III	0.474489974390851	0.255563531513452	1
Myelin basic protein MBP	0.475440062454806	0.257589314061601	1
U1-snRNPC	0.46217296050785	0.262548197527058	1
Histone H2A	0.466965703852492	0.266296085379866	1
Histone H2B	0.465737149656575	0.268576815824855	1
Complement C1q	0.439802692810305	0.277794779991863	1
Factor P	0.446356498174316	0.278677784982	1
Vitronectin	0.44583928696326	0.279615141007869	1
Collagen IV	0.438978485497777	0.284283621084963	1
CD4+	0.433108322686165	0.294254096667874	1
Aggrecan	0.424758623075263	0.301394005794703	1
Insulin	0.42562475025545	0.301779863801971	1

RoSSA52Kda	0.41813612200498	0.302191996454443	1
Complement C3 C3a	0.421671680228058	0.309217187816583	1
Factor B	0.414110890094157	0.312813660690339	1
Collagen I	0.403742492263122	0.325041280876971	1
Troponin-I	-0.401467759123666	0.329971398760098	1
GAD65GAD2	0.394594025957283	0.335606528568468	1
Fibrinogen IV	0.391325624616435	0.343565697960615	1
Intrinsic Factor IF	0.383553853835513	0.357265239922073	1
U1-snRNPBB	0.380683031656116	0.359768375870375	1
Collagen II	0.363668712354197	0.380330878697016	1
Scl-70 TopoisomeraseI	0.359059018508864	0.382197975966867	1
Muscarinic receptor	0.355422683579875	0.385443938894869	1
Phosphatidyl-serine PS	0.35332939237238	0.392473698855586	1
GP2	0.348126333750717	0.39429273989011	1
Histone H3	0.352203239521329	0.396057572787021	1
LPS	0.342458179668399	0.399872801746563	1
GP210	0.344022707046255	0.403671880115724	1
Histone H4	0.348310938218432	0.406052082647412	1
Factor H	0.341474956761419	0.407174915162368	1
Chondroitin Sulfate	-0.346250102214839	0.409394457390897	1
Myosin heavylight chain	0.338308556560305	0.41162300504257	1
PMScl-75	0.321838573466536	0.434974151063357	1
IFN-L2	0.327301318388909	0.440059266586406	1
MDA5	-0.314707437096117	0.440897179105812	1

Nup62	0.3123397590351	0.448509346183919	1
MPO	0.310318149196279	0.449113205202103	1
CENP-B	-0.301099519177202	0.461929707909833	1
Amyloid	0.291318551729398	0.473568051602452	1
Alpha-actinine	-0.278197719619058	0.491158398539909	1
IFN-r	0.286269127350501	0.491766743440059	1
Heparan Sulphate	0.278643932320928	0.501904251962297	1
B2glycoprotein1	0.266549266233029	0.51243903703836	1
B-actin	0.271487915122349	0.513666888940622	1
CENP-A	0.26261710865939	0.519811348151998	1
PL-12	0.265292807071059	0.521776027923	1
Calprotectin	0.258506523871819	0.533804331869931	1
U1-snRNP6870	0.254724423390025	0.539624948208358	1
SmD	0.250631444960269	0.543014801584964	1
GBM	0.25173224820114	0.54448890696223	1
Nucleolin	0.245670416202822	0.546877786578624	1
RiboPhospho protein P1	0.244826154670755	0.546957302361923	1
Collagen VI	0.240405803161927	0.559693250720741	1
PR3	0.243695687767565	0.559774525630296	1
EBNA1	0.235902571878014	0.561497581579268	1
Alpha Fodrin	0.237358659554475	0.568547945211272	1
Collagen V	0.223858977821849	0.584642954944695	1
IL-15	0.225413699151382	0.58624603049636	1
Cardolipin	0.225300176952817	0.589227182498349	1

RiboPhospho protein P0	0.221832618623676	0.590377387954384	1
TIF1gama	0.217144267420034	0.596880025833111	1
Myosin	0.209486721219272	0.607524646587673	1
dsDNA	0.208706476242058	0.609904865547755	1
Prothrombin protein	0.211233639250555	0.609918014103302	1
BPI	-0.20986408964629	0.618708393181123	1
IA2	0.184060768480385	0.659020779555495	1
SRP54	0.168138936436378	0.687616515852521	1
TTG	-0.164357417343902	0.689044712148979	1
PMScl100	0.166218574110711	0.691680212470815	1
LaSSB	0.162805093387162	0.693048716099673	1
GM-CSF	0.160322236365507	0.701372840515422	1
AQP4	0.158066263578073	0.701935336728644	1
LC1	-0.154236768803468	0.709796029131827	1
Mi-2	0.126396198772503	0.758024695829657	1
TNF-a	0.124594918876446	0.761417734544981	1
CRP	0.109480654151509	0.788237709751597	1
ssDNA	0.108404829295946	0.788437096780873	1
KUP70P80	0.110703317837793	0.789547301199434	1
Vimentin	0.104541892207682	0.800822424262217	1
RoSSA60Kda	0.101361967825339	0.806273190935099	1
Thyroglobulin	-0.0976749765229889	0.813629393240647	1
IL-12	0.0930193367609042	0.823764992814288	1
TPO	0.0897793451564338	0.826003152946102	1

Jo-1	0.0863605834327869	0.834765738162782	1
PL-7	0.0781701288158189	0.85035837932188	1
IFN-A1	0.0782693173768139	0.851088914088518	1
M2	0.0742350536505904	0.858352971271812	1
S100	0.0714526391105353	0.861185579935116	1
PCNA	0.0671374398454704	0.871448960211712	1
Factor D	-0.0600747291990482	0.883490425012068	1
Mitochondrial antigen	-0.0431328630573367	0.917081963354884	1
Neuropilin-1	0.023569088822746	0.954669335707447	1
TWEAK	-0.0162217783436555	0.969038603133166	1
SP100	0.0158705349916675	0.96979969693745	1
U1-snRNPA	-0.014166894143513	0.97302115383584	1
Fibronectin	0.0133784834598971	0.97416031526447	1

Table 7-4: Log2 Fold Change and Adjusted P-Values for Differential IgM Expression Across 120 Autoantigens Based on Schizont Levels

ID	log2fold	p	p.adj
Amyloid	0.614606495457576	0.093801067280287	1
Heparin	0.575733265218709	0.116477847949606	1
B2microglobulin	0.570681734144965	0.119717141185871	1
Elastin	0.55328703088503	0.131413800189261	1
FactorI	0.531648719494915	0.147178546892146	1
U1snRNPC	0.524512051685147	0.152683562954549	1

ssRNA	0.521033115097805	0.155423302209887	1
U1snRNP6870	0.512530888784646	0.162275941031137	1
TroponinI	0.5099396834704	0.164409106865618	1
TGFB1	0.506695203232937	0.167109776967553	1
Factor H	0.50392121671176	0.169445144323299	1
Nucleosome antigen	0.485274050780039	0.185782912733985	1
IFNB	0.469883212217766	0.200122643929838	1
Heparan Sulphate	0.461496285159818	0.208269178776346	1
TPO	0.447124745758926	0.222783166546207	1
Muscarinic receptor	0.446244095153944	0.223695528809417	1
Thyroglobulin	0.435343877215077	0.235210088621718	1
Vitronectin	0.433773512945515	0.236902941408234	1
Core Histone	0.428841785619056	0.242275294828937	1
HistoneH2B	0.409512611213135	0.264155566921771	1
Fibrinogen IV	0.408935782819331	0.264828830563876	1
MPO	0.405146655727202	0.269280835666167	1
Sm	0.403940709136884	0.270708471471947	1
AGTR	0.403112816524895	0.271691554851615	1
IFN r	0.402125930679559	0.272866627016349	1
Factor B	0.401149515812025	0.27403264956248	1

TNF a	0.390487191326159	0.286987164996725	1
IFN E	0.382194858920864	0.297343722792048	1
Scl70 TopoisomeraseI	0.380476840443662	0.299520283053187	1
Mi2	0.37326145355904	0.308777322784321	1
Ribo Phosphoprotein P0	0.365571966124609	0.31884875935842	1
GAD65 GAD2	0.364507988736799	0.320259079307178	1
Fibrinogen S	0.354763020673365	0.33336568511256	1
Nup62	0.354259102524035	0.334052722738617	1
GP210	0.34035694585979	0.353366368339461	1
U1snRNPA	0.339833555067389	0.354107027208267	1
EBNA1	0.333426689532058	0.363252876766816	1
Calprotectin	0.330805218834895	0.367037299922164	1
TIF1gama	0.33029943073354	0.367770288001492	1
IA2	0.327579849282953	0.371727122435548	1
Laminin	0.322178004453654	0.379664466249654	1
CD4+	0.319775065584909	0.383228543043129	1
U1snRNPBB	0.317451960767728	0.386693629729247	1
SmRNP	0.315070537004624	0.390265485460269	1
SRP54	0.312219752265345	0.394567610699099	1
Complement C1q	0.311808928116951	0.395189943644632	1

B2 glycoprotein 1	0.310680921919003	0.396901742696098	1
Complement C3 C3a	0.309635550481228	0.398492128742737	1
COL17A1	0.308783790113606	0.399790797086306	1
Histone H1	0.305290450943497	0.405143627089237	1
PR3	0.305111926460942	0.405418325651675	1
PL12	0.304087074928087	0.406997434667392	1
Collagen IV	0.300443735679915	0.412640797940872	1
CD8	0.295611972462112	0.420196103327496	1
Sphingomyelin	0.295218182115252	0.4208154257435	1
RiboPhosphoprotein P2	0.292637986187043	0.424886598366415	1
GP2	0.290680490417824	0.427990540831732	1
CENPA	0.288824354836384	0.430945919586885	1
Ro SSA 52Kda	0.288146887273329	0.432027540841866	1
GDF15	0.282539097483932	0.441040956783031	1
TWEAK	0.281829000892906	0.442189936493795	1
Collagen VI	0.280290363920427	0.444685415109329	1
GMCSF	0.280054539531042	0.445068602126407	1
HistoneH2A	0.279006454920391	0.446773893842552	1
AQP4	0.275012451498868	0.45330634348242	1
IFNL2	0.274653982267105	0.453895268688611	1

Hemocyanin	0.273415816208498	0.455932755400041	1
Alpha Fodrin	0.270346665512599	0.461005378521692	1
Ribo Phosphoprotein P1	0.267120792605105	0.466370875001051	1
Vimentin	0.265701497468928	0.468742485818543	1
Myosin	0.262046140789539	0.474881137029856	1
PMScl75	0.25530107370595	0.486323515014055	1
PMScl 100	0.252244706534094	0.491557039734592	1
Mitochondrial antigen	0.248284835230066	0.498382396926804	1
Myelin basic protein MBP	0.24717425729227	0.500305637570603	1
Factor P	0.246879732112023	0.500816340716584	1
LaSSB	0.244116026075469	0.505622009619366	1
MDA5	0.243346928882888	0.506963660659362	1
SmD	0.240620218014074	0.51173530650615	1
KU P70 P80	0.237904274878482	0.51651131522882	1
dsDNA	0.237104903893435	0.517921405384366	1
BPI	0.23698334790342	0.518136004466108	1
IL12	0.230487229124968	0.529671019597789	1
Nucleolin	0.228395332555512	0.533413158767825	1
Alpha actinine	-0.228086082937075	0.533967499497989	1
Ro SSA 60Kda	0.227464895469524	0.535081878565821	1

M2	0.225742588950722	0.53817773256396	1
Intrinsic Factor IF	0.222903043347976	0.543301386191297	1
Chondroitin Sulfate	0.22143747455385	0.545955319661612	1
ssDNA	0.219129557865832	0.550147616978899	1
HistoneH3	0.214441463371067	0.558712005161574	1
Bactin	0.21377120873581	0.559941725624534	1
GBM	0.213592016629837	0.560270712795329	1
IFNA1	0.206730977390006	0.572937184816466	1
Prothrombin protein	0.204484928156107	0.577113053954921	1
PCNA	0.204017447238729	0.577983997817583	1
Cardolipin	0.200154322793862	0.585204788886448	1
S100	0.196770290744035	0.59156432287192	1
Fibronectin	0.193502327042048	0.597735708452392	1
TTG	0.187999229467826	0.608193604057929	1
Insulin	0.160667843737276	0.661294942190085	1
LC1	0.155064030805399	0.672408123990779	1
Aggrecan	0.151327375987448	0.679858638996215	1
SP100	0.149827630662975	0.682857848907612	1
CRP	0.147277697320808	0.687968733614063	1
Myosin heavylight chain	0.146140229993426	0.690253207075279	1

Neuropilin1	0.146131604584109	0.690270541048499	1
Histone H4	0.142047323026337	0.698496595550813	1
IL15	0.126500779641839	0.730126435866895	1
Factor D	-0.117433744760554	0.748791985670797	1
PL7	0.1149907763248	0.75384693355233	1
Jo1	0.114599681948574	0.75465716646574	1
Collagen I	0.106640783010485	0.771203196161864	1
Collagen II	0.105291878137196	0.774018063308201	1
Collagen III	0.104273991635369	0.776144139882058	1
Proteoglycan	0.0921872356808964	0.801514109994882	1
Phosphatidylserine PS	0.073941959278111	0.840202255392472	1
LPS	0.0543023942113837	0.882280277693573	1
CENPB	0.0226466325966515	0.950757139321153	1
Collagen V	0.0155987565358349	0.966070714935325	1

8 List of References

1. Fernandez-Arias C, Rivera-Correa J, Gallego-Delgado J, Rudlaff R, Fernandez C, Roussel C, Götz A, Gonzalez S, Mohanty A, Mohanty S, et al. Anti-Self Phosphatidylserine Antibodies Recognize Uninfected Erythrocytes Promoting Malarial Anemia. Cell Host Microbe 2016; 19:194–203.
2. Rivera-Correa J, Conroy AL, Opoka RO, Batte A, Namazzi R, Ouma B, Bangirana P, Idro R, Schwaderer AL, John CC, et al. Autoantibody levels are associated with acute kidney injury, anemia and post-discharge morbidity and mortality in Ugandan children with severe malaria. Sci Rep 2019; 9:14940.
3. Rivera-Correa J, Guthmiller JJ, Vijay R, Fernandez-Arias C, Pardo-Ruge MA, Gonzalez S, Butler NS, Rodriguez A. *Plasmodium* DNA-mediated TLR9 activation of T-bet+ B cells contributes to autoimmune anaemia during malaria. Nat Commun 2017; 8:1282.
4. Rivera-Correa J, Mackroth MS, Jacobs T, Schulze Zur Wiesch J, Rolling T, Rodriguez A. Atypical memory B-cells are associated with *Plasmodium falciparum* anemia through anti-phosphatidylserine antibodies. Elife 2019; 8:e48309.
5. Hagadorn KA, Peterson ME, Kole H, Scott B, Skinner J, Diouf A, Takashima E, Ongoiba A, Doumbo S, Doumtabe D, et al. Autoantibodies inhibit *Plasmodium falciparum* growth and are associated with protection from clinical malaria. Immunity 2024; 57:1–11.
6. Rivera-Correa J, Rodriguez A. Autoantibodies during infectious diseases: Lessons from malaria applied to COVID-19 and other infections. Front Immunol 2022; 13:938011.
7. Dizon BLP, Pierce SK. The tangled web of autoreactive B cells in malaria immunity and autoimmune disease. Trends Parasitol 2022; 38:379–89.
8. Mourão LC, Cardoso-Oliveira GP, Braga ÉM. Autoantibodies and Malaria: Where We Stand? Insights Into Pathogenesis and Protection. Front Cell Infect Microbiol 2020; 10:262.
9. Greenwood BM, Voller A. Suppression of autoimmune disease in New Zealand mice associated with infection with malaria I. (NZB x NZW) F1 hybrid mice. Clin exp Immunol 1970; 7:793–803.

10. Greenwood BM. Autoimmune Disease and Parasitic Infections in Nigerians. The Lancet 1968; 292:380–2.
11. Essouma M, Nkeck JR, Endomba FT, Bigna JJ, Singwe-Ngandeu M, Hachulla E. Systemic lupus erythematosus in Native sub-Saharan Africans: A systematic review and meta-analysis. J Autoimmun 2020; 106:102348.
12. Essouma M, Noubiap JJ. Lupus and other autoimmune diseases: Epidemiology in the population of African ancestry and diagnostic and management challenges in Africa. Journal of Allergy and Clinical Immunology: Global 2024; 3:100288.
13. O O Adelowo MB. Systemic Autoimmune Diseases: Not So Rare in Black Africans. Rheumatology: Current Research 2014; 04:1000130.
14. Dinse GE, Parks CG, Weinberg CR, Co CA, Wilkerson J, Zeldin DC, Chan EKL, Miller FW. Increasing Prevalence of Antinuclear Antibodies in the United States. Arthritis and Rheumatology 2020; 72:1026–35.
15. Fairweather D, Root-Bernstein R. Autoimmune Disease: Mechanisms. In: Encyclopedia of Life Sciences. Wiley; 2015. page 1–7.
16. Wang L, Wang FS, Gershwin ME. Human autoimmune diseases: A comprehensive update. J Intern Med 2015; 278:369–95.
17. Ercolini AM, Miller SD. The role of infections in autoimmune disease. Clin Exp Immunol 2009; 155:1–15.
18. Kivity S, Ehrenfeld M. Can we explain the higher prevalence of autoimmune disease in women? Expert Rev Clin Immunol 2010; 6:691–4.
19. Pennell LM, Galligan CL, Fish EN. Sex affects immunity. J Autoimmun 2012; 38:J282–91.
20. Gilkeson GS, James JA, Kamen DL, Knackstedt TJ, Maggi DR, Meyer AK, Ruth NM. The United States to Africa lupus prevalence gradient revisited. Lupus 2011; 20:1095–103.
21. Lewis MJ, Jawad AS. The effect of ethnicity and genetic ancestry on the epidemiology, clinical features and outcome of systemic lupus erythematosus. Rheumatology (Oxford) 2017; 56:i67–77.
22. Bieber K, Hundt JE, Yu X, Ehlers M, Petersen F, Karsten CM, Köhl J, Kridin K, Kalies K, Kasprick A, et al. Autoimmune pre-disease. Autoimmun Rev 2023; 22:103236.
23. Hawa M, Beyan H, Leslie RDG. Principles of autoantibodies as disease-specific markers. Autoimmunity 2004; 37:253–6.

24. Ma H, Murphy C, Loscher CE, O'Kennedy R. Autoantibodies - enemies, and/or potential allies? Front Immunol 2022; 13:953726.
25. Hayter SM, Cook MC. Updated assessment of the prevalence, spectrum and case definition of autoimmune disease. Autoimmun Rev 2012; 11:754–65.
26. Koppala SN, Guruprasad V. Overview of Autoimmunity: Classification, Disease Mechanisms, and Etiology. Turkish Journal of Immunology 2023; 11:93–105.
27. Lesage S, Goodnow CC. Organ-specific autoimmune disease: a deficiency of tolerogenic stimulation. J Exp Med 2001; 194:31–6.
28. Shi G, Zhang J, Zhang Z, Zhang X. Systemic autoimmune diseases. Clin Dev Immunol 2013; 2013:728574.
29. Rosenblum MD, Remedios KA, Abbas AK. Mechanisms of human autoimmunity. Journal of Clinical Investigation 2015; 125:2228–33.
30. Bruserud Ø, Oftedal BE, Wolff AB, Husebye ES. AIRE-mutations and autoimmune disease. Curr Opin Immunol 2016; 43:8–15.
31. Serafini B, Rosicarelli B, Franciotta D, Magliozzi R, Reynolds R, Cinque P, Andreoni L, Trivedi P, Salvetti M, Faggioni A, et al. Dysregulated Epstein-Barr virus infection in the multiple sclerosis brain. Journal of Experimental Medicine 2007; 204:2899–912.
32. Li SJ, Wu YL, Chen JH, Shen SY, Duan J, Xu HE. Autoimmune diseases: targets, biology, and drug discovery. Acta Pharmacol Sin 2024; 45:674–85.
33. Rosenblum MD, Gratz IK, Paw JS, Lee K, Marshak-Rothstein A, Abbas AK. Response to self antigen imprints regulatory memory in tissues. Nature 2011; 480:538–42.
34. Zhang X, Olsen N, Zheng SG. The progress and prospect of regulatory T cells in autoimmune diseases. J Autoimmun 2020; 111:102461.
35. Theofilopoulos AN, Kono DH, Baccala R. The multiple pathways to autoimmunity. Nat Immunol 2017; 18:716–24.
36. Meng X, Layhadi JA, Keane ST, Cartwright NJK, Durham SR, Shamji MH. Immunological mechanisms of tolerance: Central, peripheral and the role of T and B cells. Asia Pac Allergy 2023; 13:175–86.
37. Hozumi N, Tonegawa S. Evidence for somatic rearrangement of immunoglobulin genes coding for variable and constant regions (K-chain mRNA/restriction enzymes/RNA*DNA hybridization). Genetics 1976; 73:3628–32.

38. Hogquist KA, Baldwin TA, Jameson SC. Central tolerance: Learning self-control in the thymus. Nat Rev Immunol 2005; 5:772–82.
39. Kisielow P. How does the immune system learn to distinguish between good and evil? The first definitive studies of T cell central tolerance and positive selection. Immunogenetics 2019; 71:513–8.
40. Schwartz RH. Historical overview of immunological tolerance. Cold Spring Harb Perspect Biol 2012; 4:a006908.
41. Szondy Z, Garabuczi É, Tóth K, Kiss B, Köröskényi K. Thymocyte death by neglect: Contribution of engulfing macrophages. Eur J Immunol 2012; 42:1662–7.
42. Xing Y, Hogquist KA. T-Cell tolerance: Central and peripheral. Cold Spring Harb Perspect Biol 2012; 4:1–15.
43. Carlow DA, Teh SJ, Van Oers NSC, Miller RG, Teh H-S. Peripheral tolerance through clonal deletion of mature CD4CD8+ T cells. Int Immunol 1992; 4:599–610.
44. Kaye Jonathan, Mei-Ling Hsu, Marie-Elizabeth Sauron, Stephen C. Jameson*, Nicholas R. J. Gascoigne*, & Stephen M. Hedrick. Selective development of CD4 + T cells in transgenic mice expressing a class II MHC- restricted antigen receptor. Letters To Nature 1989; 341:746–9.
45. Van Meerwijk JPM, Germain RN. The different roles of MHC class recognition in thymocyte CD4 versus CD8 lineage commitment and positive selection. Semin Immunol 1994; 6:231–9.
46. Korb LC, Mirshahidi S, Ramyar K, Sadighi Akha AA, Sadegh-Nasseri S. Induction of T Cell Anergy by Low Numbers of Agonist Ligands. The Journal of Immunology 1999; 162:6401–9.
47. Takahashi T, Kuniyasu Y, Toda M, Sakaguchi N, Itoh M, Iwata M, Shimizu J, Sakaguchi S. Immunologic self-tolerance maintained by CD25 CD4 naturally anergic and suppressive T cells: induction of autoimmune disease by breaking their anergic/suppressive state. Int Immunol 1998; 10:1969–80.
48. Nelson RW, Beisang D, Tubo NJ, Dileepan T, Wiesner DL, Nielsen K, Wüthrich M, Klein BS, Kotov DI, Spanier JA, et al. T Cell Receptor Cross-Reactivity between Similar Foreign and Self Peptides Influences Naive Cell Population Size and Autoimmunity. Immunity 2015; 42:95–107.

49. Lee DSW, Rojas OL, Gommerman JL. B cell depletion therapies in autoimmune disease: advances and mechanistic insights. Nat Rev Drug Discov2021; 20:179–99.
50. Nemazee D. Mechanisms of central tolerance for B cells. Nat Rev Immunol 2017; 17:281–94.
51. Nemazee D, Buerkit K. Clonal deletion of autoreactive B lymphocytes in bone marrow chimeras (immunological tolerance/transgenic mice/histocompatibility complex). Proc Nati Acad Sci USA 1989; 86:8039–43.
52. Cambier JC, Gauld SB, Merrell KT, Vilen BJ. B-cell anergy: From transgenic models to naturally occurring anergic B cells? Nat Rev Immunol 2007; 7:633–43.
53. Halverson R, Torres RM, Pelanda R. Receptor editing is the main mechanism of B cell tolerance toward membrane antigens. Nat Immunol 2004; 5:645–50.
54. Dai YC, Zhong J, Xu JF. Regulatory B cells in infectious disease (Review). Mol Med Rep 2017; 16:3–10.
55. Sakkas LI, Daoussis D, Mavropoulos A, Liossis SN, Bogdanos DP. Regulatory B cells: New players in inflammatory and autoimmune rheumatic diseases. Semin Arthritis Rheum 2019; 48:1133–41.
56. Prüßmann J, Prüßmann W, Recke A, Rentzsch K, Juhl D, Henschler R, Müller S, Lamprecht P, Schmidt E, Csernok E, et al. Co-occurrence of autoantibodies in healthy blood donors. Exp Dermatol 2014; 23:519–21.
57. Shome M, Chung Y, Chavan R, Park JG, Qiu J, LaBaer J. Serum autoantibodyome reveals that healthy individuals share common autoantibodies. Cell Rep 2022; 39:110873.
58. Teubner A, Tillmann HL, Schuppan D, Gericke G, Manns MP, Stölzel U. Prävalenz von zirkulierenden autoantikörpern bei gesunden individuen. Med Klin 2002; 97:645–9.
59. Lacroix-Desmazes S, Kaveri S V, Mouthon L, Ayouba A, Malanchere E, Coutinho A, Kazatchkinè MD. Self-reactive antibodies natural autoantibodies in healthy individuals. 1998.
60. Arbuckle MR, Mcclain MT, Rubertone M V, Scofield RH, Dennis GJ, James JA, Harley JB. Development of Autoantibodies before the Clinical Onset of Systemic Lupus Erythematosus. N Engl J Med 2003; 349:16.

61. Elkon K, Casali P. Nature and functions of autoantibodies. Nat Clin Pract Rheumatol 2008; 4:491–8.
62. Karrar S, Cunninghame Graham DS. Abnormal B Cell Development in Systemic Lupus Erythematosus: What the Genetics Tell Us. Arthritis and Rheumatology 2018; 70:496–507.
63. Ludwig RJ, Vanhoorelbeke K, Leypoldt F, Kaya Z, Bieber K, McLachlan SM, Komorowski L, Luo J, Cabral-Marques O, Hammers CM, et al. Mechanisms of autoantibody-induced pathology. Front Immunol 2017; 8:603.
64. Kohda T, Okada SI, Hayashi A, Kanzaki S, Ninomiya Y, Taki M, Sado Y. High nephritogenicity of monoclonal antibodies belonging to IgG2a and IgG2b subclasses in rat anti-GBM nephritis. Kidney Int 2004; 66:177–86.
65. Burbelo PD, Iadarola MJ, Keller JM, Warner BM. Autoantibodies Targeting Intracellular and Extracellular Proteins in Autoimmunity. Front Immunol 2021; 12:548469.
66. Rowley MJ, Whittingham SF. The role of pathogenic autoantibodies in autoimmunity. Antibodies 2015; 4:314–53.
67. Rademacher TW, Williams P, Dwekt RA. Agalactosyl glycoforms of IgG autoantibodies are pathogenic Since the Fc portion ofeach IgG molecule contains two paired carbohydrate chains, various heterologous combinations of. Immunology 1994; 91:6123–7.
68. Guo Q, Wang Y, Xu D, Nossent J, Pavlos NJ, Xu J. Rheumatoid arthritis: Pathological mechanisms and modern pharmacologic therapies. Bone Res 2018; 6:15.
69. D. Giannini1, M. Antonucci2, F. Petrelli1, S. Bilia1, A. Alunno2, I. Puxeddu1. One year in review 2020: pathogenesis of rheumatoid arthritis. Clin Exp Rheumatol 2020; 2020; 38:387–97.
70. Smolen JS, Aletaha D, Barton A, Burmester GR, Emery P, Firestein GS, Kavanaugh A, McInnes IB, Solomon DH, Strand V, et al. Rheumatoid arthritis. Nat Rev Dis Primers 2018; 4:18001.
71. Yarwood A, Huizinga TWJ, Worthington J. The genetics of rheumatoid arthritis: Risk and protection in different stages of the evolution of RA. Rheumatology (Oxford) 2015; 55:199–209.
72. Klareskog L, Rönnelid J, Saevarsdottir S, Padyukov L, Alfredsson L. The importance of differences; On environment and its interactions with genes

and immunity in the causation of rheumatoid arthritis. J Intern Med 2020; 287:514–33.

73. Catrina AI, Joshua V, Klareskog L, Malmström V. Mechanisms involved in triggering rheumatoid arthritis. Immunol Rev 2016; 269:162–74.
74. Chang KH, Hsu CC, Muo CH, Hsu CY, Liu HC, Kao CH, Chen CY, Chang MY, Hsu YC. Air pollution exposure increases the risk of rheumatoid arthritis: A longitudinal and nationwide study. Environ Int 2016; 94:495–9.
75. Safiri S, Kolahi AA, Hoy D, Smith E, Bettampadi D, Mansournia MA, Almasi-Hashiani A, Ashrafi-Asgarabad A, Moradi-Lakeh M, Qorbani M, et al. Global, regional and national burden of rheumatoid arthritis 1990-2017: a systematic analysis of the Global Burden of Disease study 2017. Ann Rheum Dis 2019; 78:1463–71.
76. Nilsson J, Andersson MLE, Hafström I, Svensson B, Forslind K, Ajeganova S, Agelii ML, Gjertsson I. Influence of age and sex on disease course and treatment in rheumatoid arthritis. Open Access Rheumatology 2021; 13:123–38.
77. Malmström V, Catrina AI, Klareskog L. The immunopathogenesis of seropositive rheumatoid arthritis: From triggering to targeting. Nat Rev Immunol 2017; 17:60–75.
78. Ishikawa Y, Terao C. The impact of cigarette smoking on risk of rheumatoid arthritis: A narrative review. Cells 2020; 9:475.
79. Van Der Helm-Van Mil AHM, Verpoort KN, Cessie S Le, Huizinga TWJ, De Vries RRP, Toes REM. The HLA-DRB1 shared epitope alleles differ in the interaction with smoking and predisposition to antibodies to cyclic citrullinated peptide. Arthritis Rheum 2007; 56:425–32.
80. Wouters F, Maurits MP, Van Boheemen L, Verstappen M, Mankia K, Matthijssen XME, Dorjée AL, Emery P, Knevel R, Van Schaardenburg Di, et al. Determining in which pre-arthritis stage HLA-shared epitope alleles and smoking exert their effect on the development of rheumatoid arthritis. Ann Rheum Dis 2022; 81:48–55.
81. Darrah E, Andrade F. Rheumatoid arthritis and citrullination. Curr Opin Rheumatol 2018; 30:72–8.
82. Liu J, Gao J, Wu Z, Mi L, Li N, Wang Y, Peng X, Xu K, Wu F, Zhang L. Anti-citrullinated Protein Antibody Generation, Pathogenesis, Clinical Application, and Prospects. Front Med (Lausanne)2022; 8.

83. Maresz KJ, Hellvard A, Sroka A, Adamowicz K, Bielecka E, Koziel J, Gawron K, Mizgalska D, Marcinska KA, Benedyk M, et al. *Porphyromonas gingivalis* Facilitates the Development and Progression of Destructive Arthritis through Its Unique Bacterial Peptidylarginine Deiminase (PAD). PLoS Pathog 2013; 9:e1003627.
84. Sakkas LI, Daoussis D, Liossis SN, Bogdanos DP. The infectious basis of ACPA-positive rheumatoid arthritis. Front Microbiol2017; 8.
85. Cheng WC, van Asten SD, Burns LA, Evans HG, Walter GJ, Hashim A, Hughes FJ, Taams LS. Periodontitis-associated pathogens *P. gingivalis* and *A. actinomycetemcomitans* activate human CD14+ monocytes leading to enhanced Th17/IL-17 responses. Eur J Immunol 2016; 46:2211–21.
86. Moutsopoulos NM, Kling HM, Angelov N, Jin W, Palmer RJ, Nares S, Osorio M, Wahl SM. *Porphyromonas gingivalis* promotes Th17 inducing pathways in chronic periodontitis. J Autoimmun 2012; 39:294–303.
87. Zhou N, Zou F, Cheng X, Huang Y, Zou H, Niu Q, Qiu Y, Shan F, Luo A, Teng W, et al. *Porphyromonas gingivalis* induces periodontitis, causes immune imbalance, and promotes rheumatoid arthritis. J Leukoc Biol 2021; 110:461–73.
88. Konig MF, Abusleme L, Reinholdt J, Palmer RJ, Teles RP, Sampson K, Rosen A, Nigrovic PA, Sokolove J, Giles JT, et al. Aggregatibacter actinomycetemcomitans-induced hypercitrullination links periodontal infection to autoimmunity in rheumatoid arthritis. Sci Transl Med 2016; 8:369ra176.
89. Elkayam O, Segal R, Lidgi M, Caspi D. Positive anti-cyclic citrullinated proteins and rheumatoid factor during active lung *tuberculosis*. Ann Rheum Dis 2006; 65:1110–2.
90. Elkayam O, Segal R, Bendayan D, van Uitert R, Onnekink C, Pruijn GJM. The anti-cyclic citrullinated peptide response in *tuberculosis* patients is not citrulline-dependent and sensitive to treatment. Arthritis Res Ther 2010; 12:R12.
91. Alpizar-Rodriguez D, Brulhart L, Mueller RB, Möller B, Dudler J, Ciurea A, Walker UA, Von Mühlenen I, Kyburz D, Zufferey P, et al. The prevalence of anticitrullinated protein antibodies increases with age in healthy individuals at risk for rheumatoid arthritis. Clin Rheumatol 2017; 36:677–82.

92. Titcombe PJ, Wigerblad G, Sippl N, Zhang N, Shmagel AK, Sahlström P, Zhang Y, Barsness LO, Ghodke-Puranik Y, Baharpoor A, et al. Pathogenic Citrulline-Multispecific B Cell Receptor Clades in Rheumatoid Arthritis. Arthritis and Rheumatology 2018; 70:1933–45.
93. Uysal H, Bockermann R, Nandakumar KS, Sehnert B, Bajtner E, Engström Å, Serre G, Burkhardt H, Thunnissen MMGM, Holmdahl R. Structure and pathogenicity of antibodies specific for citrullinated collagen type II in experimental arthritis. Journal of Experimental Medicine 2009; 206:449–62.
94. Song YW, Kang EH. Autoantibodies in rheumatoid arthritis: Rheumatoid factors and anticitrullinated protein antibodies. QJM: An International Journal of Medicine 2009; 103:139–46.
95. Demoruelle MK, Deane K. Antibodies to citrullinated protein antigens (ACPAs): Clinical and pathophysiologic significance. Curr Rheumatol Rep 2011; 13:421–30.
96. Alivernini S, Tolusso B, Petricca L, Bui L, Di Sante G, Peluso G, Benvenuto R, Fedele AL, Federico F, Ferraccioli G, et al. Synovial features of patients with rheumatoid arthritis and psoriatic arthritis in clinical and ultrasound remission differ under anti-TNF therapy: A clue to interpret different chances of relapse after clinical remission? Ann Rheum Dis 2017; 76:1228–12396.
97. Hafkenscheid L, Bondt A, Scherer HU, Huizinga TWJ, Wuhrer M, Toes REM, Rombouts Y. Structural analysis of variable domain glycosylation of anti-citrullinated protein antibodies in rheumatoid arthritis reveals the presence of highly sialylated glycans. Molecular and Cellular Proteomics 2017; 16:278–87.
98. Rombouts Y, Willemze A, Van Beers JJBC, Shi J, Kerkman PF, Van Toorn L, Janssen GMC, Zaldumbide A, Hoeben RC, Pruijn GJM, et al. Extensive glycosylation of ACPA-IgG variable domains modulates binding to citrullinated antigens in rheumatoid arthritis. Ann Rheum Dis 2016; 75:578–85.
99. Schellekens GA, Visser H, De Jong BAW, Van Den Hoogen FHJ, Hazes JMW, Breedveld FC, Van Venrooij WJ. The diagnostic properties of rheumatoid arthritis antibodies recognizing a cyclic citrullinated peptide. Arthritis Rheum 2000; 43:155–63.

100. Van Gaalen FA, Visser H, Huizinga TWJ. A comparison of the diagnostic accuracy and prognostic value of the first and second anti-cyclic citrullinated peptides (CCP1 and CCP2) autoantibody tests for rheumatoid arthritis. Ann Rheum Dis 2005; 64:1510–2.
101. Nelson HA, Banerjee D, Novis CL, Deane KD, Feser ML, Nandakumar V. A comparison of anti-cyclic citrullinated peptides (CCP3 and CCP3.1) autoantibody tests in rheumatoid arthritis. Pract Lab Med 2024; 41.
102. Kurowska W, Slowinska I, Krogulec Z, Syrowka P, Maslinski W. Antibodies to citrullinated proteins (Acpa) associate with markers of osteoclast activation and bone destruction in the bone marrow of patients with rheumatoid arthritis. J Clin Med 2021; 10:1778.
103. Kurowska W, Kuca-Warnawin EH, Radzikowska A, Maslinski W. The role of anti-citrullinated protein antibodies (ACPA) in the pathogenesis of rheumatoid arthritis. Central European Journal of Immunology 2017; 42:390–8.
104. Aggarwal R, Liao K, Nair R, Ringold S, Costenbader KH. Anti-citrullinated peptide antibody assays and their role in the diagnosis of rheumatoid arthritis. Arthritis Care Res (Hoboken) 2009; 61:1472–83.
105. Kronzer VL, Hayashi K, Yoshida K, Davis JM, McDermott GC, Huang W, Dellaripa PF, Cui J, Feathers V, Gill RR, et al. Autoantibodies against citrullinated and native proteins and prediction of rheumatoid arthritis-associated interstitial lung disease: a nested case–control study. Lancet Rheumatol 2023; 5:e77–87.
106. Crispín JC, Liossis SNC, Kis-Toth K, Lieberman LA, Kyttaris VC, Juang YT, Tsokos GC. Pathogenesis of human systemic lupus erythematosus: recent advances. Trends Mol Med 2010; 16:47–57.
107. Feldman CH, Hiraki LT, Liu J, Fischer MA, Solomon DH, Alarcõn GS, Winkelmayer WC, Costenbader KH. Epidemiology and sociodemographics of systemic lupus erythematosus and lupus nephritis among US adults with Medicaid coverage, 2000-2004. Arthritis Rheum 2013; 65:753–63.
108. Gõmez-Puerta JA, Barbhaiya M, Guan H, Feldman CH, Alarcõn GS, Costenbader KH. Racial/ethnic variation in all-cause mortality among United States medicaid recipients with systemic lupus erythematosus: A Hispanic and asian paradox. Arthritis and Rheumatology 2015; 67:752–60.

109. Marion TN, Postlethwaite AE. Chance, genetics, and the heterogeneity of disease and pathogenesis in systemic lupus erythematosus. Semin Immunopathol 2014; 36:495–517.
110. Crispín JC, Kyttaris VC, Juang YT, Tsokos GC. How signaling and gene transcription aberrations dictate the systemic lupus erythematosus T cell phenotype. Trends Immunol 2008; 29:110–5.
111. Refai RH, Hussein MF, Abdou MH, Abou-Raya AN. Environmental risk factors of systemic lupus erythematosus: a case–control study. Sci Rep 2023; 13:10219.
112. Yaniv G, Twig G, Shor DBA, Furer A, Sherer Y, Mozes O, Komisar O, Slonimsky E, Klang E, Lotan E, et al. A volcanic explosion of autoantibodies in systemic lupus erythematosus: A diversity of 180 different antibodies found in SLE patients. Autoimmun Rev 2015; 14:75–9.
113. Hoi A. Pathogenesis of Systemic Lupus Erythematosus Insights from translational research. Springer; 2021.
114. Hoi A, Igel T, Mok CC, Arnaud L. Systemic lupus erythematosus. The Lancet 2024; 403:2326–38.
115. Armstrong DL, Zidovetzki R, Alarcón-Riquelme ME, Tsao BP, Criswell LA, Kimberly RP, Harley JB, Sivils KL, Vyse TJ, Gaffney PM, et al. GWAS identifies novel SLE susceptibility genes and explains the association of the HLA region. Genes Immun 2014; 15:347–54.
116. Hagberg N, Joelsson M, Leonard D, Reid S, Eloranta ML, Mo J, Nilsson MK, Syvänen AC, Bryceson YT, Rönnblom L. The STAT4 SLE risk allele rs7574865[T] is associated with increased IL-12-induced IFN-γ production in t cells from patients with SLE. Ann Rheum Dis 2018; 77:1070–7.
117. Blazer A, Dey ID, Nwaukoni J, Reynolds M, Ankrah F, Algasas H, Ahmed T, Divers J. Apolipoprotein L1 risk genotypes in Ghanaian patients with systemic lupus erythematosus: A prospective cohort study. Lupus Sci Med 2021; 8:e000460.
118. Crow MK. Pathogenesis of systemic lupus erythematosus: Risks, mechanisms and therapeutic targets. Ann Rheum Dis 2023; 82:999–1014.
119. Iftimie G, Stoian AP, Socea B, Motofei I, Marcu D, Costache RS, Diaconu C. Complications of systemic lupus erythematosus: A review. Journal of Military Medicine 2018; 121:9–15.

120. Rosen A, Casciola-Rosen L, Ahearn J. Novel packages of viral and self-antigens are generated during apoptosis. Journal of Experimental Medicine 1995; 181:1557–61.
121. Rosen A, Casciola-Rosen L. Autoantigens as substrates for apoptotic proteases: Implications for the pathogenesis of systemic autoimmune disease. Cell Death Differ1999; 6:6–12.
122. Fransen JH, Hilbrands LB, Ruben J, Stoffels M, Adema GJ, Van Der Vlag J, Berden JH. Mouse dendritic cells matured by ingestion of apoptotic blebs induce T cells to produce interleukin-17. Arthritis Rheum 2009; 60:2304–13.
123. Levine JS, Koh JS, Subang R, Rauch J. Apoptotic Cells as Immunogen and Antigen in the Antiphospholipid Syndrome. Exp Mol Pathol 1999; 66:82–98.
124. Yung S, Chan TM. Mechanisms of kidney injury in lupus nephritis - the role of anti-dsDNA antibodies. Front Immunol 2015; 6:475.
125. Dowman B, Campbell RM, Zgaga L, Adeloye D, Chan KY. Estimating the burden of rheumatoid arthritis in Africa: A systematic analysis. J Glob Health 2012; 2:020406.
126. Usenbo A, Kramer V, Young T, Musekiwa A. Prevalence of arthritis in Africa: A systematic review and meta-analysis. PLoS One 2015; 10:e0133858.
127. Alamanos Y, Voulgari P V., Drosos AA. Incidence and Prevalence of Rheumatoid Arthritis, Based on the 1987 American College of Rheumatology Criteria: A Systematic Review. Semin Arthritis Rheum 2006; 36:182–8.
128. Almoallim H, Al Saleh J, Badsha H, Ahmed HM, Habjoka S, Menassa JA, El-Garf A. A Review of the Prevalence and Unmet Needs in the Management of Rheumatoid Arthritis in Africa and the Middle East. Rheumatol Ther 2021; 8:1–16.
129. Vento S, Cainelli F. Commentary: Systemic Lupus Erythematosus in Native sub-Saharan Africans: A Systematic Review and Meta-Analysis. Front Med (Lausanne) 2020; 106:102348.
130. Kwiatkowski DP. How Malaria Has Affected the Human Genome and What Human Genetics Can Teach Us about Malaria. Am J Hum Genet 2005; 77:171–92.
131. Piccin A, O'Connor-Byrne N, Daves M, Lynch K, Farshbaf AD, Martin-Loeches I. Autoimmune disease and sickle cell anaemia: 'Intersecting pathways and differential diagnosis.' Br J Haematol 2022; 197:518–28.

132. Duarte J, Herbert F, Guiyedi V, Franetich JF, Roland J, Cazenave PA, Mazier D, Kombila M, Fesel C, Pied S. High levels of immunoglobulin e autoantibody to 14-3-3 protein correlate with protection against severe *plasmodium falciparum* malaria. Journal of Infectious Diseases 2012; 206:1781–9.
133. Guiyedi V, Chanseaud Y, Fesel C, Snounou G, Rousselle J-C, Lim P, Koko J, Namane A, Cazenave P-A, Kombila M, et al. Self-Reactivities to the Non-Erythroid Alpha Spectrin Correlate with Cerebral Malaria in Gabonese Children. PLoS One 2007; 2:e389.
134. Shamriz O, Shoenfeld Y. Infections: A double-edge sword in autoimmunity. Curr Opin Rheumatol 2018; 30:365–72.
135. Christen U, von Herrath MG. Infections and Autoimmunity—Good or Bad? The Journal of Immunology 2005; 174:7481–6.
136. Kivity S, Agmon-Levin N, Blank M, Shoenfeld Y. Infections and autoimmunity - friends or foes? Trends Immunol 2009; 30:409–14.
137. Sundaresan B, Shirafkan F, Ripperger K, Rattay K. The Role of Viral Infections in the Onset of Autoimmune Diseases. Viruses2023; 15:782.
138. Johnson D, Jiang W. Infectious diseases, autoantibodies, and autoimmunity. J Autoimmun 2023; 137:102962.
139. Delogu LG, Deidda S, Delitala G, Manetti R. Infectious diseases and autoimmunity. The Journal of Infection in Developing Countries 2011; 5:679–87.
140. Kerr JR. The role of parvovirus B19 in the pathogenesis of autoimmunity and autoimmune disease. J Clin Pathol 2016; 69:279–91.
141. Lossius A, Johansen JN, Torkildsen Ø, Vartdal F, Holmoy T. Epstein-barr virus in systemic lupus erythematosus, rheumatoid arthritis and multiple sclerosis-association and causation. Viruses 2012; 4:3701–30.
142. Health Organization W. World malaria report 2023 -- spread view. 2023.
143. Cibulskis RE, Alonso P, Aponte J, Aregawi M, Barrette A, Bergeron L, Fergus CA, Knox T, Lynch M, Patouillard E, et al. Malaria: Global progress 2000 - 2015 and future challenges. Infect Dis Poverty 2016; 5:61.
144. Noor AM, Alonso PL. The message on malaria is clear: progress has stalled. The Lancet 2022; 399:1777.
145. Rosenthal PJ, Asua V, Bailey JA, Conrad MD, Ishengoma DS, Kamya MR, Rasmussen C, Tadesse FG, Uwimana A, Fidock DA. The emergence of

artemisinin partial resistance in Africa: how do we respond? Lancet Infect Dis 2024; 24:e591--e600.

146. Bejon P, Lusingu J, Olotu A, Leach A, Lievens M, Vekemans J, Mshamu S, Lang T, Gould J, Dubois M-C, et al. Efficacy of RTS,S/AS01E Vaccine against Malaria in Children 5 to 17 Months of Age. New England Journal of Medicine 2008; 359:2521–32.
147. Kantele A, Jokiranta TS. Review of cases with the emerging fifth human malaria parasite, *Plasmodium knowlesi*. Clinical Infectious Diseases 2011; 52:1356–62.
148. Loy DE, Liu W, Li Y, Learn GH, Plenderleith LJ, Sundararaman SA, Sharp PM, Hahn BH. Out of Africa: origins and evolution of the human malaria parasites *Plasmodium falciparum* and *Plasmodium vivax*. Int J Parasitol 2017; 47:87–97.
149. Larson B. Origin of Two Most Virulent Agents of Human Malaria: *Plasmodium falciparum* and *Plasmodium vivax*. IntechOpen; 2019.
150. Hay SI, Guerra CA, Tatem AJ, Noor AM, Snow RW. For personal use. Only reproduce with permission from The Lancet. The global distribution and population at risk of malaria: past, present, and future. LANCET Infectious Diseases 2004; 4:p327-336.
151. Piperaki ET, Daikos GL. Malaria in Europe: emerging threat or minor nuisance? Clinical Microbiology and Infection2016; 22:487–93.
152. Perkins SL. Malaria's many mates: Past, present, and future of the systematics of the order haemosporida. Journal of Parasitology 2014; 100:11–25.
153. de Korne CM, Winkel BMF, van Oosterom MN, Chevalley-Maurel S, Houwing HM, Sijtsma JC, Azargoshasb S, Baalbergen E, Franke-Fayard BMD, van Leeuwen FWB, et al. Clustering and Erratic Movement Patterns of Syringe-Injected versus Mosquito-Inoculated Malaria Sporozoites Underlie Decreased Infectivity. mSphere 2021; 6:e0021821.
154. Frischknecht F, Baldacci P, Martin B, Zimmer C, Thiberge S, Olivo-Marin JC, Shorte SL, Ménard R. Imaging movement of malaria parasites during transmission by Anopheles mosquitoes. Cell Microbiol 2004; 6:687–94.
155. Tavares J, Formaglio P, Thiberge S, Mordelet E, Van Rooijen N, Medvinsky A, Ménard R, Amino R. Role of host cell traversal by the malaria sporozoite during liver infection. Journal of Experimental Medicine 2013; 210:905–15.

156. Amino R, Thiberge S, Martin B, Celli S, Shorte S, Frischknecht F, Ménard R. Quantitative imaging of *Plasmodium* transmission from mosquito to mammal. Nat Med 2006; 12:220–4.
157. Farrant M, Roth A, Rothman J, Silver A, Wang S, Williams S, Mota MM, Pradel G, Vanderberg JP, R Hafalla JC, et al. Migration of *Plasmodium* Sporozoites Through Cells Before Infection. Trends Neurosci 1984; 291:141–4.
158. Frevert U, Engelmann S, Zougbédé S, Stange J, Ng B, Matuschewski K, Liebes L, Yee H. Intravital observation of *Plasmodium berghei* sporozoite infection of the liver. PLoS Biol 2005; 3:1034–46.
159. Graewe S, Rankin KE, Lehmann C, Deschermeier C, Hecht L, Froehlke U, Stanway RR, Heussler V. Hostile takeover by *Plasmodium:* Reorganization of parasite and host cell membranes during liver stage egress. PLoS Pathog 2011; 7:e1002224.
160. Weiss GE, Gilson PR, Taechalertpaisarn T, Tham WH, de Jong NWM, Harvey KL, Fowkes FJI, Barlow PN, Rayner JC, Wright GJ, et al. Revealing the Sequence and Resulting Cellular Morphology of Receptor-Ligand Interactions during *Plasmodium falciparum* Invasion of Erythrocytes. PLoS Pathog 2015; 11:e1004670.
161. Gerald N, Mahajan B, Kumar S. Mitosis in the human malaria parasite *Plasmodium falciparum*. Eukaryot Cell 2011; 10:474–82.
162. Baker DA. Malaria gametocytogenesis. Mol Biochem Parasitol 2010; 172:57–65.
163. Wang CYT, McCarthy JS, Stone WJ, Bousema T, Collins KA, Bialasiewicz S. Assessing *Plasmodium falciparum* transmission in mosquito-feeding assays using quantitative PCR. Malar J 2018; 17:249–56.
164. Kojin BB, Adelman ZN. The sporozoite's journey through the mosquito: A critical examination of host and parasite factors required for salivary gland invasion. Front Ecol Evol 2019; 7:284.
165. Simonetti AB. The Biology of Malarial Parasite in the Mosquito-A Review. Mem Inst Oswaldo Cruz, Rio de Janeiro 1996; 91:519–41.
166. Frischknecht F, Matuschewski K. *Plasmodium s*porozoite biology. Cold Spring Harb Perspect Med 2017; 7:a025478.
167. Song X, Wei W, Cheng W, Zhu H, Wang W, Dong H, Li J. Cerebral malaria induced by *Plasmodium falciparum*: clinical features, pathogenesis, diagnosis, and treatment. Front Cell Infect Microbiol 2022; 12:939532.

168. Bartoloni A, Zammarchi L. Clinical Aspects of Uncomplicated and Severe Malaria. Mediterr J Hematol Infect Dis 2012; 4:e2012026.
169. Arévalo-Herrera M, Lopez-Perez M, Medina L, Moreno A, Gutierrez JB, Herrera S. Clinical profile of *Plasmodium falciparum* and *Plasmodium vivax* infections in low and unstable malaria transmission settings of Colombia. Malar J 2015; 14.
170. Laishram DD, Sutton PL, Nanda N, Sharma VL, Sobti RC, Carlton JM, Joshi H. The complexities of malaria disease manifestations with a focus on asymptomatic malaria. Malar J2012; 11:29.
171. Recker M, Bull PC, Buckee CO. Recent advances in the molecular epidemiology of clinical malaria. F1000Res 2018; 7:14991.1.
172. Chandley P, Ranjan R, Kumar S, Rohatgi S. Host-parasite interactions during *Plasmodium* infection: Implications for immunotherapies. Front Immunol 2023; 13:1091961.
173. Tijani MK, Lugaajju A, Persson KEM. Naturally acquired antibodies against *Plasmodium falciparum*: Friend or foe? Pathogens 2021; 10:832.
174. S Cohen, McGregor IA, Carrington S. amma-globulin and acquired immunity to human malaria. Rev Franc et Olin Biol 1960; 260:1800.
175. Rochford R, Kazura J. Introduction: Immunity to malaria. Immunol Rev2020; 293:5–7.
176. Doolan DL, Dobaño C, Baird JK. Acquired immunity to Malaria. Clin Microbiol Rev2009; 22:13–36.
177. Langhorne J, Ndungu FM, Sponaas AM, Marsh K. Immunity to malaria: More questions than answers. Nat Immunol2008; 9:725–32.
178. Gupta S, Snow RW, Donnelly C, Newbold C. Acquired immunity and postnatal clinical protection in childhood cerebral malaria. The Royal Society 1999; 266:33–8.
179. Shelton JMG, Corran P, Risley P, Silva N, Hubbart C, Jeffreys A, Rowlands K, Craik R, Cornelius V, Hensmann M, et al. Genetic determinants of anti-malarial acquired immunity in a large multi-centre study. Malar J 2015; 14:333.
180. Beeson JG, Drew DR, Boyle MJ, Feng G, Fowkes FJI, Richards JS. Merozoite surface proteins in red blood cell invasion, immunity and vaccines against malaria. FEMS Microbiol Rev2016; 40:343–72.

181. Guevara Patiño JA, Holder AA, McBride JS, Blackman MJ. Antibodies that inhibit malaria merozoite surface protein-1 processing and erythrocyte invasion are blocked by naturally acquired human antibodies. Journal of Experimental Medicine 1997; 186:1689–99.
182. Aitken EH, Mahanty S, Rogerson SJ. Antibody effector functions in malaria and other parasitic diseases: a few needles and many haystacks. Immunol Cell Biol2020; 98:264–75.
183. Osier FHA, Feng G, Boyle MJ, Langer C, Zhou J, Richards JS, McCallum FJ, Reiling L, Jaworowski A, Anders RF, et al. Opsonic phagocytosis of *Plasmodium falciparum* merozoites: Mechanism in human immunity and a correlate of protection against malaria. BMC Med 2014; 12.
184. Murungi LM, Sondén K, Llewellyn D, Rono J, Guleid F, Williams AR, Ogada E, Thairu A, Färnert A, Marsh K, et al. Targets and mechanisms associated with protection from severe *Plasmodium falciparum* malaria in Kenyan children. Infect Immun 2016; 84:950–63.
185. Odera DO, Tuju J, Mwai K, Nkumama IN, Fürle K, Chege T, Kimathi R, Diehl S, Musasia FK, Rosenkranz M, et al. Anti-merozoite antibodies induce natural killer cell effector function and are associated with immunity against malaria on behalf of the CHMI-SIKA Study Team †, Faith H. Sci Transl Med 2023; 15:eabn5993.
186. Boyle MJ, Reiling L, Feng G, Langer C, Osier FH, Aspeling-Jones H, Cheng YS, Stubbs J, Tetteh KKA, Conway DJ, et al. Human antibodies fix complement to inhibit *Plasmodium falciparum* invasion of erythrocytes andare associated with protection against malaria. Immunity 2015; 42:580–90.
187. Kinyanjui SM, Conway DJ, Lanar DE, Marsh K. IgG antibody responses to *Plasmodium falciparum* merozoite antigens in Kenyan children have a short half-life. Malar J 2007; 6:82.
188. White MT, Griffin JT, Akpogheneta O, Conway DJ, Koram KA, Riley EM, Ghani AC. Dynamics of the antibody response to *Plasmodium falciparum* infection in African children. Journal of Infectious Diseases 2014; 210:1115–22.
189. Mugyenyi CK, Elliott SR, Yap XZ, Feng G, Boeuf P, Fegan G, Osier FFH, Fowkes FJI, Avril M, Williams TN, et al. Declining Malaria Transmission Differentially Impacts the Maintenance of Humoral Immunity to *Plasmodium falciparum* in Children. Journal of Infectious Diseases 2017; 216:879–98.

190. Osier FHA, Fegan G, Polley SD, Murungi L, Verra F, Tetteh KKA, Lowe B, Mwangi T, Bull PC, Thomas AW, et al. Breadth and magnitude of antibody responses to multiple *Plasmodium falciparum* merozoite antigens are associated with protection from clinical malaria. Infect Immun 2008; 76:2240–8.
191. Rono J, Osier FHA, Olsson D, Montgomery S, Mhoja L, Rooth I, Marsh K, Färnert A. Breadth of anti-merozoite antibody responses is associated with the genetic diversity of asymptomatic *Plasmodium falciparum* infections and protection against clinical malaria. Clinical Infectious Diseases 2013; 57:1409–16.
192. Scholzen A, Sauerwein RW. How malaria modulates memory: Activation and dysregulation of B cells in *Plasmodium* infection. Trends Parasitol2013; 29:252–62.
193. Bolad A, Berzins K. Antigenic diversity of *Plasmodium falciparum* and antibody-mediated parasite neutralization. Scand J Immunol2000; 52:233–9.
194. Illingworth J, Butler NS, Roetynck S, Mwacharo J, Pierce SK, Bejon P, Crompton PD, Marsh K, Ndungu FM. Chronic Exposure to *Plasmodium falciparum* Is Associated with Phenotypic Evidence of B and T Cell Exhaustion . The Journal of Immunology 2013; 190:1038–47.
195. Asito AS, Moormann AM, Kiprotich C, Ng'ang'A ZW, Ploutz-Snyder R, Rochford R. Alterations on peripheral B cell subsets following an acute uncomplicated clinical malaria infection in children. Malar J 2008; 7:238.
196. Sundling C, Rönnberg C, Yman V, Asghar M, Jahnmatz P, Lakshmikanth T, Chen Y, Mikes J, Forsell MN, Sondén K, et al. B cell profiling in malaria reveals expansion and remodeling of CD11c+ B cell subsets. JCI Insight 2019; 4:e126492.
197. Hansen DS, Obeng-Adjei N, Ly A, Ioannidis LJ, Crompton PD. Emerging concepts in T follicular helper cell responses to malaria. Int J Parasitol2017; 47:105–10.
198. Obeng-Adjei N, Portugal S, Tran TM, Yazew TB, Skinner J, Li S, Jain A, Felgner PL, Doumbo OK, Kayentao K, et al. Circulating Th1-Cell-type Tfh Cells that Exhibit Impaired B Cell Help Are Preferentially Activated during Acute Malaria in Children. Cell Rep 2015; 13:425–39.

199. Portugal S, Tipton CM, Sohn H, Kone Y, Wang J, Li S, Skinner J, Virtaneva K, Sturdevant DE, Porcella SF, et al. Malaria-associated atypical memory B cells exhibit markedly reduced B cell receptor signaling and effector function. Elife 2015; 4:e07218.
200. Nduati E, Gwela A, Karanja H, Mugyenyi C, Langhorne J, Marsh K, Urban BC. The plasma concentration of the B cell activating factor is increased in children with acute malaria. Journal of Infectious Diseases 2011; 204:962–70.
201. Donati D, Zhang LP, Chen Q, Chêne A, Flick K, Nyström M, Wahlgren M, Bejarano MT. Identification of a polyclonal B-cell activator in *Plasmodium falciparum*. Infect Immun 2004; 72:5412–8.
202. Donati D, Mok † Bobo, Chêne A, Xu H, Thangarajh M, Glas R, Chen Q, Wahlgren M, Bejarano MT. Increased B Cell Survival and Preferential Activation of the Memory Compartment by a Malaria Polyclonal B Cell Activator 1. The Journal of Immunology 2006; 177:3035–44.
203. Muthye V, Wasmuth JD. Proteome-wide comparison of tertiary protein structures reveals molecular mimicry in *Plasmodium*-human interactions. Frontiers in Parasitology 2023; 2:1162697.
204. Inst M, Cruz O, Brahimi K, Chaves Martins Y, Zanini GM, De M, Ferreira-Da-Cruz F, Daniel-Ribeiro CT. Monoclonal auto-antibodies and sera of autoimmune patients react with *Plasmodium falciparum* and inhibit its in vitro growth. 2011; 106:44–51.
205. Rubtsov A V, Rubtsova K, Fischer A, Meehan RT, Gillis JZ, Kappler JW, Marrack P. Toll-like receptor 7 (TLR7)-driven accumulation of a novel CD11c B-cell population is important for the development of autoimmunity. Immunobiology 2011; 118:331462.
206. Sutton HJ, Aye R, Idris AH, Vistein R, Nduati E, Kai O, Mwacharo J, Li X, Gao X, Andrews TD, et al. Atypical B cells are part of an alternative lineage of B cells that participates in responses to vaccination and infection in humans. Cell Rep 2021; 34:108684.
207. Weiss GE, Crompton PD, Li S, Walsh LA, Moir S, Traore B, Kayentao K, Ongoiba A, Doumbo OK, Pierce SK. Atypical Memory B Cells Are Greatly Expanded in Individuals Living in a Malaria-Endemic Area. The Journal of Immunology 2009; 183:2176–82.

208. Partey FD, Dowuona JNN, Pobee ANA, Walker MR, Aculley B, Prah DA, Ofori MF, Barfod LK. Atypical memory B cell frequency correlates with antibody breadth and function in malaria immune adults. Sci Rep 2024; 14:4888.
209. Portugal S, Obeng-Adjei N, Moir S, Crompton PD, Pierce SK. Atypical memory B cells in human chronic infectious diseases: An interim report. Cell Immunol 2017; 321:18–25.
210. Holla P, Ambegaonkar AA, Sohn H, Pierce S. Exhaustion may not be in the human B cell vocabulary, at least not in malaria. Immunol Rev 2019; 292:139–48.
211. Sullivan RT, Kim CC, Fontana MF, Feeney ME, Jagannathan P, Boyle MJ, Drakeley CJ, Ssewanyana I, Nankya F, Mayanja-Kizza H, et al. FCRL5 Delineates Functionally Impaired Memory B Cells Associated with *Plasmodium falciparum* Exposure. PLoS Pathog 2015; 11:e1004894.
212. Ambegaonkar AA, Kwak K, Sohn H, Manzella-Lapeira J, Brzostowski J, Pierce SK. Expression of inhibitory receptors by B cells in chronic human infectious diseases restricts responses to membrane-associated antigens. Immunology 2020; 6:eaba6493.
213. Reyes RA, Batugedara G, Dutta P, Reers AB, Garza R, Ssewanyana I, Jagannathan P, Feeney ME, Greenhouse B, Bol S, et al. Atypical B cells consist of subsets with distinct functional profiles. iScience 2023; 26:108496.
214. Kumar R, Loughland JR, Ng SS, Boyle MJ, Engwerda CR. The regulation of CD4+ T cells during malaria. Immunol Rev2020; 293:70–87.
215. Kurup SP, Butler NS, Harty JT. T cell-mediated immunity to malaria. Nat Rev Immunol2019; 19:457–71.
216. Drewry LL, Pewe LL, Hancox LS, Van de Wall S, Harty JT. CD4 T Cell–Dependent and –Independent Roles for IFN-γ in Blood-Stage Malaria. The Journal of Immunology 2023; 210:1305–13.
217. Carvalho LH, Sano G-I, Hafalla JCR, Morrot A, Curotto De Lafaille MA, Zavala F. IL-4-secreting CD4 + T cells are crucial to the development of CD8 + T-cell responses against malaria liver stages. NATURE MEDICINE • 2002; 8:166–70.
218. Poholek AC, Hansen K, Hernandez SG, Eto D, Chandele A, Weinstein JS, Dong X, Odegard JM, Kaech SM, Dent AL, et al. In Vivo Regulation of Bcl6 and T

Follicular Helper Cell Development. The Journal of Immunology 2010; 185:313–26.

219. Pérez-Mazliah D, Nguyen MP, Hosking C, McLaughlin S, Lewis MD, Tumwine I, Levy P, Langhorne J. Follicular Helper T Cells are Essential for the Elimination of *Plasmodium* Infection. EBioMedicine 2017; 24:216–30.
220. Walther M, Woodruff J, Edele F, Jeffries D, Tongren JE, King E, Andrews L, Bejon P, Gilbert SC, De Souza JB, et al. Innate Immune Responses to Human Malaria: Heterogeneous Cytokine Responses to Blood-Stage *Plasmodium falciparum* Correlate with Parasitological and Clinical Outcomes . The Journal of Immunology 2006; 177:5736–45.
221. Finney OC, Riley EM, Walther M. Regulatory T cells in malaria - friend or foe? Trends Immunol 2010; 31:63–70.
222. Gallien S, Roussilhon C, Blanc C, Pérignon JL, Druilhe P. Autoantibody against dendrite in *Plasmodium falciparum* infection: A singular auto-immune phenomenon preferentially in cerebral malaria. Acta Trop 2011; 118:67–70.
223. Mourão LC, Baptista RDP, De Almeida ZB, Grynberg P, Pucci MM, Castro-Gomes T, Fontes CJF, Rathore S, Sharma YD, Da Silva-Pereira RA, et al. Anti-band 3 and anti-spectrin antibodies are increased in *Plasmodium vivax* infection and are associated with anemia. Sci Rep 2018; 8:8762.
224. Raghavan M, Kalantar KL, Duarte E, Teyssier N, Takahashi S, Kung AF, Rajan J V., Rek J, Tetteh KKA, Drakeley C, et al. Proteome-wide antigenic profiling in Ugandan cohorts identifies associations between age, exposure intensity, and responses to repeat-containing antigens in *Plasmodium falciparum*. Elife 2023; 12:e81401.
225. Osii RS, Otto TD, Garside P, Ndungu FM, Brewer JM. The Impact of Malaria Parasites on Dendritic Cell–T Cell Interaction. Front Immunol2020; 11:1597.
226. Britta C. Urban, David J. P. Ferguson, Arnab Pain, Nick Willcox, Magdalena Plebanski, Jonathan M. Austyn & David J. Roberts. *Plasmodium falciparum*-infected erythrocytes modulate the maturation of dendritic cells. Letters To Nature 1999; 400:73–5.
227. Millington OR, Lorenzo C Di, Phillips S, Garside P, Brewer JM. Suppression of adaptive immunity to heterologous antigens during *Plasmodium* infection through hemozoin-induced failure of dendritic cell function. J Biol 2006; 5:5.

228. Arama C, Giusti P, Boström S, Dara V, Traore B, Dolo A, Doumbo O, Varani S, Troye-Blomberg M. Interethnic differences in antigen-presenting cell activation and TLR responses in malian children during *Plasmodium falciparum* malaria. PLoS One 2011; 6:e18319.
229. Urban BC, Mwangi T, Ross A, Kinyanjui S, Mosobo M, Kai O, Lowe B, Marsh K, Roberts DJ. Peripheral blood dendritic cells in children with acute *Plasmodium falciparum* malaria. 2001; 98:2859–61.
230. Vasquez M, Zuniga M, Rodriguez A. Oxidative Stress and Pathogenesis in Malaria. Front Cell Infect Microbiol2021; 11:768182.
231. Lorenz Knackstedt S, Georgiadou A, Apel F, Abu-Abed U, Moxon CA, Cunnington AJ, Raupach B, Cunningham D, Langhorne J, Krüger R, et al. Neutrophil extracellular traps drive inflammatory pathogenesis in malaria. Sci Immunol 2019; 4:336.
232. Boeltz S, Muñoz LE, Fuchs TA, Herrmann M. Neutrophil extracellular traps open the Pandora's box in severe malaria. Front Immunol2017; 8:00874.
233. Baker VS, Imade GE, Molta NB, Tawde P, Pam SD, Obadofin MO, Sagay SA, Egah DZ, Iya D, Afolabi BB, et al. Cytokine-associated neutrophil extracellular traps and antinuclear antibodies in *Plasmodium falciparum* infected children under six years of age. Malar J 2008; 7:41.
234. Fujinami RS, Von Herrath MG, Christen U, Whitton JL. Molecular mimicry, bystander activation, or viral persistence: Infections and autoimmune disease. Clin Microbiol Rev2006; 19:80–94.
235. Cunningham MW. Pathogenesis of Group A Streptococcal Infections. Clin Microbiol Rev 2000; 13:470–511.
236. Quaratino S, Thorpe CJ, Travers PJ, Londei M. Similar Antigenic Surfaces, Rather than Sequence Homology, Dictate T-Cell Epitope. PNAS 1995; 92:10398–402.
237. Macdonald SM, Bhisutthibhan J, Shapiro TA, Rogerson SJ, Taylor TE, Tembo M, Langdon JM, Meshnick SR. Immune mimicry in malaria: *Plasmodium falciparum* secretes a functional histamine-releasing factor homolog in vitro and in vivo. PNAS 2001; 98:10829–32.
238. Ludin P, Nilsson D, Mäser P. Genome-wide identification of molecular mimicry candidates in parasites. PLoS One 2011; 6:e17546.
239. Mourão LC, Roma PMDS, Sultane Aboobacar JDS, Medeiros CMP, De Almeida ZB, Fontes CJF, Agero U, De Mesquita ON, Bemquerer MP, Braga ÉM. Anti-

erythrocyte antibodies may contribute to anaemia in *Plasmodium vivax* malaria by decreasing red blood cell deformability and increasing erythrophagocytosis. Malar J 2016; 15:397.

240. Bangs SC, Baban D, Cattan HJ, Li CK-F, McMichael AJ, Xu X-N. Human CD4+ Memory T Cells Are Preferential Targets for Bystander Activation and Apoptosis. The Journal of Immunology 2009; 182:1962–71.
241. Bach FA, Muñoz Sandoval D, Mazurczyk M, Themistocleous Y, Rawlinson TA, Harding AC, Kemp A, Silk SE, Barrett JR, Edwards NJ, et al. A systematic analysis of the human immune response to *Plasmodium vivax*. J Clin Invest 2023; 133:e152463.
242. Dasari P, Fries A, Heber SD, Salama A, Blau IW, Lingelbach K, Bhakdi SC, Udomsangpetch R, Torzewski M, Reiss K, et al. Malarial anemia: digestive vacuole of *Plasmodium falciparum* mediates complement deposition on bystander cells to provoke hemophagocytosis. Med Microbiol Immunol 2014; 203:383–93.
243. Vanderlugt CL, Miller SD. Epitope spreading in immune-mediated diseases: Implications for immunotherapy. Nat Rev Immunol2002; 2:85–95.
244. Monneaux F, Muller S. Review: Epitope spreading in systemic lupus erythematosus: Identification of triggering peptide sequences. Arthritis Rheum2002; 46:1430–8.
245. Flanagan KL, Plebanski M, Akinwunmi P, Lee EAM, Reece WHH, Robson KJH, Hill AVS, Pinder M. Broadly distributed T cell reactivity, with no immunodominant loci, to the pre-erythrocytic antigen thrombospondin-related adhesive protein of *Plasmodium falciparum* in West Africans. Eur J Immunol 1999; 29:1943–54.
246. Yurasov S, Wardemann H, Hammersen J, Tsuiji M, Meffre E, Pascual V, Nussenzweig MC. Defective B cell tolerance checkpoints in systemic lupus erythematosus. Journal of Experimental Medicine 2005; 201:703–11.
247. Krumkamp R, Struck NS, Lorenz E, Zimmermann M, Boahen KG, Sarpong N, Owusu-Dabo E, Pak GD, Jeon HJ, Marks F, et al. Classification of invasive bloodstream infections and *Plasmodium falciparum* malaria using autoantibodies as biomarkers. Sci Rep 2020; 10:21168.
248. Barber BE, Grigg MJ, Piera K, Amante FH, William T, Boyle MJ, Minigo G, Dondorp AM, McCarthy JS, Anstey NM. Antiphosphatidylserine Immunoglobulin M and Immunoglobulin G Antibodies Are Higher in Vivax

Than Falciparum Malaria and Associated With Early Anemia in Both Species. Journal of Infectious Diseases 2019; 220:1435–43.

249. Saleh BH, Lugaajju A, Storry JR, Persson KEM. Autoantibodies against red blood cell antigens are common in a malaria endemic area. Microbes Infect 2023; 25:105060.
250. Moxon CA, Gibbins MP, Mcguinness D, Milner DA, Marti M. New Insights into Malaria Pathogenesis. The Annual Review of Pathology: Mechanisms of Disease 2019; 15:315–43.
251. Venkatesan P. The 2023 WHO World malaria report. Lancet Microbe 2024; 5:e214.
252. Lang B, Newbold CI, Williams G, Peshu N, Marsh K, Newton CRJC. Antibodies to Voltage-Gated Calcium Channels in Children with Falciparum Malaria. J Infect Dis 2005; 191:117–21.
253. Vera IM, Kessler A, Harawa V, Ahmadu A, Keller TE, Ray STJ, Taylor TE, Rogerson SJ, Mandala WL, Gil MR, et al. Prothrombotic autoantibodies targeting platelet factor 4/polyanion are associated with pediatric cerebral malaria. Journal of Clinical Investigation 2024; 134:e176466.
254. Katsoulis O, Georgiadou A, Cunnington AJ. Immunopathology of Acute Kidney Injury in Severe Malaria. Front Immunol2021; 12:651739.
255. Da Silva Junior GB, Pinto JR, Barros EJG, Farias GMN, Daher EDF. Kidney involvement in malaria: An update. Rev Inst Med Trop São Paulo 2017; 59:e53.
256. Mannoor K, Li C, Inafuku M, Taniguchi T, Abo T, Sato Y, Watanabe H. Induction of ssDNA-binding autoantibody secreting B cell immunity during murine malaria infection is a critical part of the protective immune responses. Immunobiology 2013; 218:10–20.
257. Sansan H. Levels of Rheumatoid Factor in *Plasmodium Falciparum* Malaria in Children and Its Association with Gender, Age and Parasite Density. International Journal of Immunology 2016; 4:46–51.
258. Piel FB, Patil AP, Howes RE, Nyangiri OA, Gething PW, Williams TN, Weatherall DJ, Hay SI. Global distribution of the sickle cell gene and geographical confirmation of the malaria hypothesis. Nat Commun 2010; 1:104.
259. Kariuki SN, Marin-Menendez A, Introini V, Ravenhill BJ, Lin YC, Macharia A, Makale J, Tendwa M, Nyamu W, Kotar J, et al. Red blood cell tension

protects against severe malaria in the Dantu blood group. Nature 2020; 585:579–83.

260. Clatworthy MR, Willcocks L, Urban B, Langhorne J, Williams TN, Peshu N, Watkins NA, Floto RA, Smith KGC. Systemic lupus erythematosus-associated defects in the inhibitory receptor FcgammaRIIb reduce susceptibility to malaria. Proc Natl Acad Sci U S A 2007; 104:7169–74.
261. Waisberg M, Tarasenko T, Vickers BK, Scott BL, Willcocks LC, Molina-Cruz A, Pierce MA, Huang CY, Torres-Velez FJ, Smith KGC, et al. Genetic susceptibility to systemic lupus erythematosus protects against cerebral malaria in mice. Proc Natl Acad Sci U S A 2011; 108:1122–7.
262. Ojurongbe O, Funwei RI, Snyder TJ, Farid I, Aziz N, Li Y, Falade CO, Thomas BN. Genetic variants of tumor necrosis factor-α -308G/A (rs1800629) but not Toll-interacting proteins or vitamin D receptor genes enhances susceptibility and severity of malaria infection. Immunogenetics 2018; 70:135–40.
263. Olaniyan SA, Amodu OK, Bakare AA, Troye-Blomberg M, Omotade OO, Rockett KA. Tumour necrosis factor alpha promoter polymorphism, TNF-238 is associated with severe clinical outcome of falciparum malaria in Ibadan southwest Nigeria. Acta Trop 2016; 161:62–7.
264. Mahto H, Tripathy R, Meher BR, Prusty BK, Sharma M, Deogharia D, Saha AK, Panda AK, Das BK. TNF-α promoter polymorphisms (G-238A and G-308A) are associated with susceptibility to Systemic Lupus Erythematosus (SLE) and P. falciparum malaria: a study in malaria endemic area. Sci Rep 2019; 9:11752.
265. Hill AVS, Allsopp CEM, Kwiatkowski D, Anstey NM, Twumasi P, Rowet PA, Bennettt S, Brewster D, Mcmichael AJ, Greenwood BM. Common West African HLA antigens are associated with protection from severe malaria. Nature 1991; 352:595–600.
266. Gourraud PA, Boyer JF, Barnetche T, Abbal M, Cambon-Thomsen A, Cantagrel A, Constantin A. A new classification of HLA-DRB1 alleles differentiates predisposing and protective alleles for rheumatoid arthritis structural severity. Arthritis Rheum 2006; 54:593–9.
267. Wijayalath W, Majji S, Villasante EF, Brumeanu TD, Richie TL, Casares S. Humanized HLA-DR4.RagKO.IL2RγcKO.NOD (DRAG) mice sustain the complex vertebrate life cycle of *Plasmodium falciparum* malaria. Malar J 2014; 13:386.

268. Olatunde AC, Cornwall DH, Roedel M, Lamb TJ. Mouse Models for Unravelling Immunology of Blood Stage Malaria. Vaccines (Basel)2022; 10:1525.
269. De Oca MM, Engwerda C, Haque A. *Plasmodium berghei* ANKA (PbA) infection of C57BL/6J mice: A model of severe malaria. Methods in Molecular Biology 2013; 1031:203–13.
270. Stephens R, Culleton RL, Lamb TJ. The contribution of *Plasmodium chabaudi* to our understanding of malaria. Trends Parasitol2012; 28:73–82.
271. Abdel-Maksoud MA, Abdel-Ghaffar FA, El-Amir A, Badr G, Al-Quraishy S. Altered renal immune complexes deposition in female BWF1 lupus mice following *Plasmodium chabaudi* infection. Saudi J Biol Sci 2018; 25:1609–16.
272. O'Donnell AJ, Schneider P, McWatters HG, Reece SE. Fitness costs of disrupting circadian rhythms in malaria parasites. Proceedings of the Royal Society B: Biological Sciences 2011; 278:2429–36.
273. Brugat T, Cunningham D, Sodenkamp J, Coomes S, Wilson M, Spence PJ, Jarra W, Thompson J, Scudamore C, Langhorne J. Sequestration and histopathology in *Plasmodium chabaudi* malaria are influenced by the immune response in an organ-specific manner. Cell Microbiol 2014; 16:687–700.
274. Ponsford MJ, Medana IM, Prapansilp P, Hien TT, Lee SJ, Dondorp AM, Esiri MM, Day NPJ, White NJ, Turner GDH. Sequestration and microvascular congestion are associated with coma in human cerebral malaria. Journal of Infectious Diseases 2012; 205:663–71.
275. Stephens R, Culleton RL, Lamb TJ. The contribution of *Plasmodium chabaudi* to our understanding of malaria. Trends Parasitol2012; 28:73–82.
276. Barnden MJ, Allison J, Heath WR, Carbone FR. Defective TCR expression in transgenic mice constructed using cDNA- based α- and ß-chain genes under the control of heterologous regulatory elements. Immunol Cell Biol 1998; 76:34–40.
277. Cambie G, Verdier F, Gaudebout C, Clavier F, Ginsburg H. Pharmacocinétique de la chloroquine chez la souris saine et infectée par *Plasmodium chabaudi*: Approche chronothérapeutique. Parasite 1994; 1:219–26.
278. Majid RA, Bello R. Progression of malaria induced pathogenicity during chloroquine therapy. Tropical Biomedicine 37(1): 2020; 37:29–49.

279. Fleischer B. Editorial: 100 Years ago - Giemsa's solution for staining of plasmodia. Tropical Medicine and International Health2004; 9:755–6.
280. Halim S, Bretschneider TR, Li Y, Preiser PR, Kuss C. Estimating malaria parasitaemia from blood smear images. In: 9th International Conference on Control, Automation, Robotics and Vision, 2006, ICARCV '06. 2006. page 1–6.
281. Knight JS, Subramanian V, O'Dell AA, Yalavarthi S, Zhao W, Smith CK, Hodgin JB, Thompson PR, Kaplan MJ. Peptidylarginine deiminase inhibition disrupts NET formation and protects against kidney, skin and vascular disease in lupus-prone MRL/lpr mice. Ann Rheum Dis 2015; 74:2199–206.
282. Maffia P, Brewer JM, Gracie JA, Ianaro A, Leung BP, Mitchell PJ, Smith KM, McInnes IB, Garside P. Inducing Experimental Arthritis and Breaking Self-Tolerance to Joint-Specific Antigens with Trackable, Ovalbumin-Specific T Cells. The Journal of Immunology 2004; 173:151–6.
283. Smith KM, Pottage L, Thomas ER, Leishman AJ, Doig TN, Xu D, Liew FY, Garside P. Th1 and Th2 CD4+ T Cells Provide Help for B Cell Clonal Expansion and Antibody Synthesis in a Similar Manner In Vivo. The Journal of Immunology 2000; 165:3136–44.
284. Al Khabouri S, Benson RA, Prendergast CT, Gray JI. TCRβ Sequencing Reveals Spatial and Temporal Evolution of Clonal CD4 T Cell Responses in a Breach of Tolerance Model of Inflammatory Arthritis. Front Immunol 2021; 12:669856.
285. Leishman AJ, Garside P, Mowat AMI. Induction of Oral Tolerance in the Primed Immune System: Influence of Antigen Persistence and Adjuvant Form. Cell Immunol 2000; 202:71–8.
286. Conigliaro P, Benson RA, Patakas A, Kelly SM, Valesini G, Holmdahl R, Brewer JM, McInnes IB, Garside P. Characterization of the anticollagen antibody response in a new model of chronic polyarthritis. Arthritis Rheum 2011; 63:2299–308.
287. Lerna M, Kerr A, Scales H, Berge K, Griinari M. Supplementation of diet with krill oil protects against experimental rheumatoid arthritis. BMC Musculoskelet Disord 2010; 11:136.
288. Leung BP, Mcinnes IB, Esfandiari E, Wei X-Q, Liew FY. Combined Effects of IL-12 and IL-18 on the Induction of Collagen-Induced Arthritis 1. The Journal of Immunology 2000; 164:6495–502.

289. Lundberg K, Kinloch A, Fisher BA, Wegner N, Wait R, Charles P, Mikuls TR, Venables PJ. Antibodies to citrullinated α-enolase peptide 1 are specific for rheumatoid arthritis and cross-react with bacterial enolase. Arthritis Rheum 2008; 58:3009–19.
290. Joester A, Faissner A. Evidence for Combinatorial Variability of Tenascin-C Isoforms and Developmental Regulation in the Mouse Central Nervous System. Journal of Biological Chemistry 1999; 274:17144–51.
291. Emeis JJ, Jirouskova M, Muchitsch EM, Shet AS, Smyth SS, Johnson GJ. A guide to murine coagulation factor structure, function, assays, and genetic alterations. Journal of Thrombosis and Haemostasis 2007; 5:670–9.
292. Díaz-Ramos À, Roig-Borrellas A, García-Melero A, López-Alemany R. α-enolase, a multifunctional protein: Its role on pathophysiological situations. J Biomed Biotechnol2012; 2012.
293. Herrmann H, Aebi U. Intermediate Filaments: Molecular structure, assembly mechanism, and integration into functionally distinct intracellular scaffolds. Annu Rev Biochem2004; 73:749–89.
294. Altschul SF, Madden TL, Schäffer AA, Zhang J, Zhang Z, Miller W, Lipman DJ. Gapped BLAST and PSI-BLAST: a new generation of protein database search programs. Nucleic Acids Res 1997; 25:3389–402.
295. Altschul SF, Wootton JC, Gertz EM, Agarwala R, Morgulis A, Schäffer AA, Yu YK. Protein database searches using compositionally adjusted substitution matrices. FEBS Journal 2005; 272:5101–9.
296. Bejon P, Berkley JA, Mwangi T, Ogada E, Mwangi I, Maitland K, Williams T, Anthony J, Scott G, English M, et al. Defining Childhood Severe Falciparum Malaria for Intervention Studies. PLoS Med 2007; 4:251–1333.
297. Mwangi TW, Mohammed M, Dayo H, Snow RW, Marsh K. Clinical algorithms for malaria diagnosis lack utility among people of different age groups. Tropical Medicine and International Health 2005; 10:530–6.
298. Ndungu FM, Marsh K, Fegan G, Wambua J, Nyangweso G, Ogada E, Mwangi T, Nyundo C, Macharia A, Uyoga S, et al. Identifying children with excess malaria episodes after adjusting for variation in exposure: Identification from a longitudinal study using statistical count models. BMC Med 2015; 13:183.

299. O'Meara WP, Bejon P, Mwangi TW, Okiro EA, Peshu N, Snow RW, Newton CR, Marsh K. Effect of a fall in malaria transmission on morbidity and mortality in Kilifi, Kenya. The Lancet 2008; 372:1555–62.
300. Kapulu MC, Kimani D, Njuguna P, Hamaluba M, Otieno E, Kimathi R, Tuju J, Sim BKL, Abdi AI, Abebe Y, et al. Controlled human malaria infection (CHMI) outcomes in Kenyan adults is associated with prior history of malaria exposure and anti-schizont antibody response. BMC Infect Dis 2022; 22:86.
301. Ndungu FM, Bull PC, Ross A, Lowe BS, Kabiru E, Marsh K. Naturally acquired immunoglobulin (Ig)G subclass antibodies to crude asexual *Plasmodium falciparum* lysates: Evidence for association with protection for IgG1 and disease for IgG2. Parasite Immunol 2002; 24:77–82.
302. Mwai K, Kibinge N, Tuju J, Kamuyu G, Kimathi R, Mburu J, Chepsat E, Nyamako L, Chege T, Nkumama I, et al. protGear: A protein microarray data pre-processing suite. Comput Struct Biotechnol J 2021; 19:2518–25.
303. Lerner A, Jeremias P, Matthias T. The world incidence and prevalence of autoimmune diseases is increasing. International Journal of Celiac Disease 2015; 3:151–5.
304. Miller FW. The increasing prevalence of autoimmunity and autoimmune diseases: an urgent call to action for improved understanding, diagnosis, treatment, and prevention. Curr Opin Immunol 2023; 80:102266.
305. Ellis JA, Kemp AS, Ponsonby AL. Gene-environment interaction in autoimmune disease. Expert Rev Mol Med 2014; 16:e4.
306. Fonseca DLM, Filgueiras IS, Marques AHC, Vojdani E, Halpert G, Ostrinski Y, Baiocchi GC, Plaça DR, Freire PP, Pour SZ, et al. Severe COVID-19 patients exhibit elevated levels of autoantibodies targeting cardiolipin and platelet glycoprotein with age: a systems biology approach. npj Aging 2023; 9:21.
307. Adib-Conquy M, Avrameas S, Ternynck T. MONOCLONAL IgG AND IgM AUTOANTIBODIES OBTAINED AFTER POLYCLONAL ACTIVATION, SHOW REACTIVITIES SIMILAR TO THOSE OF POLYCLONAL NATURAL AUTOANTIBODIES. Mol Immunol 1993; 30:119–27.
308. Scherer HU, Häupl T, Burmester GR. The etiology of rheumatoid arthritis. J Autoimmun 2020; 110:102400.
309. Khandpur R, Carmona-Rivera C, Vivekanandan-Giri A, Gizinski A, Yalavarthi S, Knight JS, Friday S, Li S, Patel RM, Subramanian V, et al. NETs Are a

Source of Citrullinated Autoantigens and Stimulate Inflammatory Responses in Rheumatoid Arthritis. Sci Transl Med 2013; 5:178ra40.

310. Foulquier C, Sebbag M, Clavel C, Chapuy-Regaud S, Al Badine R, Méchin MC, Vincent C, Nachat R, Yamada M, Takahara H, et al. Peptidyl arginine deiminase type 2 (PAD-2) and PAD-4 but not PAD-1, PAD-3, and PAD-6 are expressed in rheumatoid arthritis synovium in close association with tissue inflammation. Arthritis Rheum 2007; 56:3541–53.
311. Chavanas S, Méchin MC, Takahara H, Kawada A, Nachat R, Serre G, Simon M. Comparative analysis of the mouse and human peptidylarginine deiminase gene clusters reveal highly conserved non-coding segments and a new human gene, PADI6. Gene 2004; 330:19–27.
312. Gudmann NS, Hansen NUB, Jensen ACB, Karsdal MA, Siebuhr AS. Biological relevance of citrullinations: Diagnostic, prognostic and therapeutic options. Autoimmunity 2015; 48:73–9.
313. Alghamdi M, Alasmari D, Assiri A, Mattar E, Aljaddawi AA, Alattas SG, Redwan EM. An Overview of the Intrinsic Role of Citrullination in Autoimmune Disorders. J Immunol Res 2019; 25:7592851.
314. Aletaha D, Neogi T, Silman AJ, Funovits J, Felson DT, Bingham CO, Birnbaum NS, Burmester GR, Bykerk VP, Cohen MD, et al. 2010 Rheumatoid arthritis classification criteria: An American College of Rheumatology/European League Against Rheumatism collaborative initiative. Arthritis Rheum 2010; 62:2569–81.
315. Schwenzer A, Quirke AM, Montgomery AB, Venables PJ, Sayles HR, Schlumberger W, Payne JB, Mikuls TR, Midwood KS. Time to Include Fine Specificity Anti-Citrullinated Protein Antibodies in the Routine Diagnosis and Management of Rheumatoid Arthritis? Arthritis and Rheumatology 2019; 71:476–8.
316. Catrina A, Krishnamurthy A, Rethi B. Current view on the pathogenic role of anti-citrullinated protein antibodies in rheumatoid arthritis. RMD Open 2021; 7:e001228.
317. Deenick EK, Ma CS. The regulation and role of T follicular helper cells in immunity. Immunology 2011; 134:361–7.
318. Braddom AE, Batugedara G, Bol S, Bunnik EM. Potential functions of atypical memory B cells in *Plasmodium*-exposed individuals. Int J Parasitol 2020; 50:1033–42.

319. Cela D, Knackstedt SL, Groves S, Rice CM, Kwon JTW, Mordmüller B, Amulic B. PAD4 controls chemoattractant production and neutrophil trafficking in malaria. J Leukoc Biol 2022; 111:1235–42.
320. GS Chirivi R. Citrullination: A Target for Disease Intervention in Multiple Sclerosis and other Inflammatory Diseases? J Clin Cell Immunol 2013; 04:146.
321. Ternynck T, Falanga PB, Unterkirscher C, Gregoire J, Pereira Da Silva L, Avrameas S. Induction of high levels of IgG autoantibodies in mice infected with *Plasmodium chabaudi*. Int Immunol 1991; 3:29–37.
322. Achtman AH, Khan M, MacLennan ICM, Langhorne J. *Plasmodium chabaudi* chabaudi Infection in Mice Induces Strong B Cell Responses and Striking but Temporary Changes in Splenic Cell Distribution. The Journal of Immunology 2003; 171:317–24.
323. ANDERS RF. Multiple cross-reactivities amongst antigens of *Plasmodium falciparum* impair the development of protective immunity against malaria. Parasite Immunol 1986; 8:529–39.
324. Langhorne J, Kim KJ, Asofsky R. Distribution of immunoglobulin isotypes in the nonspecific B-cell response induced by infection with *Plasmodium chabaudi adami* and *Plasmodium yoelii*. Cell Immunol 1985; 90:251–7.
325. Bender P, Bürgin WB, Sculean A, Eick S. Serum antibody levels against *Porphyromonas gingivalis* in patients with and without rheumatoid arthritis – a systematic review and meta-analysis. Clin Oral Investig 2017; 21:33–42.
326. Yang C, Hu Z, Wang L, Fang L, Wang X, Li Q, Xu L, Wang J, Liu C, Lin N. *Porphyromonas gingivalis* with collagen immunization induces ACPA-positive rheumatoid arthritis in C3H mice. Clinical Immunology 2024; 258:109859.
327. Zhou Y, Chen B, Mittereder N, Chaerkady R, Strain M, An LL, Rahman S, Ma W, Low CP, Chan D, et al. Spontaneous secretion of the citrullination enzyme PAD2 and cell surface exposure of PAD4 by neutrophils. Front Immunol 2017; 8:1200.
328. Hou S, Gao GP, Zhang XJ, Sun L, Peng WJ, Wang HF, Ge XJ, Huang W, Sun YH. PADI4 polymorphisms and susceptibility to rheumatoid arthritis: A meta-analysis. Mod Rheumatol 2013; 23:50–60.
329. Yang X ke, Liu J, Liu J, Liang Y, Xu W dong, Leng R xue, Pan H feng, Ye D qing. Associations Between PADI4 Gene Polymorphisms and Rheumatoid Arthritis: An Updated Meta-analysis. Arch Med Res 2015; 46:317–25.

330. Alivernini S, Firestein GS, McInnes IB. The pathogenesis of rheumatoid arthritis. Immunity 2022; 55:2255–70.
331. Hussein HM, Rahal EA. The role of viral infections in the development of autoimmune diseases. Crit Rev Microbiol 2019; 45:394–412.
332. Bartold PM, Marino V, Cantley M, Haynes DR. Effect of Porphyromonas gingivalis-induced inflammation on the development of rheumatoid arthritis. J Clin Periodontol 2010; 37:405–11.
333. de Molon RS, Rossa C, Thurlings RM, Cirelli JA, Koenders MI. Linkage of periodontitis and rheumatoid arthritis: Current evidence and potential biological interactions. Int J Mol Sci 2019; 20:4541.
334. Demmer RT, Molitor JA, Jacobs DR, Michalowicz BS. Periodontal disease, tooth loss and incident rheumatoid arthritis: Results from the First National Health and Nutrition Examination Survey and its epidemiological follow-up study. J Clin Periodontol 2011; 38:998–1006.
335. Taha Rashid CW. Worldwide Links between Proteus mirabilis and Rheumatoid Arthritis. J Arthritis 2015; 04:1–7.
336. Kuwana Y, Takei M, Yajima M, Imadome KI, Inomata H, Shiozaki M, Ikumi N, Nozaki T, Shiraiwa H, Kitamura N, et al. Epstein-barr virus induces erosive arthritis in humanized mice. PLoS One 2011; 6:e26630.
337. Chu KA, Chen W, Hsu CY, Hung YM, Wei JCC. Increased risk of rheumatoid arthritis among patients with Mycoplasma pneumonia: A nationwide population-based cohort study in Taiwan. PLoS One 2019; 14:e0210750.
338. Greenwood BM, Voller A, Herrick EM. Suppression of adjuvant arthritis by infection with a strain of the rodent malaria parasite *Plasmodium berghei*. Ann Rheum Dis 1970; 29:321–3.
339. Gaballah EM, Morita K, Shimizu S, Elhenawy AA, Nabih N, Elsawey AM, Abdel-Mageed SA, Osada Y. Non-lethal rodent malarial infection prevents collagen-induced arthritis in mice via anti-arthritic immunomodulation. Parasite Immunol 2022; 44:e12901.
340. Meyer O, Labarre C, Dougados M, Goupille P, Cantagrel A, Dubois A, Nicaise-Roland P, Sibilia J, Combe B. Anticitrullinated protein/peptide antibody assays in early rheumatoid arthritis for predicting five year radiographic damage. Ann Rheum Dis 2003; 62:120–6.
341. Krishnamurthy A, Circiumaru A, Sun J, Kisten Y, Damberg P, Sakuraba K, Sandor K, Jarvoll P, Zhou T, Malmström V, et al. Combination of Two

Monoclonal Anti–Citrullinated Protein Antibodies Induced Tenosynovitis, Pain, and Bone Loss in Mice in a Peptidyl Arginine Deiminase-4–Dependent Manner. Arthritis and Rheumatology 2023; 75:164–70.

342. Kuhn KA, Kulik L, Tomooka B, Braschler KJ, Arend WP, Robinson WH, Holers VM. Antibodies against citrullinated proteins enhance tissue injury in experimental autoimmune arthritis. Journal of Clinical Investigation 2006; 116:961–73.
343. ten Brinck RM, Toes REM, van der Helm-van Mil AHM. Inflammation functions as a key mediator in the link between ACPA and erosion development: An association study in Clinically Suspect Arthralgia. Arthritis Res Ther 2018; 20:89.
344. dos Reis Neto ET, Kakehasi AM, de Medeiros Pinheiro M, Ferreira GA, Lopes Marques CD, da Mota LMH, dos Santos Paiva E, Salviato Pileggi GC, Sato EI, Gomides Reis APM, et al. Revisiting hydroxychloroquine and chloroquine for patients with chronic immunity-mediated inflammatory rheumatic diseases. Advances in Rheumatology 2020; 60:Article number 32.
345. Nazir AM, Koganti B, Gupta K, Memon MS, Aslam Zahid M Bin, Shantha Kumar V, Tappiti M, Mostafa JA. Evaluating the Use of Hydroxychloroquine in Treating Patients With Rheumatoid Arthritis. Cureus 2021; 13:e19308.
346. Scales HE, Ierna M, Smith KM, Ross K, Meiklejohn GR, Patterson-Kane JC, McInnes IB, Brewer JM, Garside P, Maffia P. Assessment of murine collagen-induced arthritis by longitudinal non-invasive duplexed molecular optical imaging. Rheumatology (United Kingdom) 2016; 55:564–72.
347. Pradhan V, Ghosh K. Immunological disturbances associated with malarial infection. Springer 2012; 37:11–5.
348. Choudhary N, Bhatt LK, Prabhavalkar KS. Experimental animal models for rheumatoid arthritis. Immunopharmacol Immunotoxicol 2018; 40:193–200.
349. Harre U, Georgess D, Bang H, Bozec A, Axmann R, Ossipova E, Jakobsson PJ, Baum W, Nimmerjahn F, Szarka E, et al. Induction of osteoclastogenesis and bone loss by human autoantibodies against citrullinated vimentin. Journal of Clinical Investigation 2012; 122:1791–802.
350. Gomez AM, Brewer RC, Moon JS, Acharya S, Kongpachith S, Wang Q, Jahanbani S, Wong HH, Lanz T V., Love ZZ, et al. Anti–Citrullinated Protein Antibodies With Multiple Specificities Ameliorate Collagen Antibody–Induced

Arthritis in a Time-Dependent Manner. Arthritis and Rheumatology 2024; 76:181–91.

351. Guiyedi V, Bécavin C, Herbert F, Gray J, Cazenave PA, Kombila M, Crisanti A, Fesel C, Pied S. Asymptomatic *Plasmodium falciparum* infection in children is associated with increased auto-antibody production, high IL-10 plasma levels and antibodies to merozoite surface protein 3. Malar J 2015; 14:162.
352. Iyengar KP, Vaish A, Nune A. Anti-cyclic citrullinated peptide antibody (ACPA) and Rheumatoid arthritis: Clinical relevance. J Clin Orthop Trauma 2022; 24:101729.
353. Sakaguchi S, Yamaguchi T, Nomura T, Ono M. Regulatory T Cells and Immune Tolerance. Cell 2008; 133:775–87.
354. Ritchie ME, Silver J, Oshlack A, Holmes M, Diyagama D, Holloway A, Smyth GK. A comparison of background correction methods for two-colour microarrays. Bioinformatics 2007; 23:2700–7.
355. Huber W, Von Heydebreck A, Sültmann H, Poustka A, Vingron M. Variance stabilization applied to microarray data calibration and to the quantification of differential expression. Bioinformatics 2002; 18:S96–S104.
356. Njuguna P, Maitland K, Nyaguara A, Mwanga D, Mogeni P, Mturi N, Mohammed S, Mwambingu G, Ngetsa C, Awuondo K, et al. Observational study: 27 years of severe malaria surveillance in Kilifi, Kenya. BMC Med 2019; 17:124.
357. Li Y, Guo R, Oduro PK, Sun T, Chen H, Yi Y, Zeng W, Wang Q, Leng L, Yang L, et al. The Relationship Between *Porphyromonas Gingivalis* and Rheumatoid Arthritis: A Meta-Analysis. Front Cell Infect Microbiol 2022; 12:956417.
358. Mehri F, Jenabi E, Bashirian S, Shahna FG, Khazaei S. The association Between Occupational Exposure to silica and Risk of Developing Rheumatoid Arthritis: A Meta-Analysis. Saf Health Work 2020; 11:136–42.
359. Holmes CL, Shim D, Kernien J, Johnson CJ, Nett JE, Shelef MA. Insight into neutrophil extracellular traps through systematic evaluation of citrullination and peptidylarginine deiminases. J Immunol Res 2019; 2019:2160192.
360. Obeng-Adjei N, Portugal S, Holla P, Li S, Sohn H, Ambegaonkar A, Skinner J, Bowyer G, Doumbo OK, Traore B, et al. Malaria-induced interferon-γ drives

the expansion of Tbethiatypical memory B cells. PLoS Pathog 2017; 13:e1006576.

361. Boyle MJ, Jagannathan P, Bowen K, McIntyre TI, Vance HM, Farrington LA, Schwartz A, Nankya F, Naluwu K, Wamala S, et al. The development of *Plasmodium falciparum*-Specific IL10 CD4 T cells and protection from malaria in children in an area of high malaria transmission. Front Immunol 2017; 8:1329.
362. Boyle MJ, Jagannathan P, Farrington LA, Eccles-James I, Wamala S, McIntyre TI, Vance HM, Bowen K, Nankya F, Auma A, et al. Decline of FoxP3+ Regulatory CD4 T Cells in Peripheral Blood of Children Heavily Exposed to Malaria. PLoS Pathog 2015; 11:e1005041.
363. Adebajo AO, Charles P, Maini RN, Hazleman BL. Autoantibodies in malaria, *tuberculosis* and hepatitis B in a West African population. Clin Exp Immunol 1993; 92:73–6.
364. Ribeiro CTD, De Roquefeuil S, Druilhe P, Monjour L, Homberg JC, Gentilini M. Abnormal anti-single stranded (ss) DNA activity in sera from *Plasmodium falciparum* infected individuals. Trans R Soc Trop Med Hyg 1984; 78:742–6.
365. Alam A. Serine proteases of malaria parasite *Plasmodium falciparum*: Potential as antimalarial drug targets. Interdiscip Perspect Infect Dis2014; 2014.
366. Houen G, Trier NH. Epstein-Barr Virus and Systemic Autoimmune Diseases. Front Immunol 2021; 11:587380.
367. Lima I, Oliveira RC, Atta A, Marchi S, Barbosa L, Reis E, Reis MG, Santiago MB. Antibodies to citrullinated peptides in *tuberculosis*. Clin Rheumatol 2013; 32:685–7.
368. Sakkas LI, Daoussis D, Liossis SN, Bogdanos DP. The infectious basis of ACPA-positive rheumatoid arthritis. Front Microbiol 2017; 8:01853.
369. Hommel B, Charuel JL, Jaureguiberry S, Arnaud L, Courtin R, Kassab P, Prendki V, Paris L, Ghillani-Dalbin P, Thellier M, et al. Chronic malaria revealed by a new fluorescence pattern on the antinuclear autoantibodies test. PLoS One 2014; 9:e88548.
370. Dema B, Charles N. Autoantibodies in SLE: Specificities, isotypes and receptors. Antibodies 2016; 5:2.

371. Richter P, Burlui A, Bratoiu I, Cardoneanu A, Rezus C, Rezus E. A Review of Anti-C Reactive Protein Antibodies in Systemic Lupus Erythematosus. Journal of Interdisciplinary Medicine 2021; 6:60–6.
372. Pisetsky DS. Evolving story of autoantibodies in systemic lupus erythematosus. J Autoimmun2020; 110.
373. Pisetsky DS, Bossuyt X, Meroni PL. ANA as an entry criterion for the classification of SLE. Autoimmun Rev 2019; 18:102400.
374. Meyer O. Anti-CRP antibodies in systemic lupus erythematosus. Joint Bone Spine 2010; 77:384–9.
375. Toussirot É, Roudier J. Epstein–Barr virus in autoimmune diseases. Best Pract Res Clin Rheumatol 2008; 22:883–96.
376. Boyle MJ, Jagannathan P, Bowen K, McIntyre TI, Vance HM, Farrington LA, Greenhouse B, Nankya F, Rek J, Katureebe A, et al. Effector Phenotype of *Plasmodium falciparum*-Specific CD4+ T Cells Is Influenced by Both Age and Transmission Intensity in Naturally Exposed Populations. In: Journal of Infectious Diseases. 2015. page 416–25.
377. Aye R, Sutton HJ, Nduati EW, Kai O, Mwacharo J, Musyoki J, Otieno E, Wambua J, Bejon P, Cockburn IA, et al. Malaria exposure drives both cognate and bystander human B cells to adopt an atypical phenotype. Eur J Immunol 2020; 50:1187–94.
378. Muellenbeck MF, Ueberheide B, Amulic B, Epp A, Fenyo D, Busse CE, Esen M, Theisen M, Mordmüller B, Wardemann H. Atypical and classical memory B cells produce *Plasmodium falciparum* neutralizing antibodies. Journal of Experimental Medicine 2013; 210:389–99.
379. Pizarro-Bauerle J, Maldonado I, Sosoniuk-Roche E, Vallejos G, López MN, Salazar-Onfray F, Aguilar-Guzmán L, Valck C, Ferreira A, Becker MI. Molluskan hemocyanins activate the classical pathway of the human complement system through natural antibodies. Front Immunol 2017; 8:00188.
380. Liu J, Gao J, Wu Z, Mi L, Li N, Wang Y, Peng X, Xu K, Wu F, Zhang L. Anti-citrullinated Protein Antibody Generation, Pathogenesis, Clinical Application, and Prospects. Front Med (Lausanne) 2022; 8:802934.
381. Pisetsky DS. Pathogenesis of autoimmune disease. Nat Rev Nephrol 2023; 19:509–24.

382. Hocking AM, Buckner JH. Genetic basis of defects in immune tolerance underlying the development of autoimmunity. Front Immunol 2022; 13:972121.
383. Ma WT, Chang C, Gershwin ME, Lian ZX. Development of autoantibodies precedes clinical manifestations of autoimmune diseases: A comprehensive review. J Autoimmun 2017; 83:95–112.